Modeling, Optimization and Control of an Integrated PEM Fuel Cell System

by

Chrysovalantou Ziogou

A Thesis

Submitted in Fulfillment of the Requirements

for the Degree of Doctor of Philosophy

Department of Engineering Informatics & Telecommunications

University of Western Macedonia

Greece

March 2013

Modeling, Optimization and Control of an Integrated PEM Fuel Cell System

by

Chrysovalantou Ziogou

A Thesis

Submitted in Fulfillment of the Requirements

for the Degree of Doctor of Philosophy

Advisory Committee

Supervisor: **Kostas Stergiou**, Assistant Professor
Department of Engineering Informatics & Telecommunications,
University of Western Macedonia (UOWM)

Members: **Michael C. Georgiadis**, Associate Professor
Department of Chemical Engineering,
Aristotle University of Thessaloniki (AUTH)

Spyridon S. Voutetakis, Research Director
Chemical Process and Energy Resources Institute (CPERI),
Center for Research and Technology Hellas (CERTH)

2013

Modeling, Optimization and Control of an Integrated PEM Fuel Cell System

by **Chrysovalantou Ziogou**

Examination Committee Members

Kostas Stergiou, Assistant Professor
Dept. of Engineering Informatics & Telecommunications
University of Western Macedonia (UOWM)

Michael C. Georgiadis
Associate Professor
Dept. of Chemical Engineering,
Aristotle University of Thessaloniki (AUTH)

Spyridon S. Voutetakis
Research Director
Chemical Process and Energy Resources Institute (CPERI), Center for Research and Technology Hellas (CERTH)

Simira Papadopoulou
Professor
Dept. of Automation,
Technological Education Institute of Thessaloniki (TEITHE)

Efstratios N. Pistikopoulos
Proffessor
Dept. of Chemical Engineering, Centre for Process Systems Engineering, Imperial College London, United Kingdom

Panos Seferlis
Assistant Professor
Dept. of Mechanical Engineering,
Aristotle University of Thessaloniki (AUTH)

Theodoros Zygiridis
Lecturer
Dept. of Engineering Informatics & Telecommunications, University of Western Macedonia (UOWM)

Chrysovalantou O. Ziogou

MSc in Mathematics, Theoretical Informatics and Systems & Control Theory,
MSc in Informatics, Management Information Systems,
BSc in Computer Engineering

Abstract

Fuel cell systems are part of a prominent key enabling technology for achieving carbon free electricity generation and can be used for stationary, mobile and portable applications. The last decade, significant research efforts have been allocated to the development of fuel cell components and integrated systems, since they constitute an efficient energy conversion technology for transforming hydrogen, and possibly other fuels, into electricity. During their operation various phenomena are evolving and their behavior is affected by many variables such as temperature, partial pressures, gas utilization and humidity. Therefore, it is necessary to be able to understand qualitatively and predict quantitatively the behavior of an integrated fuel cell system in order to protect its longevity and preserve its long-term performance. Driven by this motivation their optimum operation is of great importance. Thus, it is imperative to develop appropriate control strategies and algorithms that optimize their response so that they can accomplish certain intended functions and utilize the available resources, e.g. consumption of fuel, in an efficient manner and satisfy operating and physical constraints. The impact of control is evident not only in fuel cell systems, but also in a wide range of every day applications such as production of chemicals, automotive industry, generation and distribution of energy to name a few. Overall, control engineering provides the scientific foundation and technology for dynamically evolving systems by integrating concepts from computer science, mathematics, and systems engineering.

This thesis has a multidisciplinary scope and it is concerned with the optimal operation of an integrated Polymer Electrolyte Membrane fuel cell (PEMFC) unit and the design and development of advanced model-based control schemes which are deployed to the automation system of a small-scale experimental PEMFC unit. More specifically, a dynamic nonlinear mathematical model is developed that describes the behavior of the PEMFC and it is experimentally validated using a formal systematic estimation procedure for the determination of the empirical parameters. Also, the automation infrastructure and the architecture of the Supervisory Control and Data Acquisition (SCADA) system is presented which is used as a platform for the verification of a number of advanced controllers.

After the determination of the operational requirements of a PEMFC system a modular model predictive control (MPC) framework is designed and the PEMFC acts as a motivating system where the behavior of multivariable nonlinear MPC (NMPC) and multi-parametric MPC (mpMPC) controllers are evaluated. In addition to the NMPC and mpMPC methods, a novel synergetic strategy is proposed that empowers the performance of NMPC by exploiting a multi-parametric quadratic programming (mpQP) approach. At the core of the NMPC formulation lies a nonlinear programming (NLP) problem which is solved using a simultaneous direct transcription optimization method. The performance of the NLP solver is enhanced by a warm-start initialization and a search space reduction technique. This synergy transcends the traditional problem formulation of the NMPC aiming at the reduction of the computational time for the dynamic optimization problem without sacrificing the quality of the obtained solution.

The interconnection between the advanced model-based controllers and the automation system is facilitated through a custom developed software platform based on state-of-the-art industrial protocols. The establishment of such an infrastructure addresses the challenges related to the interface of control, computing and communication issues between the MPC and the integrated PEMFC unit. The MPC framework is deployed online to the industrial automation system and the performance of the controllers is assessed through a set of experimental studies, illustrating the operation of the PEMFC under varying operating conditions.

Περίληψη

Τα συστήματα κυψελών καυσίμου (ΚΚ) έχουν προσελκύσει το ενδιαφέρον τόσο της βιομηχανικής όσο και της βασικής έρευνας τα τελευταία χρόνια, καθώς αποτελούν μέρος μιας φιλικής προς το περιβάλλον τεχνολογίας για την παραγωγή ηλεκτρικής ενέργειας. Κατά τη διάρκεια της λειτουργίας των ΚΚ εξελίσσονται διάφορα φαινόμενα και η συμπεριφορά τους επηρεάζεται από ένα πλήθος μεταβλητών που σχετίζονται με την θερμοκρασία, τις μερικές πιέσεις των αερίων, τη χρησιμοποίηση των αντιδρώντων και την υγρασία. Σε αυτά τα πλαίσια η ανάπτυξη κατάλληλων μεθόδων ελέγχου κρίνεται επιτακτική καθώς είναι σημαντικό το σύστημα ΚΚ να καθοδηγείται στην κατάλληλη περιοχή λειτουργίας ώστε να επιτυγχάνεται η βέλτιστη απόδοση και να διασφαλίζεται η εύρυθμη λειτουργία του ενώ ταυτόχρονα να διασφαλίζεται η μακροβιότητα του.

Η παρούσα διατριβή έχει διττό αντικείμενο ενασχόλησης. Το πρώτο αφορά στην αντιμετώπιση θεμάτων διαχείρισης ενός ολοκληρωμένου συστήματος ΚΚ μέσω της μοντελοποίησης και της βέλτιστης λειτουργίας του. Ενώ το δεύτερο σχετίζεται με την ανάλυση, διερεύνηση και ανάπτυξη μεθόδων προηγμένης ρύθμισης που βασίζονται σε μαθηματικά μοντέλα χρησιμοποιώντας αλγόριθμους προρρητικού ή προβλεπτικού ελέγχου (model predictive control - MPC). Σε αυτό το πλαίσιο το σύστημα ΚΚ αποτελεί το πεδίο πειραματικής εφαρμογής, επιβεβαίωσης και αποτίμησης των αναλυόμενων και προτεινόμενων μεθόδων.

Αρχικά αναπτύσσεται ένα μαθηματικό μη-γραμμικό δυναμικό μοντέλο για συστήματα ΚΚ τύπου πολυμερικής μεμβράνης (Polymer Electrolyte Membrane – PEM) το οποίο αποτελείται από ένα σύνολο διαφορικών και αλγεβρικών εξισώσεων (ΔΑΕ) που περιγράφουν τα βασικά ισοζύγια μάζας και ενέργειας καθώς και την ηλεκτροχημική συμπεριφορά του συστήματος. Σε αυτές τις εξισώσεις εμφανίζονται κάποιες εμπειρικές παράμετροι, οι βέλτιστες τιμές των οποίων προσδιορίζονται από μια γενικευμένη συστηματική μεθοδολογία εκτίμησης. Ο στόχος της μεθοδολογίας αυτής είναι να προσδώσει πειραματικά επιβεβαιωμένη εγκυρότητα στο μοντέλο που λαμβάνει υπόψη τις αλληλεπιδράσεις των υποσυστημάτων που επηρεάζουν την ΚΚ.

Στη συνέχεια παρατίθεται μια εμπεριστατωμένη ανάλυση μεθόδων προηγμένης ρύθμισης που αποτελούν μια ανερχόμενη στρατηγική καθώς μπορούν να αντιμετωπίσουν ταυτόχρονα μη-γραμμικά συστήματα, πολλαπλά κριτήρια βελτιστοποίησης υπό περιορισμούς και να οδηγήσουν το σύστημα στην επιθυμητή κατάσταση μέσω της βέλτιστης λήψης αποφάσεων. Η μελέτη εστιάζει σε δύο μεθόδους προρρητικού ελέγχου, το μη-γραμμικό MPC (NMPC) και το πολυπαραμετρικό MPC (mpMPC). Η πρώτη βασίζεται στην online επίλυση ενός δυναμικού προβλήματος βελτιστοποίησης μη-γραμμικού προγραμματισμού (Nonlinear Programming - NLP), ενώ η δεύτερη βασίζεται στην offline επίλυση ενός προβλήματος πολυπαραμετρικού τετραγωνικού προγραμματισμού (multi-parametric Quadratic Programming - mpQP). Τέλος προτείνεται μία νέα μέθοδος που συνδυάζει τα πλεονεκτήματα των δύο προηγούμενων (mpMPC, NMPC) τροποποιώντας κατάλληλα τον χώρο αναζήτησης των μεταβλητών μέσω της δυναμικής προσαρμογής του, σε ένα υποσύνολο του εφικτού με βάση την πολυεδρική καταμέρισή του. Η συνέργεια αυτή συμβάλει καταλυτικά στην βελτίωση της απόδοσης του βελτιστοποιητή που χρησιμοποιείται για την online επίλυση ενός NLP προβλήματος και αποτελεί νευραλγική συνιστώσα του προρρητικού ελέγχου. Ακολουθεί η σχεδίαση και ανάπτυξη ενός ολοκληρωμένου πλαισίου ελέγχου το οποίο ενσωματώνει ένα πλήθος πολυμεταβλητών ελεγκτών που βασίζονται στις μεθόδους προηγμένης ρύθμισης που σχεδιάζονται για το πειραματικό σύστημα KK.

Επιπρόσθετα παρουσιάζεται η αρχιτεκτονική του βιομηχανικού συστήματος εποπτικού ελέγχου και της διεπαφής που επιτρέπει τη διασύνδεση των αλγόριθμων προηγμένης ρύθμισης με το σύστημα αυτοματισμού. Το πακέτο λογισμικού που σχεδιάστηκε και αναπτύχθηκε, αναλαμβάνει τη διασύνδεση και το συγχρονισμό της επικοινωνίας μεταξύ των ελεγκτών τύπου MPC και του εποπτικού συστήματος της μονάδας, καθιστώντας με αυτό τον τρόπο εφικτή τη μετάβαση από την θεωρητική μελέτη στην πρακτική εφαρμογή των στρατηγικών προρρητικού ελέγχου. Η μελέτη της απόκρισης των ελεγκτών και της συμπεριφοράς της μονάδας αναλύεται μέσα από ένα πλήθος πειραμάτων (σε επίπεδο προσομοίωσης και online), που παρουσιάζουν τα χαρακτηριστικά της κάθε μεθόδου σε σχέση με τους επιδιωκόμενους στόχους βέλτιστης λειτουργίας που τίθενται για το σύστημα. Για το σκοπό αυτό η μελέτη καλύπτει ένα μεγάλο εύρος λειτουργικών συνθηκών, την ύπαρξη διαταραχών και την έναρξη της λειτουργίας της μονάδας.

Acknowledgments

During my interesting and full of surprises trek towards the fulfillment of this PhD thesis, numerous people have played a role along the way and my work has been influenced by, and benefited from, my interactions with them. Thus, I would like to take this opportunity to acknowledge them.

Foremost I would like to express my deep gratitude to Prof Georgiadis for his guidance, assistance, sound advice and for shaping a smooth course for my research work. Above all he allowed me to make a dream come true, which was the realization of this thesis. I am grateful for my long lasting collaboration with Dr Voutetakis. He has been an inexhaustible source of knowledge, he taught me to think out of the box, to question everything and most importantly he believed in my potential and abilities. I wish to express my sincere appreciation for Prof Papadopoulou for always being there for me. By her constructive criticism and challenging discussions she has catalytically contributed to the outcome of my global research efforts and she helped me optimize the way that problems should be approached and solved. By their motivation and inspiration I was able to develop new ideas through the last four long years.

Furthermore I am grateful to Prof Pistikopoulos for giving me the opportunity to cooperate with him at my visit at Imperial College and for his encouraging and fruitful comments about my work, especially in the last year of my thesis. My gratitude is extended to Prof Seferlis, who has pointed out some interesting paths to follow and by his initial contribution I managed to effectively deal with my optimization-related issues.

Through countless open-minded conversations with them, an initial interesting abstract idea has evolved to a tangible set of actions that are aggregated into the work described by this thesis. By their precise feedback the quality of my work was improved and new pathways have appeared by their important comments.

I would like to thank Prof Stergiou who kindly accepted to become my final supervisor and along with Prof Zygiridis reviewed my thesis and helped to improve its quality. Also I would like to thank Dimitri T., Stella B. and Popi P. for their useful ideas and productive discussions related to fuel cell systems. A special thanks goes to Prof. Karampetakis and Prof. Vardoulakis for their lectures that enabled me to open the door to the wonderful world of mathematics and systems. I feel that a line for Prof I. Vasalo should also appear in this section, as a long time ago he told me that a person's merits are evaluated only by 50% by its studies, while the rest is its ability to cooperate as a team member. Since then I am trying to follow his advice and improve both of these fractions.

I would like to extend my thanks to Aki and Mario for their help. During the last years through their efforts I was able to focus more on my thesis and worry less about work as they successfully handled all the work-related issues. Also many thanks to Ari, Gianna, Kosta G., Kosta K., Niko, Niki and Panagioti for their collaboration at work. Furthermore, I would like to thank Dimitri, Saki and Damiano for providing a different perspective on the way that research is performed, Loukia and Martha for their optimistic thoughts and discussions, Alexi, Zisi, Thodori D. and Thodori Z. for the joyful late hour corridor meetings, and all my colleagues of LEFH and LPSDI at CPERI.

I am grateful to Dimitra and Stella for always listening to me and for being still there despite my annoying complaints and exponentially increasing whining. Many thanks to Orestis for helping me put my nonlinear worries into the right perspective and for his continuous encouragement. Last, but not least, I would like to thank Kosta for his unconstraint patience, his positive thoughts and unlimited multilevel support throughout the entire thesis. Finally I would like to thank my parents, Odyssea and Agnoula, for their endless love and the faith they have in my endeavors.

To my parents

Odyssea & Agnoula

Contents

List of Figures

List of Tables

Chapter 1

Introduction

1.1 Motivation

Energy is a fundamental determinant of the economy and plays an important part in industrial growth. At the same time the present and future global energy demand is related to the problem of climate change which constitutes a major challenge that must be addressed. It is widely known that the energy demand worldwide is increasing. In order to meet the increased demand, reserves of fossil fuels such as oil are used, which are gradually diminishing. On the other hand the use of fossil fuels is a source of greenhouse gasses and other pollutants that cause global warming with very serious and irreversible effects on the environment. For example between 1990 and 2010 90 % of the increase in CO_2 is attributed to the transport sector. More specifically road transport is responsible for 85% of the CO_2 emissions. The fact that an average lorry generates six times more CO_2 per tone/km than a train (European Commission, 2000) raises significant questions regarding the required actions that will firstly reduce this effect and secondly will decarbonize the road transport and the energy sector. Therefore, it is imperative to

transform not only the energy sector but also the transport sector into low-carbon sectors and to decouple the economic growth from resource and energy use and reduce greenhouse gas (GHG) emissions.

In order to keep climate change below 2ºC, specific targets are set towards the reduction of GHG emissions. More specifically Europe and G8 have committed to reduce their GHG emissions by 80-95 % by 2050 and in the shorter term by 2020, to reduce GHG by 20%, increase the share of renewables to 20%, and save 20% energy (European Commission, 2011). Another major issue is derived by the fact that fossil fuels are confined to a few areas of the world and their uninterruptible supply depends mainly on geopolitical, economic and sometimes ecological factors. Therefore, the energy security is vital for a stable economy. In addition, the mitigation of climate change through the reduction of GHG emissions and the security of energy supply must be considered within the context of sustainable development. All these issues constitute serious challenges that must be dealt with solutions that will provide a stable pathway towards a decarbonized energy and transport system during the next decades.

The shift towards a low carbon, efficient and secure economy requires targeted deployment of innovative technologies and increased exploitation of renewable energy sources. Furthermore, it is recognized that a technological shift and the development of new clean technologies are vital for a successful transition to a decarbonized and sustainable future economy. Although a number of diverse technologies exist that aim at the same target, such as biofuels and carbon capture and storage, the synergy between the increased use of renewable energy sources, renewable hydrogen and electricity from fuel cells represent one of the promising ways to realize sustainable energy. These technologies can simultaneously address the environmental concerns and the issues of security in energy supply and are considered as key solutions for the 21st century. Hydrogen and fuel cells can enable the so-called hydrogen economy (European Commission, 2003) and they can be utilized in transportation, distributed power and heat generation and energy storage systems.

1.1.1 The role of hydrogen

The realization of a low carbon economy can be greatly assisted by the use of hydrogen which is not a primary energy source like coal and gas but it is an energy carrier with zero carbon content. Hydrogen is a very attractive fuel that can be obtained by a variety of diverse resources which means that it can alleviate the issue of energy security which is related to the confined production of a fuel at specific regions on the planet. Since hydrogen can be produced anywhere where there is water and a source of power, generation of fuel can be distributed and does not have to be grid-dependent. Thus the long-term use of hydrogen can decouple the link between the energy needs and the energy supply. It can be produced from all primary energy sources and generates no CO_2 when used to generate electricity in a fuel cell system or alternatively it can be produced from fossil fuels with CO_2 capture and storage technologies. Furthermore, it can be used in a number of applications ranging from devices and products powered by fuel cells to heat and power generators in stationary systems for industrial and domestic use. Thus, the use of hydrogen could drastically reduce GHG emissions from the energy sector. Fig. 1.1 presents the diversity of the hydrogen production and its use (European Commission, 2003).

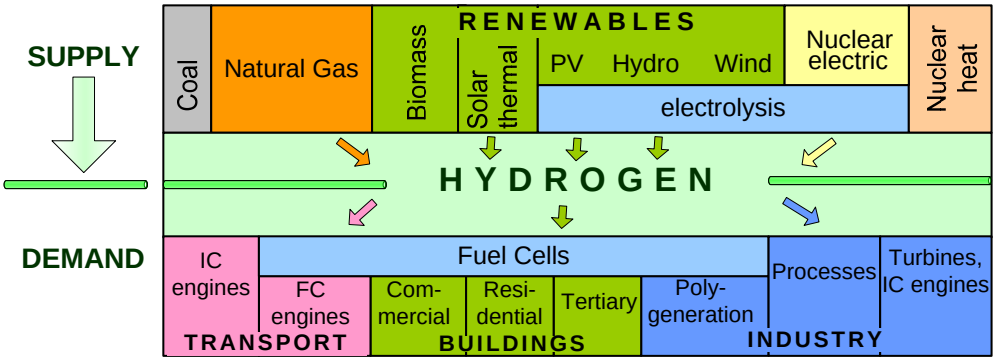

Figure 1.1 Hydrogen energy sources, energy converters and applications

Hydrogen as an energy carrier can create links between a multitude of production methods and sources to various applications including fuel cell systems. But its usefulness is not limited to those. It offers an interesting solution for both short and long-term storage in small or bulk quantities. In cases where the supply is more than the demand, the excess of energy can be transformed into hydrogen that can be easily

transported or remain onsite and serve the needs for power on demand. The transportation of hydrogen can be achieved by a number of alternatives including vehicle, ships and pipelines. Thus, the most cost-efficient method can be selected per case. Also, it can facilitate the integration of renewables in the energy supply system and offer the opportunity to increase the share of renewable energy. In the case of intermittent sources hydrogen can act as a temporary energy storage option that utilizes the excess of energy supply subsequently used to balance the demand upon request.

Today, large quantities of excess hydrogen are already available in some regions around the world. For example Germany has a surplus of 850 million Nm^3 per year (European Hydrogen Association, 2008) which is burnt for thermal uses. This constitutes an interesting option for initial applications in transport and stationary that can use the hydrogen which is generated as a by-product in chemical processes. Nowadays the hydrogen distribution network is under design and it constitutes a major challenge for the availability of hydrogen worldwide and the penetration of fuel cells in the transportation sector.

Overall hydrogen is expected to play an important role in the future low carbon energy landscape and it can be used to close the cycle of energy generation, distribution and demand and has the potential to reduce emissions to half of those projected in a business as usual scenario by 2050 (IEA, 2007). However, the transition from a carbon-based energy economy to a hydrogen-based one involves significant scientific and technological challenges for the implementation of hydrogen in conjunction with fuel cells as a clean energy solution of the future.

1.1.2 The role of fuel cells

Hydrogen and fuel cell technology have clear and mutually enforcing benefits for a sustainable growth. Fuel cells open a path to integrated energy systems that are able to simultaneously address environmental challenges and major energy issues since they have the flexibility to adapt to intermittent and diverse renewable energy sources. They are part of a promising environmentally friendly and benign technology that has attracted the attention of both industrial and basic research in the recent years. Significant effort has been allocated to fuel cell components and integrated system development since they

constitute the most efficient conversion device for transforming hydrogen, and possibly other fuels, into electricity. Furthermore, they have the flexibility to adapt to different intermittent renewable energy sources, enabling a wider energy mix in the future (Mishra *et al.*, 2005). Fuel cells are electrochemical devices that convert the chemical energy of a gaseous fuel, usually hydrogen, directly into electricity (Fig. 1.2) without any mechanical work (Pukrushpan *et al.*, 2004). The only by-product from their operation is heat and water.

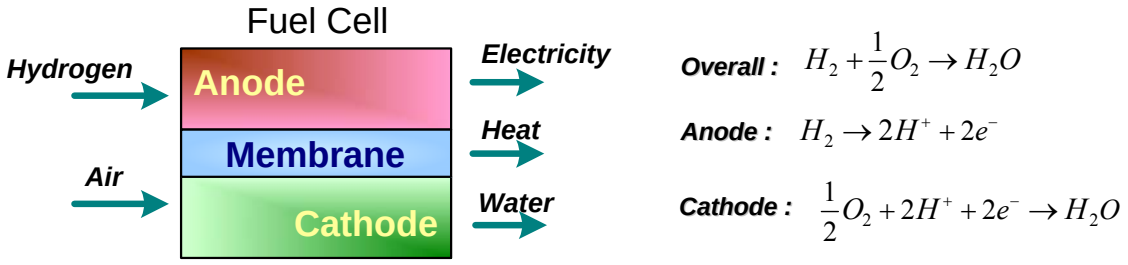

Figure 1.2 Fuel Cell and energy conversion

Fuel cells have various advantages compared to conventional power sources, such as internal combustion engines (ICE) or batteries. For instance compared to ICE the fuel is not combusted. Instead, the energy is released electrocatalytically leading to high energy efficiency, which is increased when the generated heat by the reaction is also harnessed. Fuel cells can be placed close to the point of end-use, allowing exploitation of the heat generated in the process. As the fuel is not burnt the process is quiet and carbon free. Most fuel cells operate silently, compared to internal combustion engines. They are therefore ideally suited for use within buildings or for road transport. From the efficiency point of view, fuel cells are two to three times more efficient than ICE. Furthermore, a fuel cell system can be a zero-emission source of electricity when renewable hydrogen is used and subsequently reduce the carbon footprint of the end product of application.

Batteries and fuel cells produce electricity from an electrochemical reaction. However, a battery contains a specific amount of energy according to its capacity and once this is depleted the battery must be recharged using an external supply of electricity. On the other hand, in a fuel cell the electricity production is continuous as long as fuel and oxidant, usually air, is supplied. Unlike batteries, fuel cells do not have the "memory

effect" when they operate, although in the long term there are some degradation issues. Table 1.1 presents some of the challenges that must be dealt in order to realize a low carbon future economy and the way that fuel cells can help towards this direction.

Table 1.1 The role of fuel cells towards a low carbon economy

Challenges towards a low-carbon economy	Fuel cell potential
▪ Reduce GHG emissions that cause climate change	▪ Combined with renewable hydrogen, fuel cells have a near zero carbon footprint
▪ Energy self-sufficiency and security of supply	▪ Fuel cells can be used in a wide range of applications while hydrogen can be produced from a very wide variety of resources in distributed or centralized way
▪ Decarbonization of the road transport that has a significant impact on urban areas and public health	▪ Fuel cells allow considerable reduction of noise and air pollution
▪ Management of the intermittency of renewable energy sources and energy storage	▪ Fuel cells, coupled with hydrogen, facilitate the integration and storage of renewable energy sources
▪ Energy efficiency and energy savings	▪ Fuel cells are the most efficient energy conversion technology

In order to take advantage of fuel cell's great potential a number of technological challenges must be addressed that require significant efforts of research and development before they can be overcome. In addition, fuel cells are not likely to be implemented isolated, but as a part of a larger shift in fuel infrastructure and efficiency standards, which will require sustained efforts from industry and research sectors.

1.1.3 The role of control

Nowadays, the increase in energy demands, the tighter environmental regulations and various economic considerations require for the systems and processes to operate over a wider range of conditions and often near the boundaries of their admissible region. Moreover, the interconnection and cooperation of various systems into integrated units is a prerequisite for efficient resource handling and allocation. In the sight of these issues, control is an important area both from scientific and technological point of view, able to facilitate the improvement of the response and overall behavior of systems, processes and

end-user applications. Thus, it is important for the control technologies to be built upon a rigorous sensing, modeling, decision making and optimization basis as in many situations, the subsystems of a process have high degrees of autonomy and heterogeneity. Therefore, a continuous research effort is imperative for the realization of system-level goals for performance, predictability, stability, and other properties through appropriate analysis, design and implementation. In this context, the proper control structure and methods can function as a catalyst that transforms technological innovation to systems engineering and process novelties (Fig. 1.3).

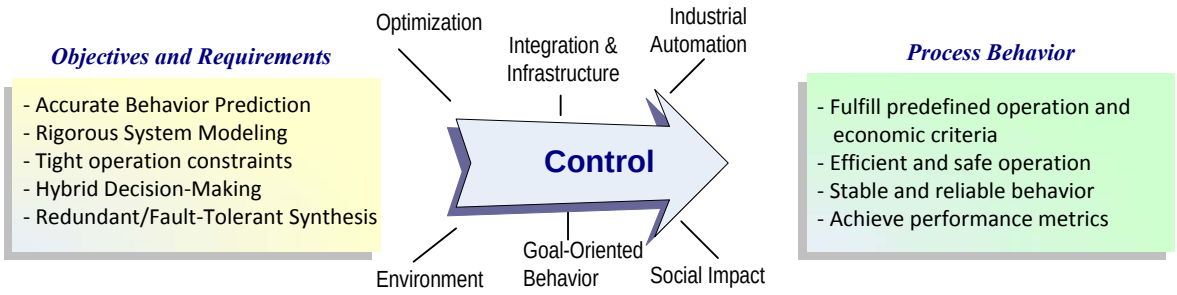

Figure 1.3 Role of control

At a wider context, control engineering tools and platforms are used to facilitate the analysis and modeling of the system and explore its response and behavior. Besides that, control is necessary to overcome the limits of ad hoc solutions as it is a highly scalable technology. Nowadays, control is present at various levels of a system or a process, initially it is applied to individual sensors and actuators, then on multivariable systems, and finally at plant wide scale.

The operation of a process involves a large number of decisions which are distributed into a hierarchically connected structure (Fig. 1.4). At the top of the structure there exist the planning and scheduling layer that focuses on economic forecast, providing production goals and schedule the timing of actions which are obtained using various mixed integer programming formulations (Biegler *et al.*, 2002). The time horizon in the planning layer is typically in months or weeks while for scheduling is weeks or days. The derived decisions are forwarded to the two-layered process operation level consisting of real-time optimization (RTO) and advanced process control. RTO is

concerned with the implementation of business decisions and production schedules based on a steady state model of the plant in order to optimize the profit of the plant and seeks additional profit margins based on parameter estimation and data reconciliation. The advanced process control (APC) layer adjusts the inputs to keep the process at the desired set-points at all times. One of the methodologies of APC is model Predictive Control (MPC) which uses a dynamic model of the process to predict the future dynamic behavior over a time horizon and therefore, allowing the computation of the optimal control actions to minimize the deviation of the output from the desired target (set-point tracking) (Mayne *et al.*, 2000). The set points from the APC layer are subsequently fed to the regulatory level which communicates with the instrumentation and data acquisition layer where the Input/Output (I/O) field of the unit exists.

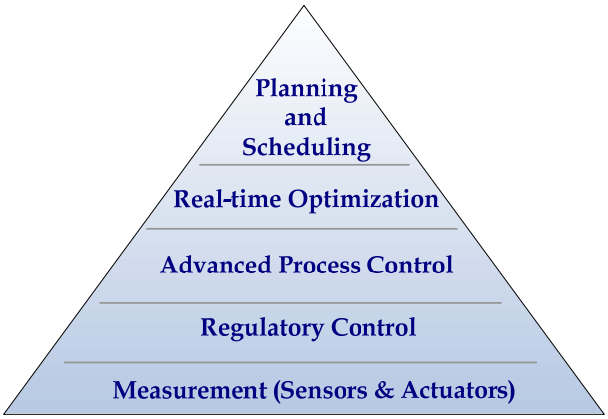

Figure 1.4 Hierarchical process structure

The impact of control technology is evident in a wide range of application areas, including fuel cells, as it is the necessary facilitator for achieving desired objectives and fulfilling application-specific goals. Fuel cell systems exhibit fast dynamics, nonlinearities and uncertainties that constitute challenges requiring appropriate control in order to be confronted effectively. The use of efficient control strategies would not only increase the performance of these systems, but would increase the number of operational hours as their lifetime is preserved by operating at optimal levels and also reduce the cost per produced kilowatt-hour. Overall control can be considered as a key enabling technology for the deployment of fuel cell systems as well as renewable energy systems.

1.2 Fuel cell technology

In general fuel cells represent a versatile and efficient electricity generation source that can be applied in a wide range of industries - from vehicles and primary energy systems to autonomous back-up power systems and portable consumer electronics devices. Although there are several types of fuel cells, all of them are structured around a central design which includes two electrodes, named anode and cathode and between them there is an electrolyte that facilitates the movement of the electrons. This electrolyte can be either solid or liquid and carries the ions between the electrodes. Also, in order to enhance and accelerate the reaction a catalyst is used. The electrodes and the electrolyte constitute the basic structure of a fuel cell and when a number of individual cells are composed they form the fuel cell stack. A fuel cell system has a number of subsystems and peripherals that control the flows of fuel and oxidant, the produced power, water and heat. However even though all types of fuel cells have the same structure, each one is suitable for different applications, uses different materials and requires specific fuel. Each fuel cell type also has its own operational characteristics which makes them a very versatile and flexible technology. Table 1.2 presents the basic characteristics of each type of fuel cell (Fuel Cell Today, 2011; U.S. Department of Energy, 2012).

Table 1.2 Types of fuel cells

Fuel cell type	Electrolyte	Operating Temperature	Electrical efficiency	Electrical power
Polymer Electrolyte Membrane (PEMFC)	Ion exchange membrane (water-based)	40-100°C	40-60%	< 250kW
High Temperature PEM (HT-PEMFC)	Ion exchange membrane (acid-based)	120-200°C	60%	<100kW
Alkaline (AFC)	Potassium hydroxide	60-90°C	45-60%	10-100kW
Direct Methanol (DMFC)	Polymer membrane	60-130°C	40%	<1kW
Phosphoric Acid (PAFC)	Liquid phosphoric acid	150-200°C	35-40%	>50kW
Molten Carbonate (MCFC)	Liquid molten carbonate	600-700°C	45-60%	>200kW
Solid Oxide (SOFC)	Ceramic	600-1000°C	50-65%	<200kW

The existing categories of fuel cell systems are mainly classified according to type of the electrolyte that plays an important role as it allows the passing through of only certain appropriate ions and blocks the movement of the electrons. The list of fuel cell types (Table 1.2) does not include the types of fuel cells which are at the research and development only stage such as microbial fuel cells. As can be seen from Table 1.2, fuel cells are a collection of technologies that operate based on the same principle. Each type has different operating characteristics and is suitable for different applications offering different benefits in each case. In general the fuel cell technology is used in a number of applications that are categorized into three broad areas:

- Stationary: provide primary or back-up power to fixed locations, such as uninterruptible power supply systems (UPS) or combined heat and power (CHP) facilities with power ranging from 0.5kW to few MWs.
- Transportation: provide primary propulsion or range extension for vehicles, such as busses, trucks, material handling vehicles (e.g. forklifts) or scooters with typical power from 1kW to 100kW.
- Portable: provide power or charge systems that are designed to move, including auxiliary power units for off-road vehicles, such as battery chargers, small personal electronics (mp3 players) or skid-mounted generators with power ranging from 5W to 20kW.

Each area has its own characteristics regarding the maturity of applications, the power level, the cost, durability and size. Nevertheless fuel cell technology (European Commission, 2003) is flexible and covers an evolving area of applications (Fig. 1.5).

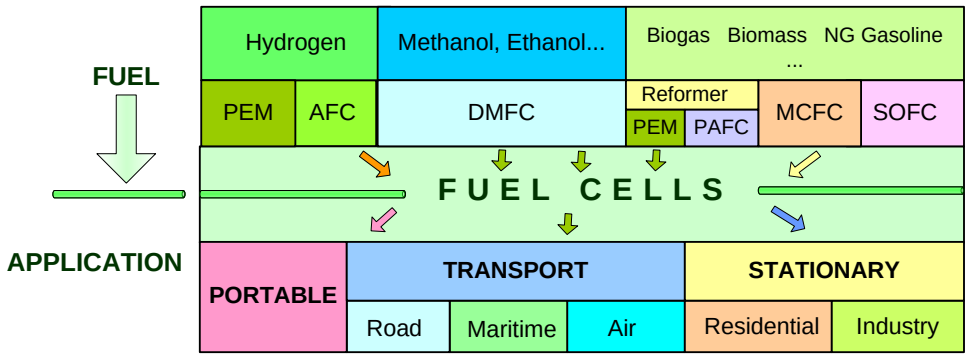

Figure 1.5 Fuels and applications related to fuel cells

The commercialization of fuel cells for various applications began in 2007 (Fuel Cell Today, 2011) and although the market is very young, it is expected to move from a niche to a mainstream market by 2017. With a compound annual growth rate of 83% for the period of 2009 to 2011 (Adamson and Jerram, 2012) and an increasing number of shipments and installed megawatts by application (Fuel Cell Today, 2011), fuel cells are an emerging technology that will play in the long-term an important role in the future energy landscape.

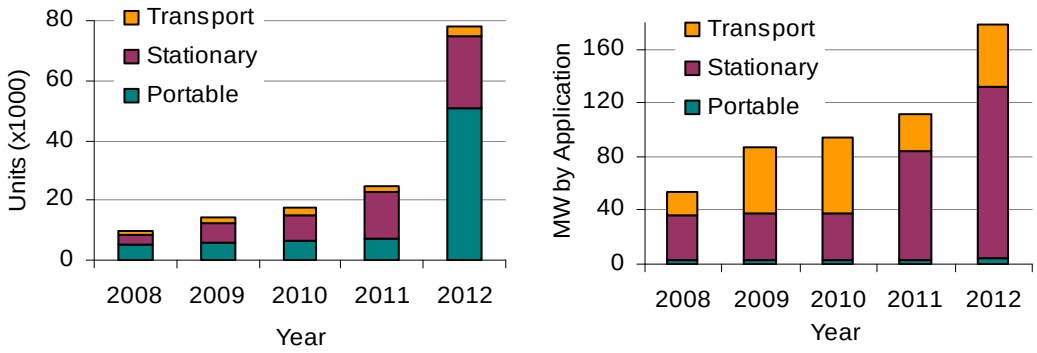

Figure 1.6 Fuel cell shipments and megawatts by application over the last 5 years

Fig. 1.6 illustrates that the shipments and installed megawatts per market segment are increasing the last 5 years and constitutes a clear indication of the fuel cell technology trend. The transport applications have increased in 2012 compared to 2011, due to the respective demand in material handling vehicles, especially in the US (Fuel Cells 2000, 2012), whereas the fuel cell electric vehicles (FCEV) are not in commercial state yet. Although every major automotive company has announced that starting from 2015 a commercially model will be available, the share of FCEVs comparing to other electric vehicles or conventional ICE is expected to increase only after 2025 (McKinsey and Company, 2010). A significant increase in shipments is noticed in 2012 which is caused by the introduction to the market of portable chargers. But as they are small in produced power they do not affect the distribution of megawatts per application. On the other hand Fig. 1.7 shows the shipments per fuel cell type and the respective megawatts per type during the last 5 years.

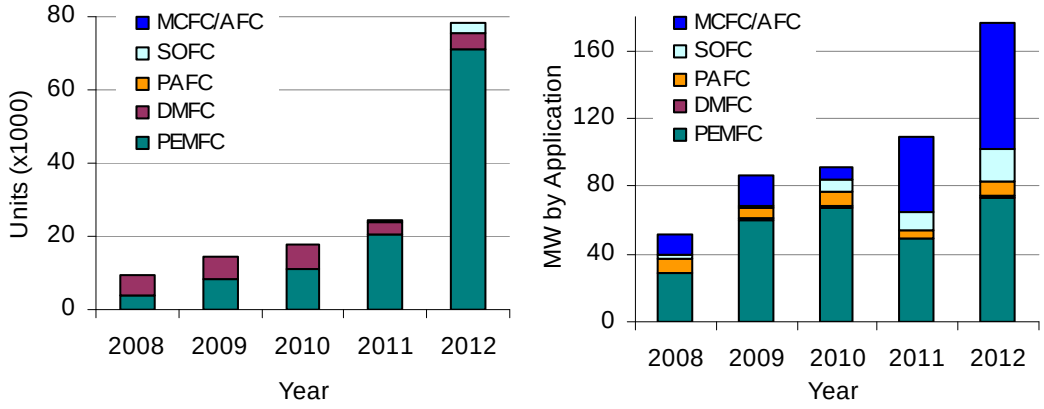

Figure 1.7 Shipments and megawatts by fuel cell type over the last 5 years

In terms of shipments, PEMFC systems are the dominant type due to their ability to be used in a number of applications. The growth that appears in 2012 is caused by the increase on portable consumer electronic devices. The rest of the shipments are by DMFC systems which are mostly used in portable generators. Finally in 2012 there is an increase in SOFC systems caused by a respective demand in Europe and in Japan.

On the other hand, the distribution in terms of megawatts per type is quite different, as expected, since PEMFCs are used in small systems while MCFC and SOFC systems are used for large stationary applications. The increased use of MCFCs in 2012 is due to the high demand by South Korea (Fuel Cell Today, 2011). Also, as multinational companies need to reduce their carbon footprint (Yang, 2010), a number of large scale fuel cell installations are expected in the near future since they can alleviate the burden on GHG emissions.

Fuel cell technology and research directions

Since fuel cell technology is relatively new and has not reached its full maturity, research efforts are necessary in order to improve the characteristics and overcome the challenges that these systems are facing. Research in the area of fuel cell systems is aimed at reducing the cost and improving the performance, durability and safety for stationary and transport applications. This includes development of process and materials, optimization of fuel cell components and sub-systems as well as modeling, testing and

validation. Furthermore, system integration is an important issue. Integrated fuel cell systems must present an optimized behavior in order to reduce the cost of electricity and exhibit their full potential to the end-user. Thus, research and development efforts related to integrated fuel cell systems are necessary that will include: power inverters and power conditioners, hybrid system designs and testing, operation and maintenance issues, and appropriate control for integrated systems. Overall the role and use of fuel cells in stationary and portable applications could be significant, especially if opportunities for integrated renewable systems are considered.

1.2.1 Polymer Electrolyte Membrane (PEM) Fuel Cell

Among the various fuel cell type, PEMFCs have some very appealing characteristics. Their low operating temperature, size and weight are only few of the features that make them more suitable for use in vehicles and portable devices. Thus, they have an increased role compared to other fuel cell types, derived by the fact that they are selected for a number of applications that currently are in an early market entrance stage (material handling equipment - MHE) or are expected to enter the market in the near future (such as FCEVs). Also, PEMFCs can be widely used in a number of small portable devices or small stationary applications to provide primary power (telecommunication stations) or backup power (autonomous power units). The range of the application that PEMFCs are suitable continues to grow. Also, the global goal to reduce GHG emissions in the road transport sector, up to 95% until 2050 (European Commission, 2011), signifies that PEMFCs systems will be part of the future automotive industry, including busses and light duty vehicles (LDV).

PEMFC technology challenges

PEM fuel cells have many advantages, but there are also a number of challenges that must be considered in order to be widely used. These challenges are mainly related to cost and performance issues while other issues include size, weight and management of water and heat (Martin *et al.*, 2010). The main key challenges include:

• Cost. The cost of fuel cell power systems is by far the largest factor that limits the market penetration of fuel cell technology.

• Lifetime and reliability. The durability of fuel cell systems is a challenging issue and specific targets are set that will make them more competitive.

• Size. The size and weight of a PEM fuel cell system must be further reduced especially if they are designed to be used in the transport segment, transport vehicles or material handling vehicles. This applies not only to the fuel cell stack, but also to the components and subsystems that form the system's balance of plant (BOP).

• Air management. Air compressor technology needs to be further optimized since it is an important part that needs significant amount of energy to operate, especially for automotive fuel cell applications.

• Thermal and water management. The temperature and hydration of the fuel cell are important factors that must be properly handled in order to have a stable system behavior.

In order to overcome the barriers that are raised by these challenges, significant scientific and technological developments are required, complemented by proper regulatory codes and standards in order to advance the penetration of fuel cell technology and allow its wide commercialization. More specifically there are three distinct areas where the research efforts and development strategies are focusing on:

- Stack components: Catalysts, electrolytes, MEAs, gas diffusion media, bipolar plates and interconnects.
- System and Balance of Plant (BOP): BOP components, electronics, controls, instrumentation, assembly components, conditioning.
- Operation and Performance: durability, operation in wide ranges of temperature and humidity, higher operating temperatures and improvements in efficiency for stationary fuel cells, higher energy density for portable fuel cells.

According to the market segment where the PEMFC systems are used, these challenges have different impact on the final product. For instance in the transport segment the most important issues are the cost and the durability compared to ICE, whereas in the stationary segment, where cogeneration of heat and power is desired, the use of PEM fuel cells would benefit from improving the heat recovery mechanism.

1.2.2 Current status and perspective of PEM fuel cell systems

The past few years PEM fuel cell technology has evolved significantly. The durability and the cost of a PEM fuel cell system have very specific targets to reach. More specifically, the lifetime required by a commercial fuel cell is over 5000 operating hours for light-weight vehicles and over 40,000 hours for stationary power generation with less than 10% performance decay (Wang *et al.*, 2011). On the other hand, fuel cell components, such as the MEA (membrane electrode assembly), exhibit performance degradation after long-term use which significantly affects the lifetime of the system. However, research efforts have yielded substantial improvements in durability, with automotive fuel cell stack and system durability in laboratory testing increasing from approximately 2000 hours in 2006 to 4000 hours in 2011 (Kurtz *et al.*, 2011). This improvement is also verified in the testing of automotive PEMFC stacks, from under 1,000 hours in 2006 to 2500 hours in 2009 (Schmittinger and Vahidi, 2008). Table 1.3 shows the evolution of some basic characteristics of an 80kW PEM fuel cell system based on projection to high-volume manufacturing (500,000 units/year) and the evolution of these characteristics over the last six years (U.S. Department of Energy, 2012).

Table 1.3 Characteristics and cost analysis of PEMFCs over the last six years

Characteristics	Units	2007	2008	2009	2010	2011	2012
Stack power	kWgross	90	90	88	88	89	88
System power	kWnet	80	80	80	80	80	80
Cell power density	mWgross/cm^2	583	715	833	833	1,110	984
Peak stack temperature	°C	70-90	80	80	90	95	87
Platinum Group Metal loading	mg/cm2	0.35	0.25	0.15	0.15	0.19	0.2
Platinum Group Metal content	g/kWnet	0.68	0.39	0.2	0.2	0.19	0.22
Cost analysis							
Stack cost	$/kWnet	50	34	27	25	22	20
Balance of plant cost	$/kWnet	42	37	33	25	26	26
System Assembly and Testing	$/kWnet	2	2	1	1	1	1
System cost	$/kWnet	94	73	61	51	49	47

Table 1.3 shows that significant improvements have been achieved the last few years regarding the power density and the platinum content, as well as in the cost of the system.

Fig. 1.8 illustrates the modeled cost and its evolution towards a specific target which is set to reach by 2017 (U.S. Department of Energy, 2012b).

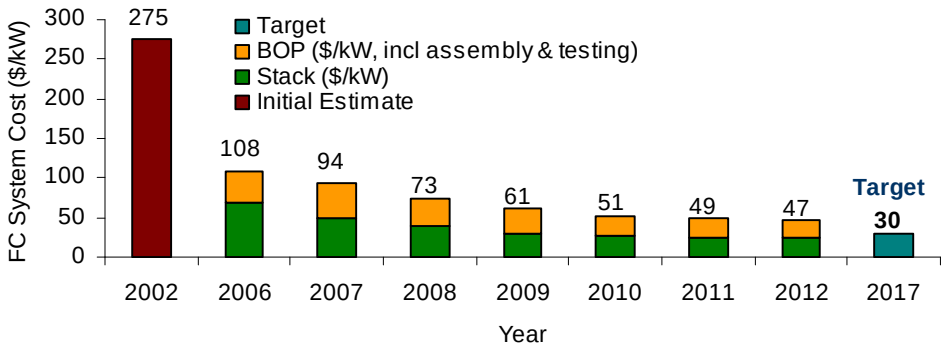

Figure 1.8 PEMFC system cost evolution from 2002 to 2012

Figure 1.8 shows the current trend of production cost of a PEM fuel cell system during the last decade (2002-2012) which is steadily decreasing. The cost of PEMFC system has dropped 83% compared to 2002 and 36% compared to 2008. Currently (2012) its status is $47/kW. This reduction in cost is caused by a decrease of the loading of the platinum-based catalyst, and by the reduction of the overall balance of plant (BOP) of the system. The same trend is observed in smaller production rates (Fig. 1.9).

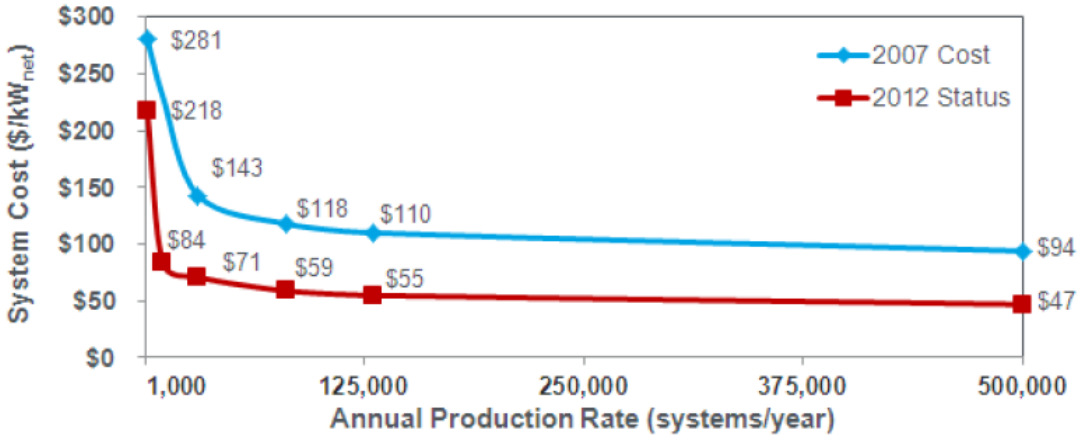

Figure 1.9 System cost and production rate

It is observed that even at a lower-volume production rate the cost is significantly reduced over the last five years. Overall the cost of the system is reducing while the

lifetime is increasing. In that context the PEM fuel cell technology shows a promising future perspective.

A further analysis of the PEM fuel cell components can provide an overview of the areas and the respective impact that research and development efforts would have on the overall cost contribution. Fig. 1.10 illustrates the cost breakdown for a 5kW system used for a small stationary application. The analysis focuses on the fuel cell system and it is based on an annual production of 50000 units (Yang, 2010).

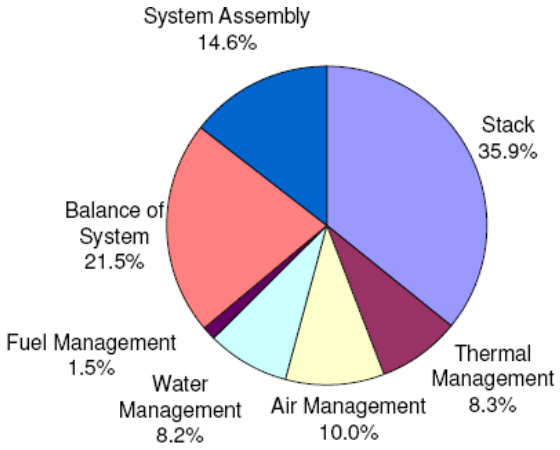

Figure 1.10 Contribution of each component to the overall PEMFC cost

From Fig. 1.10 it is interesting to notice that the stack is only 35.9% of the overall cost compared to the rest of the subsystems and the BOP of the system. Also, this analysis presents the distinct, yet interacting, subsystems that exist on a PEM fuel cell system and their significance to the system cost. Each subsystem requires monitoring and control actions which are imposed by the various actuators of the system. The development of appropriate control strategies has a strong effect not only at the performance of the stack, but also at the fuel, air, water and thermal management which is directly related to optimal response and the integrated operation.

.

1.2.3 Monitoring and Control of a PEM fuel cell system

Fuel cell systems (FCSs) have various electrochemical, mechanical and electronic components and subsystems along with a control system that ideally should enable proper functioning of all devices and components within predefined constraints considering the efficiency, safety and long-term reliability of the system. Nowadays, most of the developed systems contain only basic controllers, i.e. load control, stack temperature control, DC/DC converter voltage control and do not take into account the behavior of the load, the importance of optimization of the system's operation and information related to the overall system's performance. One of the reasons is the fact that there are still significant efforts that focus on the improvement of the materials for the MEA and the stack, less expensive catalysts, defining optimal working conditions, etc. Furthermore, even the manufacturers of commercially viable FCSs are satisfied with existing controls that enable only basic operational control of FCS with no or little regard towards an optimum state of operation. The reason for such decisions is the fact that the efforts focus on promoting the new technology and that the issues of its optimal operation can be resolved later.

On the other hand, control theory has developed to a great extent in the last two decades (Biegler *et al.*, 2002; Engell, 2007). The concepts of supervisory control and advanced control algorithms together with modern data acquisition modules can assure proper conditions for the involved components and equipment (Pregelj *et al.*, 2011) and can effectively handle the dynamics of a fuel cell. With an aim to industrialize and commercialize the fuel cell systems the need of developing suitable control strategies is becoming more and more important. The driving force behind the research and development efforts is the fact, that a customized control system can greatly improve the behavior and durability of FCS and also reduce its operating costs. In general the optimal control of a FCS is vital for improving the operation, as it influences the performance, the lifetime, the fuel utilization and the response times. For this purpose, it is necessary to develop strategies and advanced control algorithms which will also contribute to the long-term operation of the system.

Systemic development process

Overall, the utilization of hierarchical supervisory control algorithms and advanced control methodologies that incorporate a priori knowledge and integrate additional online information gained from models can contribute to a great extent to the optimum operation and can also significantly reduce the long-term operating costs. Therefore, computer-aided modeling and optimization methodologies are necessary to develop and implement these control related goals. Fig. 1.11 shows the whole analysis and design process of a typical fuel cell system.

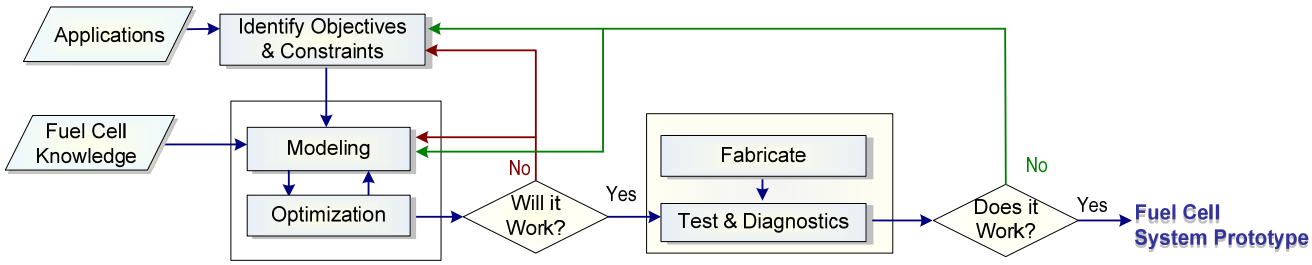

Figure 1.11 Fuel cell systemic analysis and design process

The process starts by identifying a set of specifications and constraints, which mainly depend on the intended application of the fuel cell and results to a fully operational system that fulfils the predefined objectives. This systematic approach is coupled with the online deployment to a process unit and includes the integration of the various components at hardware, equipment and software level. In this thesis the development is based on this approach that will be analyzed in the subsequent chapters.

1.3 Advanced Process Control

The increasing design and operating complexity which is encountered at technologically evolving systems, such as fuel cells, requires an interdisciplinary research approach and development process based on a concrete control framework. It is a fact that the collaboration between control and other fields has been consistently productive. Wherever dynamics and feedback are involved, the role of control is very important and

in some applications it is regarded as crucial (CSS, 2011). The objective of the control is to achieve a set of predefined conditions for the process and maintain the operation at the desired or optimal values (Qin and Badgwell, 2003). In general process control refers to the technologies that are necessary to design, develop and implement control systems for a process. The process control technologies include a multitude of components that constitute an integrated framework:

- automation hardware and software (such as actuators, measuring instruments, communication infrastructure),
- control structure design,
- physical and empirical modeling,
- computer-aided simulation and optimization,
- advanced control strategies and related technologies such as process monitoring/diagnosis,
- planning and scheduling solutions.

Theoretical and practical approaches through the effective integration of software and hardware components, aim at the development of a systemic methodology of measuring, controlling and decision-making techniques. The utilization of such methodology is expected to achieve increased energy efficiency, robust, predictable and adjustable behavior along with flexibility regarding potential system scale-up or application on similar existing and under development systems. The impact of process control (CSS, 2011) can be viewed from two different perspectives, the technical that prevails from the process design phase to the commissioning of a process, and the performance which is activated when the process is in its working phase. Once the basic control infrastructure is in place, advanced process control is one of the technologies most often used for improving the overall performance and behavior of the process. Once the process is constructed and delivered for operation, process control provides the means for maximizing efficiency and product quality.

Conventional control algorithms such as on-off, proportional integral derivative (PID) and heuristic controllers are considered for some processes inadequate solutions to optimally fulfill the operating objectives of these systems. On the other hand, advanced

control methodologies are applied to an even wider range of processes and applications as over the past few years there were significant improvements to the control theory and the computational requirements of such methodologies. Fig. 1.12 presents a comparative analysis related to the frequency that various advanced process control approaches are used (Bauer and Craig, 2008).

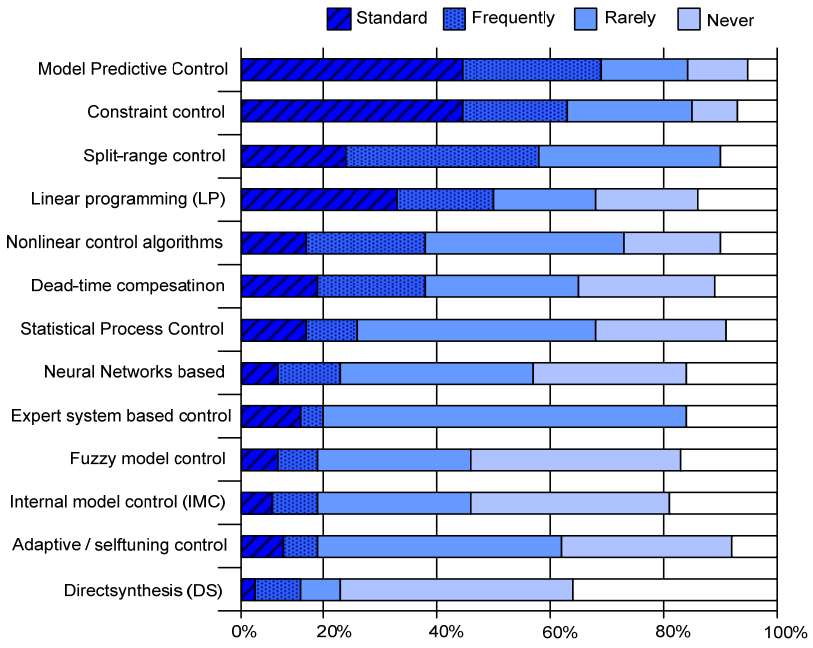

Figure 1.12 Industrial Use of Advanced Process Control

One of the factors that contribute to the success of advanced control technologies is the ability to model and optimize (online or offline) the process and then build appropriate strategies around this optimized model. Historically the process industries have been a major beneficiary of advanced control solutions. Auto tuning of PID loops, model predictive control (MPC), and real-time optimization have all had a substantial impact on the cost, efficiency and safety of the various process operations (CSS, 2011). But nowadays the implementation of MPC is expanding from the chemical and refining plants to industrial energy and power generation utilities.

1.3.1 Model Predictive Control (MPC)

Model predictive control (MPC) also known as receding horizon control (RHC), is becoming a preferred control strategy for a large number of industrial processes (Bauer and Craig, 2008). The main reasons for the increased popularity include the ability to explicitly handle constraints and dynamics of the system. Moreover, the use of MPC can simultaneously consider economic and operating objectives based on an optimizing strategy. More specifically, the MPC approach has the following capabilities and features:

- Model-based engineering approach that considers process dynamics and accelerates the development of accurate single variable or multi variable controllers.
- Handling of input and output plant constraints based on specific process variables.
- Consider the complex interactions between different subsystems of a process including various variables.
- Integrating of powerful and robust optimization algorithms for the decision making process related to the manipulated variables, able to set priorities and weights for every objective.
- Disturbance rejection due to the predictive nature of the controllers that compensate processes variations.

In general MPC refers to a methodology which makes explicit use of a process model to optimize the future predicted behavior of a process (Qin and Badgwell, 2003). The main objective is to obtain control actions that minimize a cost function related to selected objectives or performance indices of the system (Fig. 1.13).

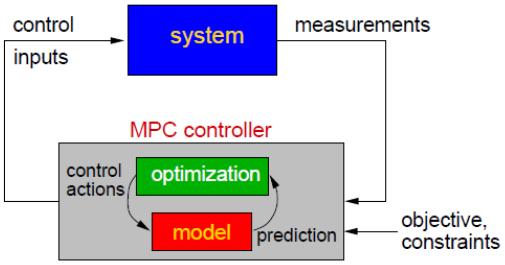

Figure 1.13 Model Predictive Control concept

At each sampling time an optimal control problem is solved using measurements acquired from the system and it yields the appropriate control inputs for the system (Allgöwer *et al.*, 2004). MPC is very flexible regarding its implementation and can be deployed and adjusted to a wide range of systems since its development is based on a model of the system.

During the past decades, model predictive control (MPC) has become a preferred control strategy for an increasing number of processes and integrated systems. For example in the petrochemical industry MPC is often combined with online optimization of the set-points on the basis of large, rigorous nonlinear stationary plant models (Biegler *et al.*, 2002). Nevertheless, despite its well-known acceptance both in a theoretical and industrial level, the various categories of MPC are still subject to in-depth analysis and evaluation. Especially, nonlinear MPC is currently in a top position in the evolving area of advanced control as its use can lead to more accurate results, increased robustness and flexibility in hardware development, compared to the linear case of MPC and other conventional approaches. In this thesis MPC will be used as the selected method of APC that will be deployed to the PEM fuel cell unit under consideration.

1.3.2 Overview of the development procedure

Although the selection of the control strategy is very important, it constitutes only one of the various steps that are necessary to achieve the desired outcome, which is a fully functional system for a specific process. These steps constitute a generic development procedure (Fig. 1.14) and they are categorized into two main sets of actions related to:

- Research and development
- System engineering

The first set is developed using a top-down approach while the later a bottom-up approach. Initially the objective is to specify a well determined set of requirements and specifications that will be used throughout the entire procedure. Also, it is important to select the appropriate topology and tools as by their integration the system structure will result. Finally, a decisive element to the success of the whole procedure is the automation and control system, since it constitutes the interface between the process and the rest of

the world. Fig. 1.14 illustrates a procedure where an APC methodology is present and more specifically MPC. This procedure involves the development of a model of the process and a simulation study that explores the response of the developed model prior to the development of the MPC controller which is based on the dynamic model.

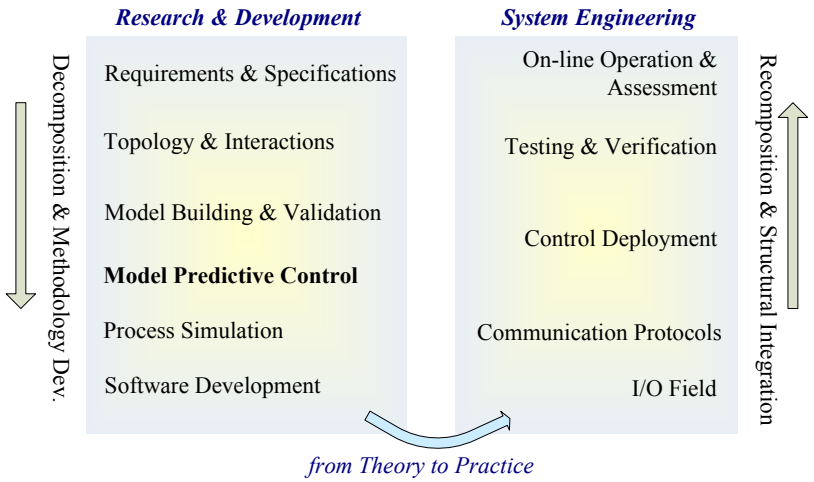

Figure 1.14 Development Procedure

More specifically, the actions that are involved during the analysis and design of the control system are:

- Determine the requirements and the boundaries of the system derived by the process operating specifications.
- Select appropriate topology where the various components will be placed and also define the interactions between the components and the subsystem of the process.
- Build a dynamic mathematical model of the process and validate its behavior against either experimental data supplied by the manufacturer or from the literature.
- Analyze and design the control architecture based on the requirements and the control objectives of the process. When feasible use rapid prototyping tools to speed up the procedure.
- Simulate the behavior and response of the process.
- Develop the software that will be used by the automation system in order to deploy the selected advanced controller to the process.

Besides the definition of the boundaries and structure of the system, the outcome of these actions is a software platform able to communicate with the rest of the system according to the predefined specifications of the process operation. After these actions the rest of the procedure involves a number of steps which are necessary to develop and implement the selected topology and control structure:

- Setup the I/O field by connecting the sensors and actuators of the process to the selected data acquisition system and configure the equipment in order to communicate using the appropriate industrial protocols.
- Deploy the control infrastructure to the process and the software installation provided by the automation system's vendors.
- Perform a set of tests to verify the control structure, including the signal tracing.
- Commission the process for nominal operation.
- Assess the behavior of the process after an initial period of operation and tune the control loops if necessary.

The fine tuning of the control system is of high importance since the overall response of the process depends on it. In the aforementioned procedure a number of challenges like computational issues, uncertainties and communication problems are of major concern that are confronted during software and hardware implementation. The ultimate aim is to select, according to needs of the system, a flexible, expandable, efficient and well defined control structure.

In this thesis this development procedure was used in order to parameterize and extend the control and automation infrastructure, including the mathematical model of the process under consideration as well as integrating to the system the advanced model-based controllers which are applied to a small scale fully-automated PEM fuel cell unit.

1.4 Research objectives and Thesis Scope

The main research objective of this thesis is to address a number of issues related to the advanced control and optimization of a PEM fuel cell system. More specifically the objectives are:

- Develop a fuel cell mathematical model to accurately capture the behavior of the system.
- Develop new algorithms to improve the performance of a typical NMPC formulation by exploiting features of the dynamic optimization problem.
- Design and implement an integrated industrial automation system able to incorporate advanced model predictive controllers.
- Demonstrate the applicability and efficiency of the newly developed algorithm and tools in the operation of a real experimental PEM fuel cell unit.
- Monitor and evaluate the system's performance at real time.

In order to achieve these objectives various interdisciplinary actions are necessary, related to the analysis, design and development of a fuel cell system along with advanced model-based control techniques. Furthermore, emphasis is placed on the structure of the optimization problem which is solved online at each time interval. The latter objective is realized though the development of a framework with the following features:

- Fast calculation of the optimal control action while taking into account the physical and operating constraints.
- Flexibility to adapt to changing fuel cell response under the influence of disturbances or during start-up and shutdown.
- Incorporation of a multitude of performance criteria under strict computational time demands.
- Easily deployable and maintainable control and optimization solutions.

The scope of this thesis is an interdisciplinary one involving:

- the model predictive control (MPC) framework,
- the fuel cell system and its subsystems,
- the industrial automation system and the respective I/O field.

1.5 Thesis Outline

The work in this thesis is organized into three interrelated parts. The first part (Chapters 1-2) is concerned with the system engineering of the PEM fuel cell, whereas the second part (Chapters 3-5) includes the design and development of the mathematical model of the system and its control. Finally the third part (Chapter 6) focuses on the implementation and testing of the developed control framework in a Fuel Cell System.

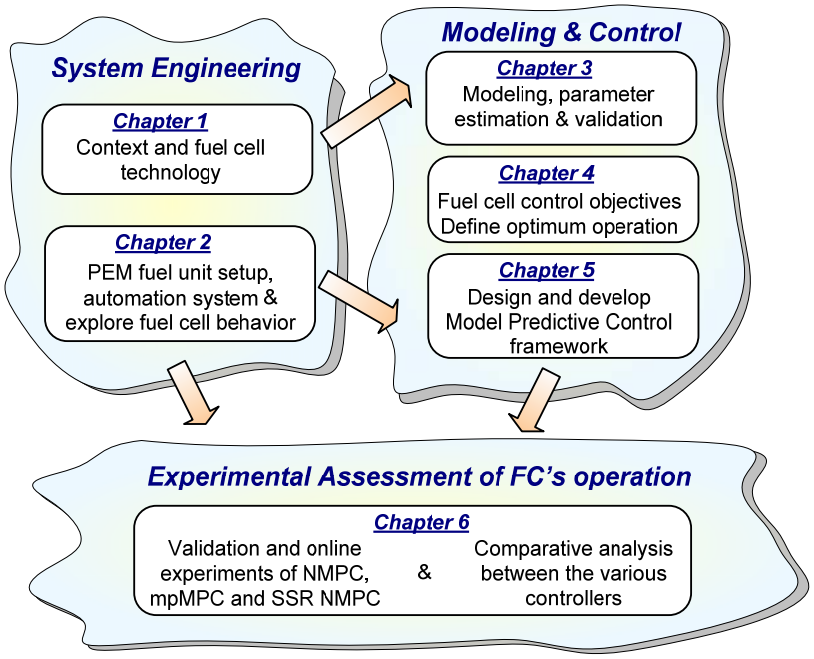

Figure 1.15 Thesis outline

More specifically:

- A detailed analysis of the PEM fuel cell unit which is used throughout this work is presented in Chapter 2. Furthermore, the automation infrastructure and the basis of the Supervisory Control and Data Acquisition (SCADA) system is also demonstrated as the basic platform for the verification of a number of advanced model-based controllers. Finally Chapter 2 presents the results of the stabilization and activation procedure that was applied to the PEM fuel cell and finally explores the behavior of the fuel cell at open loops at various conditions in order to test its operation.

- Chapter 3 presents a mathematical nonlinear dynamic model for the PEM fuel cell system involving a number of differential and algebraic equations. In this model a number of empirical parameters are used and are estimated using a formal parameter estimation method which is based on experiments performed specifically for this purpose. After the determination of the optimal values for these parameters, a number of validation tests were performed in order to experimentally validate the response of the model at various operating conditions.
- Chapter 4 specifies the control objectives of the PEM fuel cell that will be used in the design of the various controllers developed in subsequent chapters. Also, an experimental analysis is performed in order to define the behavior of the system with respect to key objectives involving the determination of the optimum region of operation for the minimization of the supplied fuel and oxidant.
- Chapter 5 presents a thorough analysis of two well established model-based predictive control methods, the multi-parametric MPC (mpMPC) and the Nonlinear MPC (NMPC). Moreover, a simultaneous direct transcription dynamic optimization method that recasts the multivariable control problem into a nonlinear programming problem (NLP) using a warm-start initialization method is analyzed. The chapter concludes with the analysis and algorithmic development of a newly developed integrated control framework that empowers the performance of the NMPC, using a Search Space Reduction (SSR) technique, with the aid of multi-parametric Quadratic Programming (mpQP) method.
- Chapter 6 discusses the deployment of the multivariable controllers to the fuel cell system and explores the response of the PEM fuel cell with respect to the control objectives introduced at Chapter 4. A number of experiments were performed revealing the potential and the performance of each control method and the overall framework is assessed. Chapter 6 is complemented by an analysis that focuses on the impact of the newly developed control method in both simulation and experimental level. Furthermore, the behavior of the fuel cell unit is investigated through a comparative analysis between various control configurations.
- Finally, Chapter 7 outlines the results of this thesis, summarizes its contribution and draws up suggestions for future developments.

Chapter 2

PEM Fuel Cell Unit

The scope of Chapter 2 is to present the overall design of the system and to specify the operation requirements and the technical features that are necessary for the implementation of an integrated supervisory control framework for a small scale automated PEM fuel cell unit. Furthermore, the structure of the automation system with its control topology is outlined and the architecture of the software that was utilized is presented. Finally the procedure for activation of the single PEM fuel cell is described, including a number of experimental tests that explore the behavior of the system. Overall Chapter 2 provides the basis of the subsequent work of the thesis as this experimental unit serves as the real-life application platform of the various control developments. The objectives of Chapter 2 are summarized as follows:

- Definition of the requirements of the process subsystems (heat up, water management, power) and the equipment that were used (sensors, acquisition modules, supervisory system).
- Definition of the synergies among the unit's subsystems.
- Derivation of a suitable architecture and a set of technical specifications of all components for the integrated system.
- Development of the automation system and its user interface.
- Exploration of the behavior of the selected PEM fuel cell under various operating conditions.

2.1 Requirements and specifications

The main features of a PEM fuel cell is its fast response, the low operating temperature, high efficiency and low corrosion (Stefanopoulou and Suh, 2007). Overall the operation of a fuel cell is a multidisciplinary one, since various phenomena occur related to electrochemical reactions, mass and heat transfer. Therefore, it is necessary to design and develop a control system able to handle a number of issues related to power management, in the context of a safe operation which is achieved by proper fuel/air delivery and temperature control. Moreover, the need for a flexible system that can modify the operating conditions is regarded as an important component of the Balance of Plant (BOP) for an integrated fuel cell system (Bavarian *et al.*, 2010). The development of an automated unit is realized through a decision making procedure that begins with the following basic steps:

- Definition of the system's boundaries.
- Determination of the unit's requirements.
- Determination of the automation system's specifications.

The information which is gathered through these steps direct the selection of the topology and architecture of the unit based on which the system is built. In the case of the PEM fuel cell unit and its automation system the main requirements are:

- Ability to test various fuel cells and stacks.
- Modular and scalable architecture (e.g. bypass of hydrators).
- Modifiable operating conditions related to temperature, humidity and pressure.
- Consistent startup and safe shutdown procedures.
- Supervisory monitoring and data archiving capabilities.
- Flexible automation framework able to incorporate different model-based control schemes.

Considering these requirements a small scale fully automated plant is designed and constructed at the laboratory of Process Systems Design and Implementation (PSDI) at CPERI/CERTH. The unit is able to measure all the necessary input signals, control the appropriate variables and adjust several system parameters. A dedicated hardware for the

data acquisition and system control of the unit is configured and successfully integrated with the unit's components. This chapter aims to give an overview of the experimental unit and provide information about the selected design and the implemented choices of the automation system.

2.2 Experimental setup of the unit

Overall there are five distinct subsystems, the power, the gas supply, the temperature, the pressure and the water management subsystem. However, each subsystem interacts with the others although it has its own control objective (Vahidi *et al.*, 2006). An integrated fuel cell system is equipped with various electrochemical and electronic components which are combined to form an integrated unit. Fig. 2.1 illustrates the simplified process and instrumentation diagram (P&ID) of the unit.

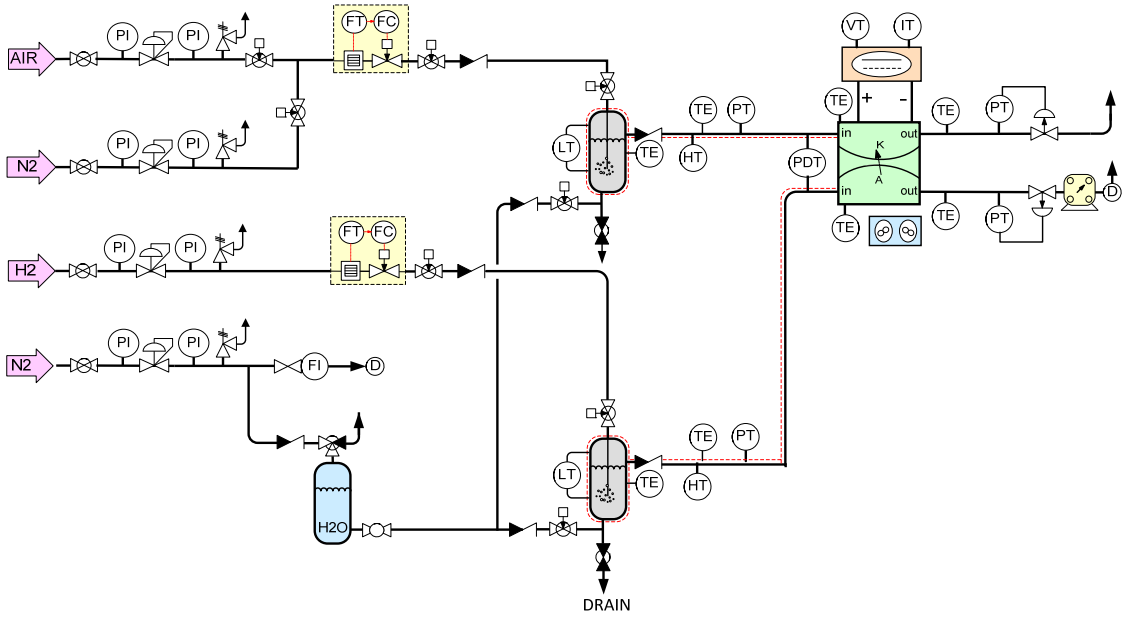

Figure 2.1 Simplified Process and Instrumentation Diagram of the PEMFC Unit

A brief description of the unit's subsystems with their main features and equipment, along with the main specifications of the PEM fuel cell that is used is presented.

2.2.1 Fuel cell specifications

In this thesis a single PEM fuel cell was used. The components were purchased by Electrochem Inc., whereas the assembly was made at CPERI. At Table 2.1 the detailed physical specifications of the fuel cell are presented.

Table 2.1 PEM Fuel cell physical parameters

Description	Value
Nominal Cell Voltage	0.6 +/- 0.05 V
Nominal Current Density	400 +/- 50 mA/cm^2
Operating temperature	60-75 °C
Total mass	1.378 kg
Specific heat capacity	772.57 J/kg·K
Active area	25 cm^2 (5cm x 5cm)
Channel Volume (anode,cathode)	$0.136 \cdot 10^{-4}$ m^3
Membrane type	Nafion 1135
Membrane thickness	0.0035in (89 microns)
Backing layer catalyst loading	20wt.% Pt/C
GDL type	Carbon paper
GDL thickness	0.019mm
Bulk density	0.44 g/cm^3
Porosity	78%
Heater resistance	0.867kΩ (55.8 W)

The core component of the fuel cell is the membrane electrode assembly (MEA) that consists of the electrolyte membrane, anode and cathode catalysts, and the gas diffusion layers. The catalyst layer is made of carbon supported platinum loading. The (MEA) is placed between two current collectors and then between two non-porous graphite current collectors plates. A graphite separator plate is attached on each side of the electrodes of the fuel cell. These plates act as conductors and are gas impermeable. They distribute the flow of the reactant gas or liquid across the electrode covered by the flow field, making

sure that the maximum amount of the gas and liquid comes in contact with the electrode. The unit cell contains a parallel serpentine flow channels for gas delivery to both the cathode and anode of the cell. The channel width is 1.25mm and the depth is 1.72mm. Figs. 2.2 and 2.3 illustrate the graphite plate and the basic configuration of the fuel cell.

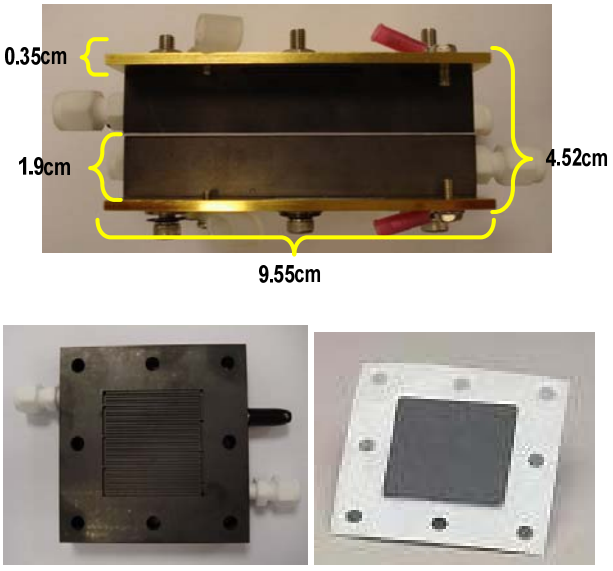

Figure 2.2 Flow plate, MEA and FC side view

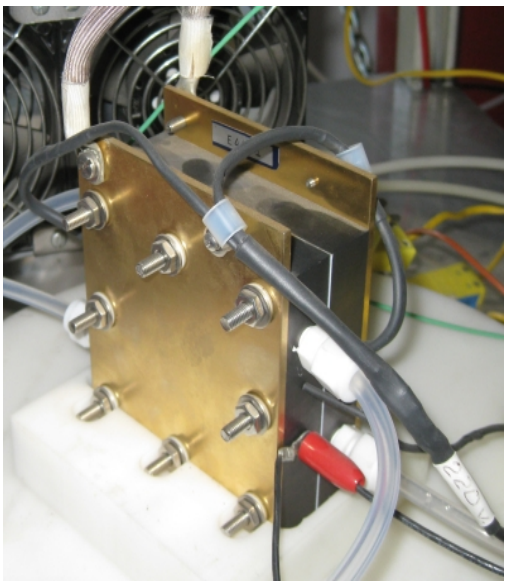

Figure 2.3 Single PEM FC connected to the unit

2.2.2 Power management

The integrated system is equipped with an electronic load from KIKUSUI (PLZ1004W) which simulates the power demands or the power fluctuations that occur in real systems where fuel cells are used for power generation. The electronic load has programmable characteristics that can be modified or adjusted according to the output load requirements. It operates in four different modes:

- Constant Current (CC) mode: In this mode the load current is constant even though the voltage at the terminals of the load changes.
- Constant Voltage (CV) Mode: In this mode the load voltage is constant even though the current into the load changes.
- Constant Resistance (CR) mode: The load behaves like a constant resistance.

- Constant Power (CP) mode: The load power is kept constant.

The activation procedure is performed using the CV mode to avoid any damages to the MEA and to determine the current span the experiments for model validation were conducted in CC mode. After the determination of the maximum allowable current and since the activation stabilized the underlying system, the electronic load is operated in CC mode. In an application where a DC/DC converter is connected to the fuel cell, the converter requires a constant current. However, other applications might demand for variable voltage and current. Finally, a sequence of small current steps can be implemented with appropriate programming for the load in order to measure the dynamic response of the fuel cell.

2.2.3 Gas supply subsystem

The gas supply subsystem has two main lines, one for the hydrogen and one for the air or oxygen supply. A third auxiliary line for nitrogen supply is also present which is used for purging of the anode and the cathode of the fuel cell as gas sections must be flushed with nitrogen before opening. In each line a thermal mass flow controllers (MFCs) is used that consist of two separate items. The first is a flow meter while the second is a flow control valve based on a built-in controller. Prior to the MFC the pressure of the gas is adjusted through a manual pressure reducing regulator.

Hydrogen and air are sent through a heated humidifier before being fed to the anode and the cathode side respectively. At the end of each line, just before the vent, there is an outlet pressure control valve which is used for conducting experiments at elevated pressure conditions. The pressure loops are controlled by the automation system. Fig. 2.4 illustrates the front panel of the unit where the three lines are shown along with the respective hand valves and manometers before and after the inlet pressure regulator. Fig. 2.5 illustrates the back view of the panel. The MFC's of each line are shown along with the respective check valves and piping.

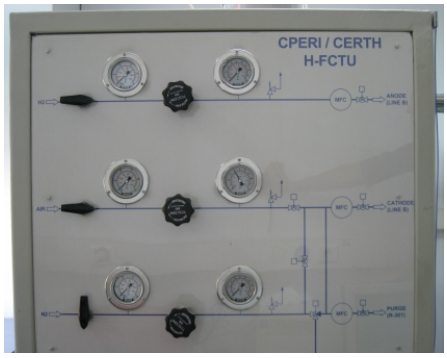

Figure 2.4 Front panel of the unit

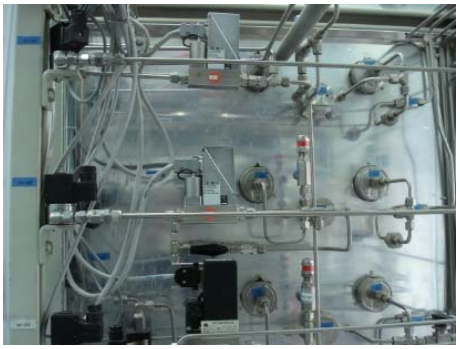

Figure 2.5 Back panel of the unit (MFCs)

Figure 2.6 Hydrators at the anode's line

Figure 2.7 Pressure control valves

2.2.4 Water management

The water management subsystem maintains the hydration of the fuel cell membrane. Humidification of the feed streams is necessary to maintain conductivity of the electrolyte membrane. The unit was designed to be able to adjust the humidity of the inlet gasses which are supplied in dry form by the pressurized cylinders. For this purpose one hydrator per line is used that employs a heated vessel with deionized water which is placed after the mass flow controller in each gas line. This vessel is equipped with a level indicator and when the water drops below a predetermined level a solenoid valve opens and water from a water tank is filled up to the nominal point. The humidity can be

adjusted independently through respective temperature control loops. Fig. 2.6 shows the hydrator which is placed at the anode's line.

The two hydrators maintain proper humidity conditions inside the cell, which is crucial to ensure the optimal operation of the membrane. To prevent water from condensing in the line between the hydrators and the FC, a heated line was used to maintain the line temperature. The heating of the humidifiers and the lines is accomplished using a heating tape. This subsystem can be bypassed in case we want to perform experiments without humidified gases.

2.2.5 Fuel cell thermal management

The temperature management is based on a fan assisted air cooling and an electrical heat up subsystems that allow to either heat the fuel cell to its operating temperature or maintain a temperature under reduced load conditions. The operation range is between 45°C and 75°C. The thermal management subsystem is active through the entire operation of the unit, during startup, shutdown and at nominal operation. During startup the fuel cell is heated in order for the temperature to reach at least 45°C, whereas at shutdown it is cooled down to avoid unnecessary heat stress to the membrane. When the fuel cell operates at nominal temperature levels the heat-up and cooling subsystems are used interchangeably depending on the load conditions. The process specifications are summarized in Table 2.2

Table 2.2 Process specifications

	Range
Hydrogen Feed (gas)	Flow Range : 0..2500 cc/min
Nitrogen Feed	Flow Range : 0..2500 cc/min
Air Feed	Flow Range : 0..4000 cc/min
Water quality (Resistivity)	~2MΩ/cm
Hydrators and Heated Line Temperature	0..120°C
Operating Pressure	0..3 bar

The various components of each individual subsystem were assembled at CPERI/CERTH and as a result a small-scale rig that houses all of them was developed. Next to the unit rig the electrical cabinet or interface box (IBX) was constructed and inside this cabinet the automation system was placed which gives life to the unit from the electrical point of view.

The IBX accepts power supply from the building which is converted to appropriate form (e.g. from 220V to 12V) and distributes it to various components. The role of the IBX is to establish a bidirectional connection between the unit and control station, which is a computer based system. The IBX accepts various types of process signals, converts them to digital signals and transmits them through the data acquisition system and vice versa (Fig. 2.8).

Figure 2.8 I/O terminals and concentration couplers

As the scope of this thesis is to explore and optimally control the unit, the focus is towards the automation system and its operations. Thus, the electrical cabinet and its design are not analyzed although it is an essential communication intermediate between the process and the control station.

2.3 Automation System

Although each subsystem has its own control objective, they also interact with each other. Therefore, the exploration of the PEM fuel cell's behavior is realized through the measurement of a variety of variables that reveal the status of each subsystem. Also, it is important to be able to adjust the operating environment on-demand through respective actuators. Thus, actuators at specific points of the unit are placed that apply the corresponding action based on the desired set of operation. Overall, the variables related to sensors and actuators constitute the unit's Input/Output (I/O) field and their respective signals must be properly acquired by the automation system of the unit which is selected for the specific application, a fuel cell testing unit.

2.3.1 Supervisory Control and Data Acquisition (SCADA)

Based on the aforementioned requirements the online monitoring of the unit and the flexible control structure is a prerequisite that the automation system must fulfill. This objective is accomplished by the use of an industrial Supervisory Control and Data Acquisition (SCADA) system. Although there are various alternatives for the selection of the automation system, such as simple data acquisition systems or PLCs, the most appropriate solution that can accomplish the requirements of this thesis, is a SCADA system. This choice was made based on the SCADA's features in conjunction with the operation objectives of the fuel cell unit. The main features that made this type of system attractive for this thesis are:

- Open architecture able to incorporate a wide range of process equipment
- Ability to send data to information systems for archiving purposes
- Communicate with heterogeneous software platforms based on OPC protocol
- Supervisory functions that support rapid software prototyping

Apart from these interesting features the selected type of system is implemented on a computer-based architecture which means that the software platform is installed, developed and parameterized on a PC. The use of a computer-based system has many advantages as it allows the use of a common place for software development including

I/O drivers and programming platforms such as Matlab, gPROMS or simple programming languages such as Fortran. Particular emphasis was placed on being able to integrate advanced process controllers.

In general a SCADA system is a process control platform that collects data from sensors or other devices on a plant level or in remote locations. The data is then sent to a central computer for management and process control. SCADA systems provide data collection features and allow manipulation of output variables through the respective software for monitoring and reporting. A typical characteristic of SCADA systems is its flexible, dynamic and often centralized architecture, which makes possible their interoperability with other systems. There are two basic parts in a SCADA system, the client part, which handles the human machine interaction and the data server part which handles most of the process control activities. The data server communicates with the devices at the I/O field through dedicated input/output measurement systems.

From the software point of view, the development of a SCADA system involves a multitude of different programs that are executed upon request or continuously when the SCADA system is enabled. The programs that are used in order to result to a fully functional automation system are related to:

- System configuration: the environment of the project is setup, including unit name, I/O drivers that will be used, enabling of appropriate network protocols.
- I/O drivers: the link with the various drivers (such as OPC servers) is established and the required I/O points are configured. This is the place where the MPC controllers are linked with the SCADA system.
- Process database: define the process variable with respect to the data from the I/O drivers and determine their characteristics such as range of measured values, sampling time, alarm levels, addressing and signaling options.
- Monitoring interface: design a graphical interface that represents the simplified P&ID of the unit with respect to the measured variables. Also, a full featured menu that includes the necessary subinterfaces for the control of the unit is developed.
- Historical data archiving: determine which of the variables from the PDB are important to be archived and at what sampling rate.

This list clearly indicates that the development procedure demands a multitude of actions involving various software programs that are collaborating to form the final SCADA system. The automation system of the developed unit is based on the industrial platform Proficy iFIX from General Electric. All system components (pumps, heaters, valves and so forth) are controlled through a computer based system by digital commands and pre-programmed procedures. The various temperatures and pressures are maintained at the desired set points by the SCADA system, via decentralized PID controllers, allowing for independent gas conditions to the fuel cell. Furthermore, the automation system allows the executions of predetermined operations, offers safety management, alarm handling and performs data archiving.

2.3.2 From the I/O signals to the information flow

As stated earlier the automation system of the unit is based on a SCADA that acquires and monitors the I/O field. In order to implement the interfacing of the various components that comprise the integrated unit, different communication methods and respective protocols are utilized. The path that the I/O signals have to take in order to be converted into data and then into useful information for the SCADA system has two parts. The first starts from the field and ends at the computer of the unit where the signals are transformed into data through the respective network protocol. The second part involves the transformation of the data into a homogenous format for the SCADA system using a common standard regardless of the physical or network protocol.

Signals to data

Initially the signals from the unit's I/O field are collected using terminals from Beckhoff according to their type, e.g. 4-20mA, 0-10V, etc. These signals are handled by the bus terminals which are organized into acquisition couplers that form a distributed bus type network that connects the I/O field to the SCADA system. A bus terminal is the interface between a fieldbus system and the sensor / actuator level. For each signal type, a respective terminal is available with I/O channels. All the terminal types have the same mechanical construction, so that difficulties of planning and design are minimized.

The industrial protocol that was selected for the implementation of this connectivity is Profibus which is a manufacturer - independent, open fieldbus standard with a wide range of applications in manufacturing and process automation. It allows devices from different manufacturers to communicate without the need for specially adapted interfaces and it is suitable both for fast, time-critical applications and for complex communication tasks. The unit's programmable electronic load communicates through a serial interface (RS232). A driver for this communication was also developed during this thesis.

Measurement accuracy

The operating decisions for each subsystem are based on the data acquired by the I/O field. Thus, it is important to rely on precise measurements in order to be able to make the optimal decisions for the operation of the unit. The variables acquired from the field are related to pressure, temperature, air flow, hydrogen flow, power, current and voltage. The transmission of the analog measurement signals is made through the input terminals to the automation system. The sensor signals are wired to the I/O terminals which are connected in a centralized way to the bus coupler. These I/O terminals transform the sensor signals with a 12bit resolution into digital data which are subsequently processed by the SCADA system. The measurement error is less than ±0.3% of the full range scale and each input signal is represented by 16 bits. The polling time of each measurement is set to 500ms.

Data to OPC format

The second part of the data path is necessary for the creation of a homogeneous format for all data based on a common standard. Since the SCADA system is structured upon an open architecture, the appropriate format for the data is selected to be the OPC standard. By this formation a uniform standard of communication is adopted at the application layer which is independent of the physical medium used for the data transmission.

In general OPC is an open standard specification that refers to open connectivity via open standards and it is the interoperability standard for industrial automation and

other related domains. This standard specifies the communication of real-time plant data between control devices from different manufacturers. It is not just a typical application level communication protocol but a collection of a standard set of objects, interfaces and methods which are used in process control and automation systems to facilitate interoperability. The vision of interoperability in multi vendor systems has become a reality, via the OPC standards. OPC servers provide a method for many different software packages of software platforms to access and send data to process devices, such as PLCs and data acquisition systems. The purpose of the OPC is to define a common interface that is developed once and then it can be connected by any OPC-enabled software.

The considered SCADA requires two OPC servers for I/O field data, one for the data originating from the Profibus network and one for the data acquired from the serial interface. Also, a number of OPC servers will be attached to the system in order to enable the communication with the model-based controllers that are developed at Chapter 6. The utilization of such architecture creates a uniform centralized environment for the SCADA system.

OPC data and process database

The role of the process database (PDB) with respect to the information flow, is to send and receive I/O values from the Driver Image Table (DIT), which is the place where the OPC client places the process values collected from the lower level OPC servers. The value of each I/O point is compared against alarm levels and there is an initial check of validity. On this level the SCADA system handles the process values according to user instructions or a predefined control strategy. The various functions involving the PDB and the DIT are performed by a dedicated system program which is responsible for the scan, the alarm and the control (SAC) of the process data. Some of the most important functions are:

- Data retrieval from the various I/O sources through the DIT.
- Translation of the data into the format expected by the PDB.
- Cross-checking whether the values of the data against the alarm limits.

- Generation of alarm messages.
- Execution of the control logic.
- Updating the database.

Once the data reach the SCADA system they are organized in the PDB and each I/O signal is assigned to a record named tag. Each tag can be sampled at different rate which is selected according to the nature of the measured input. The values at the PDB are updated based on the scan period setting, although the data from the I/O field can be acquired at smaller intervals, depending on the communication protocol and the driver (polling time). The SCADA system enables us to acquire all the available signals (analogue and digital) and to manipulate all system components (heaters, valves and so forth) by D/A commands.

Flow of information and archiving

Overall the control framework used in this thesis, has a number of interacting entities that form a common platform for the monitoring and control of the PEM fuel cell unit. The path of the process measurements from all the devices starts from the sensor signaling and finishes at the archiving system. This information flow, from the I/O field to the end user, is shown in Fig. 2.9. Furthermore Fig. 2.9 illustrates the interconnection of the control system's entities and the I/O field including the conceptual flow of information from the signal acquisition to the final presentation at user level through the development of a graphical interface. Throughout this hierarchically layered infrastructure the raw data are transformed into meaningful information blocks.

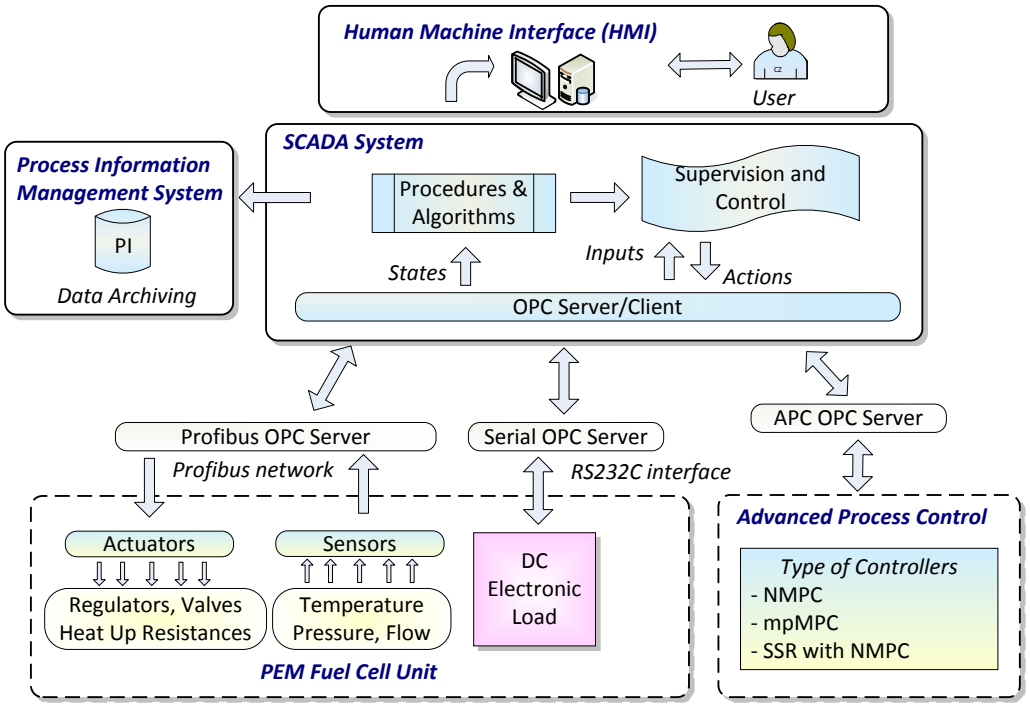

Figure 2.9 Interconnection of the control system and the I/O field

Besides the control and the data acquisition, it is important to be able to monitor the long-term system behavior. A comprehensive way to view the evolution of each experiment and the response of each subsystem is the use of diagrams based on historically acquired data. The SCADA system is able to communicate with other process system or information management system due to its open architecture. In our case a Process Information Management System (PIMS) from OSISoft is used in order to archive the online data of the PEM fuel cell unit through the SCADA. The use of a PIMS increases the visualization of the unit's behavior and enhances the decision making at the supervisory level.

Integration of Advanced process control features to the unit

Although the basic data acquisition and process is performed by the SCADA software platform, the supervisory framework is complemented by custom-made software (Appendix A) related to the advanced controllers and more specifically to model-based

predictive controllers (MPC). The programming environment for this communication software is LabView from NI. This software acts as an intermediate between the optimization solver with the dynamic mathematical model and the automation system with the signals from the I/O field and has the following features:

- Model-based engineering approach that considers process dynamics and accelerates the development of accurate single variable or multi variable controllers.
- Handling of input and output plant constraints based on specific process variables.
- Consideration of the complex interactions between different subsystems of the process based on a multivariable approach.
- Integration of powerful and robust optimization algorithms to the automation system, able to set priorities and weights for every objective.
- Disturbance rejection due to the predictive nature of the controllers that compensate processes variations.
- User friendly environment that provides an interface to the tuning parameters of the MPC algorithm ensuring flexible behavior.

The communication is based on the OPC protocol which is enabled in both software platforms, the SCADA and the custom-made APC software platform. A thorough analysis of its purpose and objectives will be presented in subsequent chapters.

2.3.3 Interactive Monitoring Interface

All the system components (mass flow controllers, heaters, valves, etc) are controlled by digital commands which are initiated by an interactive monitoring interface which is connected with the server part of the SCADA. This monitoring interface constitutes the client part of the SCADA and it is responsible for presenting process data to the user by interacting with the database system of the server part and it is often referred as the Human Machine Interface (HMI). In a system that works exclusively with sensors, controls, and process hardware, the HMI provides a graphical representation of the overall process. The development of user friendly graphical interfaces enables us to monitor, supervise, apply control actions to the system and be aware of any alarm conditions. This graphic representation is an important feature as it minimizes the

deployment cycle compared to traditional programming of user interfaces. On these interfaces real-time data are presented. A representative screen of the HMI for the monitoring of the fuel cell unit and the control of the various set-points is illustrated in Fig. 2.10.

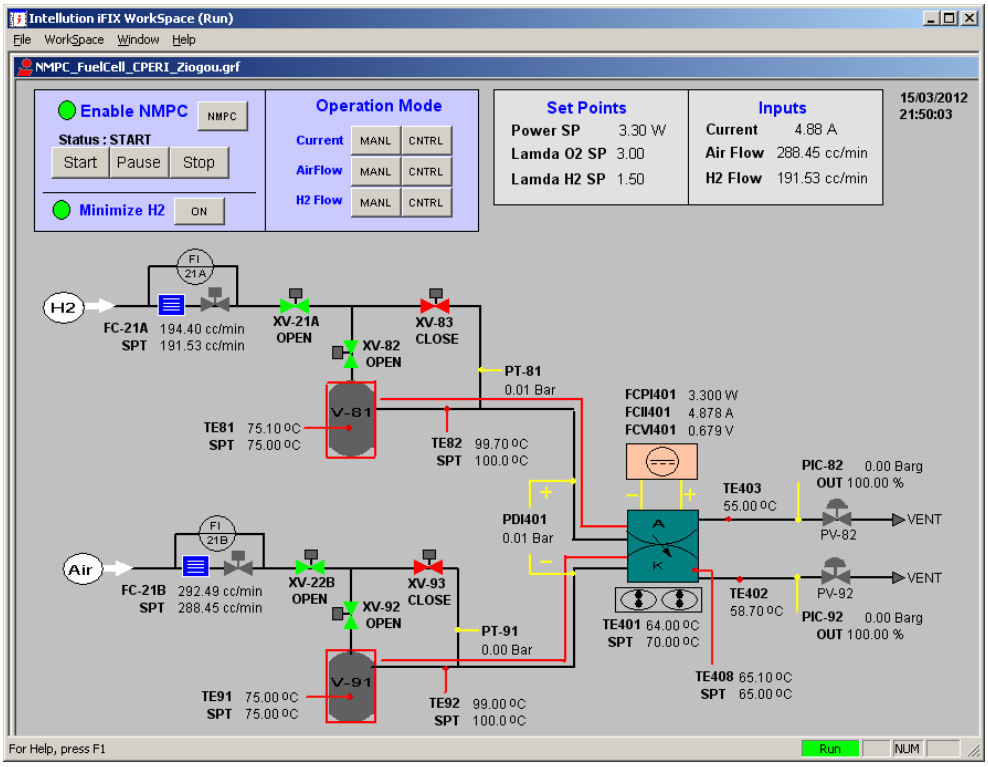

Figure 2.10 Human-machine interface (HMI) for the monitoring of the fuel cell unit

The interface of Fig. 2.10 is a simplified version of the unit's P&ID in a graphical form. Real-time data are shown as graphic shapes over a static background. As the data change in the I/O field during the operation of the fuel cell the corresponding values on the interface are updated, e.g., a valve may be shown as open (green) or closed (red). The HMI includes a number of interfaces which are presented in Appendix A.

One of the requirements for the automation framework is to have the ability to incorporate different model-based control schemes and provide a flexible way to evaluate their response and modify the parameters that are related to the various control

objectives. This requirement is realized through a user friendly interface with the following functions:

- Enable or disable the MPC framework.
- Start, pause or stop the operation of an MPC controller.
- Select the type of the MPC controller.
- Enable or disable auxiliary schemes that enhance the fuel cell operation, such as the minimization of the hydrogen consumption.
- Modify the set-point for each control loop.
- Override a controller by turning to manual the respective control action.
- Overview of the current status of each available function.

Fig. 2.11 illustrates the visualization of these functions which is part of the HMI system that was developed during this thesis.

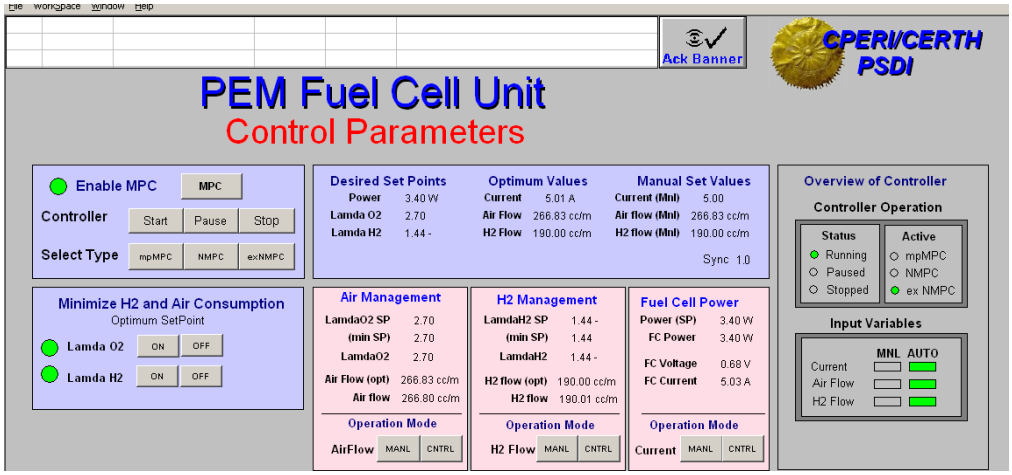

Figure 2.11 Overview of the control parameters

The interfaces that were developed for the fuel cell unit also have navigation and reporting features that enable the supervision of the state of the overall system and the user can select from a central menu screen or navigate from one screen to another.

2.3.4 Input and output variables

A number of sensors measure a variety of signals from the unit along with the respective actuators that control each of the unit's subsystems. A subset of these signals is of interest for the control problem formulation and they are considered as variables at the APC framework which is developed in the subsequent chapters. These signals are categorized into analog input and analog output. The available analog input measurements as shown in Fig. 2.12 are:

- the inlet flows of air and hydrogen ($\dot{m}_{air,in}, \dot{m}_{H2,in}$),
- the temperature of the hydrators ($T_{h,ca}, T_{h,an}$),
- the line temperature, before and after the fuel cell ($T_{ca,in}, T_{an,in}, T_{ca,out}, T_{an,out}$),
- the fuel cell temperature (T_{fc}),
- the inlet and outlet pressure at the anode and cathode ($P_{ca,in}, P_{an,in}, P_{ca,out}, P_{an,out}$),
- the pressure difference between the anode and the cathode (ΔP),
- the DC load which provides the measurement of fuel cell voltage (V_{fc}).

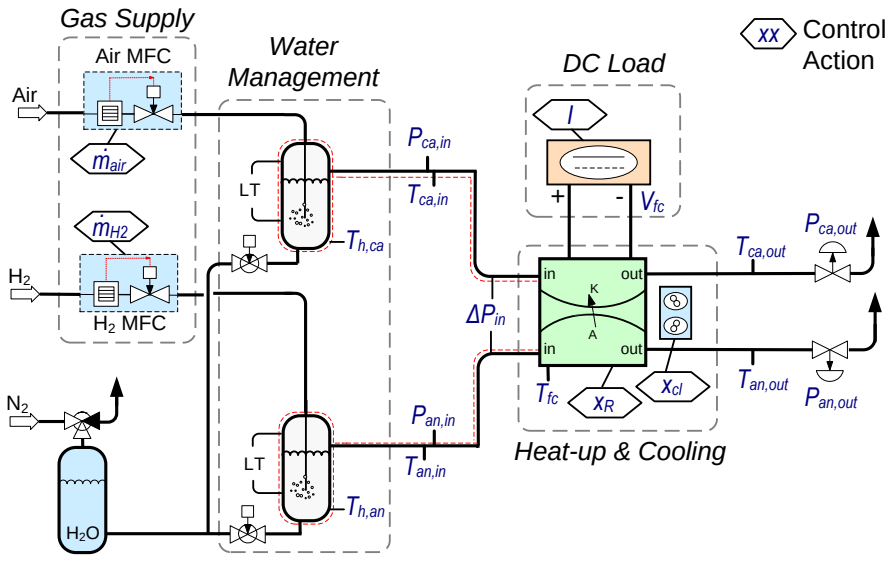

Figure 2.12 Analog input and output variables with respect to the unit flowsheet

Furthermore, a number of analog output signals exist in the unit:

- flow of the gases ($\dot{m}_{air}, \dot{m}_{H2}$),
- heat-up and the cooling percentage (x_{ht}, x_{cl}),
- current (I_{fc}) or the voltage (V_{fc}) applied by the DC electronic load depending on the mode of operation,
- percentage of operation for the temperature of the hydrators and the heated lines ($x_{ht,an}, x_{ht,ca}, x_{\ln,an}, x_{\ln,ca}$).

Finally, there are a number of digital signals (with Boolean state, open/close, high/low) related to the electro-valves of the unit, e.g. there are valves after the MFCs, at the top and at the bottom of the hydrators, valves at the inlet and at the outlet of the fuel cell and indication of the status level of the water at the hydrators (high/low). During the normal operation of the unit these valves do not change therefore they are not considered as variables for the control studies that will be presented in the subsequent chapters.

2.4 Initial behavior of the fuel cell unit

After the setup of the unit and the adjustment of its automation system, an experimental procedure was performed that explores the initial response of the unit and the behavior of the fuel cell. The purpose of this experimental study is twofold. Firstly, the fuel cell unit had to be initially stabilized (temperature and pressure loops) and the MEA of the fuel cell had to be activated. Secondly, the nominal point of operation, as provided by the manufacturer, had to be achieved in order to explore whether the system can reach its expected behavior or not. A performance metric during these experiments is the polarization curve of the fuel cell, cell voltage vs. current density. Another measure of performance is the power density, a product of voltage and current density which is proportional to the efficiency. The higher achievable power density means smaller fuel cell size which directly affects the cost of the system. Although maximum power density is achieved at ~0.5 V, the nominal power density is typically selected at 0.6-0.7 V to get a higher efficiency.

The single cell that was used during this thesis was not conditioned by the manufacturer, therefore after initial stabilization of the unit; the membrane had to be activated. The activation procedure was divided into two stages, the initial activation and the full activation of the membrane. The distinguishing characteristic between these stages was the minimum allowable voltage.

Various experimental studies can be found in the literature exploring the behavior of a PEM fuel cell system. Each study focuses on a different aspect of the fuel cell operation such as step changes in current at various temperatures (Kim and Min, 2008), start-up behavior (Chen and Zhou, 2008), characterization of the electrical behavior (Kunusch *et al.*, 2010), individual cell behavior (Jang and Chiu, 2008; Sun *et al.*, 2009). In the following analysis the performance of the system was tested against various operating conditions, involving different temperature, humidity, pressure and flow rates.

2.4.1 Stabilization phase

The purpose of this stage was to investigate the response of the developed fuel cell unit and to startup the system in a systematic way. Initially the fuel cell was purged with nitrogen. Subsequently, the gases were humidified using the hydrators that were set at low temperature (45°C) while the lines between the hydrators and the fuel cell were set at 80°C. The flow rate of the hydrogen and air was set at 500cc/min and 1000cc/min respectively. The initial load that was applied to the fuel cell by requesting a constant voltage demand at 0.70V and the corresponding current density steadily increased from 0.2 A/cm^2 to 0.23A/cm^2.

The current density was monitored by the respective interface of the SCADA system and when it reached a steady state the load was modified through a preprogrammed procedure. This procedure involves a series of small fixed length step changes in current load with a specific range, which constitute a cycle. The variations of the voltage were applied through a ramp procedure from 1.0V to 0.50V and conversely with a step change of 100mV every 10s. During each step, the 10s interval, the voltage was constant and it was observed that after each cycle the current density increased (Fig. 2.13).

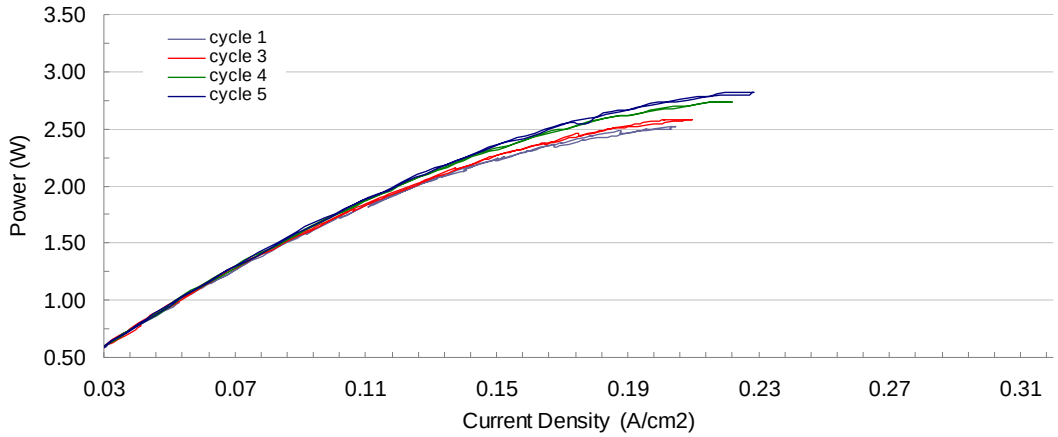

Figure 2.13 Initial fuel cell cycles (without external heating)

The fuel cell temperature was between 35°C and 40°C which indicated that the system should be heated in order to reach the working temperature (at least 50°C). Thus the respective control loops were activated using a PID algorithm controller implemented by the SCADA system. Also, the hydrators were controlled at 5°C higher than the desired temperature and a minor modification was made to the ramp procedure. The minimum voltage was set to 0.45V and a hold period of 4min was inserted when the minimum voltage was reached. Although the line between the hydrators and the inlet of the fuel cell was heated, some water droplets appeared after some time. In order to avoid this phenomenon the line heating temperature was increased by 20°C.

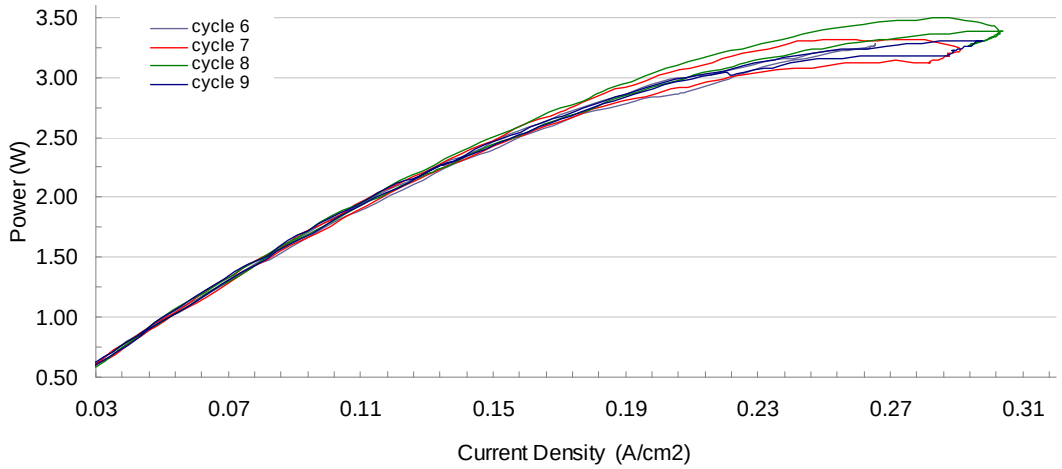

Figure 2.14 Initial cycles (with heat-up at 50°C)

The system performs as it was expected which is illustrated at Fig. 2.14 where it is observed that at the same voltage point (0.45V), the maximum power increases with respect to the current density after each cycle. The next step, before the fuel cell activation stage, involves the test of the pressure control loop. The response of the overall system was investigated at slight overpressure by activating the pressure control loop at 1barg. Initially the system was not able to reach steady state at the elevated pressure because the valves could not control the outlet pressure (Fig. 2.15). Both anode and cathode outlet valves presented oscillatory behavior and the produced power was unstable, due to abrupt controller changes.

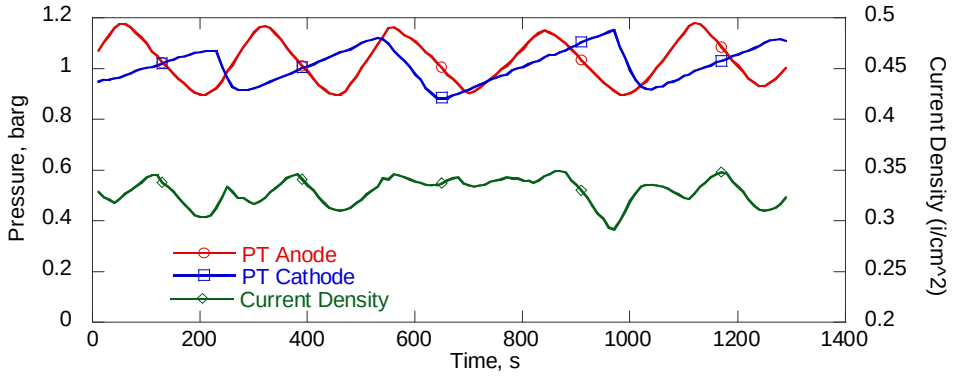

Figure 2.15 Pressure control loop (unstable)

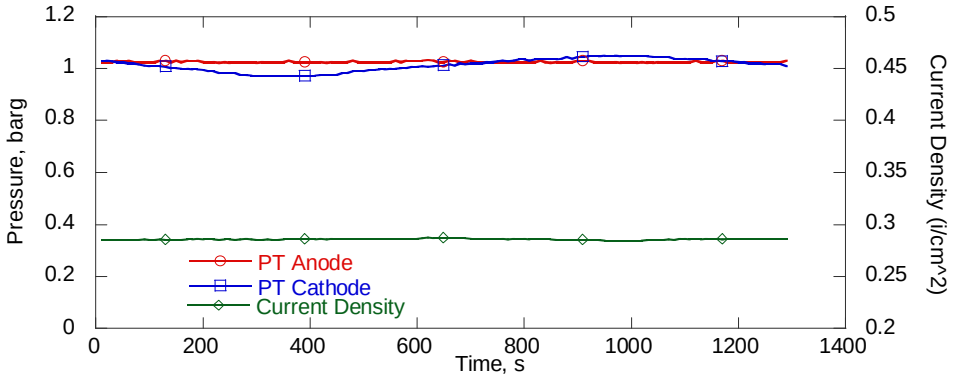

Figure 2.16 Adjusted pressure control loop (stable)

Such behavior was caused because the single cell was operated with low flow rates while the setup of the valves was for larger flows. As a consequence the valves were unable to control the pressure and proper tuning actions were applied. The system stabilization was tested once more at the same conditions (anode and cathode pressure at 1 barg). Also, the overall system was fine-tuned through the properly selected proportional and integral control parameters for the PIDs and as a result the current density and the corresponding produced power were stabilized. This behavior is depicted in Fig. 2.16, where the current density remains stable at constant voltage (0.45V).

The purpose of this stabilization phase was to ensure that the experimental unit was able to provide a stable environment for the activation of the single cell and that it could be used for the overall study. Also, we wanted to be able to monitor the various phenomena that are evolving during the fuel cell testing procedure.

2.4.2 Activation Procedure

Overall the procedure is divided into two stages, the initial and full activation, where different low voltage points were targeted. In both stages the response of the fuel cell is measured after the occurrence of small changes in the voltage demand. During the first stage a reference voltage point was set at 0.45V (V_{ref}) and used as an indicative point of comparison between each cycle in order to measure the evolution of the membrane activation. The nominal point of operation, provided by the manufacturer, was 0.40A/cm^2 at 0.6V and it constitutes an indication that the membrane is ready for use. During the initial activation the voltage demand was regulated through a ramp procedure and gradually decreased from 1.0V to 0.45V and conversely with a step change of 100 mV every 10s. Fig. 2.17 illustrates that the current density was steadily increasing, from line A to line D. However, after a series of cycles it reached a certain point where the response was stable, but compared to the nominal point it could be further improved. Therefore, the full activation procedure was employed by applying the same ramp profile with some modification to the step interval (from 10s to 30s) and to the hold time at the lowest point (from 4 min to 1min).

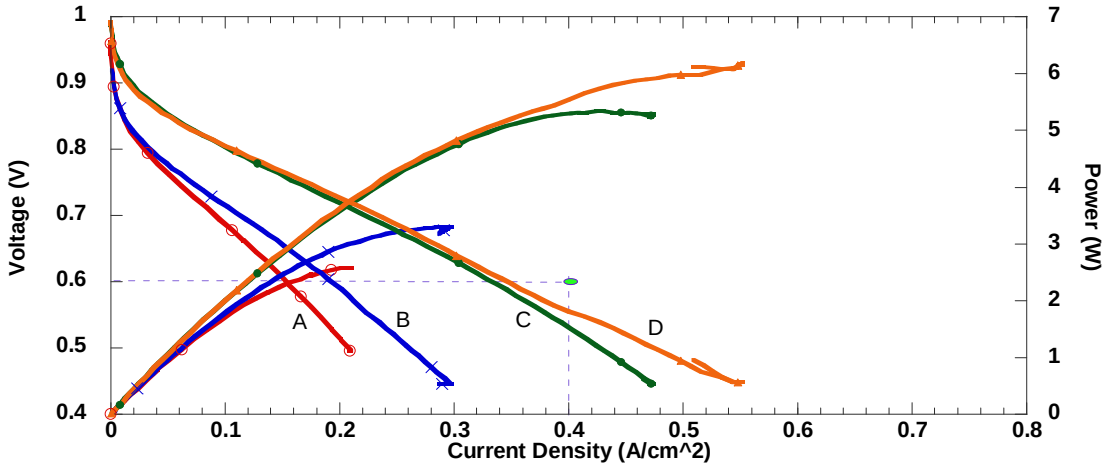

Figure 2.17 Initial activation stage

After each cycle the fuel cell remained under constant voltage (V_{ref} =0.45V) at the same conditions until the voltage is stabilized. The conditions of the activation stage are described in the Table 2.3.

Table 2.3 Operating conditions for full activation

Description	**Value**
Pressure (anode & cathode)	1barg
Temperature : fuel cell	65°C
Temperature : hydrators	70°C
H2/ Air flow rate	2000cc/min / 3000cc/min

Since the membrane was fresh we decided to use rather high hydrogen and oxygen flow rates. The flow rates were deliberately kept very high to avoid any stressful conditions to the system and to avoid voltage drops due to the lack of oxidant concentration. Each cycle uses the abovementioned ramp procedure to gradually decrease the voltage, so initially there were five cycles with a sequentially decreasing minimum voltage of 0.45V, 03V, 02V, 0.1V, 0.0V. Between consecutive cycles the system remained for ~20min at V_{ref} . Table 2.4 presents the evolution of the current density and the respective power. It is

observed that the current density at V_{ref} is increased and is at the nominal point that was initially targeted (0.6 A/cm^2).

Table 2.4 Activation cycles - Evolution of current density and power

	Current Density (start)	Current Density (end)	Power (start)	Power (end)
Before the cycles	0.592 A/cm^2	0. 619 A/cm^2	6.62W	6.90W
Cycle V_{min}: 0.45V	0.606 A/cm^2	0. 631 A/cm^2	6.78W	7.10W
Cycle V_{min}: 0.3V	0.626 A/cm^2	0. 638 A/cm^2	7.00W	7. 17W
Cycle V_{min}: 0.2V	0.615 A/cm^2	0. 645 A/cm^2	6.90W	7.26W
Cycle V_{min}: 0.1V	0.633 A/cm^2	0. 644 A/cm^2	7.10W	7.25W
Cycle V_{min}: 0.0V	0.645 A/cm^2	0. 667 A/cm^2	7.22W	7.49W

Table 2.4 illustrates that after each set of cycles the membrane is further activated, since the current density increases. During these tests the input pressure was slightly increased both in anode (30 to 50 mbar) and cathode (90 to 110 mbar) due to the large flow rates, but as we mentioned earlier these rates were selected only for the initial and full activation of the system. After these series of cycles, the flows are reduced to normal rates and the pressure loop was deactivated.

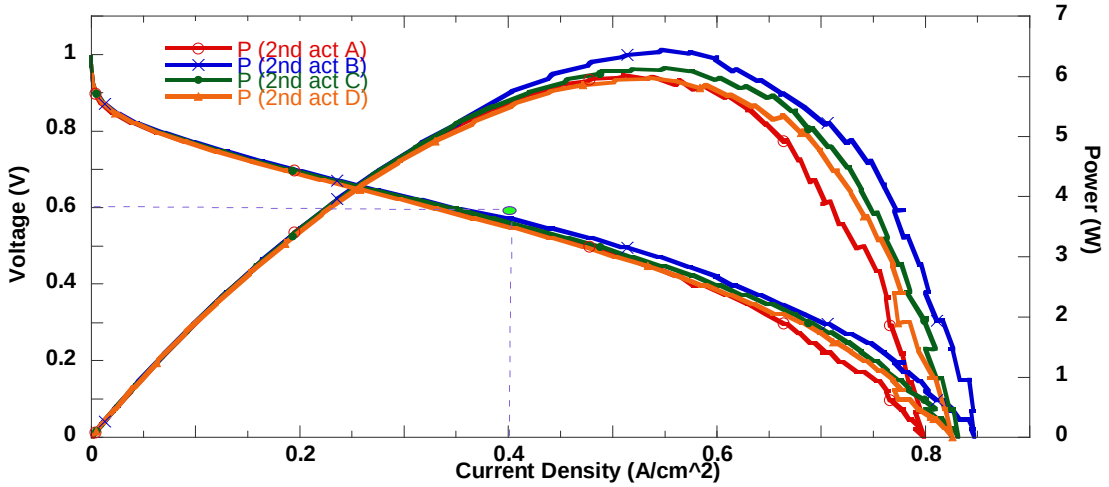

Figure 2.18 Full activation stage

Fig. 2.18 illustrates that the current density was very close to the nominal one and after a series of cycles at the same conditions the membrane presented a repeatable and stable behavior, which was a clear indication that the membrane was fully activated.

2.4.3 Response of the System under Different Operating Conditions

A detailed experimental study was performed in order to investigate the behavior of the system under different operating conditions to obtain a better understanding of the developed unit. Thus, a similar to the above cyclic operation procedure was applied involving a ramp procedure of fixed length voltage steps. The scope of this study is to explore the response of the fuel cell unit under a wide range of normal and stressful conditions (elevated pressure, low gas flows) in order to explore the boundaries of its performance. The objective of the study is to analyze the influence of the tested measured variables (temperature, pressure, mass flow rates and humidity) on the dependent variable (voltage) and to quantify their effects.

For each condition a series of cycles were performed. Only one operating variable was altered while the rest remained at a predetermined value. To avoid any influence on the measurements from one cycle to the next or between different conditions, the fuel cell was operated for at least 60min at nominal steady-state load (0.45V). The conditions that were modified were related to temperature, humidity, excess ratio of oxygen and pressure. The excess ratio of oxygen is calculated based on:

$$\lambda = \frac{\text{flow applied}}{\text{stoichiometric flow at maximum current density}} \tag{2.1}$$

For every experiment the flow rate of reactants was kept constant at a flow relative to the maximum theoretical stoichiometric flow predicted by the maximum achievable current density of the fuel cell system under consideration.

2.4.4 Experiments at different temperature levels

Initially a number of experiments were performed at different temperatures levels (50°C, 60°C, 65°C, 70°C). The hydration temperature was fixed at 70°C, the system operated at ambient pressure (0barg) and the excess flow ratio for anode and cathode flows were 2.3

and 1.5 respectively. Fig. 2.19 illustrates the effect of temperature on the performance of the fuel cell in terms of power versus current density and voltage versus current density.

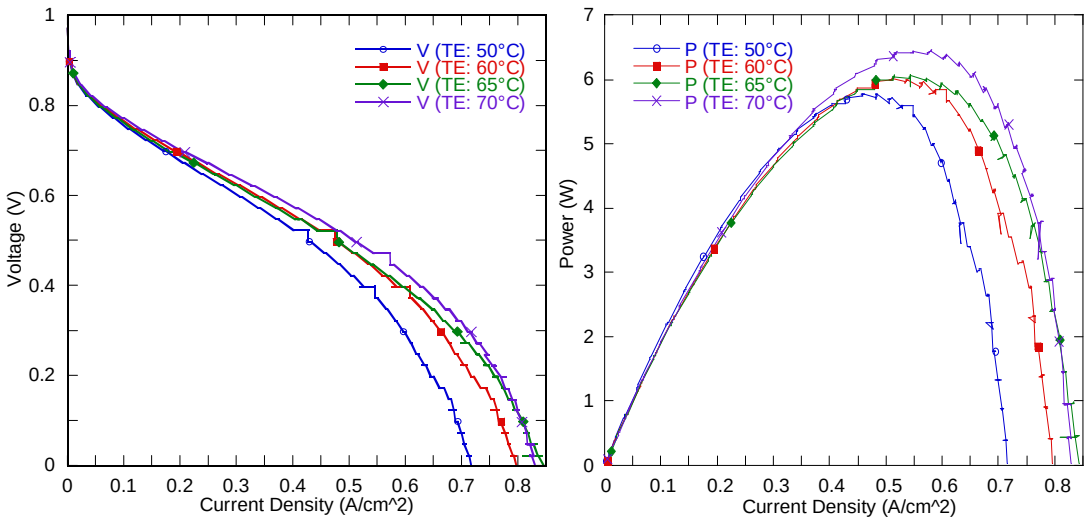

Figure 2.19 Effect of temperature to voltage and power

The lower operating temperature provided by the membrane manufacturer was 60°C. At the low temperature (50°C) a significant decrease in maximum power and current density was observed, which indicated that the full capacity of the fuel cell was not utilized. Between 60°C and 65°C the performance was similar up to the maximum delivered power but after that, the power at the elevated temperature was decreased at higher current densities. Finally a small difference exists between 65°C and 70°C.

These results indicate that overall the performance is improved as temperature increases and that the supply of fuel and water is sufficient to improve the proton conductivity. Also, it is observed that at low current densities a small difference in voltage and power exists, but as the current density increases the difference is more obvious. Although the operation at higher temperature could deliver more power, to preserve the lifetime of the membrane, the chosen temperature for the experiments was 65°C.

2.4.5 Experiments at different humidity levels

The second testing condition was the change of the hydration temperature at 65°C, 80°C and 90°C, for both anode and cathode electrodes. The second testing condition was related to the modification of the hydration temperature and more specifically three different point were applied (65°C, 80°C and 90°C) for both anode and cathode electrodes. The effect of the humidity on the fuel cell voltage and power is illustrated in Fig. 2.20.

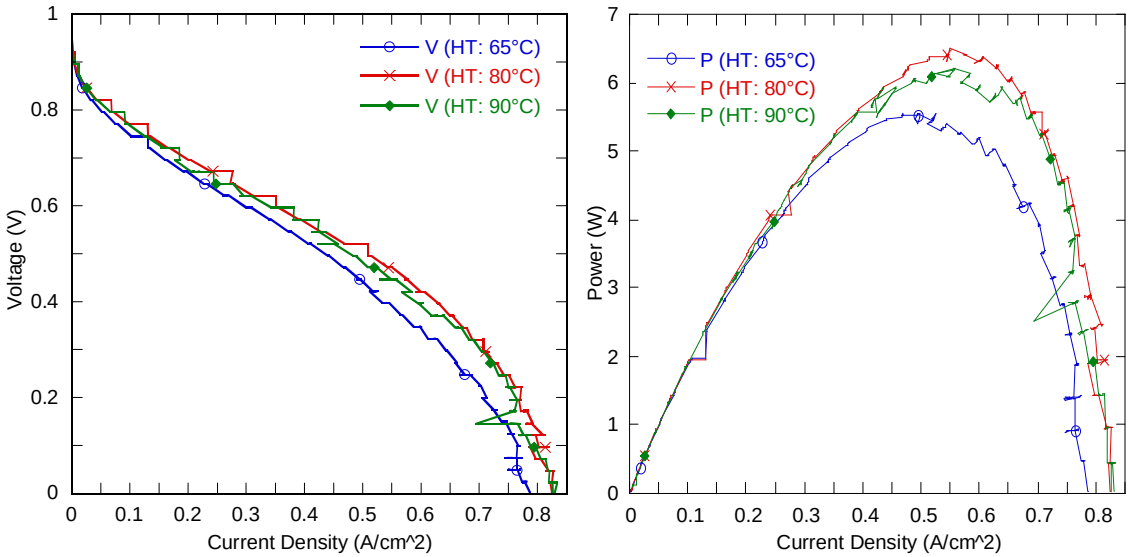

Figure 2.20 Effect of humidity to voltage and power

The performance was improved for hydrator's temperature up to 80°C. This is because the increased humidity in the gases, results in a decrease of the internal resistance of the cell. However the performance is decreased at 90°C due to flooding phenomena. The water content inside the fuel cell is accumulated at a rate higher than it can be removed therefore the produced voltage decreases. The accumulation of water increases the inactive area and the gas diffusivity is reduced. Since the suggested operating temperature from the previous experiment is 65°C the hydrator's temperature is chosen to be 5°C to 10°C higher. This would avoid flooding and at the same time it would keep the membrane adequately hydrated.

2.4.6 Experiments at different flow rates

After the selection of the operating temperature and the humidity points, experiments with different excess ratio levels. More specifically the experiments were performed at excess ratios for air of 1, 2, 4, 6 which were translated to flow rates of 500cc/min, 1000cc/min, 2000cc/min and 3000cc/min respectively. Fig. 2.22 illustrates the effect of the flow rate to the voltage and power of the fuel cell.

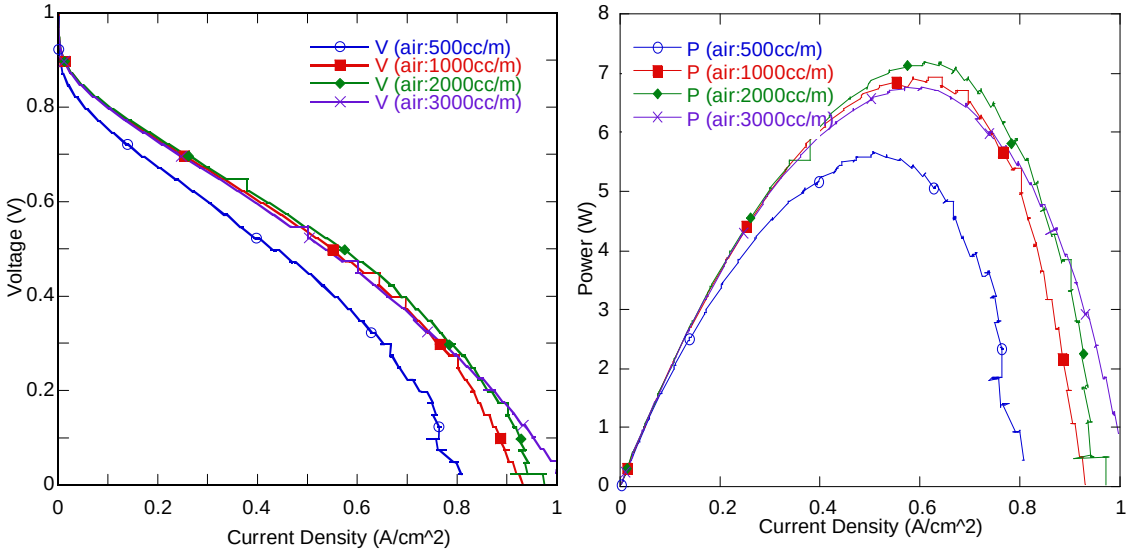

Figure 2.21 Effect of flow rates to voltage and power

At low excess ratio the oxidant is not sufficient and even at low current densities a fluctuation of the produced voltage is observed. Also, after the maximum power point a sharp voltage drop appears which indicates a lack of oxidants in the channels. On the other case side at high excess ratio (λ=6) the produced power was lower than the one with ratio 2 and 4. The water removal rate is analogous to the air flow rate which causes drying of the membrane and an increase to the electrical resistance. Therefore, any ratio between 2 and 4 can deliver satisfactory results. The air flow rate affects the performance of the system which is verified by the experimental analysis. Fig. 2.22 shows two step changes of current (8A, 12A, 8A) at different flow rates and the respective produced voltage.

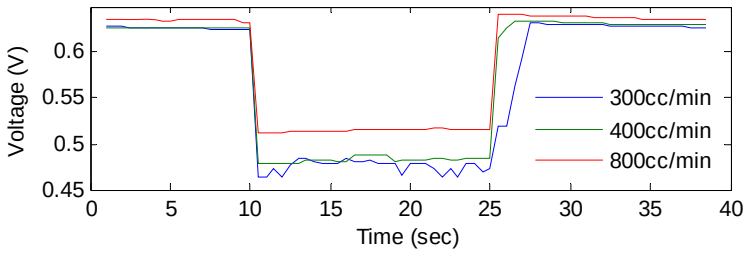

Figure 2.22 Dynamic response of the voltage at different flow rates

On the other hand, the hydrogen flow rate had very limited influence on the performance and it was selected at a stoichiometric ratio of 2.3 (500cc/m) to maintain sufficient reaction.

2.4.7 Experiments at different pressures

Finally, the pressure is an important parameter for the fuel cell, since it affects the homogeneity and the partial pressure of the reactants in the channels, the inlet gas compositions and the diffusivities of the gases through the gas diffusion layers and the rate of electrochemical reaction. The pressure was maintained at a certain level by two pressure regulators at the outlet lines. By controlling the outlet pressure the pressure inside the cell was also regulated. Fig. 2.23 shows the effect of the pressure (0 to 2barg) to the produced power and the voltage.

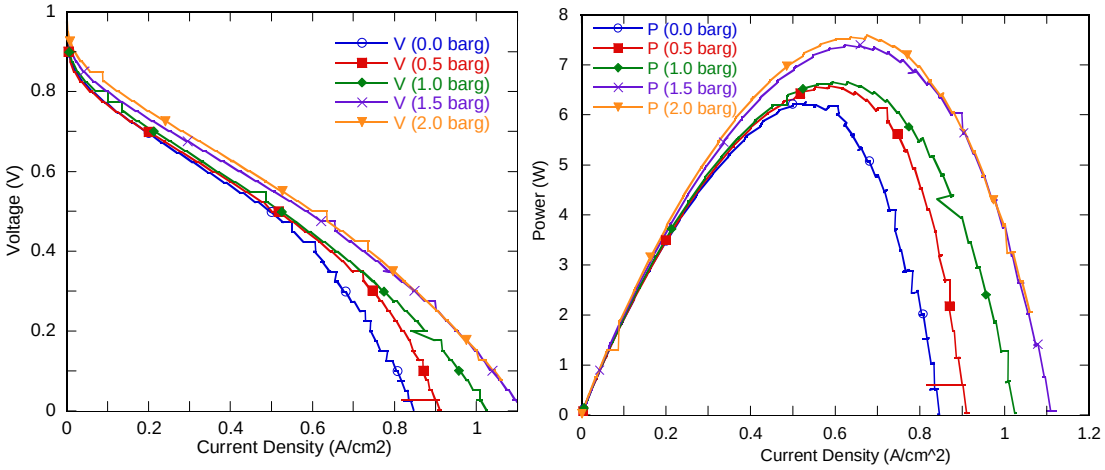

Figure 2.23 Effect of pressure to voltage and power

It is observed that the elevated pressure is beneficial to the performance. Even at low current densities a noticeable improvement is observed as the activation overpotential decreases with an increase of the pressure. Between 1.5barg and 2barg there was no apparent improvement. Furthermore, at 1.5barg, the inlet pressure at the cathode side was increased and consequently the pressure difference was increased between the anode and the cathode. This is an unsafe operating condition which should be avoided for lifetime and safety issues. Therefore, the preferred pressure would be between 0barg and 1barg.

The experimental results show that the increase of pressure results to an increase of the produced power. But a side effect is that a small change of the operating conditions can influence the stability of the system and most importantly the pressure difference between the anode and the cathode, which could cause an irreversible damage to the system. Also, there are a number of implementation issues when considering pressure control loop which would not make the elevated pressure a practical choice. Therefore, the ambient pressure is selected to be used at further studies.

2.4.8 Steps changes at constant current mode

The aforementioned experimental study was conducted with the DC electronic load set at constant voltage mode. A similar study was performed that explores the behavior of the system at constant current mode. This procedure was performed with fixed length changes of the current demand and applied at the fuel cell.

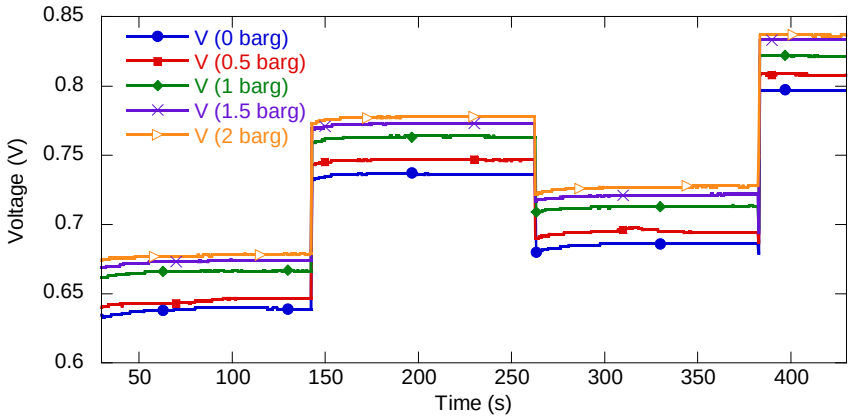

Figure 2.24 Voltage response to current step changes

An indicative plot involving few steps at different pressures is shown for completeness reasons as this mode will be used at the subsequent chapters. Fig. 2.24 illustrates the produced voltage after two current step changes for various pressure levels. The first change was from 8A to 4A and after 120 s a second change occurred, from 4A to 6A and finally from 6A to 2A. It is observed that the voltage increases as the pressure increases and the system has the same fast dynamic response to current changes, regardless of the pressure level. Similar experiments were performed for different temperature, flow rates and humidity levels and they revealed the dynamic nature of the experimental system.

2.4.9 Selected conditions for the fuel cell operation

It is clearly derived from the results that the temperature and pressure have a predominant effect on the system. Also, proper gas and water management are essential to achieve and maintain high power output. The increased gas flow rate is beneficial to fuel cell operation if the positive effects of increased availability of oxygen offset the negative effects of membrane dehydration. The objective of this study was to determine the operating conditions for safe and reliable operation of the PEM fuel cell unit as summarized in Table 2.5.

Table 2.5 Selected operating conditions for the estimation procedure

Pressure (anode & cathode)	0barg
Temperature : fuel cell	65°C
Temperature : hydrators / line	70°C / 120°C
H_2/ Air flow rate	500cc/min / 750cc/min

The aforementioned experimental study will provide the basis for the determination of the values of certain empirical parameters of the model.

2.5 Concluding remarks

The design and development of an experimental integrated fuel cell unit is a combined effort that involves a number of multidisciplinary actions from the fields of control engineering, chemical engineering and computer science. It is important to specify the scope of the system and its specifications at an early stage of the whole procedure as the requirements and the boundaries of a unit determine the overall framework that will be eventually developed and constructed.

This chapter presented the basic entities for the development of a small-scale PEM fuel cell unit, used for system evaluation purposes. The characteristics of the various subsystems of the unit were described along with the respective variables that constitute the I/O field of the process. Furthermore, specific emphasis was given to the analysis and synthesis of the automation system of the unit which is oriented towards industrial standards as the rest of the construction. Also, the interoperability of the unit with other information systems based on an open architecture was considered throughout the development procedure. The criteria that led to the selection of a SCADA system were derived by the overall research objectives of this thesis and more specifically the imperative need for flexibility of the control structure that will be explored in subsequent chapters.

Finally, an experimental study was performed at the developed unit that initially conditioned the PEM fuel cell based on an activation process. A number of tests were performed at various operating conditions that explored the behavior of the PEM fuel cell and the overall response of the unit. The results obtained by these experiments were analyzed and a set of operating conditions was selected to be used in the subsequent Chapter 3 for the modeling of the system.

Chapter 3

A Modeling Framework of a PEM Fuel Cell System

The scope of this chapter is a new dynamic nonlinear mathematical model that takes into account the main variables and parameters of a fuel cell, such as the partial pressures of all gases, the fuel cell current and the operating temperature. The main prerequisite that directed the development choices is that the model should be oriented towards optimization and control as it will be used for the formulation of advanced model-based controllers. For this reason it should simulate the dynamic behavior of the fuel cell unit under fast execution times and enough accuracy for control purposes. Thus, a semi-empirical approach was selected where first-principle equations are combined with equations having empirical parameters. In order to increase the model's accuracy a systematic parameter estimation procedure was developed that can determine the empirical parameters of the model using experimental data under various operating conditions.

3.1 Importance of modeling

In order to study and improve the behavior and performance of PEM fuel cell systems it is important to measure a variety of variables. But some of them are difficult to measure or even inaccessible due to the physical nature of the system, due to its layered structure and the fact that each cell is sealed. Also, it is difficult to understand the phenomena evolving inside the cell due to the variable's interrelations. Therefore, it is important to be able to study these phenomena and extract information about the time evolution of them by simulation methods. Such methods can provide a better insight of the system, as mathematical equations can be used to describe the various phenomena.

A simulation methodology utilizes mathematical models that play an important role in the development of fuel cells and describe the real behavior of the physical system. The aim of the current analysis is to provide an overview of the most important criteria that are considered for the selection of the proper modeling technique according to the requirements of the specific fuel cell system. Mathematical modeling is an important tool that can be used to determine the performance of new designs without the need for experimental investigations. Therefore, the models are used to improve performance and reduce design cycle times which can lead to the minimization of the development cost. Overall models play an important role in the development of PEM fuel cell technology as they facilitate the understanding of the electrochemical reaction, thermal dynamic phenomena, and fluid transfer mechanisms. Also, an important issue which can be resolved with the use of models is that the difficulty of direct measurements of the various phenomena is eliminated, because models provide details on the physical processes occurring within the fuel cell during its operation. Regarding the performance, it is important to determine the factors that affect it and to investigate the role of each fuel cell parameter to these factors with the aid of mathematical models.

There are many models or types of models available in the open literature and each one serves a different purpose or it is oriented toward a specific issue or application involved, with varying degrees of simplifications. Each modeling attempt has a specific goal, to describe a phenomenon or to be used in a specific study. For example if the purpose of the project is to study thermal and water transport phenomena, the model

should contain not only electrochemical relationships but also thermodynamic and fluid dynamic equations. On the other hand if the purpose of the modeling is an initial study of the behavior of an integrated system, then the model can contain only simplified semi-empirical electrochemical equations that mimic the polarization curve for certain operating conditions. Both models are correct and useful, since the degree of complexity and the amount of details are specified by the overall project that the fuel cell system is going to be used for.

3.1.1 Type of models and structural criteria

The most important key features of a model are defined by making the following choices: the modeling approach, the system boundary, the state and the spatial dimension. Also the level of complexity is an important characteristic of a model which is defined after the previous desired features are set. In Haraldsson and Wipke (2004) criteria on how to select a fuel cell model according to its application are presented and several models proposed in the literature are described. Overall PEM fuel cell modeling has evolved from steady state to dynamic, from lumped or simple zero-dimensional to complex three-dimensional models, from isothermal to non-isothermal, from single phase to multi phase, and recently from straight channels to more complex field structures, like serpentine flow fields.

Prior to the development of a model it is very important to set the boundary of the system that will be studied, which corresponds to the area of interest of the model and to define the key features for the desired model. Usually the categories are related to the scope of the study and most importantly to the boundary of the system:

- Inner level: includes the membrane, electrodes, the geometry of the flow fields etc.
- Cell level : single fuel cell or fuel cell stack as an autonomous entity
- System level: fuel cell stack with auxiliary components such as an air compressor

This is a very important decision as it affects the overall outcome of the modeling procedure and although vital, these initial criteria often tend to be overlooked or not specified in detail. It is useful to state the simulation objective clearly. If the simulation objective is to provide a tool for control studies, the development and validation of a fuel

cell model based on semi-empirical equations is a useful way of gaining knowledge. Thus, the optimal model choice differs for each application and the initial decisions are important to avoid costly changes later in the model evaluation process. Once the initial criteria are defined further structural details can be set.

Modeling approach

The modeling approach plays an important role on simulating the behavior of the system and is closely related to the purpose of each project or application that the model will be used for. The optimal modeling approach differs for each application and there are several types of approaches. The line separating these approaches is often blurry. Essentially however, the approaches may be classified as theoretical or semi-empirical.

The theoretical models are detailed and complex and various phenomena are described. The theoretical approach can be subdivided into (a) analytical and (b) mechanistic that use computational fluid dynamics (CFD) simulation. The semi-empirical models on the other hand can include first-principle equations or be completely empirical. Each approach has advantages and disadvantages, as discussed in (Haraldsson and Wipke, 2004). When the boundary of the simulation study is an integrated system, fuel cell stack and auxiliaries, a combination between the theoretical and the semi-empirical models can co-exist. For example a simplified approach for the electrochemical aspects such as electrode kinetics can be used since the focus is on the system level.

State of the model

Besides the modeling approach, a structural characteristic that should be defined is the state of the model, which is closely related to the purpose of the modeling study and the modeling approach. The state of the model is either steady state or dynamic in nature. Dynamic models are used to analyze step changes in operating variables, such as temperature, for start-up and shutdown procedures, analysis of the influence of various flows during operation and optimization of the response time on load demands. For example, for vehicular applications it is important to be able to respond to variable

fluctuations, therefore the model should be dynamic to some degree to account for the important transients in the system.

Steady-state models, using one operating point in each step, are useful for sizing components in the system, calculating amounts of materials such as catalysts and parametric studies (Haraldsson and Wipke, 2004). Typically, laboratory fuel cells are operated at steady-state. Therefore, when the purpose of the study is component design, where accuracy and detailed modeling of each component is required, a steady state model is necessary, since the simulation involves specific points of operation.

Dimensionality

Spatial dimension is also an important structural characteristic of a model, which is application dependent. In general, models can be distinguished by their dimensionality to lumped or zero-dimensional, one-dimensional or multi-dimensional. Usually when there is no spatial consideration the model is also semi-empirical in nature and they are used for polarization curve analysis. The zero and one-dimensional describe the fuel cell layers in a macroscopic manner and although they don't provide detailed analytical representation, they can incorporate all the dynamics involved in a fuel cell system and the interactions between the subsystems. Therefore, models with one-dimensional approach are preferred for investigating the dynamics of the system. A description of a fuel cell that takes into account mass transport limitation phenomena is represented with at least one dimension. On the other hand, to understand the water transport phenomena that occur, two-dimensional representation is required. These models are useful in providing insight when intermediate details are necessary, such as water transport.

In order to have a better understanding of how the phenomena are evolving and to gain detailed results, it is necessary to have a three-dimensional model. The multi-dimensional model solves governing equations by using CFD methods and provides a high resolution of flow characteristics of reactants, fuel, byproducts, and transport of charges. For example if the study focuses on the electrode layer it is necessary to model the spatial distribution of the current density on the membrane in both the direction of the flow and the direction which is orthogonal to the flow but parallel to the membrane (Lum

and McGruik, 2005). Usually 3D models are applied to the study of complex parts such as flow fields of a single cell.

3.2 Literature review on PEM fuel cell modeling

The aim of the current literature review is to provide a generic overview of the evolution of PEM fuel cell models since many theoretical works can be found in the literature. As stated earlier the categories which are defined by the scope of approach are analytical, mechanistic CFD and semi-empirical models. Initially a brief description of analytical and CFD models is provided. Subsequently, the analysis focuses on semi-empirical models since the subsequent developed model is developed for control purposes and used a semi-empirical approach.

3.2.1 Analytical PEM fuel cell models

Analytical models are based on electrochemical, thermodynamic and recently fluid dynamics and they tend to use various assumptions in order to represent the system with a theoretical perspective. The early fuel cell models were analytical in nature. The milestone for the analytical models is the work of Bernardi and Verbrugge (1991) and Springer *et al.* (1991). They developed a one-dimensional, steady-state, isothermal models of the membrane electrode assembly (MEA) and the gas flow channels. However, the two models differed in the way that they handle the transport of ions and water in the polymer electrolyte and the treatment of the catalyst layers. Bernardi and Verbrugge (1991) developed a model based on fundamental transport properties where the cell voltage is reduced due to losses incurred by the activation overpotential of the anode and cathode reactions, the ohmic losses due to the resistance in the membrane and to the electrodes. The model does not account for the concentration overpotential region of the polarization curve. They assumed that the membrane is fully humidified and the void regions of the catalyst layer are assumed to contain membrane phase only. In Springer *et al.*, (1991) they considered only the losses caused by the cathode reaction and the membrane. The membrane model allowed for variable hydration between the anode and cathode and thus variable ohmic resistance due to the hydration of the membrane. An

empirical formula was used to relate the hydration of the membrane to the conductivity. The entire polarization curve was modeled by incorporating flooding in the catalyst and backing layer, which was achieved by decreasing the porosity of the catalyst and backing layers that resulted in the increase of the transport losses and the cathode overpotential.

Weisbrod *et al.* (1995) used the membrane model of Springer *et al.* (1991) with the catalyst layer model of Bernardi and Verbrugge (1991) and added to it an activation overpotential term. But they ignored the concentration losses as they didn't consider the diffusion through the membrane phase of the catalyst layer and they assumed that the catalyst layer was not flooded.

However in these early models, the temperature of membrane and electrodes were not differentiated, despite that a significant temperature variation in those regions exists in both the through-membrane and flow directions depending on the geometric and operating conditions. Furthermore, the major heat source terms, the entropic and irreversible reaction heats, were not specified in their models. Based on the concentrated solution theory, Fuller and Newman (1993) built a more compact quasi two-dimensional, steady state model to describe the water transportation mechanisms and investigated strategies for thermal management. The model accounts for one-dimensional mass transfer in the through-membrane direction and one-dimensional heat transfer in the flow direction. Based on the known enthalpy change of the overall electrochemical reactions, the model calculated also the temperature rise of the flowing gas streams with various external heat transfer coefficients.

In Nguyen and White (1993) a similar model approach was used, except that the electrolyte model of Springer *et al.* (1991) was used and the catalyst layers were treated as interfaces. They developed a quasi two-dimensional model to account for heat and mass transport between the electrode and reactant gas mixture in the flow channel. The model considers phase change of water in the flow channel as the only heat source, allowing convective heat transfer between gas and solid phases. They modeled the water and heat management to describe the electro-osmotic drag and back diffusion process, heat transfer from solid phase to gas phase, latent heat associated with water evaporation and condensation in the flow channels.

Both, Nguyen and White (1993) and Yi and Nguyen (1998) developed two-dimensional, steady state models that considered both the changes across the membrane and in the direction of the bulk flow. In these models, the authors demonstrated the important roles played by water and thermal management in maintaining high performance of PEM fuel cells. In Yi and Nguyen (1998) the work of Nguyen and White (1993) was extended to include the entropic and irreversible reaction heats along with the phase change heat. However, this model allowed the temperature variation of the solid phase in the flow direction only, assuming uniform temperature in the through-membrane direction.

At Eikerling and Kornyshev (1998) some approximations were used in order to find analytical solutions to the governing equations of the PEMFC for different regions in the cell polarization curve. But their model does not incorporate the concentration at the overpotential region. The importance of accounting for temperature gradients in fuel cells modeling was demonstrated in the work of Wohr *et al.* (1998) and Djilali and Lu (2002). Wohr *et al.* (1998) developed a one-dimensional thermal model for heat and mass transfer in the through-membrane direction, particularly for PEMFC stacks. Accounting for the entropic and irreversible reaction heats, they computed the temperature profile in the through-membrane direction and predicted the maximum temperature as a function of the number of cells contained in a stack.

In Marr and Li (1999) a steady-state, isothermal engineering model of a PEMFC was developed based on the catalyst layer of Weisbrod *et al.* (1998) and the membrane model of Bernardi and Verbrugge (1991), including the electrochemical kinetics and mass transport processes of reactant gases to provide the optimal operating and design parameters in aiding the design of PEMFC system. Also, they considered the flow in the gas flow channels as one-dimensional pipe flow. Baschuk and Li (2000) further modified the catalyst layer model, considering it composed of reactant gases, liquid water and polymer electrolyte. Rowe and Li (2001) also developed a one-dimensional model in the through-membrane direction. Including entropic, irreversible, and phase change heats, they further took account of Joule heating in the membrane and anode/cathode catalyst layers. This work predicted the temperature variation in the through-membrane direction

under the various current densities and electrode thermal conductivities. In Wu *et al.* (2007) the objective was to extend the steady-state model of Hum and Li (2004) by considering the transient effects of different transport phenomena. A two-dimensional, isothermal, transient model has been developed. For comparison purposes, both steady-state and transient analysis have been conducted. The variation of reactants concentration, activation overpotential, reaction rate and corresponding current density distribution in the catalyst layer (CL) was analyzed in detail.

At Kulikovsky (2001) an analytical quasi-three-dimensional model was developed for studying the catalyst layer performances with respect to feed gas consumption in the channels. Furthermore, this work was extended in Kulikovsky (2004) developed a semi-analytical model 1D+1D taking into account oxygen and water transport across the cell and deriving an expression for the limiting current density. Finally Cheddie and Munroe (2007) presented a two-phase model of an intermediate temperature PEMFC taking into account polarization and transport phenomena. Their model considers also the dependence of the fuel cell performance on membrane level, catalyst activity, and transport properties of dissolved gases in the electrolyte medium. The aforementioned models are some of the representative works that summarize the evolution of analytical modeling.

3.2.2 CFD PEM fuel cell models

The evolution of computing technology made feasible the development of complex, more comprehensive three-dimensional full-cell models. Such technology enables the investigation of the phenomena within the cells, a task hardly achievable through experimental studies. Earlier models were primarily analytical and used a number of assumptions due to limitations posed by the numerical techniques. More recently, a general trend can be observed to apply the methods of computational fluid dynamics to fuel cell modeling. Also, multi-dimensional thermal models were presented by many PEMFC modeling groups.

The work of Gurau *et al.* (1998) was the first to use computation fluid dynamics (CFD) in the PEM fuel cells and their model is a fully two-dimensional model of a whole fuel cell, two gas-flow channels separated by the MEA. They developed a unified model that used the water transport model of Bernardi and Verbrugge (1991) and the ion transport model of Springer *et al.* (1991). They presented a unified approach by coupling the flow and transport governing equations in the flow channel and the gas diffuser, but only single-phase and incompressible fluid model was used.

To accurately represent the important transport phenomena in PEM fuel cells, a two-phase flow model is necessary because both liquid and gaseous phases exist under normal fuel cell operating conditions. With the representative work of Natarajan and Nguyen (2004) and Wang *et al.* (2001), the analytical fuel cell models have been developed into three-dimensional, two phase, non-isothermal, transient ones nowadays. Natarajan and Nguyen (2004) presented a two-dimensional, two-phase, transient model for the PEMFC cathode. Both multi-species flow and capillary flow of liquid water are accounted for in their model, and they concluded that the performance of the cell is dominated by the dynamics of liquid water rather than gas reactants transport. Wang and his associates (Um *et al.*, 2000; Wang and Wang, 2005) have also championed a unified approach, using a different water transport model than that of Gurau *et al.* (1998).

Um *et al.* (2000) have developed a similar 2D model and included two phase flow along with the description of the transient behavior of the bulk flow, species and electro-chemical reactions in a single cell. However, the underlying assumption was isothermal behavior, which is a serious modeling limitation. In following work Um and Wang (2004) the model was extended to 3D, elucidated electrochemical kinetics, current distribution, hydrodynamics, and multi-component transport.

Furthermore, Wang and Wang (2005) presented a three-dimensional dynamic, single-phase, isothermal model of a PEMFC to investigate the transient phenomena of electrochemical double layer discharging, gas transport through the gas diffusion layer (GDL) and membrane hydration as well as the evolution of water accumulation in the membrane corresponding to operating condition changes. They simulated a single cell

with 36 gas serpentine channels taking a low humidity condition and presented the mechanism of the species transport and the associated current density distribution.

In Berning *et al.* (2002) the need to account for thermal gradients and multi-dimensional transport simultaneously was addressed that couples convective transport in the gas-flow channels with transport and electrochemistry in the MEA. They developed a 3D non-isothermal two-phase model which simplified the water transport by assuming liquid phase water transport in both GDL and the membrane layer. This work was extended in Berning and Djilali (2003) with the inclusion of phase change in the model. They presented a two-phase flow model for GDL and flow channel in both anode and cathode sides; however, the MEA was excluded from simulation.

At Dutta *et al.* (2000) a similar work to Berning *et al.* (2002) was published based on a three-dimensional non-isothermal computational model except that it accounts for a partially dehydrated membrane using an empirical approach and includes the modeling of the isothermal flow in a cell that embeds a serpentine-type gas channel. In Kim *et al.* (2004) reported the influences of reservoirs, fuel dilution and gas stoichiometry on the dynamic behaviors during load changes and they observed the overshoot/undershoot of the current density during cell voltage switch. The work of Shimpalee *et al.* (2006a) uses a commercial CFD solver to simulate the transient response of a PEM fuel cell subjected to a variable load and particularly focused on the overshoot/undershoot behavior under different flow stoichiometry conditions. Their modeling study was based on their previous experimental observation of overshoot/undershoot in transient state presented in Kim *et al.* (2004).

The aforementioned studies focused on the description of a single cell, ignoring a stack and time-varying behaviors. On the other hand, the dynamic behavior of a stack can be improved by adding a simplified thermodynamic model, which is proposed by Sundaresan and Moore (2005). The model regards a cell as a composition of layers and is used to analyze the start-up behavior from a sub-freezing temperature. The model regards a cell as a composition of layers and is used to analyze the start-up behavior from a sub-freezing temperature. The work of Siegel *et al.* (2004) developed a multi-phase, two-dimensional model to take into account the liquid water saturation and flooding effect,

and they have studied transport limitations due to water build up in the cathode catalyst region. In Promislow and Wetton (2005) a stack thermal model with the coolant channel coupled with a 1D cell model was proposed that shows a significant temperature gradient of the stack, but with no dynamics.

In Shan and Choe (2006) an enhanced quasi 1D stack model was proposed that considers the thermal and fluid dynamics, resulting in the capturing of the dynamic temperature distribution including the asymmetrical effects in the stack, but missing the water distribution that are improved by adding an empirical relationship between the flooding effect and the current density and temperature. At Al-Baghdadi and Al-Janabi (2007) a three-dimensional CFD model was presented that accounts for species mass transport, heat transfer, potential losses, electrochemical kinetics, and transport of water through the membrane. Also, a two-dimensional CFD model of a PEM fuel cell was developed by Sahraoui *et al.* (2009) by taking into account electrochemical, mass and heat transfer phenomena.

The work of Li's group (Baschuk and Li, 2000; Rowe and Li, 2001; Wu *et al.*, 2007) was extended in Baschuk and Li (2009) by the development of a unified model that utilizes a membrane transport model that is based on the generalized Stefan–Maxwell equations. Finally in Wu *et al.* (2009) a comprehensive 3D model was developed with appropriate water production assumption which can be readily switched between single- and two-phases, steady and unsteady, isothermal and non-isothermal modeling approaches. Furthermore, both non-equilibrium membrane water sorption/desorption processes and non-equilibrium condensation/evaporation processes have been incorporated in this model.

All these models describe the evolution of mechanistic models that use CFD methods. These CFD models are steady state in nature and they study the design characteristics using a multidimensional approach. Each work has a specific purpose oriented towards the evolution of a certain phenomenon inside the cell or the behavior of the materials under different conditions.

3.2.3 Semi-empirical PEM fuel cell models

A interesting and comprehensive review of PEM fuel cell models can be found in Cheddie and Munroe (2005) and Haraldsson and Wipke (2004) where the focus is on the evaluation of models, whereas the review by Sousa and Golzalez (2005) is concerned with modeling at the cell level. More recently, a detailed review of PEM modeling and SOFC modeling is presented in Bavarian *et al.* (2010). In general, mechanistic modeling has many advantages regarding the thorough investigation of the fuel cell's insight and increased accuracy on phenomena analysis, but in some cases a model that responds in real time without many internal details is adequate enough. On the contrary, the semi-empirical approach can rapidly produce models able to describe the fuel cell response without the need of insight process details. Therefore, they can be used to accurately predict the fuel cell system performance for engineering applications, such as small distributed electrical generation systems, portable electronics and vehicles (Moreira and da Silva, 2009). All of these models are reduced in terms of dimensionality and comprehensiveness.

At his context a pioneering work on PEM fuel cell modeling is presented by Amphlett *et al.* (1995a) and Amphlett *et al.* (1995b), where a steady-state model for the Ballard Mark IV fuel cell has been proposed that combines performance losses into parametric equations based on operating conditions, such as the pressure and the temperature. The work of Mann *et al.* (2000) extended that model and presented a generalized steady-state electrochemical model, based also on Springer *et al.* (1991) and on the experimental data of Buchi and Scherer (1996) for the resistance of the membrane. The work of Amphlett *et al.* (1996) proposed a transient model to predict efficiency in terms of voltage output and heat losses and included heat transfer coefficients for the stack and an energy balance.

In Golbert and Lewin (2004) a transient along-the-channel model for control purposes was developed, which includes mass balances of liquid water and water vapor and heat transfer between the solid, the channels and the cooling water. Pukrushpan *et al.* (2004) presented a transient dynamic model, which includes the in-compressor flow and inertia dynamics, the manifold filling dynamics, the reactant partial pressures and the

membrane humidity. Yerramalla *et al.* (2003) considered the humidifier and stack pressure. A linear and a nonlinear model were developed and the results showed the risk involved with linearizing the model.

A common simplification in contributions Pukrushpan *et al.*, (2004), and Yerramalla *et al.*, (2003) is that the temperature transient behavior is neglected. Xue *et al.* (2004) considered the effect of temperature transient behavior and used a three control volume approach to develop a set of dynamic equations that govern the system dynamics. Pathapati *et al.*(2004) developed a complete fuel cell system-level that include mass and energy balance equations for the gases and the dynamics of flow and pressure in the channels, along with the capacitor effect of charge double layer. Muller and Stefanopoulou (2006) presented a model for the thermal dynamics containing a power section and a humidification section and have compared experimental and theoretical data to validate it.

Lee and Lalk (1998) used an object-oriented approach based on stationary equations and they analyzed the temperature variation and thermal efficiency under regular load fluctuation. The influence of flooding on the dynamic behavior was modeled by McKay *et al.* (2005). Both gas diffusion layers (GDLs) and gas flow fields have been modeled, considering lumped parameters, by dividing each GDL into three control volumes and each flow field into one. More recently, a simple empirical equation has been introduced by del Real *et al.* (2007), to model the fuel cell voltage with variations in main variables. The fluid dynamics part of their model is based on (McKay *et al.*, 2005) but the GDL has simpler structure reducing the computational cost.

The aforementioned models describe the evolution of the semi-empirical modeling approach. Although these models do not include many details of the system and they focus on specific operating conditions, in contrast with the analytical and mechanistic CFD models, they are very useful for application to real systems and control studies. A significant modeling effort has been done recently aiming to achieve the proper tradeoff between the usability and the accuracy of the semi-empirical based models. A summary of key contributions from the open literature are presented in Table 3.1. The enumeration is based on the year of publication. For each work a summary is presented along with the dimensionality and the state.

Table 3.1 Indicative semi-empirical PEM fuel cell models

	Author	Description and Focus
1	Fowler (2002)	Study of the voltage degradation and the end of life issue
2	Ceraolo *et al.* (2003)	Identification of numeric values for parameters, assumption of uniform pressure, procedure for evaluation of the parameters
3	El-Sharkh *et al.* (2004)	Stand alone PEM fuel cell power plant for residential applications, gas reformer and power conditioning
4	Al-Baghdadi (2005)	Investigate the impact of operating conditions on performance, not extensive calculations
5	Caux *et al.* (2005)	Modeling of control auxiliaries, control, boost conv, quasi static, use in vehicular applications
6	Pathapati *et al.* (2004)	Effects of charge double layer & behavior on sudden load changes, transient phenomena
7	Wishart *et al.* (2006)	Develop a methodology to obtain optimal operating conditions, include BOP. Two performance objectives: maximize net system power and the efficiency
8	Zong *et al.* (2006)	Analyze water transport across the membrane and shift change effect, pressure variation along the channel
9	del Real *et al.* (2007)	Development and experimental validation of a dynamic model. Suitable for control studies
10	Hou *et al.* (2007)	Simplified model applied for vehicle applications. Effect of temperature & pressure into performance
11	Litster and Djilali (2007)	Ambient air breathing fuel cell for portable devices. Effects of coupling between ambient air temperature and humidity
12	Wingelaar *et al.* (2007)	Electric circuit representation with small signal and large signal characteristics. Use electrochemical impedance spectroscopy
13	Andujar *et al.* (2008)	Linearized state space approach and representation electrical circuit. Model a DC/DC & boost converter to control duty cycle
14	Huisseune *et al.* (2008)	FC behavior Based on two discrete models : thermodynamic & electrochemical
15	Outeiro *et al.* (2008)	A parameter optimized model as an electrical equivalent circuit including temperature effects
16	Al-Dabbagh *et al.* (2009)	Use of conditioning circuits & controllers. DC/DC converter and AC inverter
17	Caux *et al.*(2010)	Model suitable for energy optimization purposes with electrochemical & electrical characteristics
18	Lazarou *et al.* (2009)	Electric circuit model, use of simple lumped electric circuit elements. Case study: connection or disconnection of load
19	Li *et al.* (2009)	Fast approach to predict the performance. Analysis through a series of experiments
20	Miansari *et al.* (2009)	Thermodynamic approach with study of channel dimension. Effect of temperature, pressure and air stoichiometry on the irreversibilities
21	Moreira *et al.* (2009)	Practical model for performance evaluation with few calculations and sum up into one equation

Fig. 3.1 illustrates the dimensionality and the system state, along with the existence of temperature and water management subsystems.

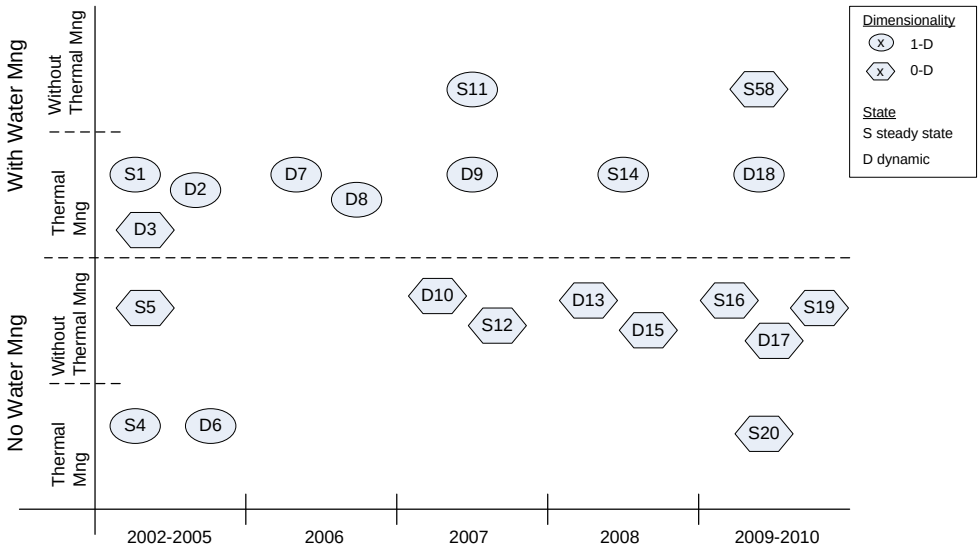

Figure 3.1 Characteristics of PEM fuel cell models

The presented models can be steady state or dynamic and they study the response of the system to changes and its performance under various conditions. Each work has a specific purpose oriented towards fast development and considers only the required amount of detail needed for the scope of the project involved. It is important to note that these models are either one dimensional or lumped parametric models. When the dimensionality is ignored, usually the temperature variation and the water handling are also ignored and vice versa. The former focuses on simulating the fuel cell polarization curve while the latter generally pays more attention to thermodynamic aspects. These models are used in practical applications and it has been recognized that although a large number of theoretical models have been developed recently, an analogous number of semi-empirical models has been developed too.

Compared to all these models, the model presented in this work is developed for the purpose of online control in the PEM fuel cell unit described in Chapter 2. As such, it needs to have reduced execution times and enough accuracy for control. It is important to include details regarding the thermal behavior of the system as the regulation of the flow and the temperature are considered. Thus an approach that combines both empirical and mechanistic equations is employed. The proposed model has the potential to couple both the theoretical validity and the inherent simplicity of the empirical application.

3.3 Structural model analysis and assumptions

In general mechanistic models are being valid over a wide range of process operations and provide physical insight into the reaction processes. However, mechanistic models have increased computational needs and require the knowledge of parameters which are not readily available, such as transfer coefficients or active catalyst layer thicknesses. Empirical models, on the other hand, are developed rapidly by utilizing experimental data without requiring detailed insight into the process. In the published literature there exist many models based on empirical equations. Such models are developed for a specific set of operating conditions and are adapted to specific applications. They are used in engineering studies, as they provide a rapid start into fuel cell modeling.

An approach combining both theoretical and empirical modeling techniques can take advantage of the theoretical validity and the semi-empirical simplicity (Li *et al.*, 2009). However, a semi-empirical model needs thorough validation and possible parameter adjustment for new applications or operating conditions, as their empirical coefficients need to be adjusted for every new configuration. They are validated against experimental data and they typically do not provide as many details as theoretical models do. Such models are suitable for initial system optimization or control studies using realistic time scales.

The proposed model relies on mass and energy conservation equations combined with equations having experimentally defined parametric coefficients thus resulting in a semi-empirical dynamic model. To model mass transport phenomena a five volume approach was adopted. The model accounts for mass dynamics in the gas flow channels, the gas diffusion layers (GDL) and the membrane. The equation of the voltage as a function of the current and the relationship between the current drawn from the fuel cell and the consumption of the reactants describe the operation of the fuel cell. Finally, in this scheme the energy balance of the fuel cell was also considered.

To simplify the overall modeling framework and reduce the computational requirements several assumptions have been employed without sacrificing the accuracy

of the model. Some of these are theory related and others were derived from the operation of the testing unit. The theory related assumptions are:

a) the ideal gas law holds for gases which are uniformly distributed,

b) the temperature is uniform at the anode and the cathode side,

c) each channel is homogeneous in respect to pressure as all channels have a fixed length volume.

The assumptions derived from the operation of the fuel cell testing unit are:

a) humidified hydrogen and air are fed in the fuel cell

b) the produced water is continuously removed through the cathode flow

c) the condensed water in the anode channel is dragged by the flow of the unreacted hydrogen.

3.4 Mass dynamics

The model equations consist of material balances of all components whereas every gas follows the ideal gas law. Therefore, the mass of each gaseous component is described through the partial pressure of each gas in the material balances. The mass balance is applied to the cathode and the anode channel volumes for the respective species. Also, the inlet and outlet flows of each channel and the exchange flow between the gas diffusion layers are incorporated. The mass transport throughout each FC volume that has been considered in the model is graphically illustrated in Fig. 3.2.

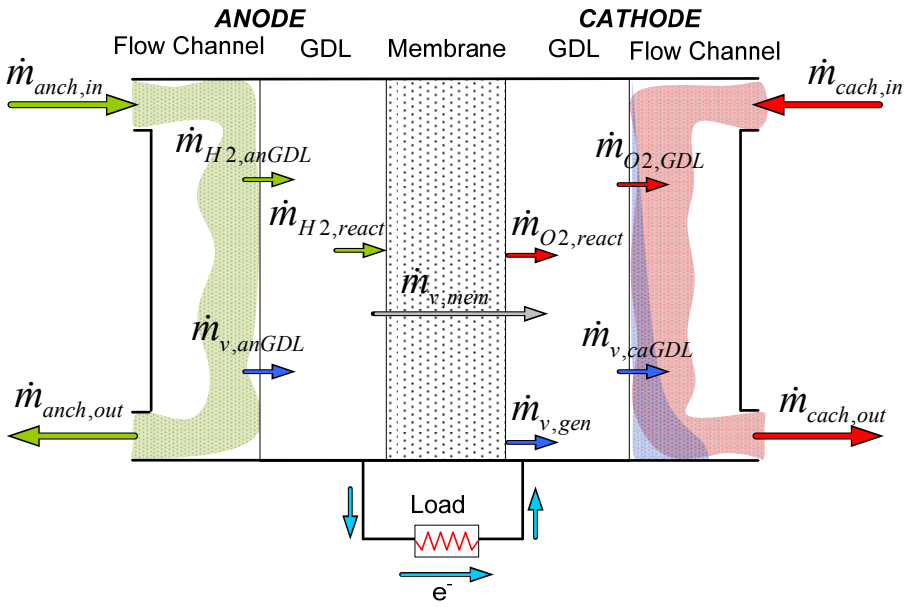

Figure 3.2 Structure of the Dynamic Model

3.4.1 Mass balances in cathode and anode channels

The model equations consist of the material balances of each species. Every individual gas follows the ideal gas equation. The concentration of each gas in the channel is calculated based on conservation of mass assuming that the channel is homogeneous with respect to concentration and temperature. Applying mass balance to the cathode channel volume, assessing the inlet and outlet flows of the channel and the exchange flow between the channel and the gas diffusion layer, the following equations are derived:

$$\frac{dm_{O2,cach}}{dt} = \dot{m}_{O2,cach,in} - \dot{m}_{O2,cach,out} - \dot{m}_{O2,GDL} \tag{1.1}$$

$$\frac{dm_{N2,cach}}{dt} = \dot{m}_{N2,cach,in} - \dot{m}_{N2,cach,out} \tag{1.2}$$

$$\frac{dm_{v,cach}}{dt} = \dot{m}_{v,cach,in} - \dot{m}_{v,cach,out} + \dot{m}_{v,caGDL} + \dot{m}_{evap,cach} \tag{1.3}$$

$$\dot{m}_{l,cach,in} - \dot{m}_{l,cach,out} - \dot{m}_{evap,cach} = 0 \tag{1.4}$$

In order to calculate the inlet mass flow rate of the individual species at the cathode (oxygen, nitrogen, vapor) the ratio of the mass of water vapor to the mass of dry air (ω) is used which is also referred to as humidity ratio.

$$\omega_{ca,in} = \frac{m_{v,cach,in}}{m_{a,cach,in}} = \frac{M_v}{M_a} \frac{\phi_{cach,in} p_{sat}\left(T_{cach,in}\right)}{p_{cach,in} - \phi_{cach,in} p_{sat}\left(T_{cach,in}\right)} \tag{1.5}$$

The relative humidity (φ) gives a good representation of the humidity of the mixture as the maximum amount of water that the air can hold (saturation) is included. The saturation pressure (p_{sat}) is calculated using the equations proposed in Nguyen and White (1993).

The mass flow rate of dry air ($m_{a,cach,in}$) and vapor ($m_{v,cach,in}$) entering the cathode is

$$\dot{m}_{cach,in} = \dot{m}_{a,cach,in} + \dot{m}_{v,cach,in} \tag{1.6}$$

$$\dot{m}_{a,cach,in} = \frac{1}{1+\omega_{ca,in}} \dot{m}_{cach,in} \tag{1.7}$$

$$\dot{m}_{v,cach,in} = \frac{\omega_{ca,in}}{1+\omega_{ca,in}} \dot{m}_{cach,in} \tag{1.8}$$

The mass flow rates of the oxygen and nitrogen to the cathode channel are calculated as follows:

$$\dot{m}_{i,cach,in} = x_i \dot{m}_{a,cach,in} = x_i \frac{1}{1+\omega_{ca,in}} \dot{m}_{cach,in} \quad ,i = [O_2, N_2] \tag{1.9}$$

The mass fraction of oxygen (x_{O2}) and nitrogen (x_{N2}) in the dry air are defined as:

$$x_{O_2} = y_{O_2} M_{O_2} M_a^{-1} \tag{1.10}$$

$$x_{N_2} = (1 - y_{O_2}) M_{N_2} M_a^{-1} \tag{1.11}$$

The molar mass of dry air (M_a) is expressed by the sum of the mass fraction of oxygen and nitrogen and the respective molar masses:

$$M_a = y_{O_2} M_{O_2} + (1 - y_{O_2}) M_{N_2} \tag{1.12}$$

The above equations (1.1-1.12) describe the dependence of masses from the inlet mass flows in the channel and the dynamics in the cathode's GDL. The outlet mass flows are also required to conclude the description of the dynamics evolving at the cathode. We

assumed that no liquid water enters the cathode or the anode channel. Also, the membrane allows only the transport of water in vapor state due to its waterproof nature. Therefore, the liquid water is produced by the reaction inside the cathode and part of it is evaporated or condensed inside the channel. The evaporation/condensation dynamics inside the cathode are expressed by:

$$\dot{m}_{evap,cach} = \left(p_{sat}\left(T_{fc}\right) - p_{v,cach} \right) \frac{V_{cach} k_{cond} M_v}{R T_{fc}} \tag{1.13}$$

The overall mass balance of the water in liquid phase is:

$$\dot{m}_{l,cach,out} = \dot{m}_{l,caGDL} - \dot{m}_{evap,ca} \tag{1.14}$$

The outlet mass flow rate of the oxygen, nitrogen and vapor in the cathode channel can be determined by:

$$\dot{m}_{k,cach,out} = \frac{m_{k,cach}}{m_{a,cach} + m_{v,cach}} \dot{m}_{cach,out} \quad ,k=[O_2, N_2, v] \tag{1.15}$$

At the cathode the condensed liquid water is dragged by the air, so the outlet flow is:

$$\dot{m}_{cach,out} = K_{cach,out}\left(p_{cach} - p_{out}\right) \tag{1.16}$$

The partial pressures of the gases in the channel are calculated using the ideal gas law and the overall cathode pressure is determined by the summation of the partial pressure of each species:

$$p_{k,cach} = \frac{R T_{fc}}{V_{cach} M_k} m_{k,cach} \quad ,k=[O_2,N_2,v] \tag{1.17}$$

$$p_{cach} = p_{O2,cach} + p_{N2,cach} + p_{v,cach} \tag{1.18}$$

The equations that describe the anode part of the fuel cell are analogous to the ones describing the cathode part. The values of all parameters used for channel dynamics are summarized in Table 3.2.

Table 3.2 Flow channel parameters

Parameter	Value
m_{fc}	1.378 kg
Cp_{fc}	772.57 J/kg·K
A_{fc}	25 cm^2
V_{anch} , V_{cach}	$0.136 \cdot 10^{-4}$ m^3
δ_{anch} , δ_{cach}	1.25mm
$K_{anch,out}$	0.001kg/(bar·s)
$K_{cach,out}$	0.001kg/(bar·s)
k_{cond}	100 s^{-1}

3.4.2 Gas Diffusion Layer (GDL) dynamics

Each gas diffusion layer is considered a volume with homogeneous properties. A mixture of hydrogen and water vapor flows through the anode GDL, while a mixture of oxygen, nitrogen, and water vapor flows through the cathode GDL. The above gases must diffuse throughout the GDL to reach the membrane. Nitrogen diffusion is neglected since it is an inert gas. The oxygen and hydrogen mass flow rates between the GDL and the cathode and the anode channel respectively are described by:

$$\dot{m}_{k,GDL} = A_{fc} M_k N_{k,GDL} \quad ,k = [O_2, H_2] \tag{1.19}$$

The molar flux of the vapor that is generated via the electrochemical reaction and the molar fluxes of the reactants are calculated from the electric current and the stoichiometry of the reaction as follows:

$$N_{v,gen} = \frac{I}{2FA_{fc}} \tag{1.20}$$

$$N_{O_2,GDL} = \frac{I}{4FA_{fc}} \tag{1.21}$$

$$N_{H_2,GDL} = \frac{I}{2FA_{fc}} \tag{1.22}$$

The water vapor mass flow rate depends on the membrane active area, the vapor molar mass and the vapor diffusion molar flux flow between GDL and anode and cathode:

$$\dot{m}_{v,kGDL} = A_{fc} M_{H2O} N_{v,k} \quad ,k = [an, ca] \tag{1.23}$$

where $N_{v,k}$ is the molar flow rate per unit area (flux) of the vapor diffusion which is calculated by the effective diffusivity (D_{eff}) the thickness of the diffusion channels (δ_{GDL}) and the concentration gradients ($c_{v,anGDL}$,$c_{v,caGDL}$):

$$N_{v,k} = -D_{eff,H_2O} \frac{\left(c_{v,kch} - c_{v,kGDL}\right)}{\delta_{GDL}} \quad , k = [an, ca] \tag{1.24}$$

As the oxygen is assumed to be in the same pressure with the channel, diffusion will be imposed by the electrochemical reaction. The effective diffusion coefficient that will be used for the calculation of the pressure is a function of the porosity (ε_{por}) of the layer as described in Nam and Kaviany (2003):

$$D_{eff} = D_{ref} \varepsilon por \left(\frac{\varepsilon_{por} - \varepsilon_p}{1 - \varepsilon_p} \right)^{da} \tag{1.25}$$

where ε_p is a percolation threshold which for porous media is composed of two-dimensional, long and overlapping, random fiber layers, ε_p is equal to 0.11 and *da* is an empirical constant which is 0.785 for cross-plane diffusion (Dutta *et al.*, 2001).

The partial pressure of water vapor in each GDL is calculated through the respective mass balance equation:

$$\frac{dp_{v,caGDL}}{dt} = RT_{fc} \left(\frac{N_{v,gen} + N_{v,mem} - N_{v,ca}}{\delta_{GDL}} \right) \tag{1.26}$$

$$\frac{dp_{v,anGDL}}{dt} = RT_{fc} \left(\frac{N_{v,an} - N_{v,mem}}{\delta_{GDL}} \right) \tag{1.27}$$

Since a uniform diffusion is assumed, the partial pressures of oxygen and hydrogen inside the respective GDL are expressed by:

$$p_{O_2,GDL} = p_{O_2,cach} - \frac{RT_{fc}\delta_{GDL}}{D_{eff,O_2}} N_{O_2,GDL} \tag{1.28}$$

$$p_{H2,GDL} = p_{H2,anch} - \frac{RT_{fc}\delta_{GDL}}{D_{eff,H2}} N_{H_2,GDL} \tag{1.29}$$

3.4.3 Membrane model

The membrane hydration model calculates the water mass flow rate that crosses the membrane and the water content in the membrane. Given that the membrane only allows the transport of vapor water, the following equations are only considering gaseous water, which is also assumed to be uniformly distributed over the surface area of the membrane. A set of semi-empirical equations are employed from Dutta *et al.* (2001). The overall mass flow rate of vapor that crosses the membrane is given by:

$$\dot{m}_{v,mem} = M_{H_2O} A_{fc} N_{v,mem} \tag{1.30}$$

The flow of vapor water through membrane is affected by two phenomena, the electro-osmotic drag ($N_{v,osm}$), caused by hydrogen ion drag, and the back diffusion ($N_{v,diff}$), caused by water concentration gradient between the cathode and the anode. These two phenomena are mathematically expressed by:

$$N_{v,osm} = n_d \frac{I}{A_{fc} F} \tag{1.31}$$

$$N_{v,diff} = a_w D_w \frac{c_{v,cach} - c_{v,anch}}{\delta_{mem}} \tag{1.32}$$

Where n_d is the drag coefficient, D_w is the diffusion coefficient, δ_{mem} is the membrane thickness and $c_{v,anch}$, $c_{v,cach}$ are the water concentration in anode and cathode channel

respectively. Based on the combination of those phenomena the net overall vapor molar flow ($N_{v,mem}$) across the membrane is expressed by:

$$N_{v,mem} = N_{v,osm} - N_{v,diff} \tag{1.33}$$

The vapor concentration at anode and cathode surfaces ($c_{v,anch}$, $c_{v,cach}$) of the membrane is a function of the water content at these surfaces and it is calculated by the membrane dry density $\rho_{mem,dry}$ and the membrane dry equivalent weight $M_{mem,dry}$:

$$c_{v,k} = \frac{\rho_{mem,dry}}{M_{mem,dry}} \lambda_k \quad \text{,k=[anch,cach]} \tag{1.34}$$

To calculate the water content at the membrane surfaces the vapor activity inside each GDL is (Springer *et al.*, 1991):

$$\lambda_{kch} = 0.043 + 17.81a_k - 39.85a_k^{\,2} + 36a_k^{\,3} \quad \text{,k=[an,ca]} \tag{1.35}$$

The vapor activity (α_κ) is the ratio of the water vapor pressure to the saturation pressure which in case of gas it is equivalent to relative humidity (φ_κ) of each GDL channel.

$$\phi_{kGDL} = \frac{p_{v,kGDL}}{p_{sat}(T_{fc})} \quad \text{,k=[an,ca]} \tag{1.36}$$

The relationship between the water content at the anode surface of the membrane and the electro-osmotic drag coefficient n_d is given by Dutta *et al.* (2001):

$$n_d = 0.0029\lambda_{anch}^{\,2} + 0.05\lambda_{anch} - 3.4 \cdot 10^{-19} \tag{1.37}$$

The water diffusion coefficient (D_w) is expressed by the membrane water content at the anode surface:

$$D_w = D_{\lambda anch} \exp\left(2416\left(\frac{1}{303} - \frac{1}{T_{st}}\right)\right) \tag{1.38}$$

Where ($D\lambda_{anch}$) is modified based on the relative humidity level that affects the water content at the anode surface (λ_{anch}):

$$D_{\lambda_{anch}} = \begin{cases} 10^{-10} & \lambda_{anch} < 2 \\ 10^{-10}(1 + 2(\lambda_{anch} - 2)) & 2 \le \lambda_{anch} \le 3 \\ 10^{-10}(3 - 1.67(\lambda_{anch} - 3)) & 3 < \lambda_{anch} < 4.5 \\ 1.25 \cdot 10^{-10} & \lambda_{anch} \ge 4.5 \end{cases} \tag{1.39}$$

The physical parameters in the membrane model and the GDL dynamics are taken from the fuel cell specifications used on the actual unit. These parameters are summarized in Table 3.3.

Table 3.3 Membrane parameters

Parameter	Value
$M_{mem,dry}$	1.1 kg/mol
$\rho_{mem,dry}$	$1.98 \cdot 10^{3}$ kg/m^3
δ_{mem}	$8.89 \cdot 10^{-5}$ m
δ_{GDL}	$1.9 \cdot 10^{-5}$m
ε_{por}	78%

3.5 Energy Balance

A dynamic thermal model describes the behavior of the fuel cell temperature based on the overall energy balance equation of the fuel cell. The amount of energy which is not converted to electrical power is expressed by a set of various energy terms that are associated with the fuel cell operation:

$$m_{fc} Cp_{fc} \frac{dT_{fc}}{dt} = \Delta\dot{\mathrm{H}}_{an} + \Delta\dot{\mathrm{H}}_{ca} + \Delta\dot{\mathrm{H}}_{chem} + \dot{Q}_R - \dot{Q}_{rad} - \dot{Q}_{\mathrm{conv}} - P_{elec} \qquad (1.40)$$

where m_{fc} denotes the mass of the fuel cell and Cp_{fc} is the specific heat calculated for the system under consideration. The above equation takes into account the differences of the energy flow rates between the input and output streams at the anode ($\Delta\dot{\mathrm{H}}_{an}$) and the cathode ($\Delta\dot{\mathrm{H}}_{ca}$), the rate of energy produced by the chemical reaction ($\Delta\dot{\mathrm{H}}_{chem}$), the rate of energy which is released to the environment through radiation ($\dot{Q}_{rad}$) and the rate of heat losses to the environment ($\dot{Q}_{amb}$). Also, the heat supplied by the heating resistance ($\dot{Q}_R$) is included along with the heat which is removed by the air cooling system ($\dot{Q}_{cl}$).

The last term P_{elec} is the amount of energy which is converted to electrical power. The changes of the anode and cathode energy flow rates are given by the changes of enthalpy as follows:

$$\Delta\dot{H}_{an} = \Delta\dot{H}_{H_2} + \Delta\dot{H}_{H_2O,an} \tag{1.41}$$

$$\Delta\dot{H}_{ca} = \Delta\dot{H}_{Air} + \Delta\dot{H}_{H_2O,ca} \tag{1.42}$$

Only a part of the oxygen and hydrogen fed in the inlet channels participate in the reaction. Therefore, the remaining amount of energy passes through the system to the outlet. For each gas the enthalpy change is calculated as follows:

$$\Delta\dot{H}_{H_2} = \dot{m}_{H_2,anch,in}\Delta h_{H_2,an,in} - \dot{m}_{H2,anch,out}\Delta h_{H_2} \tag{1.43}$$

$$\Delta\dot{H}_{Air} = (\dot{m}_{O_2,cach,in}\Delta h_{O_2,ca,in} + \dot{m}_{N_2,cach,in}\Delta h_{N_2,ca,in}) - (\dot{m}_{O_2,cach,out}\Delta h_{O_2,ca} + \dot{m}_{N_2,cach,out}\Delta h_{N_2,ca}) \tag{1.44}$$

$$\Delta\dot{H}_{H_2O,k} = \dot{m}_{v,kch,in}\Delta h_{H_2O,v,k,in} - \left(\dot{m}_{v,kch,out}\Delta h_{H_2O,v} + \dot{m}_{l,kch,out}\Delta h_{H_2O,l}\right) \quad ,k = [an, ca] \tag{1.45}$$

It is assumed that the required energy for the change of water phase is negligible therefore it is not incorporated in the above equations. In order to calculate the enthalpy differences at the anode and the cathode, the changes of mass specific enthalpies with respect to a reference state of the participated gases are used, assuming constant specific heat.

$$\Delta h_{i,an,in} = Cp_i\left(T_{an,in} - T_{ref}\right) \quad ,i = [H_2, H_2O,_v] \tag{1.46}$$

$$\Delta h_{i,ca,in} = Cp_i\left(T_{ca,in} - T_{ref}\right) \quad ,i = [O_2, N_2, H_2O,_v] \tag{1.47}$$

$$\Delta h_i = Cp_i\left(T_{fc} - T_{ref}\right) \quad ,i = [H_2, O_2, N_2, H_2O,_l, H_2O,_v] \tag{1.48}$$

Where T_{ref} is the reference temperature.

The reaction that converts the chemical energy into electricity and forms liquid water is always exothermic and the produced enthalpy is calculated as the difference between the enthalpy of the produced water and that of the reactants at the anode and the cathode GDL.

$$\Delta\dot{H}_{chem} = \dot{m}_{H_2,GDL}\Delta h_{H_2,an,in} + \dot{m}_{O_2,GDL}\Delta h_{O_2,ca,in} - \dot{m}_{H_2O,gen}\left(\frac{\Delta H_r(T_{ref})}{M_{H2O}} + \Delta h_{H_2O,v}\right) \tag{1.49}$$

Where ΔH_r^o is the mass specific enthalpy of formation of liquid water.

A part of the produced heat is released to the environment through radiation:

$$\dot{Q}_{rad} = \varepsilon_{em}\sigma\, A_{tot}(T_{fc}^4 - T_{ref}^4) \tag{1.50}$$

Where ε_{em} is the emissivity of the fuel cell body, the σ is the Stefan-Boltzmann constant and A_{tot} denotes the overall outer surface of the fuel cell.

As stated earlier due to the reaction an excess amount of heat is generated during the operation of the fuel cell since only a part of the produced enthalpy is converted to electrical energy and the rest is converted to thermal energy, resulting in an increase of the temperature. Also, as the fuel cell has a different temperature than its environment, heat is lost through convection ($\dot{Q}_{\mathrm{co}nv}$) to its environment. The amount of heat which is transferred to the surroundings consists of a natural convection term and a forced convection term.

$$\dot{Q}_{conv} = \dot{Q}_{amb} + \dot{Q}_{cl} \tag{1.51}$$

The heat loss to the environment caused by natural convection is expressed by:

$$\dot{Q}_{amb} = h_{amb} A_{tot}\left(T_{fc} - T_{amb}\right) \tag{1.52}$$

where h_{amb} is the natural convection heat transfer coefficient.

A cooling system is used for the removal of the excess heat and to maintain the desired fuel cell temperature. The heat energy removed by the cooling system is expressed by:

$$\dot{Q}_{cl} = h_{forc} A_{cl}\left(T_{fc} - T_{cl}\right) \tag{1.53}$$

$$h_{forc} = K_{cl1} P_{cl}^{K_{cl2}} \tag{1.54}$$

where h_{forc} is the forced convective heat transfer coefficient and A_{cl} is the effective surface for the cooling system. The forced convection heat transfer coefficient is calculated based on two experimentally defined parameters (K_{cl1},K_{cl2}) and the power (P_{cl}) of the fans.

The heat supply for the initial heat up of the fuel cell is expressed by:

$$\dot{Q}_R = P_R x_R \tag{1.55}$$

where P_R is the power of the heater and x_R is the fraction of power used for heating. The parameters used in the energy balance are summarized in Table 3.4.

Table 3.4 Thermal model parameters

Parameter	Value
A_{tot}	$355.27 \cdot 10^{-4}$ m^2
A_{cl}	$311.84 \cdot 10^{-4}$ m^2
h_{amb}	$1.73 \cdot 10^{-3}$ W/(m^{2}K)
K_{cl1}	1.24
K_{cl2}	1.38
P_R	55.8W
P_{cl}	25W

3.6 Electrochemical equations

The typical characteristics of the fuel cell are normally expressed in the form of a polarization curve, which is a plot of cell voltage versus cell current density. To determine the voltage-current relationship of the cell, the cell voltage has to be defined as the difference between an ideal Nernst voltage and a number of voltage losses (Fig. 3.3) as it is described in the current section.

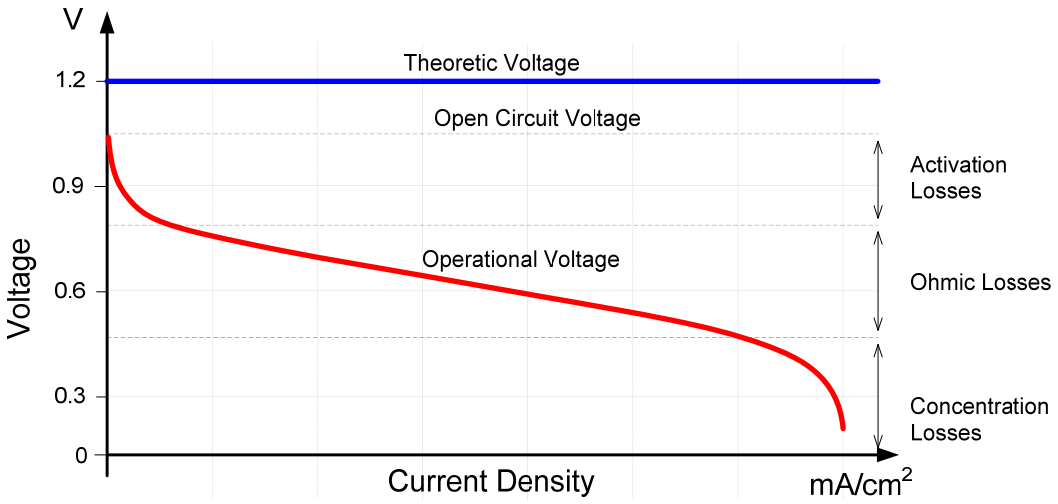

Figure 3.3 Theoretic vs. operational voltage

The main losses are categorized as activation, ohmic and concentration losses. The equation that takes under consideration the above losses expresses the actual cell voltage:

$$V_{cell} = E_{nernst} - V_{act} - V_{ohm} - V_{conc} \tag{1.56}$$

The above equation is able to predict the voltage output of PEM fuel cells of various configurations. Depending on the amount of current drawn the fuel cell generates the output voltage. The electric power produced by the system equals the product of the stack voltage V_{cell} and the current drawn I:

$$P = I \cdot V_{cell} \tag{1.57}$$

The Nernst voltage or open circuit voltage (OCV) falls as the current supplied by the stack increases. The reversible thermodynamic potential is calculated using the Nernst equation and can be expressed as:

$$E_{nernst} = E^0 + \frac{RT}{2F} \ln\left(\frac{p_{H_2} \sqrt{p_{O_2}}}{p_{H_2O}} \right) \tag{1.58}$$

The activation losses are caused by the slowness of the reactions taking place on the surface of the electrodes. A portion of the voltage generated is lost because of the chemical reaction that transfers the electrons to or from the electrodes. The activation losses are described by the Tafel equation (Mann *et al.*, 2000), which can be calculated as:

$$V_{act} = \xi_1 + \xi_2 T_{fc} + \xi_3 T_{fc} \ln(I) + \xi_4 T_{fc} \ln(c_{O2}) \tag{1.59}$$

This description for the activation overvoltage takes into account the concentration of oxygen at the catalyst layer and various experimentally defined parametric coefficients.

At a later stage of the fuel cell operation, as current density rises, ohmic losses (V_{ohm}) prevail. They are derived from the membrane resistance to the flow of electrons through the material of the electrodes and the various interconnections, as well as by the resistance to the flow of protons through the electrolyte (Pathapati *et al.*, 2004):

$$V_{ohm} = (\xi_5 + \xi_6 T_{fc} + \xi_7 I) I \tag{1.60}$$

Finally the mass transport or concentration losses result from the change in concentration of the reactants at the surface of the electrodes as the fuel is used. To calculate the diffusion losses a semi-empirical equation by (Kim *et al.*, 1995) was used:

$$V_{conc} = \xi_8 \exp(\xi_9 I) \tag{1.61}$$

The empirical parameters are related to the conductivity of the electrolyte (ξ_8) and to the porosity of the gas diffusion layer (ξ_9).

In the above equations ξ_k,(k=1..9) represent experimentally defined parametric coefficients the value which can vary from stack to stack. The values of these parameters are presented in Table 3.5. Some of these parameters are defined by the estimation procedure as described in the subsequent section.

Table 3.5 Electrochemical parameters

Parameter	Value
$\xi_1, \xi_2, \xi_3, \xi_4$	1.3205, $-3.12\cdot10^{-3}$, $1.87\cdot10^{-4}$, $-7.4\cdot10^{-5}$
ξ_5, ξ_6, ξ_7	$3.3\cdot10^{-3}$, $-7.55\cdot10^{-6}$, $7.85\cdot10^{-4}$
ξ_8, ξ_9	$3\cdot10^{-5}$, $6\cdot10^{-2}$

The developed model can couple both the theoretical validity (mechanistic equations) and the inherent simplicity of the empirical application (semi-empirical equations). Based on the aforementioned equations the model structure and the interactions between its parts are shown in Fig. 3.4.

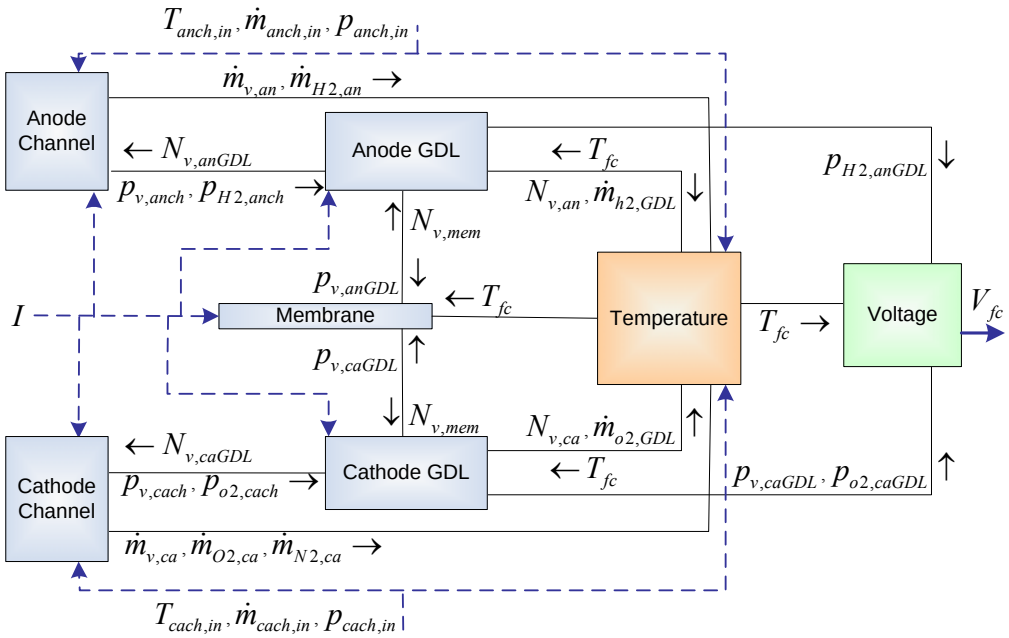

Figure 3.4 Fuel cell model structure

The described dynamic model is not system dependent as it can be adjusted to describe any other PEM fuel cell system by performing a number of sequentially executed actions. These actions are related to the determination of the physical characteristics of the PEM fuel cell, the unit specific parameters and finally the empirical parameters utilized by the electrical subsystem of the model. The value of the empirical parameters can be specified by a systematic parameter estimation procedure as long as experimental data or data from the manufacturer are provided. Finally the resulted estimated values are included to the model and a different set of data is necessary to explore the validity of the model against the fuel cell unit. The following section described the necessary actions to implement such procedure.

3.7 Parameter estimation and model validation

In order to assess the validity of the developed model, the PEM fuel cell unit described in the previous chapter, was used to generate experimental data under various conditions. Power load profiles up to the maximum point have been used for the estimation of model parameters and for the experimental validation of the model. There are two sets of model parameters: physical or estimated. The physical parameters are based on the fuel cell hardware specifications and listed in Tables 3.2, 3.3, 3.4 along with their values. The estimated parameters are the ones that cannot be physically determined. For this reason a formal systematic parameter estimation technique was employed in order to find the optimal values for the parameters. The purpose of this formal technique is to minimize the deviation between the model predictions and the experimental data.

The aforementioned model describes voltage as a function of the current, temperature and partial pressures. The polarization curve resulting from a set of electrochemical equations includes a few parameters, some of which are unknown, depending on the operating conditions, while others have been taken from the open literature. When an experiment is executed, to obtain the polarization curve, the voltage (dependent variable) is measured directly, but the parameters are not. Therefore, an estimation of these critical parameters is necessary in order to increase the predictive power of the model. The estimation procedure results in the determination of the optimal

values for these parameters. After the adjustment of the model to the optimal values, a validation procedure was performed under different operating conditions to assess the model accuracy.

3.7.1 Procedure and Representative set of data used

The technique that was followed for the parameter estimation relies on the variation of current, which is directly connected to the actual power demand and affects the temperature and the partial pressures of the reactants in the fuel cell. Consequently the change of the current affects voltage according to the polarization curve. Thus, the focus of the parameter estimation procedure is on the semi-empirical equations that describe the voltage losses. The estimation of critical voltage drop coefficients was made with using measurements that allowed the optimal tuning of the semi-empirical model.

The experimental procedure consists of reading the dynamic response of the cell voltage and cell power after the occurrence of small successive changes in the load demand. This experimental procedure intended to derive the fuel cell polarization curve and acquire data from the overall operational range. Two sets of experiments were conducted for the generation of data for the parameter estimation procedure. More specifically, in each experiment 11 different load levels were requested from the fuel cell. The duration of each request was set to 2min which is sufficient enough to obtain a steady-state voltage. The requested load varied from 0A to 20A with a step change of 2A. The varying operating condition was the pressure, 0barg and 1barg. The FC temperature was kept constant at 65°C and the humidification temperature was 75°C. The air flow was 2000cc/min and the hydrogen flow 500cc/min. The reproducibility of the experimental procedure and the accuracy of the results were ensured by the two above mentioned sets of experiments, consisting of four experiments at each condition.

3.7.2 Parameter Estimation and Results

The developed model has been implemented in the gPROMS modeling environment (PSE Ltd, 2010). Once the model was constructed, a sensitivity analysis was performed to identify the most critical model parameters which were further optimally selected. A detailed sensitivity analysis based on simulation results revealed the most critical parameters to be estimated. Thus comparing the prediction of the model to the experimental data a major deviation was observed at the beginning of the polarization curve, the area where the activation losses appear. Therefore, a parameter related to the activation losses equation was selected for the estimation procedure. Another important deviation was observed in the slope of polarization curve at the area of the ohmic losses. This indicates that the parametric coefficients at the ohmic losses should optimally be estimated. Finally the area of the concentration losses were not considered, as it should be avoided during normal operation, in order to avoid system failure.

A nonlinear regression technique with a constant variance model defining a maximum likelihood estimation problem was employed to determine the optimal values for the selected parametric coefficients. For the scope of the estimation procedure the model parameters (ξ_1, ξ_7) were expressed as (θ_1, θ_2) representing the estimated variables used in the maximum likelihood problem.

In the estimation procedure the parameters can be fitted independently or simultaneously. Although the independent parameter estimation is numerically more reliable, it cannot represent the coupling between the parameters; therefore the simultaneous approach is used. The data acquisition of the system variables is performed by various sensors. Each variable is associated with one sensor, which introduced an uncertainty in the data measurements or otherwise stated a measurement error. When solving an estimation problem the measurement errors (ε_i) are modeled by a variance model. In the aforementioned testing unit the measurement errors are assumed to be statistically independent and normally distributed with zero mean and therefore a constant variance model was used:

$$\sigma^2 = \sigma^2(z, B) = \omega^2(z^2 + \varepsilon) \tag{1.63}$$

where z is the model prediction of the measured quantity, ω is a parameter of the variance model and ε is a small but non-zero constant that ensures that the variance is still defined for predicted values that are equal to zero or very small.

Table 3.6 Parameters of the estimation procedure

Model Prediction	Measurements	Parameter ω	Constant ε
z_1	$\tilde{z}_1$	ω_1=0.05	ε_1=0.1·10^{-3}
z_2	$\tilde{z}_2$	ω_2=0.0047	ε_2=0.1·10^{-5}

The proposed nonlinear regression technique attempts to model the relationship between the measured data and the response of the model by fitting a quadratic equation to observed data. The estimation procedure is based on a maximum likelihood formulation which provides simultaneous estimation of parameters in the dynamic model of the fuel cell and the variance model of the measuring sensors. The maximum likelihood goal can be expressed by the objective function:

$$J_\theta = \frac{N}{2}\ln(2\pi) + \frac{1}{2}\min_\theta \sum_{i=1}^{nE}\sum_{j=1}^{nV_i}\sum_{k=i}^{nM_{ij}}\left[\ln(\sigma_{ijk}^2) + (\tilde{z}_{ijk} - z_{ijk})^2(\sigma_{ijk}^2)^{-1}\right] \tag{1.64}$$

where N is the total number of measurements taken during all experiments, θ are the model parameters to be estimated, constrained between a lower and an upper bound, nE are the number of experiments performed (nE=8), nV_i are the number of variables measured in the ith experiment (nV_i=2) and nM_{ij} are the number of measurements of the jth variable in the ith experiment (nM_{ij}=660).

The solution of the maximum likelihood problem determines the values for the uncertain physical and variance model parameters, (ξ_1, ξ_7). These values maximize the probability that the dynamic model will predict the measurement values obtained from the experiments. The measured variables ($\tilde{z}_1, \tilde{z}_2$) are the produced voltage and power, having a sample time of 2s and (z_1,z_2) are the model predicted values. The variation of the load is handled as a piecewise constant term during the estimation procedure, using the same interval duration (2min) as described in the experimental procedure. After the

solution of the aforementioned problem in gPROMS the estimated parameter values are summarized in Table 3.7.

Table 3.7 Results of the parameter estimation procedure

Variables	Est. Value	Up Bound	Low Bound	Std. Dev	95% Conf Int	95% t-value	Ref. t-value
θ_1	1.3205	1.4	0.954	$1.04 \cdot 10^{-3}$	$2.04 \cdot 10^{-3}$	$6.464 \cdot 10^{2}$	1.645
θ_2	$7.85 \cdot 10^{-4}$	$4.3 \cdot 10^{-3}$	$1.1 \cdot 10^{-6}$	$4.12 \cdot 10^{-6}$	$8.1 \cdot 10^{-6}$	$0.969 \cdot 10^{2}$	

The estimation results have sufficient accuracy and therefore the values of the parameters can be applied to the model for its validation. This is justified by the fact that the standard deviation is more than two orders of magnitude lower than the estimated value. Also, a clear indication of this accuracy is the 95% t-values of both estimated parameters which are larger than the reference t-value.

Besides the 95% confidence interval of each estimation parameter, another measure that indicates that the parameters are optimally defined is the confidence ellipsoid. It takes into account the correlation between the estimates of *θ1* and *θ2*. The individual 95% confidence intervals are appropriate to validate the possibility of specifying the range for each parameter under consideration independently of the value of the other parameter. The confidence ellipsoid interprets these intervals simultaneously. This alternative significance test is considered in Fig. 3.5 and it is based on whether the elliptically shaped area representing the joint confidence region encloses the optimal point at its center neighborhood. The joint confidence region illustrates that the parameters are known with the same precision and that the estimated point is optimal for both of them.

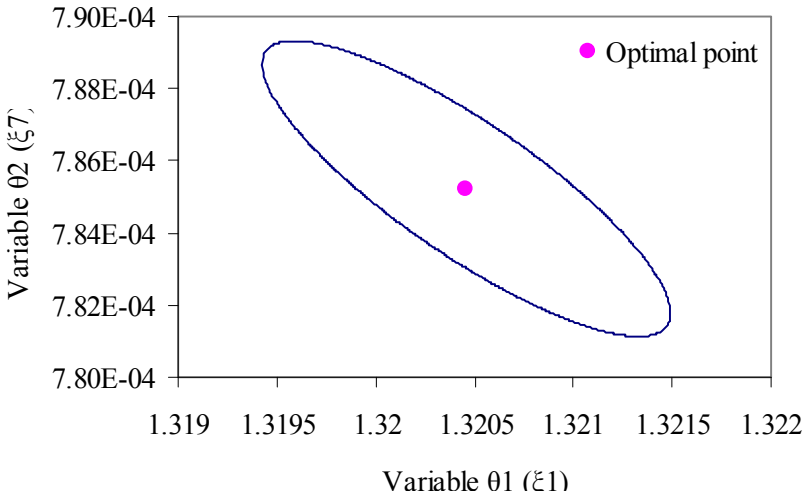

Figure 3.5 95% Confidence ellipsoid of the estimated values

Another measure which indicates that the estimation was performed successfully is the examination of the residuals using a corresponding diagram which illustrates the distribution of the observed error against time.

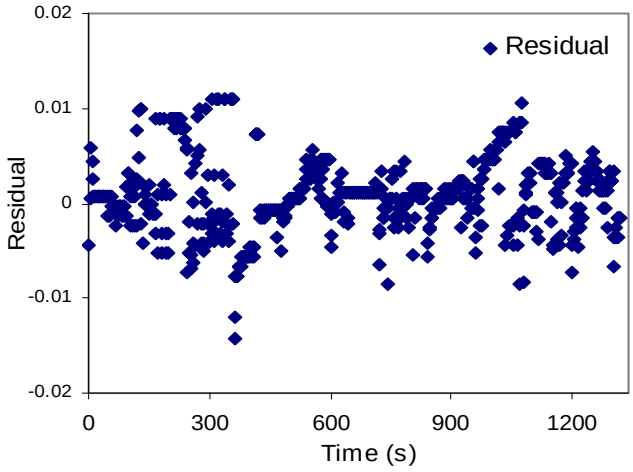

Figure 3.6 Residual Analysis

Fig. 3.6 illustrates a horizontal band of residuals which is indicative that a long-term effect is not influencing the data. Also, the observed error between the experimental and the predicted data is independent and it is randomly distributed. There are no significant outliers present which confirms that the applied regression technique provided accurate

results. This accuracy is better depicted by the corresponding polarization and power curves in Fig. 3.7.

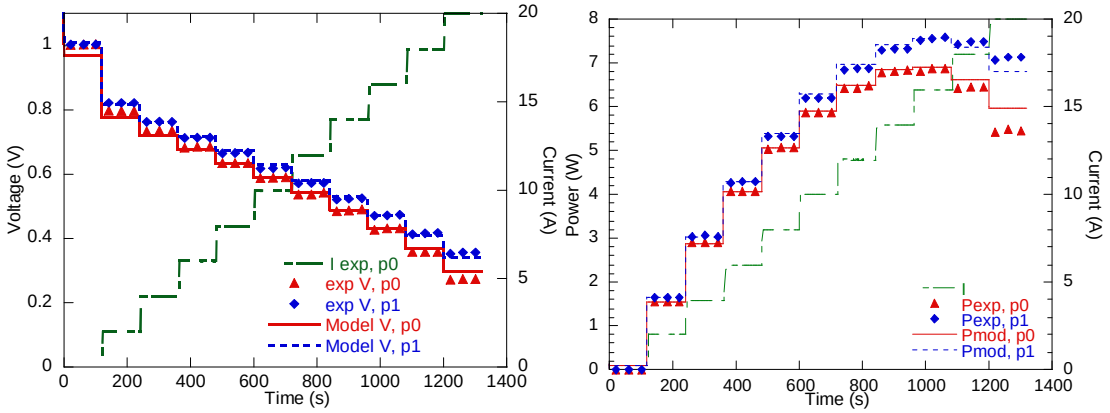

Figure 3.7 Experimental and model voltage and power (0barg, 1barg)

Model predictions are in a very good agreement with the experimental data for both conditions. It is found that the mean square-root difference between the experimental and the predicted voltage is 0.0389V. Thus, the optimal parameters provide to the model the accuracy to properly describe the behavior of the output voltage.

The optimal values for parameters $\xi_1(\theta_1)$ and $\xi_7(\theta_2)$ are presented in the second column of Table 3.7. It is not possible to fairly compare these parameters with those from other fuel cells units, since they are related to the specific system and they are empirical in nature. This is clearly illustrated in both the statistical metrics (Table 3.7, Fig. 3.5-3.6) and the comparison against experimental data (Fig. 3.7).

3.7.3 Model validation

To perform a comprehensive model validation study, the model with the optimal parameters was simulated with a few step changes of the input variable (current). In this section in order to validate the accuracy of the derived model (which incorporates the optimal parameter values), we compare its predictive power with new experimental data at various operating conditions. These conditions are different from the ones used for the parameter estimation procedure. An indicative set of experiments are presented to

demonstrate the accuracy of the model. The varying condition between the validation experiments is related to the pressure at two different levels, 0.5barg and 1.5barg. Fig. 3.8 illustrates a comparison between model prediction and experimental data. Again a good agreement is achieved.

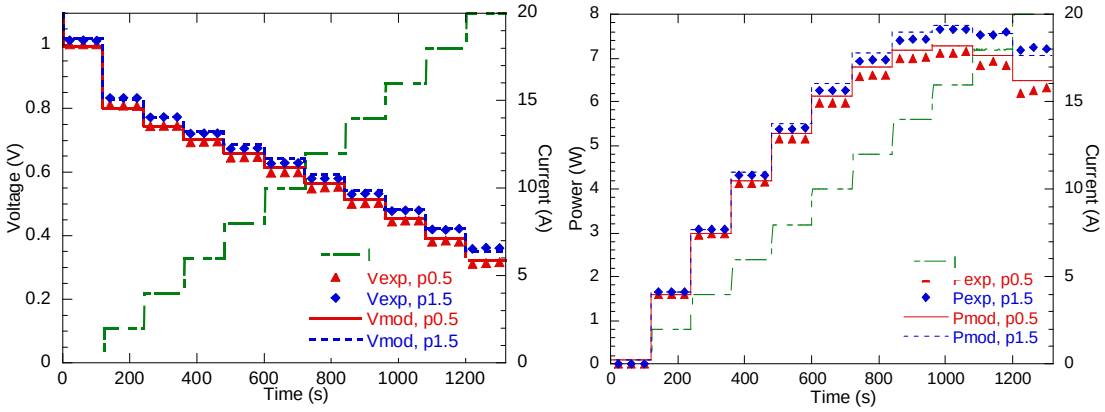

Figure 3.8 Experimental and model voltage and power (0.5barg, 1.5barg)

It is clear that under different pressure conditions the model response is very close to the experimental behavior for the whole range of current variation. Fig. 3.9 further illustrates the accuracy of the model with respect to response in two step changes in current (6A, 8A). The sampling time is 500ms and the duration of each step is 120s. A good agreement is observed between the measurements and the model predictions with a maximum error of 0.0027V.

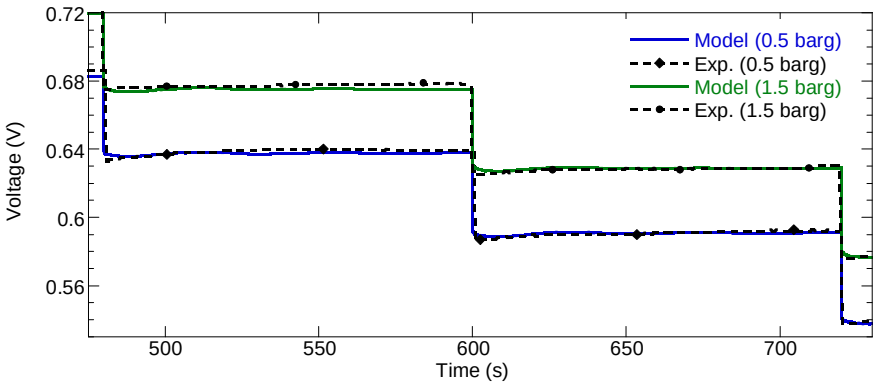

Figure 3.9 Voltage validation (0.5 barg, 1.5 barg)

During step changes in current an adequate voltage prediction is achieved by reproducing both the steady-state behavior between the step change and the dynamic behavior due to the instantaneous increase in current. In summary the proposed model demonstrates an excellent behavior both at steady and transient conditions and therefore it can be used both in startup and during variable load changes.

Figs 3.12 and 3.13 illustrate the steady-state and the dynamic response of the model against the experimental data from the unit at different temperature (55°C) compared to the one where the parameter estimation took place (65°C) the FC. It is observed that a negligible error exists between the model prediction and the real operation of the system both at steady-state and dynamic conditions.

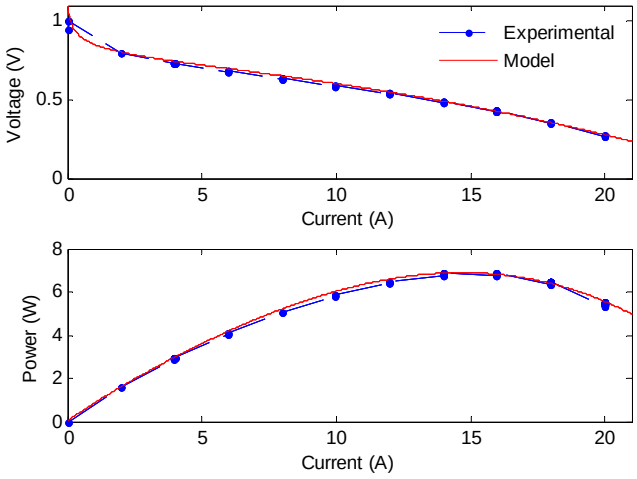

Figure 3.10 Steady State Response

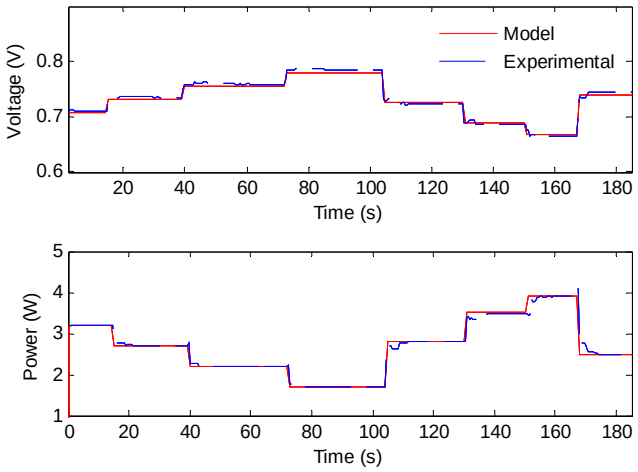

Figure 3.11 Dynamic Response

The mean square-root difference at steady-state was 0.018V while at dynamic step changes was 0.024V. The above metric was calculated using 600samples over a period of 600s and 660samples over a period 1320s for the steady-state and the dynamic case respectively. This measure is a clear indication that the model has the required accuracy to describe the behavior of the system.

3.8 Concluding remarks

In this chapter the basic criteria for selecting the appropriate modeling approach and model features are outlined along with an extensive literature review on the available PEM fuel cell models. Then a new dynamic model is presented relying on mass balances, an energy balance and electrochemical equations. To model mass transport phenomena a five volume approach is adopted that considers the mass dynamics in the gas flow channels, the gas diffusion layers (GDL) and the membrane. The energy balance includes all the necessary terms that describe the energy flow rate at the anode and the cathode, the rate of produced energy by the chemical reaction, the heat supplied by the resistance along with the various heat losses and the energy which is removed by the cooling system. Finally the electrochemical part includes a number of empirical parameters that model the voltage losses for the entire operating range of the fuel cell. Based on a formal parameter estimation procedure the optimal values for the empirical parameters are derived and the predictive power of the resulted model is validated against experimental data at different pressure and temperature conditions.

Overall the qualitative and quantitative response of the developed model indicated that it can capture accurately enough the behavior of the PEM fuel cell unit, a fact that guarantees its suitability for the subsequent model-based control studies.

Chapter 4

Control Issues and Challenges of PEM Fuel Cell Systems

The performance of a PEM fuel cell (PEMFC) is affected by the operating conditions and the subsystem's interactions as various phenomena are evolving during its operation. Therefore, it is necessary to be able to understand qualitatively and predict quantitatively the optimal operation of an integrated fuel cell system in order to protect its longevity and preserve its long-term performance. To achieve that it is important to apply a control scheme able to address the numerous challenges that arise during the operation of the fuel cell and to ensure a stable performance. But prior to the selection of an appropriate control scheme, it is essential to fully comprehend the nature of the control problem. Based on this motivation the scope of this chapter is to:

- provide an overview of the operating issues that affect the response of the system,
- determine the desired operating goals,
- propose an appropriate control configuration (in terms of manipulated and controlled variables of the system),
- formulate a mechanism to improve the operation of the PEMFC unit,

Furthermore, a literature review with some indicative control studies is provided that set the context for the control framework.

4.1 Operating issues and management subsystems

The response of a PEMFC system is affected by a number of design and operating factors, such as the properties of the materials that are used, the component of the subsystems, the partial pressures of hydrogen and oxygen in the gas channels, humidity of the membrane and the fuel cell temperature. Some of these factors are determined by the design specifications of the system and cannot be modified during the operation of the system while other factors, that influence the environment and the operating conditions, can be managed by proper control actions (Yuan *et al.*, 2010). Overall the behavior of a PEMFC is highly nonlinear and is governed by the complex interaction of its subsystems. Within a PEMFC several processes occur, but those that have the greater influence on the performance are related to the:

(a) the electrochemical reactions in the catalyst layers,

(b) the proton transfer in the electrolyte membrane layer and

(c) mass transport within all regions.

From these processes some management issues arise related to water, heat and gas management. To achieve a stable and good performance these issues need to be carefully handled. Also, the auxiliary subsystems and their topology are important factors that should be carefully considered. For instance an increase at the air flow rate and consequently the operating pressure, improves the produced power, but increases the auxiliary consumption. Humidification of the reactant gas is essential to keep the membrane hydrated, but too much humidification can cause water flooding. So there must be a balancing point for the operating conditions (Berg *et al.*, 2004). Furthermore, it is necessary to analyze the trade-off between the various parameters of the system in order to define the optimum region of operation as this choice leads to different characteristics for the unit regarding its performance, effectiveness and safety. However this is only feasible by optimizing the corresponding operating parameters such as the humidity, the temperature, the gas flow rate and the pressure as these parameters directly affect the water, heat and gas management, so that the fuel cell performance is finally determined.

4.1.1 Water and heat management

As the fuel cell operates the fuel cell produces, besides the useful power, two by-products, water and heat. Thus, the integrated system must include the means for their removal. A common practice is to direct the water to a drain while the heat can be discarded to the environment through the cooling system. The performance of PEM fuel cells is affected by the water formation and its removal especially when the operation is at high current densities, where the hydration of the membrane plays any important role in the overall behavior of the system (Bao *et al.*, 2006). The water transport can be determined by three different mechanisms:

(a) the electro-osmotic drag from the anode to the cathode due to potential difference

(b) the back diffusion from the cathode to the anode due to concentration gradient

(c) the pressure difference between the cathode and anode.

These water transport mechanisms result in a conflict that on the anode side, the membrane tends to dry out due to the electro-osmotic transport while on the cathode side, flooding caused by excessive liquid water accumulation may block the pores of the catalyst layers, the gas diffusion layers or even the gas channel (Baschuk and Li, 2005). Also, the excess of water also aggravates other problems such as corrosion and contamination of components. On the other hand the flooding phenomenon is dominated by the condensation and evaporation process in the cathode (Nguyen *et al.*, 2003), which is strongly affected by the temperature distribution. Therefore, a proper balance between water formation and water removal is necessary (McKay *et al.*, 2005).

The heat management in a PEMFC is inherently coupled with the water transport. Overall the balance between the produced heat and its removal determines the operating temperature of a PEMFC. Subsequently the temperature and water vapor pressure profiles within the MEA dictate the phase of water present in various regions and its transport from the membrane to the gas channels (Adzakpa *et al.*, 2008). Overall the fuel cell temperature is influenced by the inlet flows and the reaction rate. Thus, thermal and water transport mechanisms are intimately interlinked and one cannot study the fuel cell behavior without considering both of them (Muller and Stefanopoulou, 2006). Improper

heat management can cause membrane dehydration or cathode flooding. From the electrochemical point of view, an excessive increase of temperature increases the membrane resistance to the conduction of the protons and as a result the ohmic losses are intensified.

These stringent thermal requirements present a significant heat management challenge that affects the humidity of the gases and the temperature of the fuel cell. The water and heat management subsystem include the hydrators heating system, the heated lines between the hydrators and the inlet of the anode and the cathode, the air cooling fans and the heat-up resistances of the fuel cell.

4.1.2 Gas supply management

The gas supply management is concerned with the proper supply of the hydrogen and air to the fuel cell system. As the fuel cell operates there must be available a specific stoichiometric ratio of air and hydrogen as the power demand changes. On one hand the air supply should be carefully handled as it allows the electrochemical reaction to take place by utilizing the reactant and it determines the quality of the energy conversion rate (Djilali and Lu, 2002). On the other hand the hydrogen is the fuel that drives the reaction so respective management should take place. An insufficient oxidant supply might lead to an undesirable starvation phenomenon that can cause performance deterioration and accelerate the fuel cell degradation.

In commercial systems the air is supplied to the cathode by an air compressor while in small-scale systems, such as the one used in the current thesis, the air is provided by a pressurized cylinder due to the low flow rate requirements. On the anode side the hydrogen is usually stored in high pressure cylinder and is supplied through a mass flow controller.

4.1.3 Power management

An equally important factor, as the heat and water management, is related to the power of the fuel cell. In various works the demanded power which is achieved though proper current or voltage manipulation (depending on the mode of operation of the converting device), is treated as an external disturbance when power management is not considered (Vahidi *et al.*, 2006). But when an overall power management scheme is designed and developed it is important to be able to determine the current that will be applied to the fuel cell for the fulfillment of the requested load. More specifically when a centralized approach is used the demanded power is achieved though a multivariable control approach that considers the current as a manipulated variable. The appropriate current is determined by the control configuration and is set to the DC/DC converter or to the DC electronic load when the converter and the load are topologically merged into one common device. The later configuration is a common practice where fuel cell stations are used for testing purposes or during the initial setup of a stationary system where the load in not connected from the beginning.

4.1.4 Temporal behavior and membrane degradation

Another interesting factor that should be considered during the design of a control system is the temporal behavior of the fuel cell. As the fuel cell system operates over time, the produced voltage might deviate from its nominal. There are two main reasons that justify this deviation, hydration issues related to temperature and water management and material issues related to membrane degradation.

The voltage deviation which is caused by the lack of hydration is reversible while the deviation caused by degradation is not reversible. The main consequence of dehydration is drying of the proton-conducting membrane. When the system starts-up a temporary deviation may occur by the fact that the membrane might not be fully hydrated. This deviation is reduced after a while when the membrane is properly hydrated and afterwards the system's response is stable when repeated experiments are performed at the same conditions.

On the other hand, for longer periods of time, (e.g. few months) a deviation from the expected behavior is observed due to the degradation in the membrane and this is a permanent deviation. The voltage degradation rate is normally an indication of the fuel cell state of health and it ranges between 1 and 10 μV/hr (Schmittinger and Vahidi, 2008) which can be increased at extreme operating conditions. The performance of the fuel cell deteriorates through time and this is one of the main issues that affect the durability of fuel cell systems.

Such behavior is also encountered by the system that was used during this thesis. Driven by these practical issues it is important to rely on a control scheme able to compensate such an offset in the system's behavior and simultaneously can handle the management of the interacting subsystems.

According to the aforementioned issues the performance of an integrated fuel cell system is highly affected by the proper water, heat and gas supply management which are governed by a respective set of operating parameters and variables. Based on that, the optimum operation can be defined by the use of a control approach, able to provide information regarding the state of the water, the evolution of the humidity level and the gas flow. Fig. 4.1 illustrates the conceptual boundaries of the management subsystems of the PEM fuel cell unit which was described in Chapter 2.

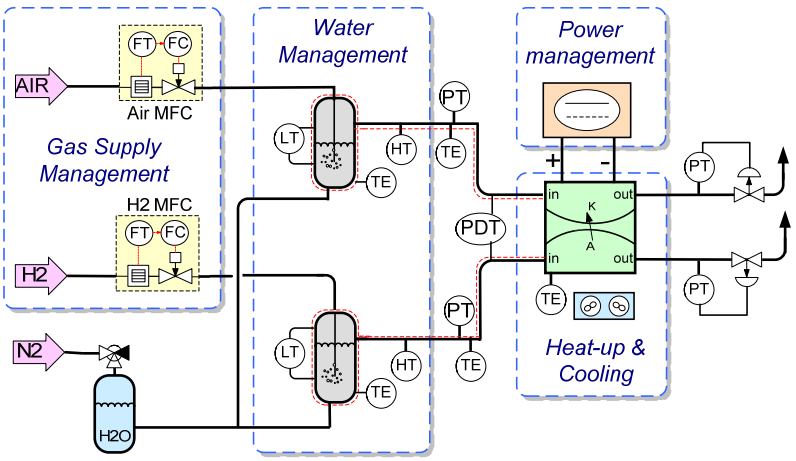

Figure 4.1 Management subsystems of the PEM fuel cell unit

4.2 Literature review on control of PEM fuel cell systems

Based on the aforementioned analysis a fuel cell system typically consists of various subsystems for power conditioning, air, fuel and heat management. Although there is a coupling among these subsystems, the control strategies proposed in the literature deal with the respective control issues in a decentralized or centralized manner. Some strategies focus in a particular objective aiming at the regulation of a specific subsystem while others on the overall integrated system. Also, besides the control objective which is related to the respective subsystem of the fuel cell, a multitude of different type of controllers have been proposed in the literature and different control configurations can be employed for achieving the same objective. Over the past few years significant developments have been made in the area of fuel cell control. An indicative only review of the various control approaches using different type of controllers follows.

4.2.1 Feedforward and feedback control strategies

A feed-forward/feedback scheme for power tracking based on manipulations of cathode flow as well as fuel cell current output was proposed in Pukrushpan *et al.* (2004) where the feedback scheme also employs a state observer driven by a system model and measurements of compressor flow rate, manifold pressure and stack voltage. The issue of air starvation in PEMFCs has also been extensively studied in Pukrushpan *et al.* (2004b) while another approach includes the use of a reference governor formulation that imposes an oxygen concentration constraint (Sun and Kolmanovsky, 2005). A feedback control structure can address several PEMFC control objectives, including power, temperature, humidity and oxygen control. For example the cell power was controlled by a cascade control structure in Lauzze and Chmielewski (2006). Another approach for the air feed control problem of a fuel cell is the use of single input single output sliding mode controller making that utilizes a low-order linear model (Garcia-Gabin, 2009). The regulation of the output power is addressed in Woo and Benziger (2007) by employing a feedback control strategy using dry feeds at exact stoichiometry with complete utilization of the hydrogen and the oxygen. In Zenith and Skogestad (2007) a control system based on switching rules in order to control the converter's output voltage using a simplified

dynamic model, while in Zenith and Skogestad (2009) the study deals with the relatively slow transients associated with the mass and energy balances resulting a control scheme with the control loops for power (or voltage), hydrogen pressure, temperature and oxygen concentration. An optimal control strategy that minimizes the hydrogen consumption in a hybrid fuel cell system is proposed in Rodatz *et al.*(2005).

4.2.2 Adaptive control strategies

A number of adaptive control strategies have also been proposed in the literature. An adaptive control algorithm (ARMAX model based) that dynamically stabilizes the oxygen excess ratio around an optimal level is presented in Zhang *et al.* (2008). In Zumoffen and Basualdo (2010) an adaptive predictive control with robust filter is analyzed using a nonlinear dynamic control oriented model and the feedforward actions are improved by an adaptive feedback structure while in Jiang *et al.* (2007) an adaptive strategy that adjusts the output current set-point of the fuel cell is presented. A linear and a nonlinear adaptive controller are synthesized in Bao *et al.* (2006) that aim to the control independently the air stoichiometric ratio, gas pressures and power output by manipulating the air compressor and the output valves. A simulation study is performed in Kolavennu *et al.* (2011) using a SISO adaptive controller in conjunction with a linear reference model for tracking the power profile in a fuel cell system. In Methekar *et al* (2010) the power density is controlled by the voltage and air flow manipulation targeting the power peek of the fuel cell incorporating a nonlinear black box time series model in conjunction with a parameter estimation scheme using recursive least squares.

4.2.3 Advanced control strategies

Some other approaches proposed advanced control strategies for the PEMFC. For instance in Wu *et al.* (2009) a multivariable predictive control with constraints using a reduced order model is presented that guarantees a safe operation as well as long lifetime of the fuel cell in a hybrid system. On the other hand, a single variable model-based predictive control is presented in Gruber *et al.* (2009) to control the oxygen excess ratio using the compressor motor voltage to manipulate the air flow rate which is also tested experimentally. In Danzer *et al.* (2008) a model-based multivariable controller is

developed that aims at the control of the cathode pressure and the oxygen excess ratio of a PEMFC using the oxygen mass flow controller and the outlet throttle as actuators. A tracking observer was employed to estimate the partial pressure using the measurement of the air pressure at the outlet throttle of the fuel cell system. A nonlinear model predictive controller was designed in Golber and Lewin (2004) to cope with the static gain reversal and control the power using current as manipulated input. The issue of power control is addressed by the use of unconstrained linear MPC and linear quadratic Gaussian (LQG) controllers that incorporate state space models in Methekar *et al.* (2010b), where the behavior of the unconstrained LMPC and the LQG is experimentally explored using a single fuel cell. Overall the dynamics of the PEM fuel cell are highly nonlinear and they are affected by the operating conditions, which include the effects of the output current, the temperature and the humidity (Cho *et al.*, 2008; Benziger *et al.*, 2006).

In the context of advanced control strategies an approach that utilizes explicitly a MPC formulation has been also proposed. Puig *et al.* (2007) proposed a fault tolerant explicit formulation that uses as manipulated variables the air feed through the compressor voltage and includes the detection of faults in the actuator that affect the compressor range of operation. Arce *et al.* (2010) developed an explicit predictive control strategy in conjunction with a load governor and a PI controller that aims at the avoidance of oxygen starvation criterion and the maximum efficiency of the system.

4.2.4 Experimentally validated control studies

Besides the numerous works that perform simulation-based design and analysis of the behavior of the fuel cell system, there is a need for experimental verification through online deployment of the various proposed control schemes Varigonda and Kamat, (2006). A number of experimental studies can be found in the literature that exemplify the use of various control configurations focusing on one objective at a time. The safety of the system which is maintained by avoiding air starvation has been experimentally achieved by an adaptive controller (Yang *et al.*, 2007), a sliding mode controller (Gabin *et al.*, 2010), (Talj *et al.*, 2010), a super twisting algorithm (Kunusch *et al.*,2012), a combined mpMPC with a PI control scheme (Arce *et al.*, 2010) and an NMPC approach based on a Volterra series model (Gruber *et al.*, 2012).

On the other hand, the temperature management can be achieved by a PI loop (More *et al.*, 2010) or an explicit MPC controller (Arce *et al.*, 2011) while the pressure is controlled using an adaptive state feedback scheme (Tong *et al.*, 2009). Another interesting work addresses the issue of maximum efficiency as a function of stoichiometry, temperature and humidity using an adaptive control scheme (Kelouwani *et al.*, 20012).

4.3 Control objectives for the PEM fuel cell unit

As stated earlier the durability and performance of a PEM fuel cell are influenced by the operating conditions. Therefore, it is of vital importance to control the various subsystems responsible for maintaining a stable operating environment while ensuring an economically attractive operation. Overall the objectives for the control system are to effectively address the issue of power generation in an optimum manner. In this context the optimality is defined by the three constituents:

- Operation at a safe region regardless of the load fluctuations.
- Minimization of the fuel consumption and air supply.
- Maintenance of stable temperature conditions ensuring proper gas humidification.

One of the most important considerations for the control of the fuel cell is to guarantee that the operation is within a safe region which is expressed by avoiding fuel and oxidant starvation. It is important to prevent such phenomenon as it affects the longevity of the fuel cell and can cause irreversible damage to the membrane (Schmittinger and Vahidi, 2008). Moreover this is very critical when abrupt changes on the load occur. Such case can cause a sudden increase for gas supply demand since the oxygen and hydrogen react instantaneously and the level of the gases are reduced drastically.

From the fuel point of view, it is desirable to supply the amount of hydrogen close to the required one. A recycling line is not yet present at the fuel cell unit which means that the unreacted hydrogen will be released to the vent. Therefore, one of the control objectives is to minimize the supplied hydrogen in conjunction with the previous objective for safe operation.

Another significant factor that should be considered is the proper handling of the operating temperature, as it affects the long-term performance of the fuel cell. The operation at an elevated temperature accelerates the degradation phenomena and can influence the durability of the fuel cell. Furthermore, the temperature directly affects the rate of chemical reactions and transport of vapor and reactants (Ahn and Choe, 2008). As the hydrators, used for the humidification of the gases, operate at a stable temperature point, it is important to maintain the fuel cell operating temperature, in order to keep the water content of the gases at a desired level.

4.3.1 Variables and control configuration

In the considered system there are four distinct control objectives, one direct external and three indirect internal objectives. The main control objective is to fulfill the varying power demand at acceptable response time, avoiding oxygen starvation while minimizing the hydrogen consumption at stable temperature conditions. Once the environment of fuel cells has been clearly determined, it is necessary to identify the controlled and corresponding manipulated variables which will be used to device the appropriate control scheme that make the system to respond as requested.

More specifically the desired power (P_{sp}) is delivered by properly manipulating the current (I) which is applied to the fuel cell by the converter (DC electronic load) connected to the system. In our case the mode of operation for the electronic load is set to constant current (CC) since the boundaries of the system were identified by the experimental study performed during the activation of the fuel cell.

The safe operation is maintained by controlling the reactants at a certain excess ratio level in order to avoid starvation caused by sub-stoichiometric reaction conditions at the cathode and the anode. The safe operating region for the cathode and the anode is defined by two unmeasured variables, the oxygen and hydrogen excess ratios (λ_{O2}, λ_{H2}), expressed as the ratios of the input flow of each gas to the consumed quantities per unit time due to the reaction (Pukrushpan *et al.*, 2004):

$$\lambda_{O2} = \frac{\dot{m}_{O2,cach,in}}{\dot{m}_{O2,caGDL}} \tag{4.1}$$

$$\lambda_{H2} = \frac{\dot{m}_{H2,anch,in}}{\dot{m}_{H2,anGDL}} \tag{4.2}$$

where $\dot{m}_{O2,cach,in}, \dot{m}_{H2,anch,in}$ are the oxygen and hydrogen input flows at the channels while $\dot{m}_{O2,caGDL}, \dot{m}_{H2,anGDL}$ are the respective reacted quantities. In order to reach the required excess ratio set-point the air and hydrogen flows ($\dot{m}_{air}, \dot{m}_{H2}$) are used as manipulated variables. The safety of the operation is ensured by maintaining the excess ratios above one ($\lambda_{O2,SP} > 1, \lambda_{H2,SP} > 1$).

The power generation and the starvation avoidance objective can be achieved by control actions that aim at an accurate set-point tracking of $P_{SP}, \lambda_{O2,SP}, \lambda_{H2,SP}$. On the other hand the temperature control ($T_{fc,SP}$) involves two mutually exclusive subsystems, one for the heat-up and another for the cooling; therefore a number of requirements are considered besides the set-point tracking ability of the controller:

- Maintain the temperature at the desired level having an allowable deviation of +/- 1°C
- Avoid concurrent operation of the heat-up and cooling
- Exhibit stable operation
- Avoid large overshoot after step changes

The fuel cell temperature is controlled by manipulating the operating percentage of the heating resistance (x_{ht}) and of the cooling fans (x_{cl}) of the system, respectively. Based on these variables the resulted conceptual control configuration is shown by Fig. 4.2.

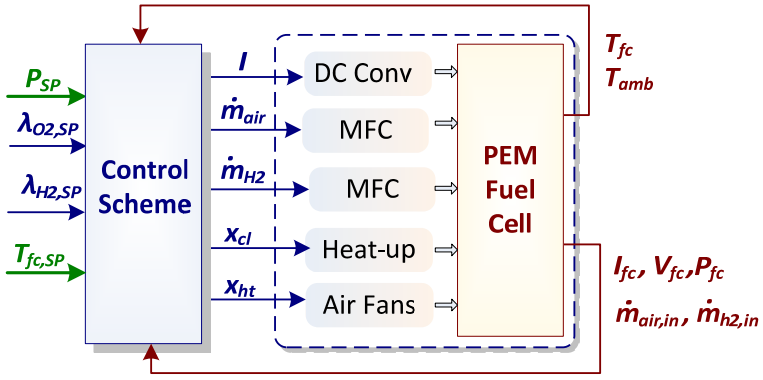

Figure 4.2 Control configuration

Fig. 4.2 illustrates the entities of the system and the flow of information related to the controller and the fuel cell including the measured variables from the unit:

- the power, current and voltage (I_{fc}, V_{fc}, P_{fc}),
- the ambient and fuel cell temperature (T_{fc}, T_{abm})
- the mass flow rates ($\dot{m}_{air,in}, \dot{m}_{h2,in}$).

The type of the controller and the number of the controllers per objective are the subject of the subsequent sections.

4.4 Experimental analysis of O_2 and H_2 excess ratios

The control of the air supply is critical for the safety of the system while the control of hydrogen supply can set the inlet hydrogen flow rate to the required one which results to fuel savings. To achieve these objectives it is important to be able to adjust the set-point of the respective excess ratios to achieve a safe and economic operation. But the appropriate set-point selection is accomplished only if the relationship between the produced power and the excess ratio levels of oxygen and hydrogen is known for the specific fuel cell unit. Therefore, an experimental analysis under a wide range of flow rates and input current is performed that reveals this correlation.

Moreover, an additional design constraint is imposed at the earlier described control configuration related to a physical limitation of the hydrogen mass flow controller used in the unit. According to the calibration sheet of the mass flow controller (MFC) the accuracy of the measurement or the control of the flow rate is questionable below 180cc/min. Thus, this is the lower bound that the controller of the unit must consider.

The set of experiments were performed at constant current level (1A – 9A). During each experiment the flow rate was modified from 180cc/min to 800c/min with a step increase every 30 seconds by 50cc/min until the upper point was reached. As λ_{O2} and λ_{H2} are unmeasured variables they are calculated online by the nonlinear model of the fuel cell. Figs 4.3 and 4.4 show the relationship between the produced power, the flow rate and the excess ratio of oxygen and hydrogen respectively.

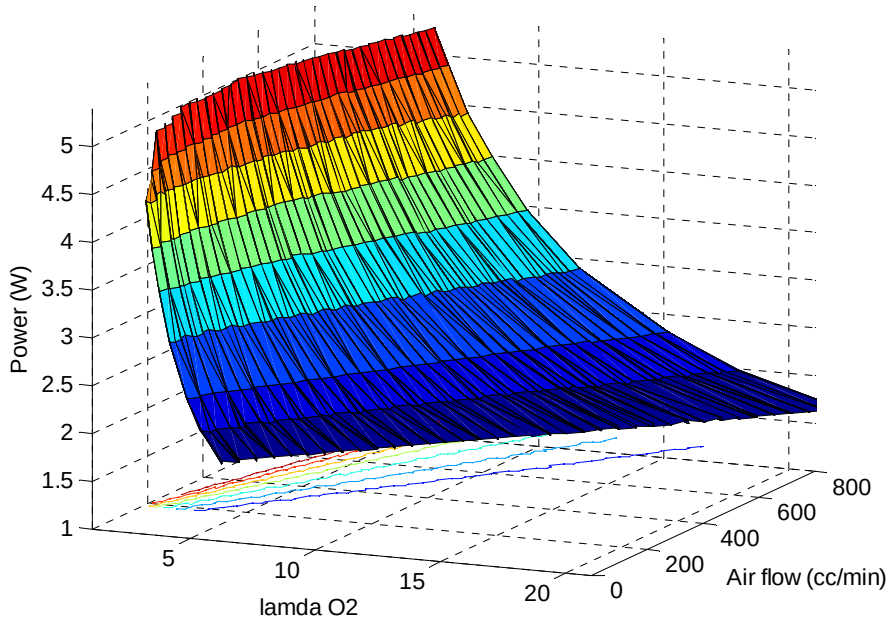

Figure 4.3 Produced power at various air flow rates and oxygen excess ratio

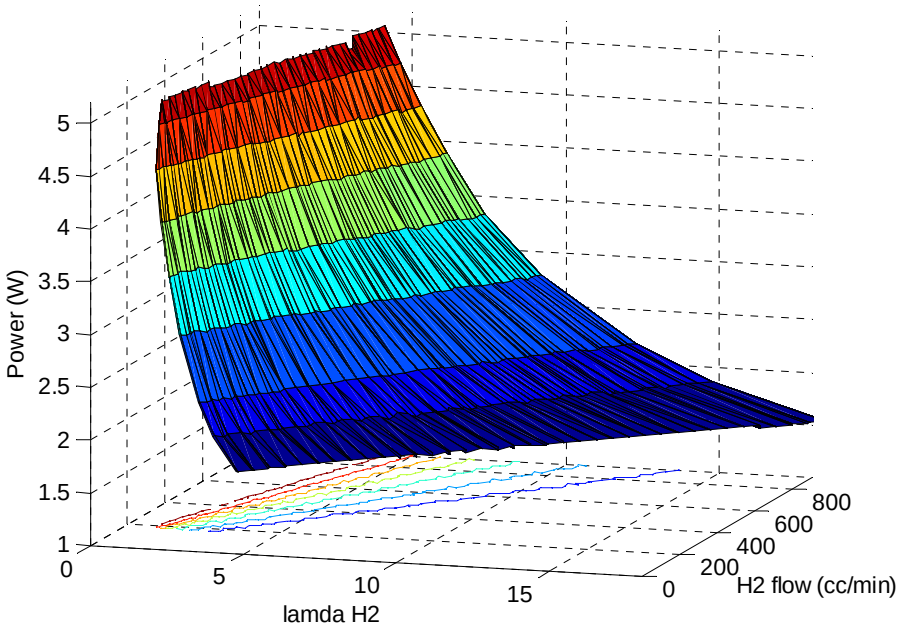

Figure 4.4 Produced power at various hydrogen flow rates and hydrogen excess ratio

It is observed that at low current levels the influence of air and hydrogen excess ratios is limited while at high current levels the excess ratios affect the stability and performance of the system. For certain current levels the increase of excess ratio causes an increase of the power but after a point the power decreases as the electrical resistance rises due to the increase of water removal rate which probably causes dehydration. To overcome the combined effects of such complex phenomena, the nominal values of λ_{O2} and λ_{H2} which are used as set-points of the respective control objectives of the control scheme, are determined from these experiments. Table 4.1 shows the minimum and the maximum achievable excess ratio levels of each experiment for the different current.

Table 4.1 Minimum and maximum achievable excess ratios (current 1A – 9A)

Current	O_2 Excess ratio		H_2 Excess ratio	
	minimum	maximum	minimum	maximum
1A	4.20	21.04	3.66	18.43
2A	3.36	16.83	2.92	14.75
3A	2.80	14.02	2.44	12.29
4A	2.10	10.52	1.83	9.21
5A	1.68	8.41	1.46	7.37
6A	1.40	7.01	1.22	6.14
7A	1.20	6.01	1.04	5.26
8A	1.168	5.26	1.02	4.60
9A	1.142	4.67	1.005	4.09

It is interesting to note that at low current levels the minimum feasible set-point increases. This is caused by the fact that the MFC cannot accurately operate below 180cc/min. On the other hand, as the power increases the minimum excess ratio is reduced accordingly until the constraint of safety is reached ($\lambda_{O2,SP} > 1, \lambda_{H2,SP} > 1$). As a result a feasible excess ratio set-point that could cover the full operating range (1..5W) for the anode is 4.2 and for the cathode is 3.66. These experimental results indicate that

an adjusted set-point for the excess ratios would be beneficial for the overall operation without compromising the safety of the system.

4.5 Systematic determination of $\lambda_{o2,SP}$ and $\lambda_{H2,SP}$

In addition to the safety of the system, the overall performance can be further improved by properly selecting the set-point for the excess ratios. Based on this new goal the control configuration (Fig. 4.2) can be expanded to include a feedforward mechanism that will determine the set-points for λ_{O2} and λ_{H2} based on the minimum gas criteria. This expansion employs an adaptive set-point determination which is applied in a feedforward manner to the controller ($\lambda_k^{SP} = f_{\lambda k}(P_{sp}), k \in [O_2, H_2]$). The aim of the adaptive set-point determination is to reduce the amount of hydrogen which will not be consumed by the reaction, for the given operating conditions, based on the requested power drawn from the fuel cell.

In order to define a feedforward set point derivation mechanism the results from the open loop experimental analysis that was previously analyzed are used. For each power-excess ratio curve (Fig. 4.5a,b) a minimum feasible point of the excess ratio is determined.

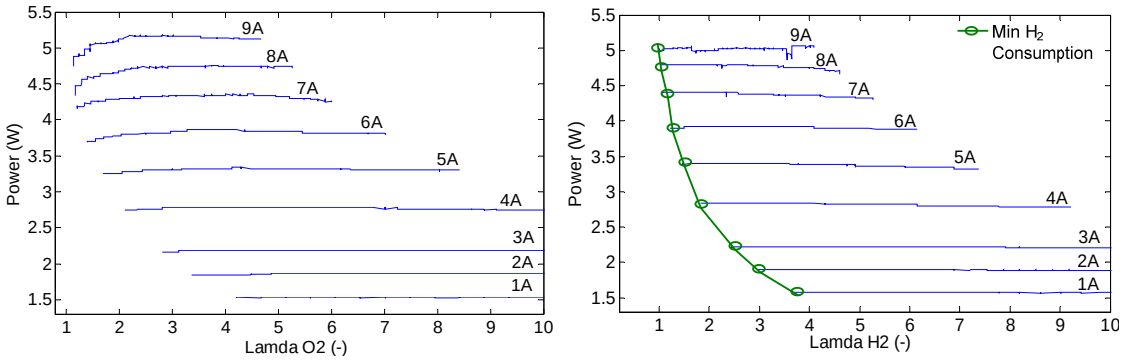

Figure 4.5 Power vs. oxygen and hydrogen excess ratio at various current levels

Fig. 4.5b illustrates the minimum allowable hydrogen excess ratio points at each current level. The set of all these points forms a steady-state path that could be approximated by a polynomial. Thus, a curve fitting process was performed in order to determine the

polynomial that could express the curve formed by these points and the order of the polynomial. The results from the curve fitting process of the excess ratio of hydrogen are presented at Fig. 4.6 and 4.7.

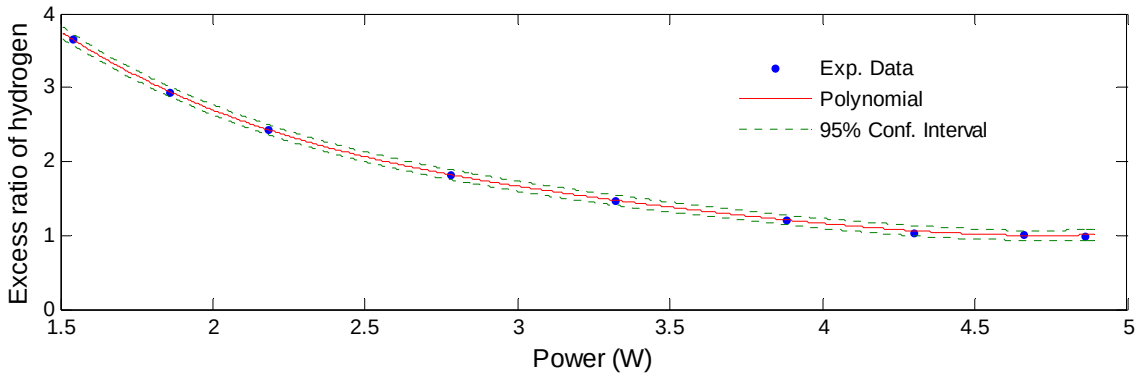

Figure 4.6 Experimental data and fitted curve

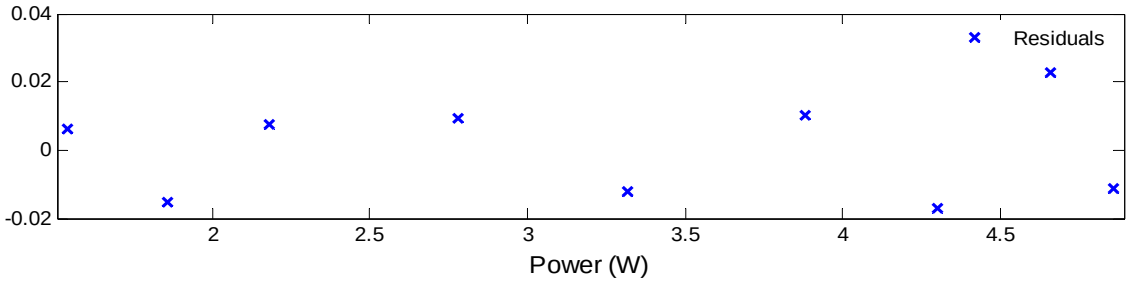

Figure 4.7 Distribution of the residuals

Fig. 4.6 shows the 95% confidence interval along with the fitted curve and the data. The residuals (Fig. 4.7) appear randomly scattered around zero which is a clear indication that the method and the model that was used for the fit can describe the experimental data well. From the above process a 4th degree polynomial is derived that can be used to define the set-point for the excess ratio of hydrogen as a function of power ($\lambda_{H2}^{SP} = f_{\lambda H2}(P_{sp})$). A similar analysis was performed using a linear, a 2nd degree and a 3rd degree polynomial.

Table 4.2 presents some statistics about the goodness of the fit for each polynomial.

Table 4.2 Statistics for various degrees polynomials

	linear	quadratic Polynomial	cubic Polynomial	4th deg. Polynomial
Sum of squares due to error (SSE)	0.7748	0.05508	0.01215	0.00161
R-square	0.8953	0.9926	0.9984	0.9998
Adjusted R-square	0.8804	0.9901	0.9974	0.9996
Root mean squared error (RMSE)	0.3327	0.09581	0.0493	0.02006

Except from the linear polynomial all the others could also be used but the 4th degree polynomial provides more accurate results. Moreover, the computational burden caused by the use of the 2nd, 3rd or the 4th degree polynomial is negligible. Therefore, the 4th degree polynomial was selected to be applied to the unit ($f_{\lambda H2}(P_{sp}) = a_1 P_{SP}^4 + a_2 P_{SP}^3 + a_3 P_{SP}^2 + a_4 P_{SP} + a_5$). The values of the coefficients with their 95% confidence bounds are presented at Table 4.2

Table 4.3 Value of the coefficients and 95% conf. bounds for $\lambda_{H2,sp}$ feadforward function

Coefficient	Value	95% Conf. bounds
α1	0.04542	0.02078, 0.07006
α2	-0.6616	-0.9775, -0.3456
α3	3.721	2.264, 5.178
α4	-10.02	-12.87, -7.174
α5	12.43	10.44, 14.41

A similar analysis was performed for the determination of the coefficient for the oxygen excess ratio curve polynomial:

$$f_{\lambda O2}(P_{sp}) = 0.065 P_{SP}^4 - 0.896 P_{SP}^3 + 4.88 P_{SP}^2 - 12.29 P_{SP} + 14.6 \quad (4.3)$$

These polynomials are applied online in a feedforward manner to the controller ($\lambda_{H2,sp} = f_{\lambda H2}(P_{sp})$, $\lambda_{O2,sp} = f_{\lambda O2}(P_{sp})$). Once $\lambda_{O2,sp}, \lambda_{H2,sp}$ are determined by the

feedforward mechanism, the set-point can be reached by properly manipulating the air and hydrogen flows ($\dot{m}_{air}, \dot{m}_{H2}$).

4.6 Concluding remarks

This chapter presents a detailed analysis of the fuel cell subsystems that should be optimally managed in order to provide a stable environment and to protect its longevity and durability. An indicative literature review has been performed to explore the various ways that the control challenges can be addressed. Furthermore, the control objectives were defined along with the corresponding manipulated and controlled variables. Additionally an experimental analysis involving the oxygen and hydrogen excess ratios per requested power was performed and its results were used to extract a feedforward mechanism for the determination of the respective set-points for the whole operating range of the fuel cell.

Once the scope and boundaries of the overall control framework are defined, the next chapters considers the development of new control algorithms and their application for the online control of the PEM fuel cell system.

Chapter 5

An Advanced Model Predictive Control Framework

This chapter presents two advanced model-based control methodologies for the efficient real-time control of PEM fuel cell. The first methodology is an online Nonlinear Model Predictive control (NMPC) strategy, which is very appealing due to its ability to handle dynamic nonlinearities of the process into consideration, whereas the second methodology is an explicit or multi-parametric Model Predictive Control (mpMPC) strategy, that defines the optimal solution in real-time using low complexity online implementation algorithms. At the core of both methods (NMPC, mpMPC) there is an optimal control problem which is solved online for the NMPC case and offline for the mpMPC.

Then a novel unified control framework is presented which is derived by the combination of these two MPC-based strategies. This framework exploits the advantageous features of the multi-parametric offline formulation and enhances the performance of the optimization problem which is solved online by the NMPC controller.

5.1 Model Predictive Control (MPC)

Model predictive control (MPC) or receding horizon control (RHC) is part of a family of optimization-based control methods, which solves online an open loop finite horizon optimal control problem for the determination of the future control moves (Chen and Allgower, 1998). MPC is based on the fact that past and present control actions affect the future response of the system (Qin and Badwell,2003). The main objective is to obtain a control action by minimizing a quadratic cost function related to selected objectives or performance indices of the system. As the system's conditions and dynamics change and evolve through time, the optimization problem has to be solved online at consecutive sampling intervals. Thus at each sampling time a finite horizon optimal control problem is solved over a prediction horizon (T_p), using the current state of the process as the initial state. The optimization yields an optimal control sequence ($u_k..u_{k+Nc}$) over a control horizon (T_c) and only the first control action (u_k) for the current time is applied to the system while the rest of the calculated sequence is discarded. At the next time instant the horizon is shifted by one sampling interval and the optimization problem is resolved using the information of the new measurements acquired from the system (Mayne *et al.*, 2000). The concept of receding horizon adds a feedback to the whole approach that enables the compensation of disturbances affecting the system or modeling inaccuracies. Fig. 5.1 illustrates the concept of RHC.

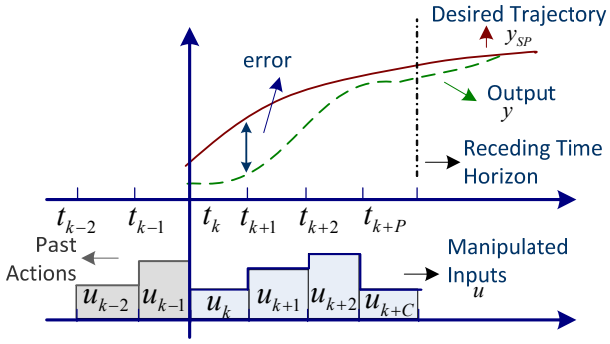

Figure 5.1 Receding Horizon concept

This methodology makes explicit use of a process model to optimize the predicted future behavior of the system. Thus, the first step in designing an MPC system is the development or selection of a suitable for control purposes mathematical model. Depending on the nature of the model, linear or nonlinear, we refer to MPC or Nonlinear MPC (NMPC) formulation. For the rest of this thesis we will use the NMPC approach as we are interested on nonlinear processes. A process model always includes some assumptions or simplifications with respect to the system which is represented, that may lead to minor inaccuracies. Also, the effect of disturbances to the process may add some extra uncertainty compared to the response of the developed model.

Deviations of the model predictions from the actual process response are calculated at each sampling instance and considered as the error of the process model. This error defines a bias term which is used to correct future predictions and it is considered constant for the entire prediction horizon step. The mathematical representation of the MPC algorithm is as follows (Allgöwer *et al.*, 2004; Mayne *et al.*, 2000):

$$\min J = \sum_{j=1}^{Np} \left(\hat{y}_{k+j} - y_{sp,k+j} \right)^T Q \left(\hat{y}_{k+j} - y_{sp,k+j} \right) + \sum_{l=0}^{Nc-1} \Delta u_{k+l}^T R \Delta u_{k+l} \tag{5.1a}$$

s.t.:

$$\dot{x} = f_d(x,u), \quad y = g(x,u) \tag{5.1b}$$

$$e_k = \left(y^{meas} - y^{pred} \right)_k \tag{5.1c}$$

$$\hat{y}_{k+j} = y_{k+j}^{pred} + e_k \tag{5.1d}$$

$$N_c = (T_c - T_k)/\Delta t_c, \; N_p = (T_p - T_k)/\Delta t_p \tag{5.1e}$$

$$u^L \le u \le u^U, \; y^L \le y \le y^u \tag{5.1f}$$

The minimization of functional J (eq. 5.1a) is subject to constraints on the manipulated (u) and controlled (y) variables (eq. 5.1f). y_k^{SP} denotes the desired reference trajectory, while f_d are the differential equations and g denote the equations of the output variables. The difference e_k between the measured variable y^{meas} and the corresponding predicted value y^{pred} at time instance k is assumed to be constant for the entire number of time intervals (N_p) of the prediction horizon T_p, T_c denotes the control horizon reached

through N_c time intervals. Tuning parameters of the algorithm are the weight factors in the objective function (Q, R) and the length of the prediction and control horizon.

5.1.1 Scope of the optimization problem

In both cases of MPC, linear and nonlinear at the core of the control problem lies an optimization problem. The solution of this optimal control problem involves an optimization procedure that aims at the determination of the best solution for a given system considering physical and operating constraints. For this purpose various elements are necessary to formulate an optimization problem:

- A model that represents the behavior of the process and it is formulated by a set of equations and constraints.
- An objective function or performance index that defines a quantitative measure that need to be minimized, usually the tracking of a desired trajectory for the MPC case.
- A set of decision variables that are appropriately adjusted to satisfy the constraints and achieve the minimization of the predetermined objective function. These variables are the degrees of freedom of the system

In order to systematically determine the optimal solution of the problem using these elements various methods and algorithms are available. Thus, the selection of the appropriate method is based on criteria derived by the nature of the system:

- Type of variables involved: discrete or continuous.
- Type of problem: differentiable or nondifferentiable.
- Type of objective function and feasible region: convex or nonconvex.

After the appropriate formulation of the optimization problem the rest of the MPC elements (e.g., control and prediction horizon, weights of terms in the objective etc., error calculation) are assembled and the integrated framework is ready to be used, initially for parameter tuning and subsequently for implementation at the process or for simulation purposes. In many cases and more specifically when a nonlinear formulation is involved, the solution of the optimization problem in each sampling instance is computationally demanding. To avoid computational delays and deterioration of the control performance,

the optimization problem must be solved in a time period smaller than the sampling time interval of the system (Würth *et al.*, 2011). Therefore, it is important to use a methodology that takes into consideration all the operating constraints which are imposed by the nature of the process into consideration.

5.2 Nonlinear Model Predictive control

MPC is a well established advanced control methodology which employs the use of a process model and it is widely used in the industry mainly because of its ability to handle multivariable systems and constraints systematically. Motivated by the impact of MPC and urged by the need for near boundary operation and highly nonlinear behavior of many processes Nonlinear MPC (NMPC) has gained significant attention over the past decade (Findeisen *et al.*, 2007; Magni *et al.*, 2009). Moreover recent advances in optimization enable the move towards direct online optimizing control (Engell, 2007). Various theoretical and practical aspects (e.g. stability, reliability, robustness, computational burden) have been recently explored and on-going research is progressing in the area of NMPC towards the industrial implementation of the methodology (Rawlings and Mayne, 2009).

5.2.1 Recent literature review of NMPC developments

Although NMPC formulation is not as developed as the linear MPC, important progress has been made the recent years regarding theoretical and practical considerations (Findeisen *at al.*, 2003; Allgöwer *et al.*, 1999; Lee *et al.*, 2002; Mayne *et al.*, 2000; Magni and Scattolini 2004). The NMPC formulation requires the online solution at each time step of an optimization problem to determine the manipulated inputs. As computational power increases and solution algorithms are evolving the application of NMPC is a viable option for the control of complex processes which are described by nonlinear differential and algebraic equations. The optimization problem derived by the control formulation generally is nonconvex and consequently, the major practical challenge associated with NMPC is the online solution of the nonlinear program (NLP).

Therefore, it is of paramount important the utilization of efficient and reliable NLP solution to make NMPC a viable control technique.

The closed-loop performance is improved when the nonlinear model is used directly in the NMPC calculations. However, standard NLP codes are not designed to handle ODE constraints (Henson, 1998). This limitation can be overcome using a two-stage solution procedure in which a standard NLP solver is used to compute the manipulated inputs and an ODE solver is used to integrate the nonlinear model equations, known as sequential solution or partially parameterized method, since only the manipulated variables are discretized (Manenti, 2011). An alternative to the sequential solution approach is to solve the optimization problem and the model equations simultaneously (Biegler *et al.*, 2002). The dynamic model is fully discretized as per the manipulated variables and it is directly integrated in the optimization problem. In this approach the numerical integration and the optimization simultaneously converge. The most well-known simultaneous method is based on collocation on finite elements (CFE) (Biegler, 1984) and multiple shooting (Diehl *et al.*, 2002). In addition, it is necessary to explore alternative formulations of the NMPC problem with improved computational properties such as the combination of multiple shooting and collocation method presented in Tamimi and Li (2010). The need for NMPC has stimulated intensive research and fast algorithms for NMPC are now available (Cannon, 2004; Diehl *et al.*, 2002; Martinsen *et al.*, 2004; Schäfer *et al.*, 2007; Zavala *et al.*, 2008).

NMPC is a nonlinear open-loop optimal control technique where feedback is incorporated via the receding horizon formulation. From a theoretical perspective, the minimum requirement of a model-based feedback controller is that it yields a stable closed-loop system if an accurate model of the plant is available, which is referred as nominal closed-loop stability. Important issues regarding stability of NMPC and the efficient solution of the open-loop optimal problem has been extensively studied by various groups (Limon *et al.*, 2006; Magni *et al.* 2001a, De Nicolao *et al.*, 2000, Mayne and Michalska, 1990). Furthermore, nominal stability can be guaranteed by making use of the inherent robustness properties of NMPC as shown in (Diehl *et al.*, 2005).

Similar formulations take into consideration the issue of computational burden, delay and stability (Findeisen *et al.*, 2004; Chen *et al.* 2000). From a practical point of

view, there are some cases where the NMPC has a non negligible computational delay. An interesting approach that takes into consideration the sampling intervals is sampled data NMPC, which refers to the repeated application of input trajectories that are obtained at discrete sampling instants (Findeisen *et al.*, 2003). This approach has and its associated proof of stability was explored in a real-time framework by (DeHaan and Guay, 2007).

Besides the stability at nominal conditions it is important to consider the case of robust stability. The primary reason for including feedback in NMPC is to account for model mismatch against the actual plant. Simulation and experimental studies demonstrate that NMPC has some degree of robustness to modeling errors. Nevertheless, it is important to incorporate a rigorous theory which allows the robustness of different NMPC formulations to be analyzed and facilitates the derivation of new formulations with improved robustness properties. Some interesting robustness results are presented by (Limon *et al.*, 2009; Cannon *et al.*, 2011; Lazar *et al.*, 2008; Imsland *et al.*, 2003).

Finally another interesting approach which applies in the nominal case of NMPC, exploits the interval between consecutive updates and thus reduce the computational delay (Zavala and Biegler, 2009). In conclusion, some open issues and unexploited application domains exist for the theoretic basis and the real-time implementation aspects of NMPC. But beyond these issues the potential and benefits of NMPC are progressively penetrating to complex processes and furthermore research is encouraged. It is clear from the above brief analysis that significant progress has been made in the control of various aspects of fuel cell systems and the application of model based control techniques can improve the understanding of these control issues and lead towards the design of better control systems.

5.3 Dynamic Constrained Optimization

As stated earlier the NMPC formulation includes the solution of an optimization problem at each sampling instance. But the online application of the NMPC framework faces a challenging dilemma (Diehl *et al.*, 2002), either the nonlinear iteration procedure is performed until a pre-specified convergence criterion is met, which might introduce

considerable feedback delays, or the procedure is stopped prematurely with only an approximate solution, so that a pre-specified computation time limit can be met. The feedback delays can lead to loss of performance and stability, caused by the online computational burden. Fortunately, considerable progress has been achieved in the last decade that allows both the decrease of computational delays and the minimization of the approximation errors. Recently NMPC controllers are based on nonlinear programming (NLP) sensitivity with reduced online computational costs and can lead to significantly improved performance (Zavala and Biegler, 2009). Overall the application of dynamic optimization in conjunction with fast optimization solvers allows the use of first-principles models for NMPC (Diehl *et al.*, 2009). In general, a DAE constrained optimization problem is considered which includes the continuous-time counterpart of the NMPC problem:

$$\min_{u(t)} J = \varphi\left(x(t), z(t), u(t)\right) \tag{5.2}$$

$$\text{s.t. } \frac{dx(t)}{dt} = f_d\left(u(t), x(t), z(t)\right) \tag{5.2a}$$

$$0 = f_a\left(u(t), x(t), z(t)\right) \tag{5.2b}$$

$$x(0) = x_0 \tag{5.2c}$$

$$x^L \le x\ (t) \le x^U\ ,\ z^L \le z\ (t) \le z^U\ ,\ u^L \le u\ (t) \le u^U \tag{5.2d}$$

where t is the scalar independent dimension defined in the fixed domain [0, t_f], x is the vector of differential (state) variables, z is a vector of algebraic variables, u is the vector of manipulated variables and x_0 are the initial conditions of the state variables, f_d and f_a are the differential and the algebraic equations. Finally eq. (5.2d) denotes the bounds. Since the implemented NMPC algorithm involves inequality constraints, direct optimization methods are used for the optimization problem which is transformed into a NLP problem.

5.3.1 Dynamic optimization methods

In principle two main numerical approaches exist for the solution of the open-loop optimal control problem, the indirect and the direct methods (Biegler and Grossman, 2004). The first relies on Pontryagin's Maximum Principle, it is suitable for problems that have only equality constraints and it is on calculus of variations. The second approach, the direct approach, transforms the optimization problem into an NLP problem. Direct methods are more general and computationally efficient comparing to the indirect methods. Furthermore, they can handle inequality constraints and find suitable initial guesses for state variables. In direct methods the original infinite dimensional problem is transformed into finite dimensional by parameterizing the input, and in some cases the states, by a finite number of parameters and by solving or approximating the differential equations during the optimization.

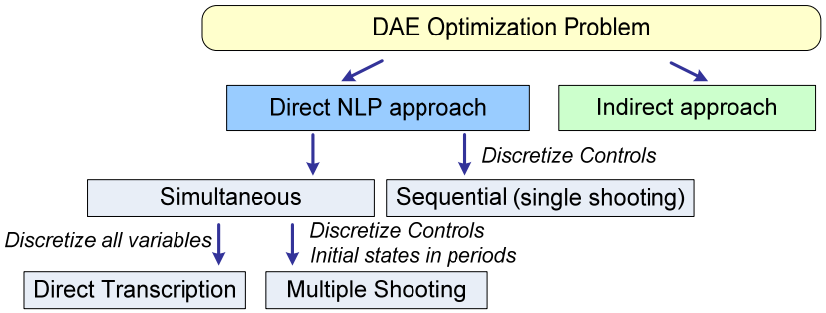

Figure 5.2 Classification of DAE optimization methods

Mainly two direct strategies for the solution of the NMPC optimal control problem using mathematical programming can be distinguished, the sequential and the simultaneous (Fig 5.2). The main difference among the direct approaches is the handling of the continuous-time DAE model.

Sequential approach

In the sequential or single-shooting approach the control trajectory of the manipulated variables is finitely parameterized or discretized, the optimization steps are performed and afterwards the NLP problem is solved. In each evaluation of the performance index

at the solution of the NLP, the process model is integrated with a DAE solver that integrates the model over the entire horizon in a single call. The NLP solver obtains a new value for the controls profile and computes the search step using either an exact Newton's method, which requires both the first and the second gradient information, a computational expensive procedure, or a Quasi-Newton's approximation, which may lead to weaker convergence properties. This approach can handle stiff dynamic systems and off-the self NLP solvers and DAE solvers can be used. The main disadvantage is that the integration step is usually computationally expensive (Biegler *et al.*, 2002).

Simultaneous approach

In the direct simultaneous approach the solution of the differential equations and the optimization is obtained concurrently. For this purpose the differential equations are discretized and enter the optimization problem as additional constraints. Typical simultaneous approaches use multiple shooting or direct transcription to parameterize/discretized the equations. The direct multiple shooting approach discretizes the optimization horizon (prediction horizon) into a number of elements (time intervals) with discretization of the manipulated variables. The differential equations on these intervals are integrated separately in each element. The guesses of the values of the parameterized inputs and the initial conditions are made at each element and similarly the evaluation of gradient information is performed separately at each element. Multiple shooting allows parallel computation since each interval is computationally decoupled. The main drawback is that the overall complexity increases when the model contains many dynamic states (Diehl *et al.*,2002).

Another simultaneous approach is the direct transcription method that explicitly discretizes all the variables (differential, algebraic, input and output) and generates a large scale but sparse NLP problem. This discretization based on orthogonal collocation on finite elements (OCFE), which can be treated as a special calls of implicit Runge-Kutta type method (Betts, 2011). Initial values for the whole state trajectory are required which may be an advantage if such knowledge is available. The direct transcription method is usually selected due to its accuracy and numerical stability properties (Diehl *et al.*, 2002; Kameswaram and Biegler, 2008). In addition, this approach does not require a

DAE integrator, as the discretized model is solved once at the optimal point and as a consequence computational intermediate solutions are avoided. Moreover, the sparsity and the structure can be exploited by modern NLP solvers.

5.3.2 Direct transcription method

In the direct transcription method the dynamic optimization problem is transformed into a large NLP formulation without an embedded DEA solver. Furthermore, the manipulated (input) and state variables profiles and consequently the output (controlled) variable profile are approximated with a family of polynomials on finite elements. The time horizon is divided in finite elements (NE) and each equally spaced finite element is partitioned in collocation points (N_{cop}). Although the resulted mesh of finite elements is fixed, this does not limit the interesting features of this method. By this formulation the differential equations are transformed into an algebraic system of equations (Fig. 5.3).

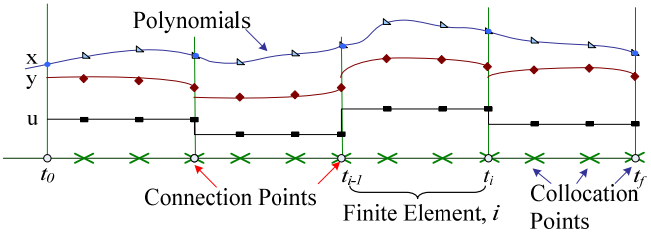

Figure 5.3 Finite elements and collocation points

The residuals of state and algebraic equations are assumed to be exactly satisfied only at the collocation points. The position of the collocation points is determined as the shifted roots of orthogonal polynomials, usually Legendre or Radau orthogonal polynomials, of order equal to the number of collocation points within each finite element. The solution is approximated with Lagrange polynomials at each finite element (Finlayson, 1992; Biegler *et al.*, 2002; Kiparissides *et al.*, 2002):

$$x(t) = \sum_{j=0}^{Ncop} x^{i,j}\Omega_j(t), \quad i = 1..NE \ , \ t \in [t_i, t_{i+1}] \tag{5.3}$$

$$\Omega_j(t) = \prod_{k=0,k\neq j}^{Ncop} \frac{(t - t_{i,k})}{(t_{i,j} - t_{i,k})} \tag{5.4}$$

where N_{cop} is the total number of the internal collocation points of each element, *NE* is the number of the finite elements, $x^{i,j}$ is the value of the state vector at collocation point *j* of the i^{th} finite element. Respectively the algebraic variables ($z^{i,j}$) and input (manipulated variables) variables (u^i) are approximated. The length of each element is $h_i = t_i - t_{i-1}$. The basis function (Ω) is normalized over each element having time $\tau \in [0,1]$ and $t = t_{i-1} + h_i \cdot \tau$. Ω_j is calculated using the shifted roots of the Legendre polynomials. After the discretization of the DAE model, the constrained optimization problem (5.2) is expressed as an NLP problem in the form (Biegler *et al.*, 2002):

$$\min_{x^{i,j}, z^{i,j}, u^i} \sum_{i=1}^{NE} \sum_{j=1}^{Ncop} w_{i,j} \phi\left(x^{i,j}, z^{i,j}, u^i\right) \tag{5.5}$$

$$\text{s.t. :} \quad \sum_{k=0}^{Ncop} \dot{\Omega}_k(\tau_{i,j}) x^{i,k} = h_i f_d\left(u^i, x^{i,j}, z^{i,j}\right) \tag{5.5a}$$

$$0 = f_a\left(u^i, x^{i,j}, z^{i,j}\right) \tag{5.5b}$$

$$x^{1,0} = x_0, \quad x(t_f) = \sum_{j=0}^{Ncop} x^{NE,j} \Omega_j(1) \tag{5.5c}$$

$$x^L \le x^{i,j} \le x^U, z^L \le z^{i,j} \le z^U, u^L \le u^i \le u^U, \quad i = 1..NE, \quad j = 1..N_{cop} \tag{5.5d}$$

$$x^{i,0} = \sum_{j=0}^{Ncop} x^{i-1,j} \Omega_j(1), \quad \mathrm{i} = 2..NE \tag{5.5e}$$

To enforce zero-order continuity of the state variables at the element boundaries the connecting equations are used (5.5e).

The use of OCFE discretization scheme allows the NLP solvers to exploit the sparsity of the system and as the discretized model is solved once at the optimal point, integration at intermediate points is avoided. On the other hand, efficient large-scale NLP solvers are necessary and careful formulation of the NLP is a prerequisite for an accurate state and profile result. Overall this method exhibits fast convergence rates and can deal with unstable systems in a straightforward manner since it allows direct enforcement of state and control variable constraints (Biegler *et al.*, 2002).

In this work the simultaneous direct transcription method is selected for the NMPC framework. The overall procedure for the development of an NMPC controller based on direct transcription method and the various conceptual stages for from the design to the online deployment are presented in Fig. 5.4.

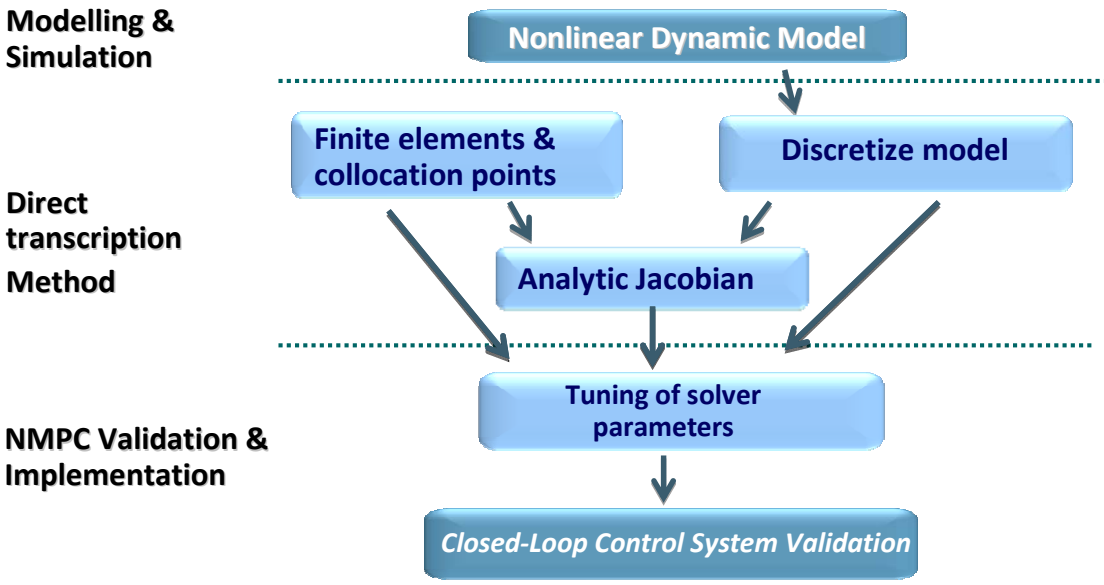

Figure 5.4 Development procedure of NMPC framework

As this is a modular design the place of the direct transcription method could take any other optimization method (single shooting or multiple shooting).

5.3.3 Numerical Algorithms for the solution of an NLP problem

Besides the selection of an appropriate optimization method, it is equally important to select a suitable NLP numerical algorithm that could handle the complexity of the DAE model and provide satisfactory response according to the problem's requirements. Therefore, specific emphasis is given to the use of an efficient solver. A number of numerical algorithms exist which are implemented by software packages for nonlinear programming (Biegler and Grossman, 2004). The available numerical algorithmic methods for constrained optimization using an NLP formulation are:

- Sequential quadratic programming (SQP) method
- Interior point (IP) method
- Generalized reduced gradient-based (GRG) or nested projection method

The main difference between these methods is the way that the variables are treated with respect to the solution of the Karush-Kuhn-Tacker (KKT) optimality conditions. More specifically the SQP and the IP methods solve simultaneously the optimality conditions whereas the GRG consider a decomposition that leads to different nested subproblems. Subsequently these subproblems can be solved using Newton-type methods. Each method has its pros and cons and all of them can be used to solve NLP problems with equality and inequality constraints. Thus, the selection is problem-depended and oriented towards application specific requirements and implementation issues. An indicative only list includes software packages like:

- SQP method: NPSOL, SNOPT, fmincon
- IP method: KNITRO, LOQO, IPOPT
- Reduced gradient: CONOPT, LANCELOT, MINOS

In case that a direct transcription method is selected the DAE model and consequently the formulated NLP problem, is represented by a large-scale set of algebraic equations. For this reason the selected algorithm should be able to handle large-scale problems where the constraints and the variables are several hundreds or several thousands.

Reduced gradient-based method

The reduced gradient-based (GRG) method is especially useful for large-scale NLPs with nonlinear objectives and constraints and problems where it is important for the solver to remain feasible over the course of successive iterations (Biegler and Grossman, 2004). There are two variants of the GRG-type method, the gradient projection and the linearly constrained augmented Lagrangian. In the first variant the nonlinear equations are solved repeatedly which introduces a significant computational expense and requires an extra step for feasibility check at every iteration. An alternative to this approach is to construct a subproblem with constraints linearized at the current point (Murtagh and Saunders,

1998). The use of successive linearizations and consecutive subproblems leads to the approach of the nonlinearly constrained problem solution.

In this method the variables (n) are first partitioned in order to deal with constrained portion of the NLP problem into three categories (Murtagh and Saunders, 1978):

- the superbasics (s): the set of superbasics is regarded as the set of the independent variables (decision variables) that are allowed to move in any desirable direction to reduce the value of the objective function
- the basics (m): the basic variables (dependent on the design variables) have a value between their bounds and when the superbasics change then the basics are obliged to change in a definite way to maintain feasibility with respect to the constraints
- the nonbasics (n-m-s): the nonbasic variables are set to their bounds at the optimal solution

This partitioning changes over the course of the optimization iterations. After the variable partitioning the GRG algorithm executes a sequence of major and minor iterations until the optimum solution is found. At every major iteration the solution of a linearly constrained NLP subproblem is performed, while in the minor iterations the reduced gradient method is applied. The subproblem in the minor iteration uses an augmented Lagrangian function (eq. 5.6) which includes a quadratic penalty function to penalize the movement from the feasible region (Murtagh and Saunders, 1998):

$$\min_{u(t),z(t)} f(x)+\lambda^T h(x)+\nu^T(g(x)+s)+\frac{1}{2}\rho\left\|h(x),g(x)+s\right\|^2 \tag{5.6}$$

$$\text{s.t.}\quad h(x^k)+\nabla h(x^k)^T p=0 \tag{5.6a}$$

$$g(x^k)+\nabla g(x^k)^T p+s=0 \quad ,s\geq 0 \tag{5.6b}$$

where λ and ν are the multipliers of equalities and inequalities, ρ is the penalty parameter and s are the slack variables. Each subproblem contains original linear constraint and bounds on variables, as well as linearized versions of the nonlinear constraints. At every minor iteration an active set of bounds and constraints is selected. After the reduced space decomposition is applied to the subproblem, a quasi-Newton method is employed

to approximate the reduced Hessian (second-order information). Once the search direction is determined for all variables a line search is performed. At the solution of this subproblem using the simplex method, the constraints are relinearized and the cycle repeats until the KKT conditions of the initial NLP are satisfied. Given that the system has few degrees of freedom, the use of a reduced gradient method is extremely efficient, even if the NLP is a large-scale one. The major iterations converge at a quadratic rate (Murtagh and Saunders, 1978) since the internal feasibility step is missing due to the linearized subproblem.

The optimization software package which is selected for this thesis is the reduced gradient-based solver MINOS (Modular Incore Nonlinear Optimization System) of Murtagh and Saunders (Murtagh and Saunders, 1978), which has been implemented very efficiently to a number of problems. MINOS requires the analytical form of the Jabobian but approximates numerically the Hessian of the problem. It takes advantage of the sparsity in the Jacobian which is present when a direct transcription method is selected and one of its merits is that it tends to be very efficient with time critical problems.

5.4 Multi-parametric MPC

The computation of an MPC law is derived by the solution of an optimization problem at each sampling instant. However this inserts a computational issue which must be carefully handled in order to avoid loss of performance due to delays. An alternative approach to classic MPC is the explicit or multi-parametric MPC (mpMPC) method that avoids the need for repetitive online optimization (Pistikopoulos, 2012). This method is suitable for linear constrained state space system with low complexity (Bemporad *et al.*, 2002; Pistikopoulos *et al.*, 2002). The development of an mpMPC controller is realized into two main steps:

- Off-line optimization: Derivation of the critical regions which are explored by an optimal look-up function.
- Online implementation: Based on the system measurements the critical regions are traversed and the corresponding optimal control action is determined.

The overall procedure of development an mpMPC controller, from design to online deployment (Pistikopoulos *et al.*, 2007; Pistikopoulos, 2012), is presented in Fig. 5.5.

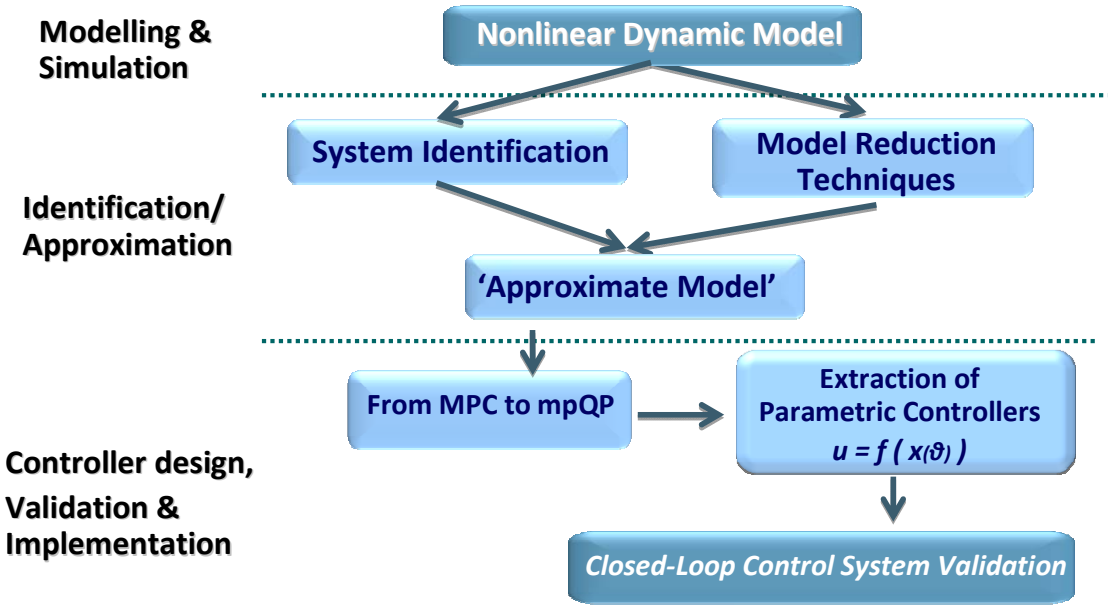

Figure 5.5 Development procedure of mpMPC framework

In mpMPC the online optimization problem is solved off-line with multi-parametric quadratic programming (mpQP) techniques to obtain the objective function and the control actions as functions of the measured state/outputs (parameters of the process) and the regions in the state/output space where these parameters are valid i.e. as a complete map of the parameters. Online control is then applied as a result of simple function evaluations since the computational burden is shifted offline. The following section presents a brief overview of the main ideas, necessary for the formulation and implementation of the mpMPC.

5.4.1 Parametric programming

Parametric programming is a generic mathematical technique that for a given objective function to optimize, a vector of optimization variables and a vector of parameters, provides the optimization variables as a set of functions of the parameters and the

corresponding regions in the space of parameters, called critical regions (*CR*). Consider the following general parametric programming problem:

$$\begin{aligned} z(\theta) &= \min_{x} f(x,\theta) \\ s.t. \quad & g(x,\theta) \le 0 \\ & x \in X \subseteq \Re^n, \theta \in \Theta \subseteq \Re^s \end{aligned} \tag{5.7}$$

where x is the vector of continuous variables and θ is the vector of parameters bounded between certain upper and lower bounds. The substitution of $x(\theta)$ into $f(x,\theta)$ result to $z(\theta)$ which is the parametric profile of the objective function. When the parameter is a vector instead of a scalar we refer to multi-parametric programming. The solution of (5.1) is given by Dua *et al.*, (2002):

$$x(\theta) = \begin{cases} x^1(\theta) & \text{if} \quad \theta \in CR^1 \\ x^2(\theta) & \text{if} \quad \theta \in CR^2 \\ \vdots & \\ x^i(\theta) & \text{if} \quad \theta \in CR^i \\ \vdots & \\ x^N(\theta) & \text{if} \quad \theta \in CR^N \end{cases}$$

such that $CR^i \bigcap CR^j = \varnothing$, $i \neq j$, $\forall i, j = 1,\ldots,N$ and CR^i denotes a critical region. In order to obtain the critical regions and $x^i(\theta)$ a number of algorithms have been proposed in the literature. The selection of the appropriate one depends on the nature of the problem, if f and g are convex, differentiable, linear, quadratic or nonlinear. For the formulation of the mpMPC f is convex and quadratic and g is linear. Thus, the resulting parametric approach is a multi-parametric quadratic program (mpQP). An algorithm for the solution of the mpQP has been proposed by Dua *et al.* (2002) where there is an iterative determination of a set of unique active constraints and the corresponding critical regions by writing the KKT optimality conditions of the mpQP.

5.4.2 From MPC to mpQP

The use of mpQP enables the derivation of the objective and optimization variable as functions of the varying parameters and the regions in the space of parameters where

these functions are valid. Thus, the solution of the optimal control problem (MPC problem) with mpQP is a multi-parametric problem. A brief outline of the standard MPC formulation is presented along with its transformation to the mpQP problem. Consider the following constrained discrete-time linear time invariant model of the system:

$$\begin{aligned} x_{t+1} &= Ax_t + Bu_t \\ y_t &= Cx_t \end{aligned} \qquad (5.8)$$

$$\text{s.t.} \quad \begin{aligned} x_{\min} \le x_t \le x_{\max} \\ u_{\min} \le u_t \le u_{\max} \\ y_{\min} \le y_t \le y_{\max} \end{aligned}$$

where $x_t \in \Re^n$ is the state vector, $u_t \in \Re^m$ is the vector of input variables, $y_t \in \Re^p$ is the vector of the output variables, $A \in \Re^{n\times n}$, $B \in \Re^{n\times m}$ and $C \in \Re^{p\times n}$ are the system matrices, t is the current time interval and the subscripts *min* and *max* denote the lower and upper bounds respectively.

The receding horizon open-loop optimal control problem regulating (5.8) to the origin has the following formulation and it is used to derive the explicit control law (Mayne *et al.*, 2000) for x_t :

$$\min_U J(U, x(t)) = x_{t+N_y|t}^T P x_{t+N_y|t} + \sum_{k=0}^{N_y-1} \left[x_{t+k|t}^T Q x_{t+k|t} + u_{t+k}^T R u_{t+k} \right]$$

$$\begin{aligned} s.t. \quad & x_{t|t} = x(t) \qquad and: \\ & x_{t+k+1|t} = Ax_{t+k|t} + Bu_{t+k}, k \ge 0 \\ & u_{t+k} = Kx_{t+k|t}, N_u \le k \le N_y \\ \\ & x_{\min} \le x_{t+k|t} \le x_{\max}, k = 1, ..., N_c \\ & u_{\min} \le u_{t+k} \le u_{\max}, \quad k = 1, ..., N_c \end{aligned} \qquad (5.9)$$

where $x_{t+k|t}$ is the prediction of x_{t+k} at time t, Q and R, are the tuning parameters which are constant, symmetric and positive definite matrices, N_y, N_u and N_c are the prediction, control and constraint horizons respectively with $N_u \le N_y$ and K is some feedback gain. The weight R penalizes the use of control action u. The sequence $U \triangleq \left[u_t^T, ..., u_{t+N_u-1}^T \right]^T$ contains the future control inputs that yield the best predicted

output with respect to the performance index for the prediction horizon. Once this is determined, the first control input u_t is applied to the system. Considering the linear model (5.8), the MPC problem (5.9) can be recast as a mpQP which can be solved with standard multi-parametric programming techniques and involves a systematic exploration of the parameter space. From (5.9) the following can be derived (Pistikopoulos *et al.*, 2002):

$$x_{t+k|t} = A^k x(t) + \sum_{j=0}^{k-1} A^j B u_{t+k-1-j} \tag{5.10}$$

The optimization problem (5.9) with the aid of (5.10) can be rewritten in a QP problem.

$$V(x(t)) = \frac{1}{2} x^T(t) Y x(t) + \min_U \left\{ \frac{1}{2} U^T H U + x^T(t) F U \right\} \tag{5.11}$$

$$\text{s.t. } GU \le W + Ex(t)$$

where U is the vector of optimization variables and *H, F, Y, G, W* and *E* are obtained from *Q* and *R*. If the weighting matrices in (5.9) satisfy $P \succeq 0$, $R \succ 0$ and $Q \succeq 0$, then H$\succ$ 0 and the problem is strictly convex and therefore *V* is continuous. The KKT conditions are then sufficient conditions for optimality and the solution is unique. Then the QP problem (5.11) is transformed into multi-parametric QP by this linear transformation by defining:

$$z \triangleq U + H^{-1} F^T x(t) \tag{5.12}$$

In particular the equivalent mp-QP formulation that corresponds to the MPC problem is defined:

$$V(x(t)) = \min_z \frac{1}{2} z^T H z \tag{5.13}$$

$$\text{s.t.} \quad Gz \le W + Sx(t)$$

which is an mpQP in *z* parameterized by $x(t)$ and $S = E + GH^{-1}F^T$.

In order to start solving the mp-QP problem, an initial vector x_0 inside the polyhedral set *X* of parameters is necessary, such that the QP problem (5.13) is feasible for $x = x_0$. Such a vector can be found for instance by solving a linear program (LP) (Bemporad *et al.*, 2002; Johansen and Grancharova, 2003).

5.4.3 Critical regions and feedback control law

The mpQP problem can be solved with any available QP solver or by the use of software packages like POP (POP, 2007) or MPT (Kvasnica *et al.*, 2004) and the solution is a set of convex non-overlapping polyhedra on the parameter space, each corresponding to a unique set of active constraints. The solution of the mpQP problem consists of several steps (Pistikopoulos *et al.* 2007):

- Find a local optimum z(x) by solving the QP problem for $x=x_0$ and identifying the active constraints.
- Find the set in the space of x(t) (critical regions) where z(x) is valid.
- Proceed iteratively until the x(t)-space is covered.

The mpQP (5.11) is solved by treating z as the vector of optimization variables and x_t as the vector of parameters to obtain z as a set of explicit functions of x_t. The optimizer z(x) is continuous and piecewise affine so will be U. Subsequently only the first element of U is applied and the control action $u(t)$ is also piecewise affine and continuous and it is expressed as an explicit function of the state variable $x(t)$ for the different critical regions, obtained though an affine mapping:

$$u(t) = f(t) = \begin{cases} K_1 x + c_1 & if \quad D_1 x \le b_1 \\ \vdots & \\ K_{Ncr} x + c_{Ncr} & if \quad D_{Ncr} x \le b_{Ncr} \end{cases} \tag{5.14}$$

where N_{CR} is the number of critical regions, K, c, D, b are constants defining each region CR, i and the derived optimal control action within. The online effort is thus reduced to the evaluation of (5.14) of the current state and the determination of the region (point location problem) in which the current state x belongs.

Although the above MPC (5.9) regulates the system to the origin or to a specific steady state, in practice MPC is used for trajectory tracking where it is required to asymptotically converge to a constant value (set-point) or to follow a reference profile that may vary in time. In order to achieve tracking the (5.9) problem is modified to include the reference profile. Thus, the objective is to minimize the error between the

system output y_t and the reference signal $y_{SP,t} \in \Re^p$ which is given by the problem specifications. Fig. 5.6 illustrates a conceptual representation of the entities that comprise the mpMPC approach (Pistikopoulos *et al.*, 2007).

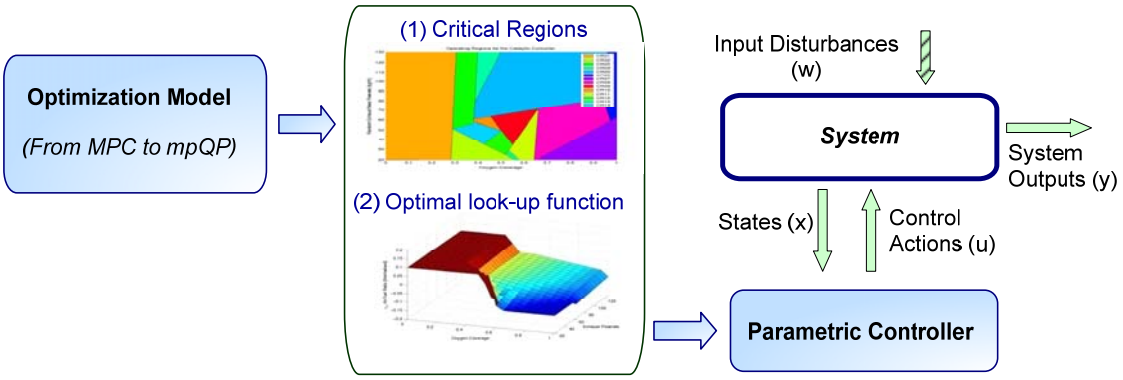

Figure 5.6 Multi-parametric control strategy

The offline preprocessing of the optimal solution allows the implementation of mpMPC with high sampling requirements whereas the look-up function offers an easy and computationally cheap implementation. But as the problem size grows (number of states and inputs, length of prediction horizon), so does the complexity of the partitioning for the critical regions due to the combinatorial nature of the mpQP problem (Tøndel *et al.*, 2003). As a consequence the mpMPC can be used to relatively small problems. An alternative approach is to employ an approximate mpMPC formulation that deals with some of these issues (Alessio and Bemporad, 2009). Nevertheless, mpMPC is the advantages of mpMPC are widely recognized and the on-going research efforts are constantly enhancing its features and characteristics.

5.5 Synergy of NMPC with mpQP

The presented advanced model-based control methodologies have many advantages and some limitations that affect their applicability. As previously stated in NMPC which is very appealing due to its ability to handle dynamic nonlinearities of the process under consideration, whereas mpMPC is based on a reduced order linear model that provides the optimal solution in real-time via a simple look-up function, as the optimization problem is computed offline. However these approaches have also some limitations. The mpMPC approach can be used to linear and relatively low dimensional systems as the complexity of the solution grows with the problem size, along with the fact that the response of the controller depends heavily on the accuracy of the derived reduced order model. In the case of NMPC the main barrier for its wider applicability arises by the requirements imposed by the online solution of the optimization problem at every iteration.

During the last decade significant effort is devoted by the research community to develop algorithms and methods that could overcome the aforementioned limitations (Pistikopoulos *et al.*, 2012). There are several very promising works that approach these issues in a systematic way and each one focus on a specific issue of the MPC-based method. In order to address the issues related to MPC, NMPC or mpMPC various approaches are developed such as:

- Reduction of the complexity of mpMPC solutions through approximate solutions or proper merging of resulted critical regions.
- Expansion of the explicit method to nonlinear systems (mpNMPC).
- Use of real-time variants and suboptimal approaches to improve the optimization time of NMPC.
- Exploit the structure of the problem through proper algorithms implemented.

However the efforts to improve the performance and limit the drawbacks of the MPC-based controllers are not limited only to different approaches to the control problem and its structure. Recently numerous methods related to algorithmic developments have been proposed. An indicative only list includes the following:

- use of a warm-start homotopy path method (Ferreau *et al.*, 2008),

- a PWA approximation for warm-starting (Zeilinger *et al.*, 2011),
- a partially reduced Sequential QP (SQP) method (Shafer *et al.*, 2007),
- an accelerated dual gradient-projection algorithm (Patrinos and Bemporad, 2012),
- new developments in interior-point methods (Wang and Boyd, 2010; Domahidi *et al.*, 2012),
- use of advanced preprocessing (Zavala and Biegler, 2009; Yand and Biegler, 2012),
- a combination of multiple shooting and direct transcription method (Tamimi and Li, 2010),
- an event-driven triggering method (Eqtami *et al.*, 2011),
- exploiting a list with frequently used active sets (Pannocchia *et al.*, 2007),
- a set-theoretic method based on an adaptive interpolation (Raimondo *et al.*, 2012),

All these approaches and methods indicate that MPC is a method of interest which is gradually evolving as its advantages are widely recognized since it has a strong potential to numerous applications from small-scale low complexity to large-scale highly nonlinear systems and processes.

5.5.1 Synergetic framework structure

Based on the above considerations this section presents a novel combination of these two well established method, NMPC and mpMPC, that cooperate in a control framework which exploits their individual characteristics. The scope of the proposed integrated framework is to combine the benefits that each control methodology has, namely the accuracy and full coverage of the system's operation for the NMPC approach and the fast execution time of the mpMPC approach. Furthermore, as the basis of the NMPC is the solution of an NLP problem it is important to reduce the computational effort (Diehl *et al.*, 2002) between successive iterations, which constitutes the primary objective of the proposed synergy.

The objective of the proposed framework is mainly the reduction of the computational effort for the solution of the NLP problem between successive iterations.

This is achieved by using a newly proposed preprocessing bound related technique and an existing technique related to the optimization problem:

- a Search Space Reduction (SSR) technique of the feasible space,
- a warm-start initialization procedure of the NLP solver.

Warm-start technique

The term warmstart signifies that information from the previously solved optimization problem is used in order to formulate the subsequent problem. More specifically the optimal solution of a problem is provided as the initial solution of a subsequent one. This technique can significantly reduce the number of iteration towards the optimum point (Benson and Shano, 2008). Therefore, it is of great importance to define a good starting point using the information gained from the previous iteration. Nevertheless, the use of a warm-start method is mainly applicable to active set solver in contrast to interior point solver where the warm-start is difficult. Furthermore, warmstarting can be applied only in situations where the successive problems are of the same size which is exactly the case for a NMPC controller. In the proposed framework a active set method is used and thus the use of warm-start is enabled to achieve better performance.

Search space exploration and region reduction/elimination

In global optimization there are two directions that the respective algorithms can follow in order to improve their performance and decrease to necessary time for the determination of the optimum solution:

- Reduce the number of variables and screen out the unimportant ones
- Reduce the search space by eliminating unpromising regions

Although both of them have interesting features and are useful for global optimization problems, in the case of control problems only the second one can be used, since all variables of the problems are important. Overall the decomposition of the search space into favorable and non-favorable areas has been previously studied for the improvement of global optimization problems using:

- domain optimization algorithms (Melo *et al.*, 2007),
- agent-based systems (Ullah *et al.*, 2008),
- metamodel based design space exploration (Booker *et al.*, 1999),
- evolutionary methods (Rowhanimanesh and Efati, 2008),
- a dividing rectangles algorithm (Jones *et al.*, 2008),
- input clustering combining with mutual information trees (Baluja and Davies, 1997),
- space exploration and unimodal region elimination (Younis and Dong, 2010).

In these algorithms, the feasible space or design space in the case of global optimization is modified by two approaches aiming to reach global solutions with the resources available and with less computation cost:

- Division into many subspaces and the search focuses on the most promising regions.
- Start of search eliminating the unpromising regions from the design space.

The benefit of using space exploration optimization algorithms is that good and acceptable solutions can be reached with fewer resources, less computation time and better accuracy. Motivated by this idea, that the feasible space can be partitioned and only part of is may be of interest, a novel method for its reduction is designed and developed in this thesis. The novel element of the newly proposed framework is the development of a search space reduction method. In the case of a tracking problem, where step changes exist, the previous computed solution, although feasible and optimal, may be away from the new set point. Therefore, after a step change the search for a new optimum solution is expanded throughout the variable's feasible space.

The main concept of the proposed framework is to define the region in a variable's feasible space that includes the optimum solution for a given objective function, by applying an SSR technique. One way to divide the feasible space into many subspaces and carrying out search in each one of these subspaces is the use of a PWA function which has been widely used on the mpMPC control method. Thus, in our case we use an mpQP formulation to define at every iteration a properly adjusted search space for the NLP solver to explore.

5.5.2 Formulation of the combined algorithm

The proposed synergy reduces the search space to a smaller subset around a suggested solution provided by a PWA approximation of the system's feasible space. Thus, the NLP solver has a reduced variable space to explore in order to locate feasible points with acceptable solution quality. Based on the fact that the special treatment of the bounds can lead to substantial computational savings (Gill *et al.*, 1984) the proposed synergy aims at the adjustment of the search space through the modification of the upper and lower bounds at every iteration. The structure of the proposed synergetic framework is illustrated in Fig. 5.7.

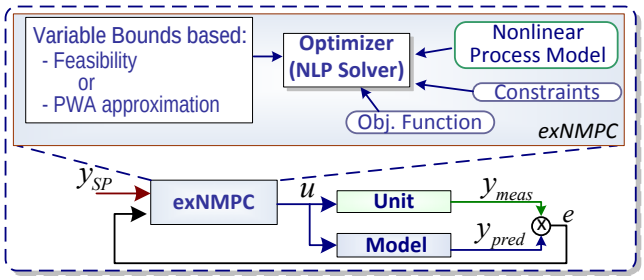

Figure 5.7 exNMPC Framework

In this context an mpMPC controller is used prior to the solution of the NLP problem in order to provide a suggested solution (u_{mp}) which is transformed into upper and lower bounds ($bu_{act,low}, bu_{act,up}$) augmented by a deviation term (e_{bu}):

$$e_{bu} = \frac{bu_{f,up} - bu_{f,low}}{by_{f,up} - by_{f,low}} e_{y,\max} \tag{5.15}$$

where $bu_{f,up}, bu_{f,low}$ are the feasible upper and lower bounds of variable u, and $by_{f,up}, by_{f,low}$ are the respective bounds for variable y. The term $e_{y,\max}$ is the maximum model mismatch between the linearized and the nonlinear model and it is determined by an offline simulation study that involves the whole operating range of y.

The space reduction methods starts by determining the upper and lower bounds utilizing information acquired by a PWA function which explores the entire feasible space. This PWA formulation yields the necessary information to be subsequently used to

update the active bounds for the selected variables. The bounds are modified at every iteration and as a consequence the search space of u is reduced to a smaller subset based on:

$$bu_{act,low} = \begin{cases} u_{mp} - e_{bu} & ,(u_{mp} - e_{bu}) \geq bu_{f,low} \\ bu_{f,low} & ,(u_{mp} - e_{bu}) < bu_{f,low} \end{cases}$$
$$bu_{act,up} = \begin{cases} u_{mp} + e_{bu} & ,(u_{mp} + e_{bu}) \leq bu_{f,up} \\ bu_{f,up} & ,(u_{mp} + e_{bu}) > bu_{f,up} \end{cases} \quad (5.16)$$

where $bu_{act,low}, bu_{act,up}$ are the active bounds for u. Therefore, the optimizer has a set of updated bounds for the respective manipulated variable u.

Apart from the bounds modification the rest of the NLP problem formulation remains the same. The proposed strategy at sampling interval k is summarized in Algorithm 1.

Table 5.1 Algorithm for search space reduction technique

Algorithm 1 SSR based on PWA and NLP problem
Input: Warm-start solution (x_k, u_k, y_k , Hessian H), measured variables (y_k^{meas}), parameters (p_k), set-points ($y_{sp,k}$)
Output: Vector of manipulated variables u_{k+1}
1: Calculate error e_k and $\hat{y}_k$
2: Locate CR_i for parameter vector ϑ_k and obtain u_{mp}
3: Calculate $bu_{act,low}, bu_{act,up}$
4: Modify bounds $u_l = bu_{act,low}, u_u = bu_{act,up}$
5: Solve NLP problem (5.5)
6: Obtain u_{k+1}^1 from $u_{k+1} = [u_{k+1}^1, ..., u_{k+1}^{NE}]$

Based on the above algorithm the explicit solution can direct the warm-start procedure for the solution of the NLP problem and thus improve its performance. One can see that the bound is constructed around the mpQP solution by considering the ratio in feasible

magnitudes of the input and output variables and the model approximation error. The bound reduction is thus ensured by considering the deviation term.

The proposed method will be further analyzed through a set of motivating simulation and experimental case studies involving the control of the PEM fuel cell unit that was analyzed in the current thesis.

5.6 Concluding remarks

The research effort in this chapter was motivated by the fact that model predictive control (MPC) is a promising control approach which is evolving and proves its agility by the results gained from its application to complex processes and multivariable systems. Thus, the formulation and basic features of two model-based predictive methodologies, NMPC and mpMPC, are analyzed along with an overview of the dynamic optimization techniques that are available for the solution of NLP problems.

Then a novel method is presented where the combination of implicit (NMPC) and explicit (exNMPC) model-based control features is exploited along with the efficient utilization of feasible space exploration and an efficient initialization technique to provide a fast control solution for complex nonlinear systems. The proposed synergetic scheme relies on an NMPC formulation that uses a simultaneous direct transcription dynamic optimization method that recasts the multivariable control problem into an NLP using a warm-start initialization method. The bounds of selected optimization variables are redefined by a search space reduction technique which is based on a PWA approximation of the variable's feasible space, computed offline by an mpQP method.

The next chapter illustrates the applicability and effectiveness of each method using simulation and real-time experimental studies of the previously described PEM fuel cell system.

Chapter 6

Application of Advanced MPC in PEMFC Systems

The aim of this chapter is to implement the results from previous chapters to the online control of the PEM fuel cell described in Chapter 2. More specifically, the dynamic model presented in Chapter 3 in conjunction with the control objectives for the PEM fuel cell introduced in Chapter 4 are used to develop various controllers based on MPC methods (Chapter 5). These methods are eventually deployed to the PEM fuel cell unit described in Chapter 2 and their efficinecy is online monitored by the automation system. The outcome of this integration is an integrated control framework which is used to evaluate the behavior of the process using different controllers under varying operating conditions, at both nominal operation and in the presence of disturbances and during system startup. Thus, the scope of this chapter is to:

- provide a thorough analysis of the design and implementation of each MPC method,
- discuss the effect of each controller to the system's behavior,
- asses the performance of each strategy with respect to the operational objectives.

Driven by this scope the chapter is divided into three parts, one for each control strategy. Extra emphasis is given to the newly developed method (exNMPC) as this is a novel

algorithmic development in the open literature. The salient features of this approach are illustrated using both simulation and real-time experimental case studies.

6.1 Design context and preparatory actions

Prior to the development of the various controllers it is important to set the context of the problem under consideration which is complimented by some necessary preparatory actions. The results from these actions constitute the basis for the development of model-based controllers in the rest of the chapter. The operation of the PEM fuel cell is strongly affected by the operating conditions (Benziger *et al.*, 2006), the interactions of the different subsystems of the fuel cell unit and the conflicting operating objectives ($P_{SP}, \lambda_{O2,SP}, \lambda_{H2,SP}, T_{fc,SP}$). All these can be handled by an advanced control framework, which enables the adjustment of the manipulated variables according to changes in the underlying process and simultaneously ensures fast response and precise tracking of the required set-points.

6.1.1 Control problem considerations

Several important issues need to be considered during the problem formulation to improve the convergence rate and the performance of the resulting controller. These aspects are related to the proper boundaries of the variables, the initial starting point and the initial conditions. Furthermore, the path towards the solution of the optimization problem can be improved by proper scaling and the use of the previously described warm-start strategy (Chapter 5).

Operation constraints of the PEMFC unit

The upper and lower bounds of the variables resulting from the operating constraints of the process guide the algorithm to avoid inappropriate and/or unsafe areas. These bounds were determined by the PEMFC system (I, V, P) in conjunction with the operating range of the mass flow controllers (MFC) ($\dot{m}_{air,in}, \dot{m}_{H2,in}$). Imposing minimum and maximum

values to the aforementioned variables, the bounds of all states were determined. The upper and lower bounds of the system operating variables are summarized in Table 6.1.

Table 6.1 Operating constraints of the PEMFC's variables

Power: 0..5.3W
Current: 2..10A
Voltage: 0.3..0.9V
Air Flow: 180..900cc/min
Hydrogen Flow: 180..900cc/min

Apart form the specification of the region of the optimization, it was necessary to provide a well scaled model during the initial problem formulation therefore all variables and parameters were properly normalized.

Model accuracy

The fuel cell model is at the heart of the optimizer, therefore its accuracy affects the prediction capability of the controller. In order to enhance the accuracy and minimize the error between the model and the fuel cell unit the results from the parameter estimation were employed as described in Chapter 3. As a result the experimentally validated model has a negligible offset from the unit's response. More specifically the mean and the maximum voltage error is 0.023V and 0.042V respectively, while the power mean and maximum error is 0.05W and 0.12W.

Initial conditions and warm-start

The initial conditions of the system and the initial starting point, as well as the proper bounds of the variables have significant influence. Therefore, the overall efficiency was improved by a proper scaling and the use of a warm-start strategy. A realistic starting point enables the first optimization step of the NMPC algorithm to result in a feasible solution for the system. In the PEMFC under consideration the starting point was selected

near the typical point of operation (0.45V), provided by the membrane manufacturer (Electrochem) that was also experimentally verified.

For a PEMFC system with moderate process disturbances, a warm-start strategy, which works well with active-set solvers like MINOS (Murtagh and Saunders, 1998), reduces significantly the number of iterations (Gill *et al.*, 1984). After the first optimization step is performed all subsequent solutions use information from the previous optimization step, such as the values of the states, the shadow variables (Lagrange multipliers), etc. Finally the Jacobian has been analytically evaluated to eliminate a costly computational step of the algorithm and to enhance the overall accuracy.

MPC related parameters

The resulting NMPC controllers are designed to be deployed and tested to the fuel cell unit. Therefore, an unstable response might cause undesirable issues to the overall fuel cell system and affect the durability and longevity of the fuel cell membrane. In order to avoid such response the prediction horizon is selected to be sufficiently long (Altmüller *et al.*, 2010; Reble and Allgöwer, 2012) with respect to the dynamics of the fuel cell (T_p=5sec) divided into N_p intervals. The control horizon (T_c) was set to be equal to the sampling time of the SCADA system (500ms) and it is divided into N_c intervals whereas the performance index to be minimized is:

$$\min_u J = \sum_{j=1}^{Np} \left(\hat{y}_{k+j} - y_{sp,k+j} \right)^T Q \left(\hat{y}_{k+j} - y_{sp,k+j} \right) + \sum_{l=0}^{Nc-1} \Delta u_{k+l}^T R_1 \Delta u_{k+l} \tag{6.1}$$

$$\text{s.t.:} \quad \begin{array}{l} \dot{x} = f_d(x,u), \quad y = g(x,u) \\ x_l \le x \le x_u, u_l \le u \le u_u, y_l \le y \le y_u \end{array} \tag{6.1a}$$

where Q and R_1 are the weighting matrices that will be fine tuned to accomplish the desired behavior. Finally the selected optimization method is the direct transcription using a reduced gradient NLP solver. The nonlinear fuel cell model is discretized based on orthogonal collocation of finite elements (OCFE). More specifically there are 10 finite elements (NE) with 4 collocation points (N_{cop}) each. All these parameters and settings

are the basis for the development of the controllers and if not otherwise stated they will be applied in every case study that follows.

6.2 Design and development of NMPC controllers for the PEMFC unit

Initially the NMPC approach as described in Chapter 5 will be used to control the PEM fuel cell. The primary objective of the subsequent analysis is the application of NMPC to the fuel cell system. To achieve this, a tailor-made optimization strategy and a proper control formulation illustrating reduced computational requirements, are proposed. A prerequisite for the online application of the controller is to exhibit both fast response and minimize the error towards the set-point. Therefore, the analysis of the behavior focuses on these two metrics: fast and accurate set-point tracking. The performance of the FC under different air and hydrogen stoichiometry was investigated considering a variable load demand. Verification and validation of the NMPC framework that deals with the control issues of the fuel cell, was performed by deploying the multivariable controller online to the unit. From the software point of view, the initial model was developed in gPROMS which is transformed into Fortran in order to be applied online to the unit. The selection of the specific programming language was based on the solver (MINOS).

A series of experiments were performed and the response of the controller at power demand changes and at variable operating conditions was explored. The behavior of the proposed scheme is exemplified here by three case studies. In the first one the accuracy of the control actions and the computational delay are shown, while in the second case study the effect of model error is explored by operating the unit at different temperatures. Finally in the third case the efficiency of the overall system is enhanced by the use of the feedforward set-point adjustment scheme that minimizes the hydrogen consumption.

6.2.1 NMPC problem formulation

From the control objectives that were analyzed in Chapter 4 we selected three of them ($y_{SP}=[P_{SP},\lambda_{O2,SP},\lambda_{H2,SP}]$) to be controlled by the NMPC whereas the heat management ($y_{SP,PID}=T_{fc,SP}$) is assigned to two PIDs, one for the heat up and one for the cooling. Thus, for the NMPC problem there are three manipulated variables, the current, the air and the hydrogen flow rates ($u=[I,\dot{m}_{air},\dot{m}_{H2}]$) and three controlled variables $y=[P_{SP},\lambda_{O2},\lambda_{H2}]$, one measured, the power and two unmeasured, the excess ratios of oxygen and hydrogen. Fig. 6.1 illustrates the control configuration which is implemented during the current case study.

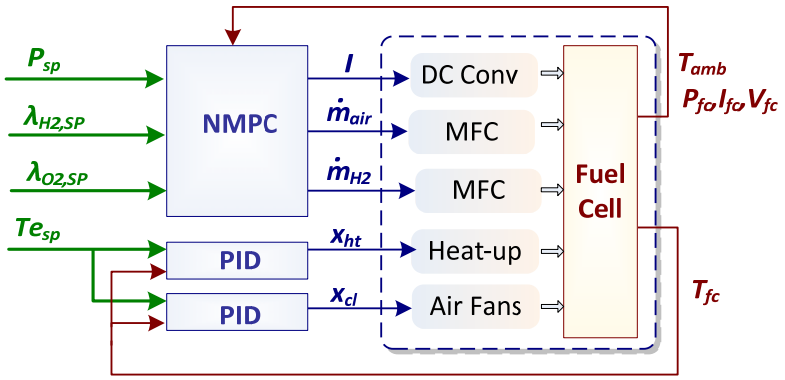

Figure 6.1 Control configuration (NMPC)

The nonlinear fuel cell model is comprised out of eight differential equations and one algebraic which are discretized into 10 finite elements (u is piecewise constant) with 4 collocation points each. At this control configuration the energy balance is not included. The resulting discretized system has 381 variables and 342 constraints and the analysis of the model discretization based on OCFE is summarized at Table 6.2.

Table 6.2 PEM fuel cell model discretization based on OCFE (NMPC)

Variables
State variables at col. points: 320
Algebraic variables at col. points: 30
Inputs at each finite element: 3
Constraints
States: 240
Algebraic: 30
Continuity at elem. boundaries: 72
Jacobian Matrix
Elements (Total/Non-zero): 130302/2520
Density: 1.934%

Furthermore, we have one more variable, corresponding to time length (t_f), which is fixed in our problem formulation. The optimization problem has 30 degrees of freedom since the control profiles are discretized into 10 finite elements (*u* is piecewise constant). At the performance index *Q* and *R* are output and input weighting matrices, respectively. Specifically $[Q_P, Q_{\lambda o2}, Q_{\lambda H2}] = diag(Q)$ and $R = R_I$, where $Q_P, Q_{\lambda o2}, Q_{\lambda H2}$ are penalties on output power ($Q_P = 1.3$), oxygen and hydrogen excess ratio ($Q_{\lambda o2} = 0.23, Q_{\lambda H2} = 0.21$) while R_I is the penalty on the change of the input current ($R_I = 0.04$).

6.2.2 Power Profile with constant excess ratios

Initially the response of the NMPC framework to various power demands was studied at specific operating conditions of temperature and pressure (*T*=338K, *Pt*=1bar). A number of power demand changes were made within a range of 1W to 5W, which covers the operational range of the system. Fig. 6.2 illustrates the experimental data showing the step changes in the power demand and the respective produced power from the FC unit.

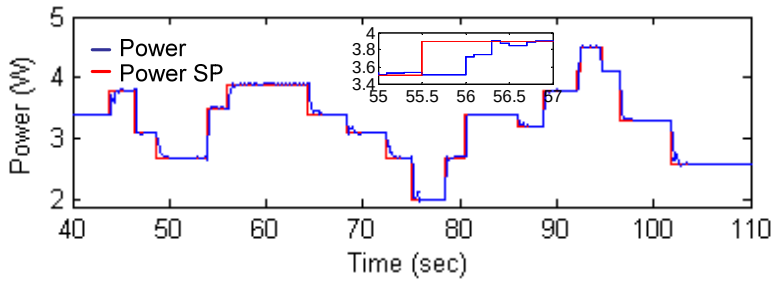

Figure 6.2 Power response at constant temperature (NMPC)

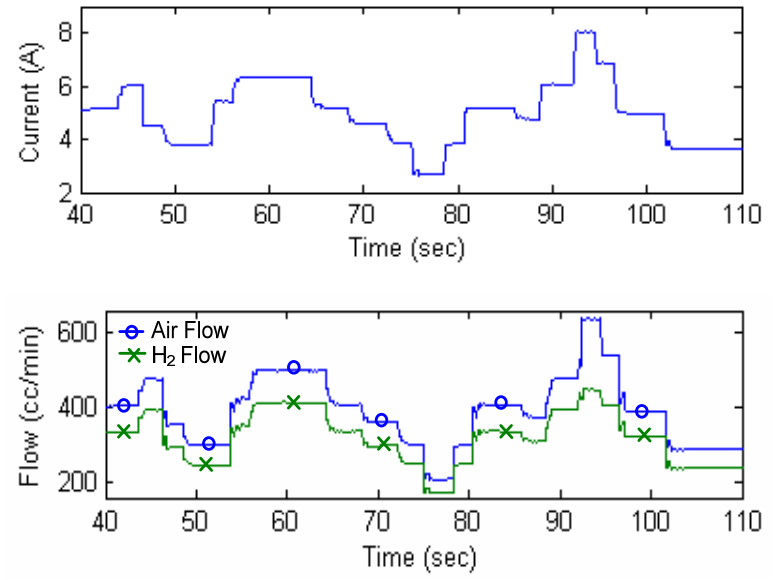

Figure 6.3 Manipulated variables (NMPC) a) current, b) air and hydrogen flow

Fig. 6.2 shows the power response to the corresponding control actions of the manipulated variables (Fig. 6.3a, Fig. 6.3b) as the power demand changes while the oxygen and hydrogen excess ratio remains at a constant set-point ($\lambda_{o2,sp}$=3.3, $\lambda_{H2,sp}$=3). The profiles of the manipulated variables are derived by the NMPC during the various changes of the power demand. It can be observed that the controller is able to steer the fuel cell power to any admissible set-point while maintaining the required excess ratio level. Also, from a simple error analysis is noticeable that the NMPC can produce a series of control actions (Fig. 6.3) resulting to a negligible offset from the desired set-point. More specifically, the mean square error (MSE) is 51mW for the power and the average oxygen and hydrogen excess ratio error is less than $3*10^{-3}$.

Besides the necessary accuracy, the second issue that the NMPC framework should address is the computational delay. Fig. 6.4 illustrates the optimization time which is required for the solution of the NLP problem at every sampling interval.

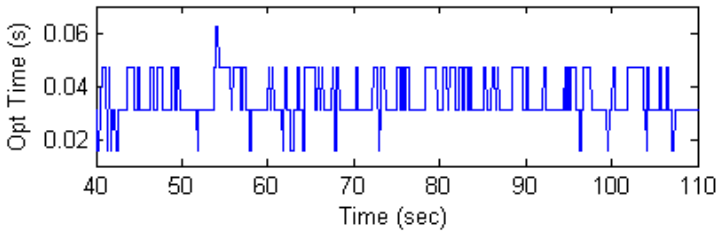

Figure 6.4 Optimization time at various power step changes (NMPC)

At every interval the optimization problem is solved and it is observed from Fig. 6.4 that the maximum optimization time is 63ms while the average optimization time is 34.7ms. This signifies that the sampling time constraint is satisfied and that the controller behaves seamlessly throughout the whole experiment regardless of the various changes of the power demand. This case study reveals that the controller is able to track the changes of the power demand accurately and with sufficient speed, while maintaining the safety of the system by keeping the excess ratio of oxygen and hydrogen at the desired level.

6.2.3 Response to disturbances and model uncertainties

The second case study where the response of the NMPC controller is explored involves the appearance of some disturbances at the system. The efficiency of the controller to confront disturbed operating conditions and unmodeled phenomena that might appear over time, such as membrane/catalyst system degradation, was verified by choosing temperature as a metric in the following studies. The case study involves two different scenarios. In the first one a variable power profile and constant excess ratios set points were required at three different operating temperatures of the FC resulting from process disturbances. In the second scenario the demanded power and the excess ratios set points are kept constant while the unit temperature decreases. The FC temperature is modified by the use of the heat-up subsystem of the unit which is controlled by a PI controller.

Controller Response at Different FC Temperatures

In the first scenario the assumed operating temperature of the FC as described by the dynamic model is 65°C while the unit operates at 65°C, 55°C and 45°C due to disturbances at the inlet temperatures of the reactants. This difference causes a deviation between the output power of the model and the actual power of the fuel cell. In the following analysis three step changes in the load demand were imposed for each different temperature. The oxygen and hydrogen excess ratios were kept by the controller at the same level (λ_{o2sp}=3, λ_{H2sp}=2.6). Fig. 6.5 shows the power tracking capability of the controller despite the disturbances effect. We observe that the power set-point is reached in all three cases.

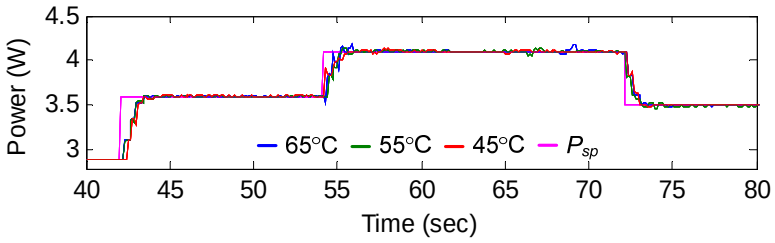

Figure 6.5 Power response at different temperatures (NMPC)

The experimental data show the demanded power profile and the respective produced power when the FC unit operates at different temperature points (45°C, 55°C and 65°C). Fig. 6.6 illustrates the effect of the operating temperature at the voltage and more specifically it shows a comparison between voltage profiles that are derived at different temperatures for tracking the same power profile and excess ratio levels. Fig. 6.7 shows the resulting control actions (current, air and hydrogen flows) for the three different operating temperatures.

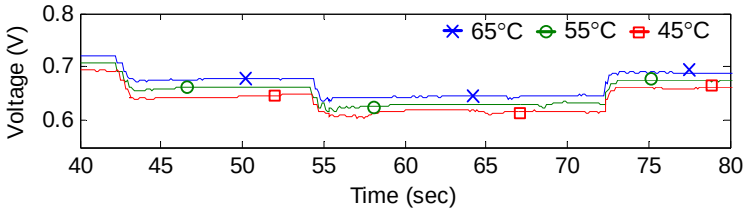

Figure 6.6 Voltage response at different temperatures (NMPC)

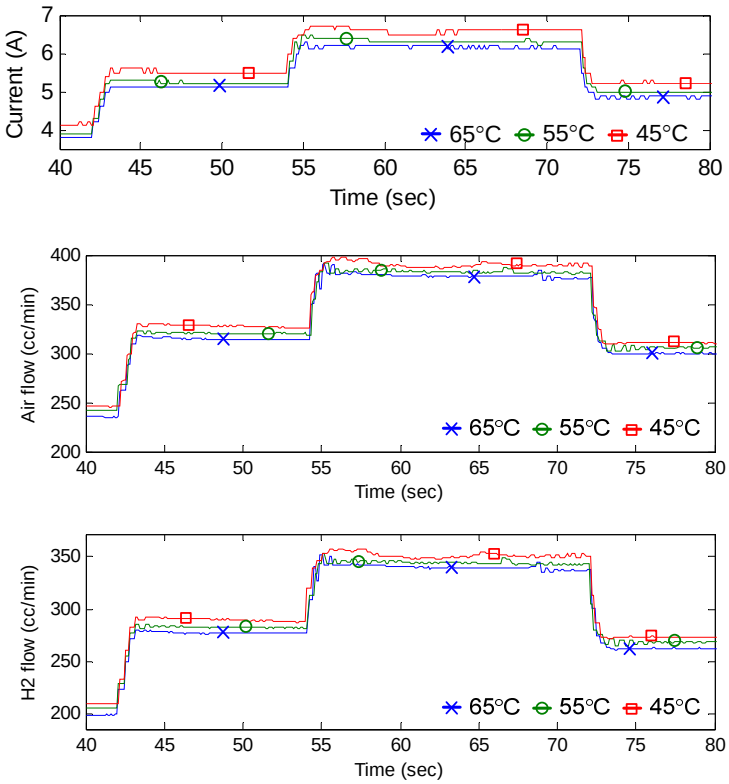

Figure 6.7 Manipulated variables profiles at different temperatures (NMPC)

Fig. 6.7 shows a comparison between the manipulated variables profiles that are applied to the FC unit in order to follow the desired power profile and excess ratio levels at different temperatures (45°C, 55°C and 65°C). From Fig. 6.7a we observe that as the temperature decreases the current is accordingly increased in order to reach the power demand. The air and hydrogen flows are adjusted (Fig. 6.7b, Fig. 6.7c) in order to reach the desired excess ratio levels.

Fig. 6.8 illustrates the required time for the solution of the NLP problem for the various temperature profiles (45°C, 55°C and 65°C) showing that the optimization time is at the same levels for each experiment.

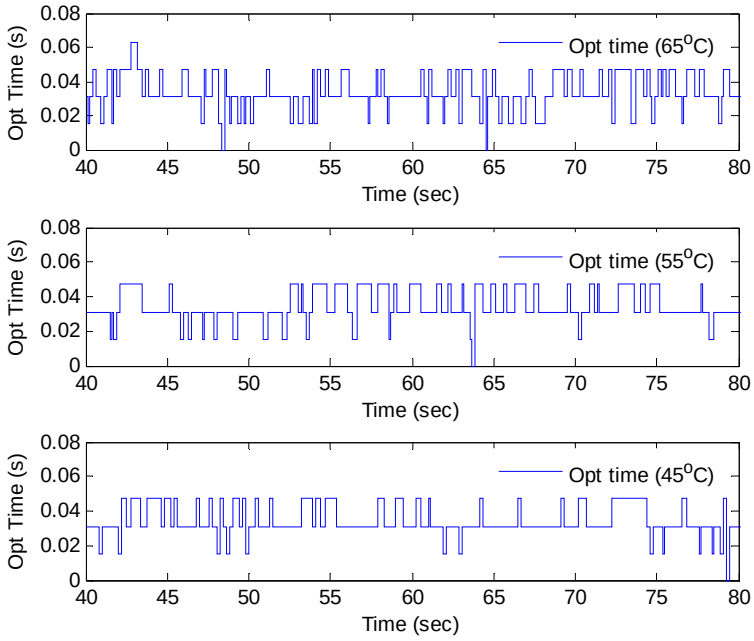

Figure 6.8 Optimization time at various temperatures (NMPC)

Fig. 6.8 shows that the optimization time is not affected when the controller has to deal with process disturbances affecting the operating temperature. Overall the controller behaves seamlessly regardless of the temperature difference.

Controller Response to Temperature decrease

In the second scenario the response of the NMPC controller in the presence of a continuous decrease of the operating temperature is explored. Initially the operating FC temperature was at 53°C, while the required set-points of power, oxygen and hydrogen excess ratios were kept constant at 3.5W, 3.5 and 3.2 respectively by the NMPC controller. As the heat-up subsystem was turned off and the cooling subsystem was enabled, the operating temperature decreases. In Fig. 6.9 the temperature drop (10°C) is shown and its effect to voltage is illustrated in Fig. 6.10. As the voltage changes the controller adjusts the inputs properly in order to maintain the desired set-points.

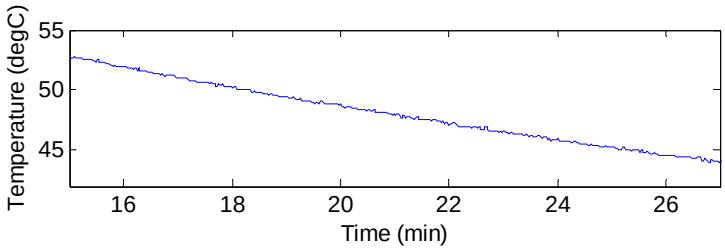

Figure 6.9 Temperature decrease as the heat-up is turned off (NMPC)

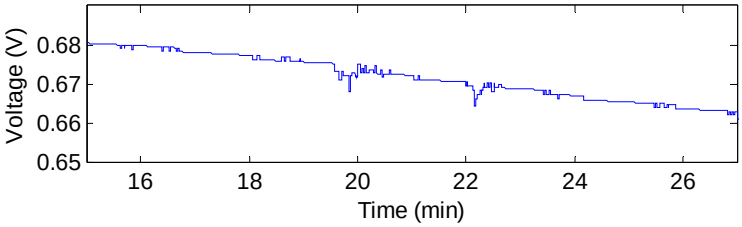

Figure 6.10 Voltage response to temperature decrease at constant power (NMPC)

Fig. 6.11 shows experimental data of the demanded and the respective produced power during the decrease of the operating temperature, while Fig. 6.12 shows the respective control actions for the current and the gas flows that are adjusted during the temperature decrease in order to maintain the produced power at the desired level.

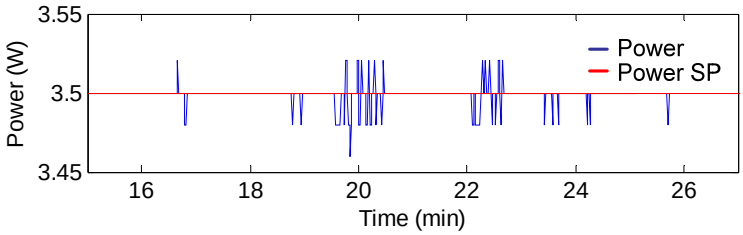

Figure 6.11 Produced power while temperature decreases (NMPC)

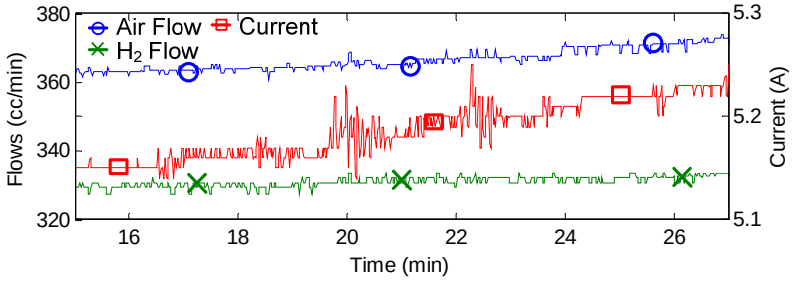

Figure 6.12 Manipulated variables at temperature decrease (NMPC)

Although the error between the actual voltage and the predicted by the dynamic model voltage increases due to the temperature difference, the execution time for the solution of the optimization problem remains at low levels (20ms-60ms) similar to the nominal case, with an average value of 36ms. Finally the average error between power, oxygen and hydrogen excess ratios and their set-points are 17mW, $2.1*10^{-3}$, $1.9*10^{-3}$ respectively.

The results from the above scenarios reveal that the multivariable NMPC controller is able to handle relatively large deviations of the temperature between the process and the model and consequently of the predicted power and although the error increases, the respective time for the solution of the optimization problem remains the same while the demanded power and excess ratio levels are reached efficiently. Furthermore, the NLP problem converges to an optimum solution at each time interval. From the above analysis we conclude that the controller can tolerate a large level of model error without any performance deterioration.

6.2.4 Minimum hydrogen supply

In the third case study where the NMPC method is used, the application of the feedforward scheme for the minimization of the hydrogen consumption to the system is explored and the control configuration presented at Fig. 6.1 is slightly modified resulting to the one of Fig. 6.13. During this case study the operating FC temperature is kept at 65°C.

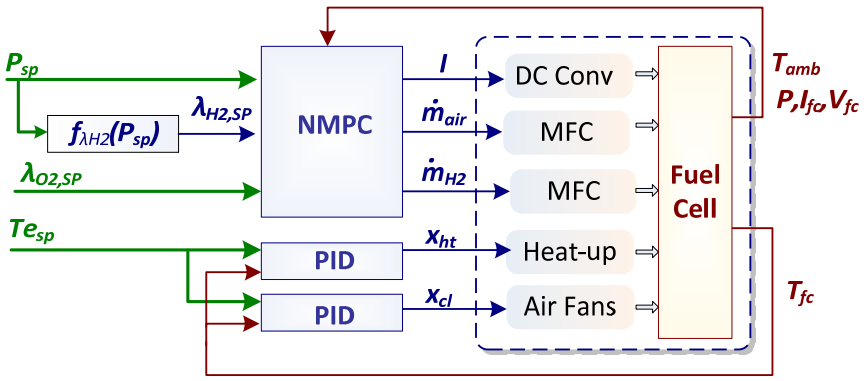

Figure 6.13 Expanded control configuration for adjusting the $\lambda_{H2,SP}$ (NMPC)

In order to determine the appropriate set-point that concurrently satisfies the manufacturers constraint (flow rate > 180cc/min) and the operating constraint (λ_{H2}>1) the 4th degree polynomial is used based on the analysis presented in Chapter 2. The effect of this control configuration is shown in the following scenario which involves a few step changes in the power demand and it is compared to the case where the hydrogen excess ratio is kept at a constant level (λ_{H2}=2.8).

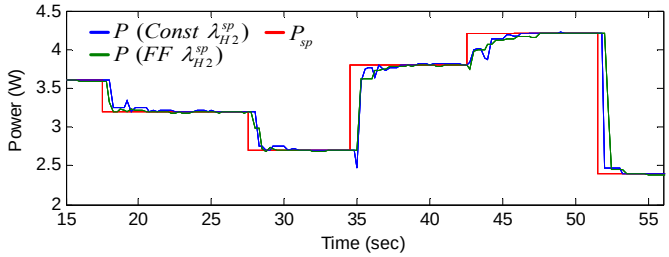

Figure 6.14 Power tracking with and without the adjustment of $\lambda_{H2,SP}$ (NMPC)

Fig. 6.14 presents a comparison of the power tracking ability of the fuel cell as the excess ratio of hydrogen is kept at constant level and as it is adjusted to the minimum allowable hydrogen flow. It is observed that the power set-point is reached in both cases. Fig. 6.15 illustrates the hydrogen excess ratio profiles based on a constant set-point and an adjustable set-point utilizing the feedforward scheme based on the power demand.

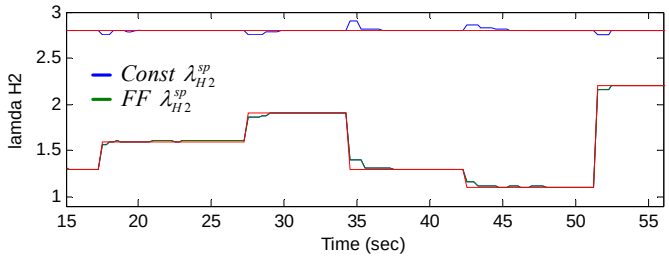

Figure 6.15 Profile tracking of $\lambda_{H2,SP}$ with and without the adjustment (NMPC)

As illustrated by Fig. 6.15 the hydrogen excess ratio ranges from 1.3 to 2.4 and the controller is able to adjust the hydrogen flow rate in order to reach the set-point which is modified in a feedforward manner. The respective flow rate for both cases, constant or adjusted set-point, is shown in Fig. 6.16.

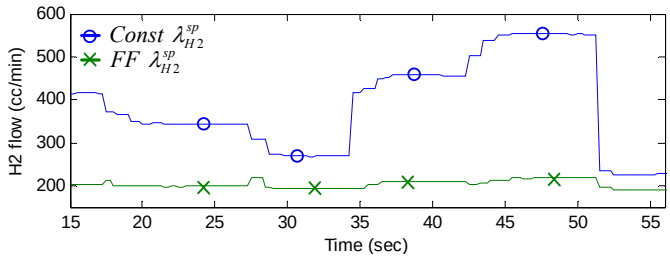

Figure 6.16 Hydrogen flows with and without the adjustment of $\lambda_{H2,SP}$ (NMPC)

Fig. 6.16 shows the modification of the hydrogen flow rates where the $\lambda_{H2,sp}$ is kept constant and when $\lambda_{H2,sp}$ is adjusted utilizing the feedforward scheme based on the power demand. It is noted that the hydrogen flow rate is significantly reduced in the second case, while the set-point is reached with the same accuracy. Therefore, the feedforward scheme can be used in order to reduce the hydrogen usage, while at the same time the safety of the system is ensured and the power is delivered as requested.

6.2.5 Overall assessment of the NMPC controller

The NMPC controller that was derived for the online control of a PEMFC system can efficiently address the issues of power generation in a safe and controlled way. From the results of the experimental case studies it is observed that the controller is able to track efficiently a variable power demand while compensating process disturbances as well as the effects of unmodeled phenomena such as degradation or variations of operating conditions. Overall, it has been clearly illustrated that the NMPC framework is able to deal with uncertainties and achieve trajectory tracking in a satisfactory manner. Also, in all three case studies the NMPC controller exhibits low optimization solution requirements without convergence failures while satisfying realistic constraints imposed by the nature of the PEM fuel cell system.

6.3 Design and development of mpMPC controllers for the PEMFC unit

The second MPC method that was developed is mpMPC. The primary objective of the subsequent analysis is to derive a number of decentralized mpMPC controllers one for each control objective and evaluate the response of the system in simulation mode. Some of these controllers will be used for the formulation of the exNMPC algorithm that will be examined in the subsequent section 6.4. Based on that, the analysis will be brief as the focus of this thesis was not on the mpMPC method. The decentralized control configuration which is developed and used is illustrated at Fig. 6.17 including the input/output variables of each controller and the interactions between them.

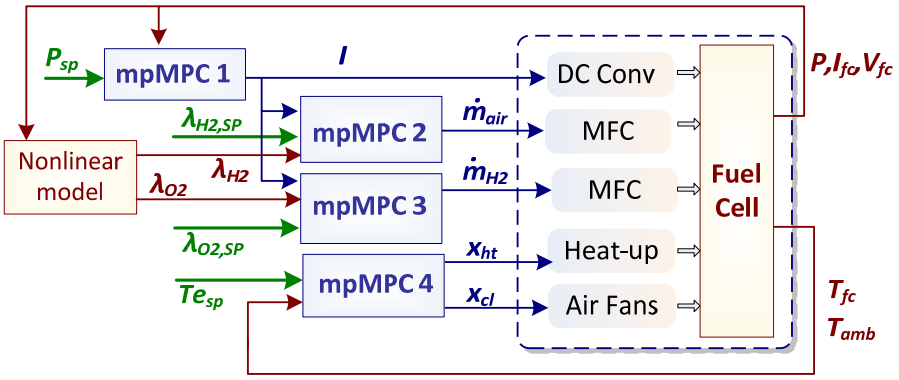

Figure 6.17 Distributed control configuration (mpMPC)

The four mpMPC controllers are designed based on an equal number of linear models that are derived using a model identification technique. From the software point of view, the initial model was developed in gPROMS which is transformed into Matlab code with Simulink for the solution of the mpQP problem and the derivation of the PWA function for the variables into consideration. The selection of the specific software package was dictated by the multi-parametric software that was used (POP) (ParOS Ltd, 2007).

A series of simulation experiments were performed and the response of the controllers at power demand and excess ratio changes was explored. The behavior of the

proposed scheme is exemplified here by a simulation case study, whereas the experimental deployment of the controller and its effect at the response of the PEM fuel cell unit is explored in the comparative case studies that will be presented in the subsequent section 6.4.

6.3.1 Linear model approximation

Prior to the control framework the nonlinear model needs to be simplified in order to be used for the MPC controller design. Therefore, a discrete reduced order state space (SS) model for each control objective is obtained using a model identification technique that reconstructs adequately the dynamic behavior of the system. The input-output data are obtained from simulations of the nonlinear model for various operating conditions and the parameters of the SS models are determined from the Identification Toolbox of Matlab. The sampling time for the data is 100ms for the power, the current and the mass flow rates, and 1s for the temperature, since temperature presents slower dynamic behavior. The mathematical representation of the SS model with additive disturbances is as follows:

$$\begin{aligned} &x(t+1) = Ax(t) + Bu(t) + Cv(t) \\ &y(t) = Dx(t) \\ &y_{\min} \le y(t) \le y_{\max}, u_{\min} \le u(t) \le u_{\max}, v_{\min} \le v(t) \le v_{\max} \end{aligned} \tag{6.2}$$

The first SS model (ss_{Pfc}) approximates the behavior of the power and has one manipulated variable (I), one control (output) variable (P) and two states.

$$A = \begin{bmatrix} 0.99904 & 0.045486 \\ 0.003633 & 0.82713 \end{bmatrix}, B = \begin{bmatrix} -0.0051039 \\ 0.019406 \end{bmatrix}, C = \begin{bmatrix} -17.482 & 0.0036194 \end{bmatrix}$$

The second ($ss_{\lambda o2}$) and the third ($ss_{\lambda H2}$) reduced order models approximate the behavior of the oxygen and hydrogen excess ratio. Both SS models have one state, one disturbance (I), one manipulated variable which is the mass flow rate of air ($\dot{m}_{air}$) and hydrogen ($\dot{m}_{H2}$) and one output variable each, the excess ratio of oxygen (λ_{O2}) and hydrogen (λ_{H2}), respectively. The system matrices are:

$$A_2 = [\text{-}0.014276], B_2 = [\,0.060283], C_2 = [\text{-}0.0088574], D_2 = [233.68]$$

$$A_3 = [\,\text{-}\,0.055887],\ B_3 = [0.0086835], C_3 = [\text{-}0.0055123],\ D_3 = [\,238.05]$$

The fourth SS model (ss_{Tfc}) represents the behavior of the temperature which is maintained at the desired set point through a heatup resistance and a set of cooling fans. The system matrices are presented bellow:

$$A_4 = 1,\ B_4 = [0.0052417\ \text{-}0.0004687], C_4 = [3.3348\text{e-}009],\ D_4 = 1$$

This model has one state, one output /control variable (T_{fc}), one known disturbance the ambient temperature (T_{amb}) and two inputs, the power to the resistance for the heatup (W_{ht}) and the power of the fans (W_{cl}), which both are transformed into operation percentage (x_{ht} ,x_{cl}). A measure of the fitness between the aforementioned models in question and the provided data for the identification is the mean square-root difference (Table 6.3).

Table 6.3 Fit results for the identified ss models

Controlled Variable	Sampling time	Samples	MSE	Fit %
Power	100ms	1200	29mW	82.9
λ_{O2}	100ms	6000	0.041	83.2
λ_{H2}	100ms	6000	0.037	84.1
T_{fc}	1sec	58000	0.004K	91.4

From the results of Table 6.3 it is apparent that the response of the approximated models would be close to the nonlinear model and that the SS models have the required accuracy to describe the behavior of the simulated system. Fig. 6.18 present the results of the fitness for the power and Fig. 6.19 for the temperature which also verifies the metrics presented at Table 6.3.

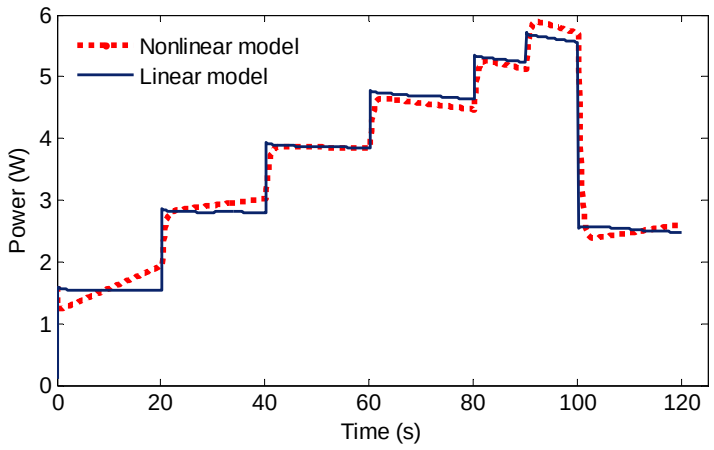

Figure 6.18 Comparison of linear vs nonlinear model (variable: power)

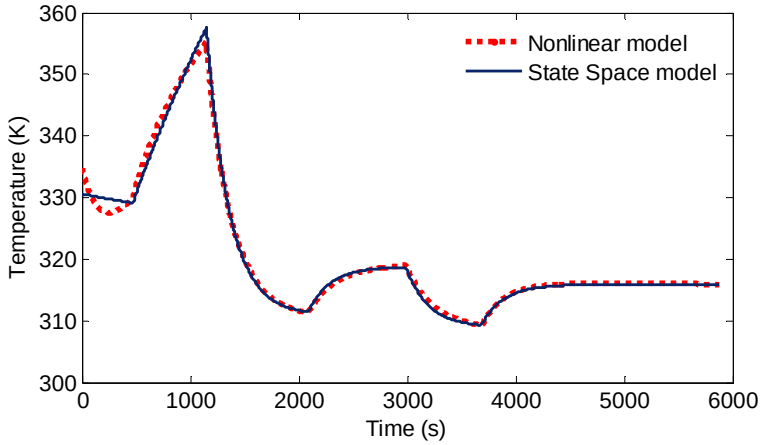

Figure 6.19 Comparison of linear vs nonlinear model (variable: temperature)

6.3.2 Design of the mpMPC controllers

The next step involves the design of mpMPC controllers for the PEM fuel cell system based on the derived SS models. Overall there are four MPC problems which are subject to constraints and they are formulated based on problem (6.1). Thus, for each control variable (represented by an SS model) an MPC problem is formulated. Subsequently, each MPC problem is transformed into an mpQP problem which involves a systematic exploration of the parameter (ϑ) space and results in a set of convex non-overlapping

polyhedra (critical regions) of this space, each corresponding to a unique set of active constraints (Chapter 5, section 5.4). The parameters for each mpQP problem are presented at Table 6.4.

Table 6.4 mpQP problem parameters

Objective	Optimization Var. (u)	Parameters (θ)
Power	Current	$\theta_1 = [x1\ x2\ I\ P\ P_{sp}]$
O2 Excess ratio	Air flow	$\theta_2 = [x1\ I\ \lambda_{O2}\ \lambda_{O2,sp}]$
H2 Excess ratio	Hydrogen flow	$\theta_3 = [x1\ I\ \lambda_{H2}\ \lambda_{H2,sp}]$
Temperature	Resistance %, Fans %	$\theta_4 = [x1\ T_{amb}\ T_{fc}\ T_{fc,sp}]$

The aforementioned mpQP problem and can be solved with standard multi-parametric techniques (mpQP) (Pistikopoulos *et al.*, 2007). In our study the explicit parametric controller was derived with the Parametric Optimization (POP) software (ParOS Ltd, 2007). The control horizon in each problem is 2, therefore there are two optimization variables (u_{t+0}, u_{t+1}). The corresponding parameters of each problem are shown in Table 6.5 along with the respective number each mpMPC controller's critical regions.

Table 6.5 mpMPC settings and resulting regions

Objective	Optimization variables (u)	Pred.Hor. (Np)	Weight (Q)	Weight (R)	CR
P	$I_{(t+0)}$, $I_{(t+1)}$	10	3	0.01	57
λ_{O2}	$m_{O2(t+0)}$,$m_{O2(t+1)}$	20	1	0.1	13
λ_{H2}	$m_{H2(t+0)}$, $m_{H2(t+1)}$	40	100	0.1	13
T_{fc}	$W_{R\ (t+0)}$, $W_{R\ (t+1),}$ $W_{cl\ (t+0)}$, $W_{cl\ (t+1,)}$	100	1000	0.001	17

A projection of the critical regions for the mpMPC controller of the power is shown in Fig. 6.20.

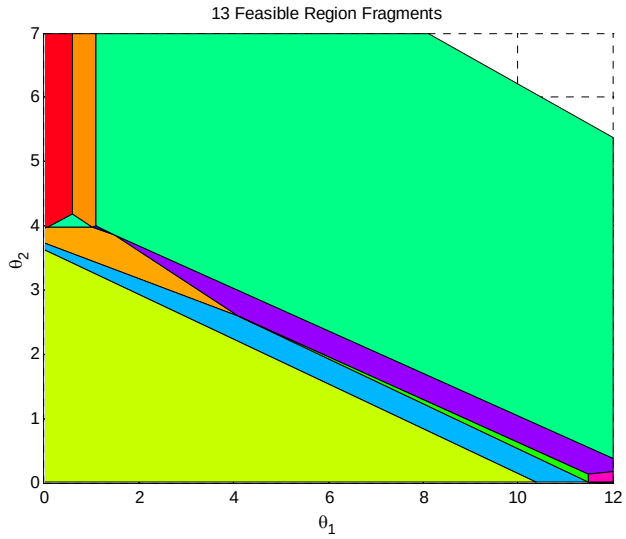

Figure 6.20 Critical regions of the mpMPC controller for the power

The result from the aforementioned actions is four mpMPC controllers and their response will be explored by a simulation study.

From the software point of view, during this thesis two main software algorithms were developed:

- An automatic transformation of the critical regions from Matlab code to Fortran language (Appendix B)
- An algorithm that implements a simple look-up function of the critical regions in Fortran language (Appendix B)

Both of them were not available in POP software and since we wanted to use the mpMPC controller to the unit and most importantly to the newly developed exNMPC algorithm (Chapter 5, Section 5.5) it was necessary to develop respective interfaces between the results of POP and Fortran language.

6.3.3 Simulation case study using the mpMPC controllers

The following case study presents the control of the fuel cell system which is simulated by the nonlinear dynamic model using the aforementioned mpMPC controllers. Figs 6.21, 6.22 and 6.23 illustrate the simulation results of the mpMPC implementation for various set-points. During the simulation we assumed that the ambient temperature was kept constant at 298K. The performance of the temperature controller is presented in Figure 4, where simulations performed with three temperature set points changes (333K, 338K, 343K) while the power controller's set point is set at constant level (5W), and it is observed that the controller follows rapidly the set point changes on the temperature without offset. Due to the small size of the PEMFC the system needs to be heated during steady state operation in order to follow the set point (the resistance is working at 1-4%).

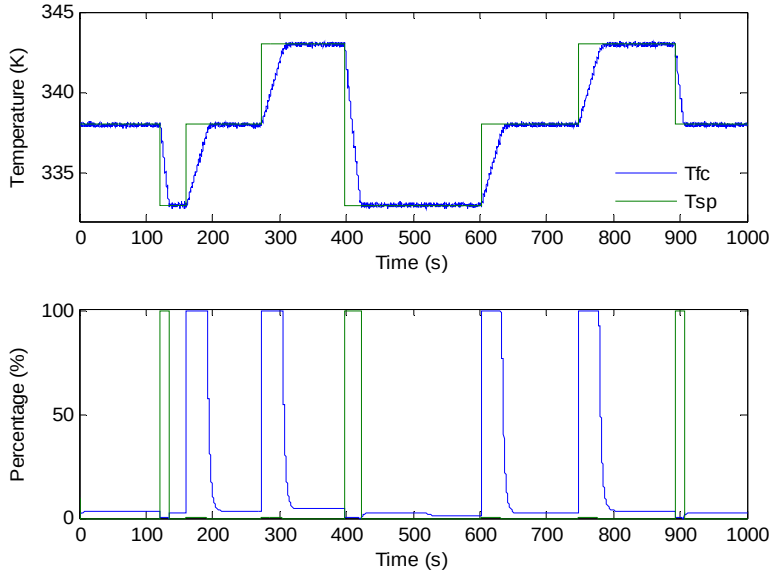

Figure 6.21 Temperature control and cooling/heatup (mpMPC)

Figs 6.22 and 6.23 illustrate the performance of the power and oxygen excess ratio controllers. During the simulated experiment the hydrogen excess ratio is kept constant through the controller (λ_{H2}=1.5) and the temperature controller has a fixed set point at 338K.

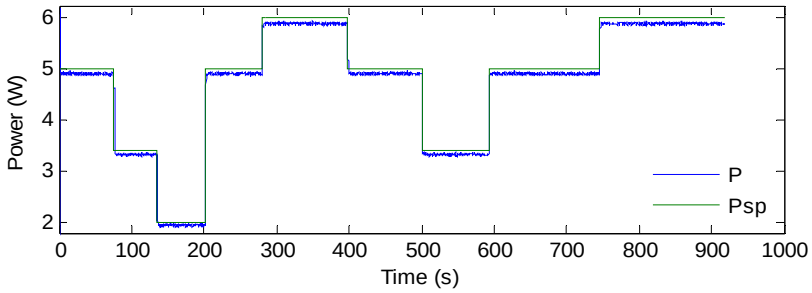

Figure 6.22 Control of power (mpMPC)

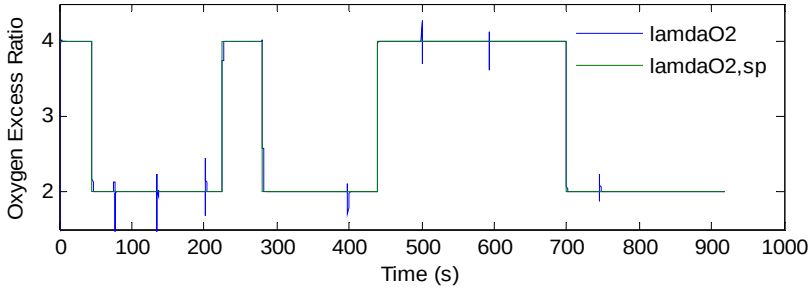

Figure 6.23 Control of λ_{O2} (mpMPC)

The power controller showed excellent response to load changes and the excess ratio controller demonstrated fast settling time (less than 2s) after current disturbances. The current (Fig. 6.24a) and the mass flow rates (Fig. 6.24b) are properly adjusted to fulfill the starvation avoidance constraint by keeping the excess ratio at constant level.

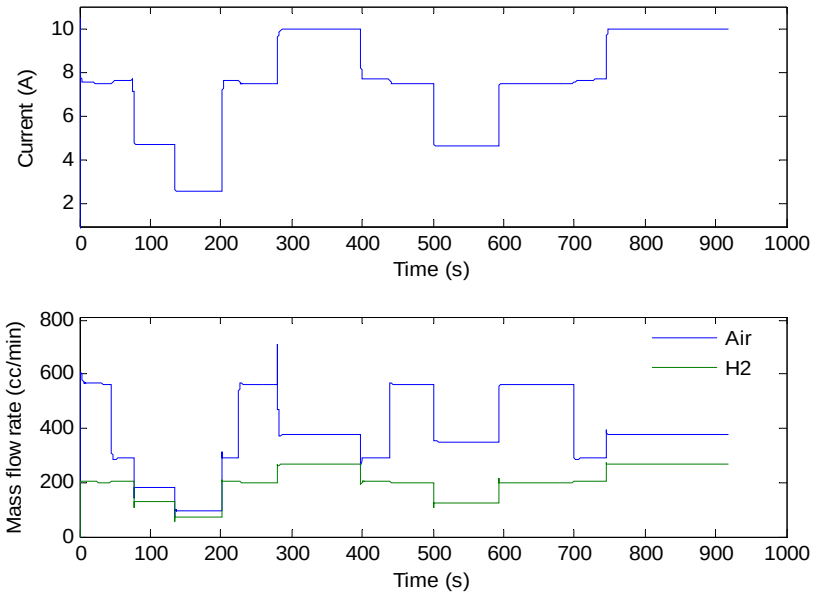

Figure 6.24 Current and mass flow rates profiles (mpMPC)

Overall the mpMPC controllers are able to track the desired reference points regardless the fluctuations of the interacting variables. Finally the system response was within the feasible area of operation since the output of the controllers was bounded by the operating constraints and the stability was guaranteed.

6.3.4 Overall evaluation of the mpMPC controllers for the PEMFC

The development procedure of mpMPC controllers requires less time as they can be derived by experimental data as well. This can be very helpful at the early stages of the development of a control system or in the case that we want to identify a trend in the response of the system. In this section a set of mpMPC controllers were developed and validated offline based on simulation data from the nonlinear dynamic model. Four controllers have been derived in order to fulfill the power demand, while avoiding starvation and maintain the fuel temperature at the desired set point. The results from their deployment to the PEM fuel cell unit will be presented in the subsequent section where a number of comparative experimental case studies will reveal their effect to the behavior of the unit and their response to varying operating controllers.

6.4 Design and development of exNMPC controllers for the PEMFC unit

The third MPC method developed and applied in the PEM fuel cell system, is the combined exNMPC method where the use of mpQP enhances the performance of a typical NMPC formulation through a search space reduction (SSR) algorithm as illustrated in Chapter 5. Based on the exNMPC method a number of controllers are developed which are used in simulation and experimental case studies, in order to exemplify the effectiveness and prove the agility of the newly proposed method approach. For this purpose three main case studies will be presented:

- Analysis of the effects of the SSR to the performance of NMPC and comparison of different initialization methods of the optimization problem (in simulation mode).
- Response of the exNMPC at nominal conditions and in the presence of disturbances, including a comparison to mpMPC and NMPC controllers (experimental deployment).
- Experimental application of exNMPC at different operating conditions and for the start-up of the PEM fuel cell system (experimental deployment).

During the experiments (simulation and experimental) the feedforward scheme for the adjustment of the hydrogen and oxygen excess ratio is also employed ensuring that the system operates not only at a safe region but also it utilizes the minimum required fuel to operate. The interconnection of the controller to the industrial SCADA system is achieved through a custom made OPC-based interface that was designed to establish the online communication between the NLP solver and the automation system.

The development of an exNMPC method is based on two main set of actions, the offline reparatory actions and the online deployment and parameter tuning of the controller. The offline actions are responsible for the development of the exNMPC controller that would satisfy the control and operation objectives of the system and include the following:

- Formulate the NMPC controller (direct transcription and NLP problem).
- Select the manipulated variables to be adjusted online.

- Approximate nonlinear model with linear state space model.
- Calculate the linearization error.
- Determine critical region for each objective by the solution of the mpQP problems.
- Derive PWA functions for each selected control objective.
- Define the SSR parameters.

These actions are implemented for the PEM fuel cell system and the resulting parameters and settings will be presented.

6.4.1 exNMPC Problem Formulation

The development of the exNMPC controller involves a typical NMPC controller which is augmented by a preprocessing algorithm (SSR) which is called prior to the solution of the NLP problem. This NMPC controller is based on the direct transcription method and it is formulated according to Section 6.2. Besides the NMPC problem formulation, the rest of the preparatory actions involve the SSR algorithm.

NMPC problem formulation based on direct transcription

According to the control objectives ($y_{SP} = [P_{SP}, T_{fc,SP}, \lambda_{O2,SP}, \lambda_{H2,SP}]$) defined in Chapter 4, there are five manipulated variables ($u = [I, \dot{m}_{air,in}, \dot{m}_{H2,in}, x_{ht}, x_{cl}]$) and four controlled variables ($y = [P_{fc}, T_{fc}, \lambda_{O2}, \lambda_{H2}]$). Two of the manipulated variables (x_{ht}, x_{cl}) are mutually exclusive and they mainly affect one of the controlled variables (T_{fc}). Fig. 6.25 illustrates the control configuration which is implemented during the current case study.

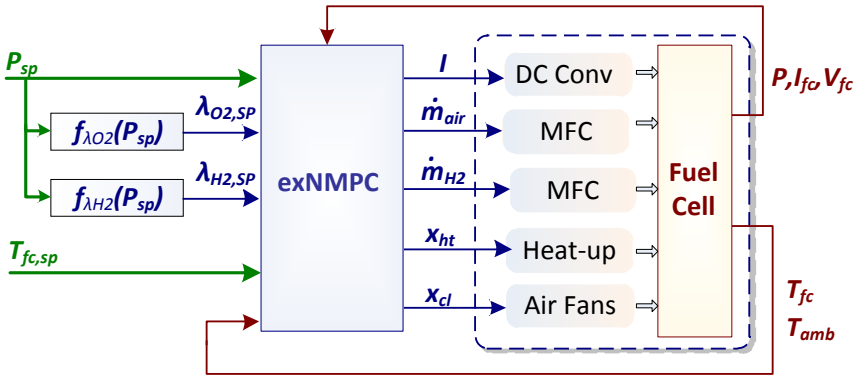

Figure 6.25 Control configuration (exNMPC)

Regarding the NMPC formulation (eq. 6.1) the weight matrix Q defines the weights for the output power, oxygen and hydrogen excess ratio and temperature ($[QR_P, QR_{\lambda o2}, QR_{\lambda H2}, QR_{Tfc}] = diag(QR)$) while $R1$ are the penalties on the change of the current, the percentage of operation of the heat-up resistance and the cooling fans ($[R1_I, R1_{xht}, R1_{xcl}] = diag(R1)$). The nonlinear dynamic model of the PEMFC, presented in Chapter 3, is comprised of nine differential equations and one algebraic, discretized at 10 finite elements (NE) having 4 collocation points (N_{cop}) each, resulting to 441 variables and 381 equations and the analysis of the model discretization based on OCFE is summarized at Table 6.6.

Table 6.6 PEM fuel cell model discretization based on OCFE (NMPC)

Variables
State variables at col. points: 360
Algebraic variables at col. points: 30
Inputs at each finite element: 5
Constraints
States: 270
Algebraic: 30
Continuity at elem. boundaries: 81
Jacobian Matrix
Elements (Total/Non-zero): 168021/3375
Density: 2.009%

SSR and PWA functions

Three of the manipulated variables (I, x_{ht}, x_{cl}) are selected to have varying bounds during the operation of the system, that mainly affect two of the controlled variables (P_{fc}, T_{fc}). The development of the SSR technique as analyzed in Section 5.4, requires a PWA function to approximate the power and the temperature behavior of the fuel cell system using the aforementioned mpMPC approach. Prior to the solution of the mpQP problem two linear discrete state space (ss) models are derived, one for each control objective. The first one (ss_P) approximates the behavior of power and has one input variable (I) and two

states ($x_{P,1}, x_{P,2}$) whereas the second ss (ss_{Tfc}) approximates the temperature behavior and has two input variables (x_{ht}, x_{cl}), one disturbance (T_{amb}) and two states ($x_{Tfc,1}, x_{Tfc,2}$).

For each linear model (ss_P, ss_{Tfc}) an mpQP problem is formulated. The first mpQP problem involves five parameters $\vartheta_P = [x_{P,1}\ x_{P,2}\ I\ P\ P_{sp}]$ and the resulting optimal map consists of $N_{CR,P} = 57$ critical regions. The second mpQP problem involves six parameters $\vartheta_{Tfc} = [x_{Tfc,1}\ x_{Tfc,2}\ T_{amb}\ T_{fc}\ T_{fc,sp}]$ while the resulting feasible space, defined by ϑ_{Tfc}, is partitioned into $N_{CR,Tfc} = 23$ critical regions. Based on a simulation analysis the linearization error ($e_{y,\max}$) and the change of bounds are determined (e_{bu}) that will by used for the online adjustment ($bu_{act,low}, bu_{act,up}$) of the active boundaries for each variable. The values of the parameters for the SSR are outlined at Table 6.7.

Table 6.7 Parameters for the SSR algorithm of exNMPC

Manipulated variable	**Linearization Error** ($e_{y,\max}$)	**Max deviations**	**Max Change of Bounds** (e_{bu})
x_{ht}, x_{cl}	8.60%	4.3°C	±8%
I	17.10%	0.684W	±2A

These parameters are used so that the bounds of I, x_{ht}, x_{cl} are adjusted while the bounds of the other two variables ($\dot{m}_{air}, \dot{m}_{H2}$) are fixed at their feasible bounds.

6.4.2 Explore the SSR effect – Different initialization methods (simulation)

In the first case study the performance of the proposed exNMPC scheme is illustrated through two simulation scenarios. In first one (S1) the analysis focuses on the temperature objective whereas in the second scenario (S2) the analysis focuses on the effect that the SSR has on the power objective. Their scope is to explore the overall behavior of the fuel cell system and concurrently evaluate four different methods regarding the initialization of the optimization problem:

- C1: A cold start initialization is performed at each iteration using a predefined set of initial values.
- C2: The cold start initialization of C1 is complemented by the SSR algorithm.
- W1: A warm start initialization method is performed at each iteration utilizing information from the previously solved NLP problem.
- W2: The cold start initialization of C1 is complemented by the SSR algorithm.

The method (W1) is the typical NMPC formulation while the (W2) is the newly developed exNMPC approach. In cases (C2) and (W2) the SSR algorithm is applied concurrently for the power and the temperature objective which means that three manipulated variables (I, x_{ht}, x_{cl}) have adjusted bounds between successive iterations. At these scenarios the analysis of the results focuses on the execution time, the set-point tracking accuracy and a number of metrics which are related to the optimization problem (e.g., total iteration, maximum function calls, etc.).

Scenario S1 - SSR for the temperature objective

The scope of the first scenario (S1) is to present the effect of the proposed SSR approach to the performance of the system. Also, the importance of the warm-start initialization of the NLP problem is illustrated and finally a comparison between the various initialization procedures is shown. Initially the analysis focuses on the accuracy regarding the control objectives and subsequently the focus is shifted towards the computational requirements.

The following simulation case study involves a scenario with few step changes at the power demand and at the fuel cell temperature. As stated earlier the scope of the study is to show the effect of the SSR technique (exNMPC) compared to the typical NMPC formulation. Therefore, the response of an NMPC controller (method W1) is compared to the proposed exNMPC controller (method W2). Both use the same nonlinear dynamic model and the same optimization method and the simulation horizon is 10min.

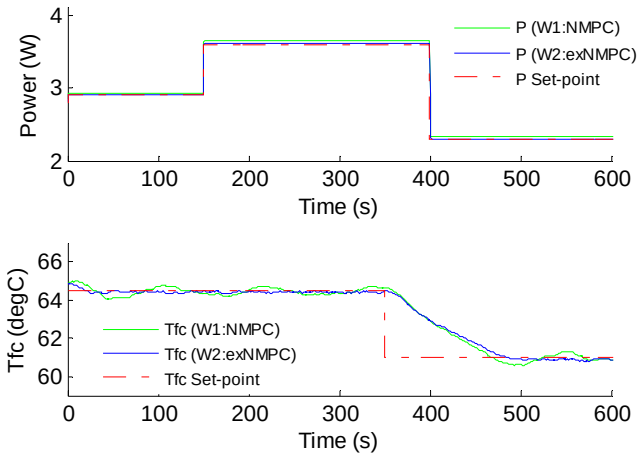

Figure 6.26 a) Power profile, b) Fuel cell temperature (exNMPC, NMPC)

Figure 6.26 illustrates that the power demand is delivered upon request by using both initialization methods (warm-start with (W2) and without the SSR (W1)) in terms of accuracy and the temperature is maintained at the desired set-point with a negligible error (±0.4°C). Figure 6.27 illustrates the corresponding oxygen and hydrogen excess ratio profiles that are adjusted according to the power demand based on the minimum air and hydrogen considerations as described earlier. The fuel cell operates at a safe region since the excess ratio of the air and the hydrogen are kept above the minimum ($\lambda_{O2}, \lambda_{H2} > 1$).

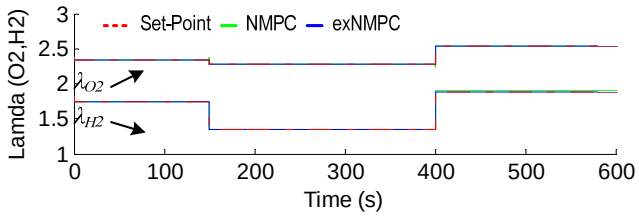

Figure 6.27 Oxygen and hydrogen excess ratio profiles (exNMPC, NMPC)

Figs. 6.26 and 6.27 show that both controllers (NMPC and exNMPC) have similar behavior in terms of accuracy which is verified by the mean squared error (MSE) for each objective as presented in Table 6.8.

Table 6.8 MSE of each control objective (methods W1 and W2)

	NMPC (W1)	exNMPC (W2)
Power	14mW	16mW
Temperature	0.3°C	0.2°C
λ_{O2}	2.7×10^{-3}	1.9×10^{-3}
λ_{H2}	8.8×10^{-4}	7.6×10^{-4}

The subsequent analysis shows the importance of the proposed SSR technique and its effect to the solution of the NLP problem regarding the computational requirements. The aforementioned simulation scenario is tested with four different methods (C1, C2, W1, W2) regarding the initialization of the optimization problem. Figs 6.26 and 6.27 present the results from W1 and W2, namely the NMPC and the exNMPC controllers. The performance of each method regarding the optimization time, the iterations and the calls to the objective function over the 10min is reported in Table 6.9.

Table 6.9 Scenario S1 - Results from various initializations (C1, C2, W1, W2)

	C1:Cold	C2:Cold+ SSR	W1:Warm	W2:Warm+SSR
Max opt time (ms)	3164	1026	493	382
Avg time (ms)	356	304	86	66
Total Iters	25187	21209	19329	10329
Max Iters.	845	539	541	373
Avg Iters.	206	203	17	8
Max Fun. Calls	2100	1589	1857	884
Avg Func. Calls	234	189	46	28

From Table 6.9 it is observed that the maximum and the average optimization time are decreased when the search space is adjusted both in cold start and warm start optimization. But when the optimization is performed using the cold start method, the maximum optimization time is beyond the system sampling time specifications.

Therefore, it is not practical to use a cold start initialization, method C1 or C2. On the other hand, the warm start initialization (W1, W2) of the optimizer shows superior performance compared to the cold start. Furthermore, a significant improvement is observed at the maximum and average optimization time in method W2 compared to method W1. This improvement is caused by the reduced number of iterations that the optimizer performs in order to find the optimum values for the decision variables of the NLP problem compared to the W1 method. When method W2 is applied the search space is adjusted around the suggested solution which is derived by the PWA approximation of the system and therefore the optimizer has a reduced space to explore. Moreover, an interesting observation is that the total number of iterations is decreased by 47% when the search space is adjusted (W2). Figs 6.28 and 6.29 illustrate the optimization time and the required iterations of methods W1 and W2.

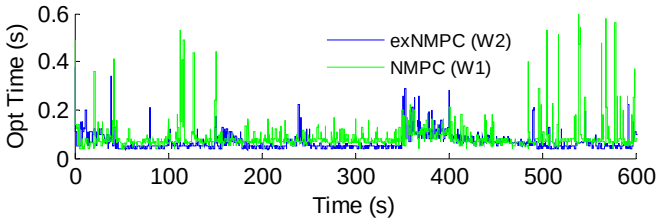

Figure 6.28 Optimization time per interval (exNMPC, NMPC)

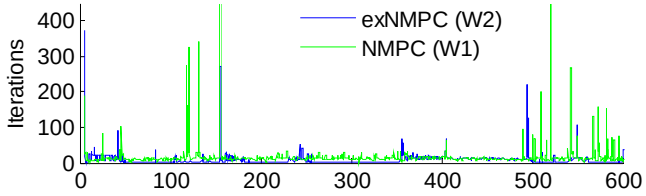

Figure 6.29 Iterations per interval for methods (exNMPC, NMPC)

In steady state both methods (W1, W2) have similar behavior with optimization time ~50ms and ~100ms respectively. But when a step change occurs or a disturbance affects the temperature of the system, W2 method requires less iterations to minimize the objective function as it searches in a reduced space for the optimum value. On the other hand, W1 requires more iterations and performs much more function calls in order to

determine the optimum value. In summary this example illustrated clearly the effect of the SSR.

From the above analysis and the performance metrics it is obvious that the proposed exNMPC framework (W2 method) that uses warm start initialization in conjunction with the SSR technique outperforms the others, for the given problem. The results indicate that the proposed controller (exNMPC) can be applied online to the fuel cell unit. Thus the next two case studies explore the online behavior of the system using the selected exNMPC controller.

Scenario S2 - SSR for the temperature and the power objectives

The second scenario (S2) involves few step changes of the power demand while the fuel cell temperature is maintained at a specific level (65°C). The response of the proposed exNMPC (W2 initialization method) is compared to an NMPC controller (W1 initialization method) using the same nonlinear dynamic model and the same optimization method. The difference from the previous scenario (S2) is that the analysis focuses on the power objective based on a simulation scenario with 40s duration. Figs 6.30 and 6.31 illustrate the behavior of the system with respect to the temperature and power profile.

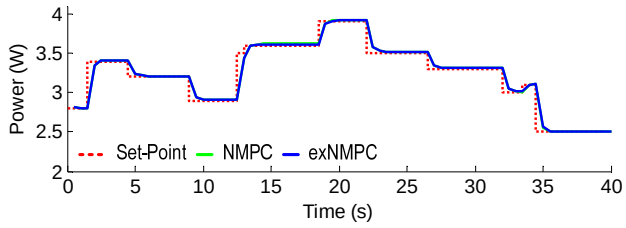

Figure 6.30 Power demand profile and produced power (exNMPC, NMPC)

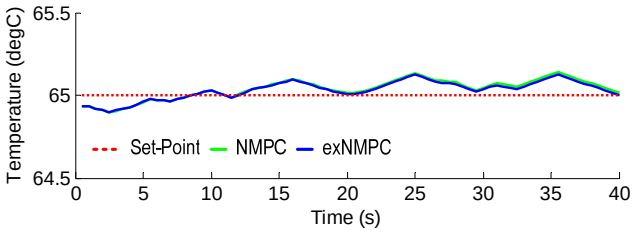

Figure 6.31 Fuel cell temperature (exNMPC, NMPC)

Fig. 6.30 illustrates that the power demand is delivered upon request by both controllers (NMPC, exNMPC) in terms of accuracy. Furthermore, the temperature is controlled at the desired set-point with a negligible error (±0.3°C). Fig. 6.31 illustrates the respective oxygen and hydrogen excess ratio profiles that are adjusted according to the power demand based on the minimum air and hydrogen considerations as described earlier. The fuel cell operates at a safe region since the excess ratios of the gases are kept above the minimum ($\lambda_{O2}, \lambda_{H2} > 1$).

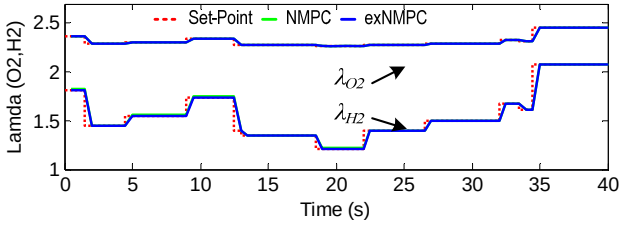

Figure 6.32 O Oxygen and hydrogen excess ratio profiles (exNMPC, NMPC)

Figs 6.30, 6.31 and 6.32 show that both controllers (NMPC and exNMPC) have similar behavior in terms of accuracy. The subsequent analysis shows the importance of the proposed SSR technique and its effect to the solution of the NLP problem regarding the computational requirements. The aforementioned simulation scenario is tested with the four different initialization methods (C1, C2, W1, W2). Figs 6.30, 6.31 and 6.32 present the results from W1, W2, namely the NMPC and the exNMPC controllers. Maximum and average optimization time per interval, maximum iterations per interval and total iterations over the 40s along with the maximum calls to the objective function are reported at Table 6.10.

Table 6.10 Scenario S2 - Results from various initializations (C1, C2, W1, W2)

Method	Max opt time (s)	Avg time (ms)	Total Iters	Max Iters.	Max Fun. calls
C1:Cold	3.93	1086	23594	1639	3443
C2:Cold+ SSR	2.30	861	20370	1063	2101
W3:Warm	0.863	413	5038	346	762
W4:Warm+SSR	0.48	207	1851	124	368

The maximum and the average optimization time are decreased when the search space is adjusted (C2) even though a cold start initialization is performed. But the maximum optimization time is beyond the system sampling time specifications. Therefore, it is not practical to use a cold start initialization method C1 or C2. On the other hand, the warm start initialization (W1, W2) of the optimizer shows superior performance compared to the cold start. We observe a significant improvement of the average optimization time in W2 method which is affected by the iterations that the optimizer performs in order to find the optimum values for the decision variables of the NLP problem that minimize the objective function. An interesting observation is that the total number of iterations is decreased by 64% when the search space is adjusted (W2).

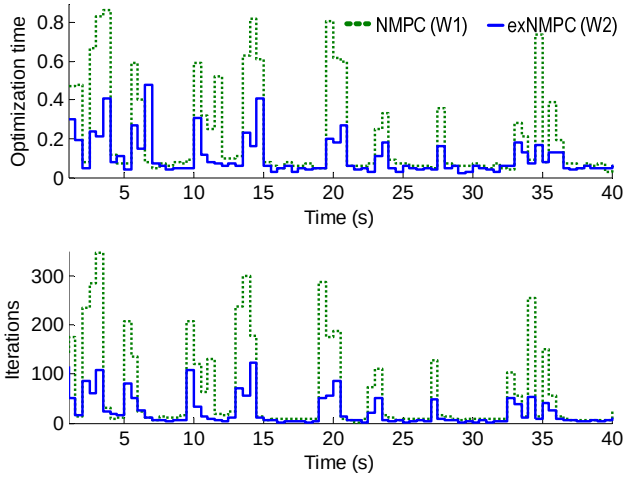

Figure 6.33 a) Optimization time and b) Iterations per interval (NMPC, exNMPC)

Fig. 6.33 shows that in steady state both methods (W1,W2) have similar behavior with optimization time 40ms to 60ms. After a step change W2 method requires less iterations to minimize the objective function as it searches in a reduced space for the optimum value. On the other hand, W1 requires more iterations and performs much more function calls.

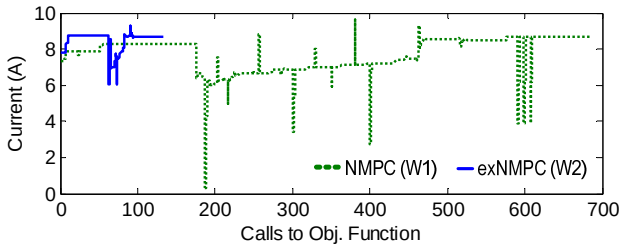

Figure 6.34 Function evaluations after a power step change

Fig. 6.34 depicts the exploration of the search space for the optimum value of I during one sampling interval after a power step change ($t = 19\,\text{sec}, P_{sp} = 3.9W$). In W1 method, I changes between 0.3A and 9.9A and the optimizer performs 685 function calls, while in W2, I deviates between 6.2A and 9.1A and only 132 function calls are performed. Both methods results to the same optimum value (M3: 8.689A, M4: 8.683A) but W1 requires 811ms while W2 requires only 201ms at this specific interval. By this illustrative example the effect of the SSR is clearly shown.

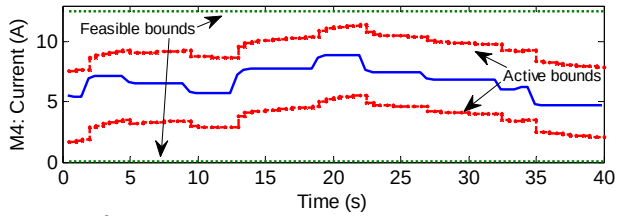

Figure 6.35 Feasible and active bounds and optimum values for I (exNMPC)

Fig. 6.35 presents the upper and lower bounds of I, along with the optimum I profile for method W2. A comparison between methods W1 and W2 regarding the optimum values of I is presented in Fig. 6.36.

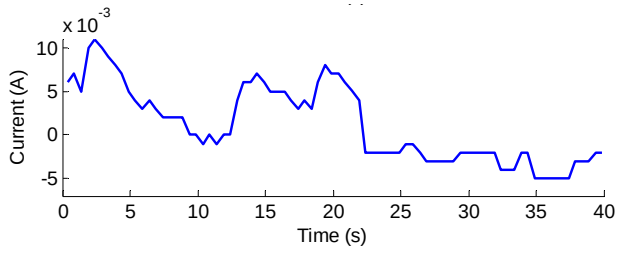

Figure 6.36 Optimum value difference as selected by NMPC and exNMPC

Both methods result to the selection of the same optimum current value since the maximum difference between them is 11mA. From the aforementioned analysis and the performance metrics it is obvious that the proposed exNMPC framework (W2 method) that uses warm start initialization in conjunction with the SSR technique outperforms the others, for the given problem.

6.4.3 Single variable SSR and comparison to NMPC, mpMPC (experimental)

The proposed exNMPC scheme, relying on the NMPC augmented by the SSR algorithm, is deployed to the industrial SCADA system and its behavior is explored through experimental scenarios. Also, the NMPC controller and the various mpMPC that were previously developed are also deployed to SCADA in order to perform a comparative case study. The performance of the underlying controllers is assessed on the basis of fast response and minimum error comparing to the set-point. Two experimental scenarios are presented. In the first one (E1) the accuracy of the control actions and the computational delay are shown, while in the second scenario (E2) the controller's response in the presence of modeling error is explored.

Their scope is to explore the overall behavior of the fuel cell system, controlled by the proposed various controllers, at nominal conditions and when disturbances appear. In order to insert the element of disturbance the control configuration was slightly modified. The exNMPC and NMPC controllers do not include the energy balance of the model. Instead they consider the temperature as a measured parameter. As a consequence the SSR algorithm is applied for the power objective only. Finally the temperature control is accomplished by the two PID controllers that where used at Section 6.2 as well. The analysis of the results focuses on the execution time and the set-point tracking accuracy.

Scenario E1 - Nominal case (comparison with NMPC)

The first scenario involves various step changes at the power demand in order to explore the behavior of NMPC and exNMPC with respect to the optimization time. It is assumed that both the model and the unit operate at the same temperature ($T=338K$) and pressure conditions ($Pt=1bar$). Fig. 6.37 illustrates the power response to the corresponding control actions of the manipulated variables as the power demand changes.

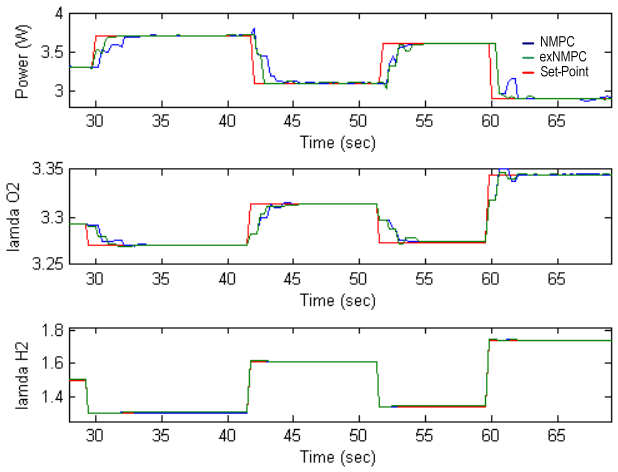

Figure 6.37 Power demand and excess ratios set-points (NMPC, exNMPC)

Also, the profiles of oxygen and hydrogen excess ratios are shown (Fig. 6.37b, Fig. 6.37c). From the power delivery point of view both controllers (NMPC, exNMPC) illustrate a very good performance and the demanded power in all cases is available on request.

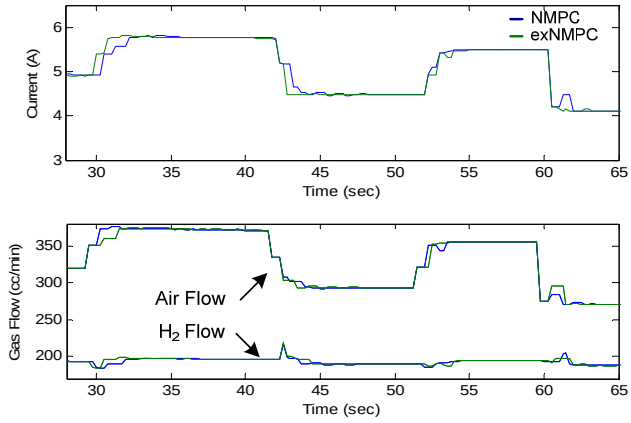

Figure 6.38 Manipulated variables (NMPC, exNMPC)

The gas flows (Fig. 6.38b) are adjusted accordingly in order to achieve the desired excess ratio levels. Both controllers are able to fulfill the power demand and guarantee a safe operation while minimizing the fuel consumption. It is observed (Table 6.11) that the exNMPC and the NMPC controllers have mean square error (MSE) of the same order of magnitude.

Table 6.11 Deviation from the set-point and optimization time (NMPC, exNMPC)

	Power MSE (mW)	O2 Excess Ratio (-)	H2 Excess Ratio (-)	Max. opt. time (ms)	Avg opt. time (ms)
NMPC	15.2	2.2×10^{-3}	6.7×10^{-4}	47	34.8
exNMPC	9.1	2.3×10^{-3}	3.2×10^{-4}	29	17.1

Besides the necessary accuracy, the second issue that the advanced control framework should address is the computational delay which is a significant challenge for the online applicability of the resulting controller. As illustrated in Fig. 6.39 and Table 6.11, the proposed exNMPC scheme can efficiently and faster provide the necessary control actions comparing to the NMPC in order to follow the power demand and the excess ratios set-point changes. The exNMPC controller shows a significant improvement in the optimization time at every instance while both controllers behave seamlessly in case of steady state or step changes.

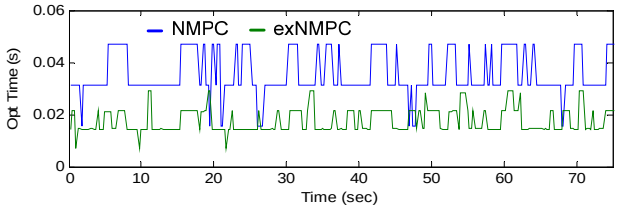

Figure 6.39 Optimization time (NMPC, exNMPC)

Scenario E2 – Temperature disturbance (comparison with mpMPC)

In the second experimental scenario the effect of a mismatch between the operating conditions predicted by the model and the actual ones of the process is explored. The temperature of the system changes while the controllers (mpMPC, exNMPC) have constant power and excess ratios set-points ($P_{SP}=3.5W$, $\lambda_{O2,SP}=3.1$, $\lambda_{H2,SP}=1.7$). This difference in temperature causes a deviation at the output power of the model comparing to the actual power of the fuel cell. The operating temperature that the model is aware of

is 65°C while the unit operates successively at 60°C, 52°C, 65°C and 58°C due to disturbances as shown in Fig. 6.40.

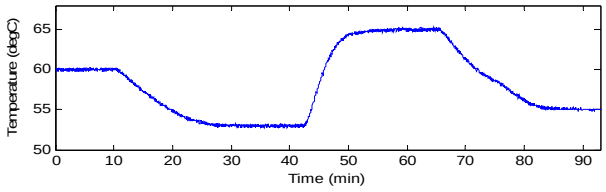

Figure 6.40 Modification of the temperature profile of the FC unit

Fig. 6.41 illustrates the response of the mpMPC controller. We notice that there exists an error between the delivered power and the power set-point that increases or decreases according to the temperature.

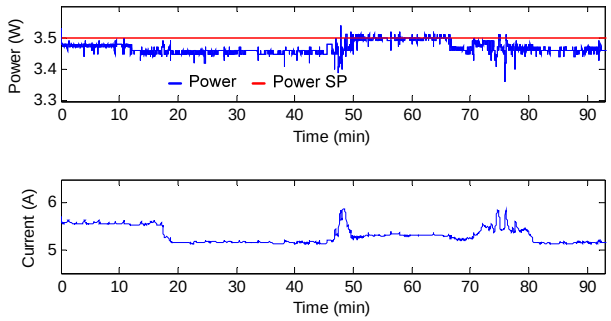

Figure 6.41 Power response during temperature changes (mpMPC)

When the system operates close to the nominal temperature (65°C), the deviation decreases while it increases as the FC's temperature deviates from the nominal. This offset is caused mainly by the difference in the temperature.

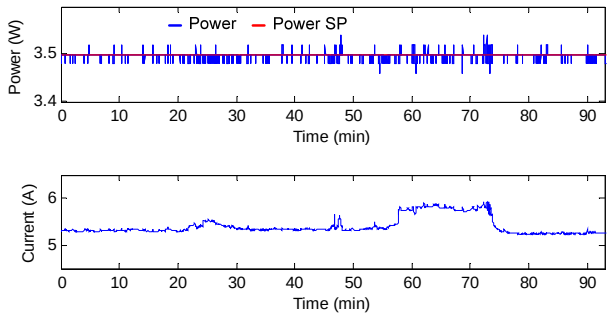

Figure 6.42 Power response during temperature changes (exNMPC)

In Fig. 6.42 the response of the exNMPC controller is shown. The average error of the exNMPC scheme is the same throughout the whole experiment regardless of the temperature differences. But this is not the case for the mpMPC controller which exhibits a deviation that varies depending on the temperature difference (Fig. 6.43).

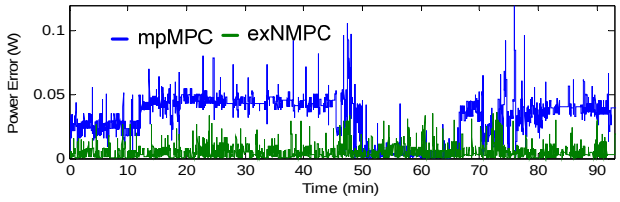

Figure 6.43 Absolute power error during temperature changes (mpMPC, exNMPC)

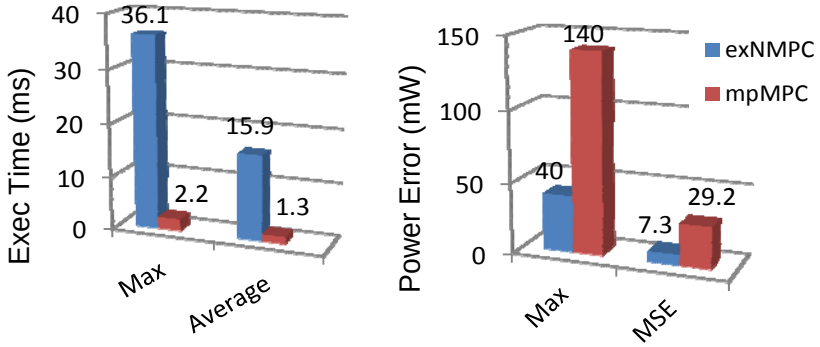

Figure 6.44 Execution/optimization time and power error (mpMPC, exNMPC)

In Fig. 6.44 the optimization time and the absolute error are shown. The exNMPC controller has the same behavior as in the nominal case. The mpMPC does not involve online optimization; therefore the solution is retrieved within 1-2ms. However the exNMPC controller behaves more accurately as the mean square error (MSE) of the power is less than 8mW regardless of the temperature change and the maximum error is 72% lower than the mpMPC error.

Overall the mpMPC can achieve trajectory tracking, but it cannot compensate for the error caused by the temperature variation (model mismatch). In contrast, the use of NMPC controller has a negligible error, but it has side-effects like increased optimization time compared to exNMPC. Obviously, the exNMPC scheme illustrates an improved behavior comparing to the other two control strategies, for the underlying control

problem in delivering accurate power tracking even in the case of a difference in the operating conditions.

6.4.4 Online deployment of exNMPC at varying operating conditions (experimental)

In the third case study the experimental behavior of the PEM fuel cell system is explored and controlled by the exNMPC approach at varying operating condition and during start-up from the environmental temperature. The response of the proposed exNMPC controller is illustrated through three scenarios. In both cases the performance is evaluated in terms of computational requirements and accuracy with respect to the control objectives analyzed at Chapter 4.

Scenario E3 - Online behavior of the PEMFC at power demand changes

The purpose of this experimental scenario is to explore the response of the proposed exNMPC controller with respect to the four control objectives. During this scenario the power and temperature profiles are externally determined while the oxygen and hydrogen profiles are derived and supplied to the exNMPC scheme based on the minimum air and hydrogen consumption functions. More specifically, a random power profile is typically demanded by the fuel cell system while the temperature is maintained at a certain level (55°C). The power demand varies between 1W and 4.2W and the duration of the experiment is 5 minutes. Fig. 6.45a illustrates the demanded and the produced power by the fuel cell while Fig. 6.45b illustrates the temperature of the fuel cell.

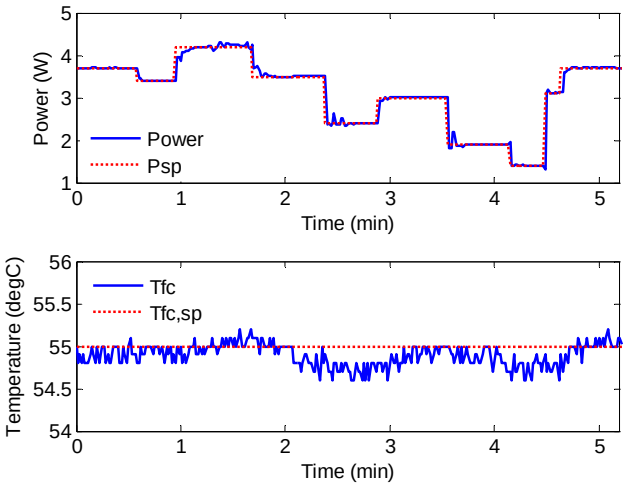

Figure 6.45 Power generation and temperature profile

A negligible error between the demanded and the delivered power is observed with a mean square error (MSE) of 12mW. Also, the temperature deviates from the desired set-point between -0.4°C to +0.1°C, which is within the initial objectives (±1°C). The oxygen and hydrogen excess ratio profiles are calculated based on the desired power profile and Fig. 6.46 illustrates that the system follows those trajectories. The oxygen excess ratio varies between 2.4 and 3.7 while the hydrogen excess ratio varies from 1.05 to 3.9.

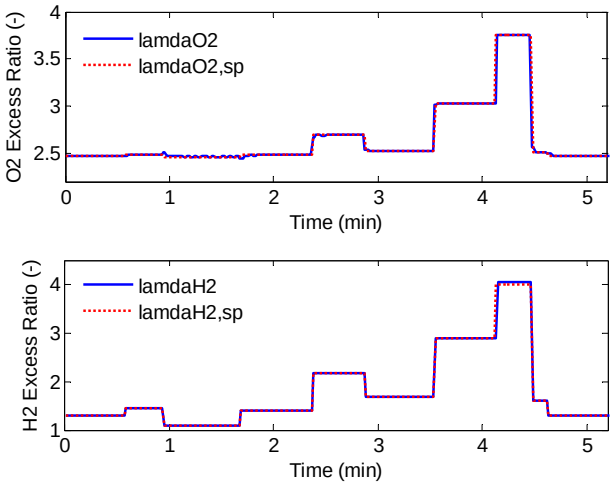

Figure 6.46 Oxygen and hydrogen profiles

As the demanded power decreases an increase to the minimum excess ratio appears. This is caused by the fact that the mass flow controllers of the unit are unable to operate below 180cc/min which is a physical design constraint imposed by the manufacturer. From Figs 6.45 and 6.46 it is obvious that the control objectives are achieved and the system operates in an optimum manner. The corresponding control actions are shown in Figs 6.47 and 6.48.

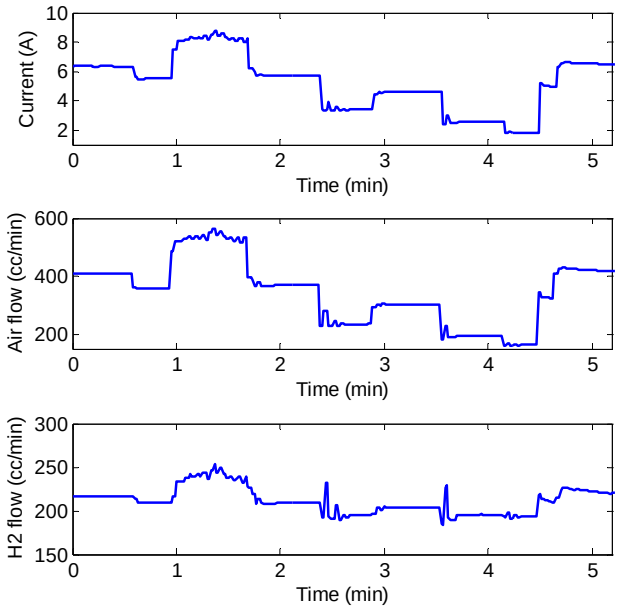

Figure 6.47 Control actions: current, air and hydrogen flows

As the power demand varies the controller calculates the optimal current (Fig. 6.49a) which is set to the DC load that subsequently applied to the fuel cell. At the same time the air and hydrogen flows (Fig. 6.47b, 6.47c) are adjusted based on the excess ratio profiles.

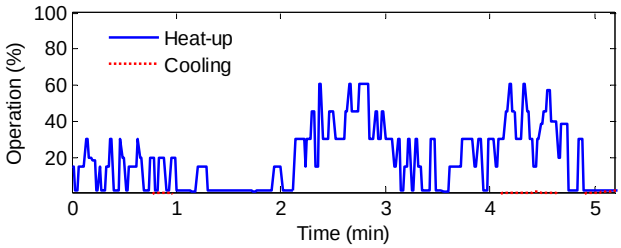

Figure 6.48 Percentage of operation of the heat-up resistance

For the given temperature the cooling fans do not operate and the temperature is maintained at 55°C by properly adjusting the percentage of operation of the heat-up resistance. As the demanded power increases so does the produced heat. Therefore, the resistance supplies less heat, as seen by the percentage of operation that decreases (Fig. 6.48). This can be clearly seen during the 1st and the 2nd minute of the experiment where the heat-up percentage is close to 2% as the required heat is produced by the fuel cell.

The computational delay caused by the optimization problem constitutes an important challenge for the online applicability of any nonlinear MPC controller. Based on that the performance of the exNMPC in terms of time response is evaluated. As stated earlier a sampling time of 500ms is chosen for the data acquisition by the SCADA system therefore the solution of the optimization problem at every time interval should be less than the sampling interval. Fig. 6.49 shows the optimization time at every iteration for the aforementioned experiment.

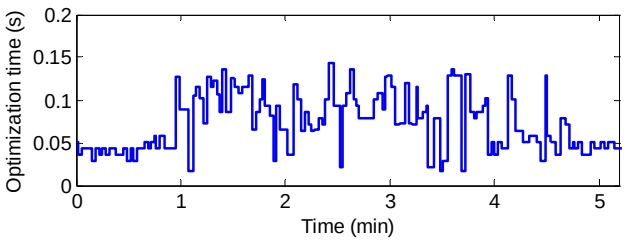

Figure 6.49 Optimization time for each sampling interval

The assessment of the performance of the controller is summarized in Table 6.12.

Table 6.12 Scenario E3 - Performance of the exNMPC controller

Performance metrics	
Max. opt. time	149ms
Average opt. time	63ms
Max. Iterations	341
Max. func. calls	712

The maximum optimization and the average time indicate that the sampling constraint is satisfied. From the above analysis it is concluded that the fuel cell system is able to provide the power demand using the minimum fuel and oxidant consumption. Furthermore, the exNMPC controller exhibits a stable behavior while achieving the predetermined objectives within the required sampling time.

Scenario E4 - Online behavior of the PEMFC at power, temperature changes

The fourth experimental scenario (E4) involves two step changes in temperature and various changes in power demand. The duration of the scenario is 19min and the sampling time is 500ms. The scope of the controller is to concurrently fulfill the four objectives ($y_{SP}=[P_{SP},T_{fc,SP},\lambda_{O2,SP},\lambda_{H2,SP}]$) within the predefined time constraints of the system. The difference from the previous scenario (E3) is that besides the power, the temperature is modified as well. Fig. 6.50 illustrates the temperature set-point profile and the fuel cell temperature. The temperature drops from 55°C to 48°C and then it rises to 61°C.

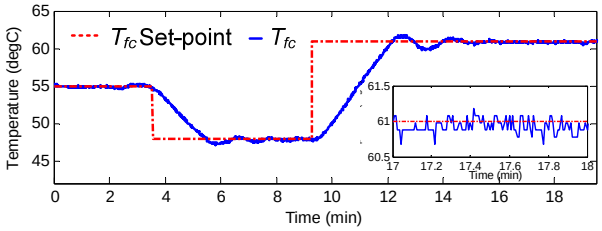

Figure 6.50 Step changes at the temperature and zoom in at steady state

When the set-point is reached the system settles to the desired value with a negligible deviation of ±0.1°C after a few oscillations. The maximum overshoot and undershoot is 0.6°C and -0.9°C, respectively. A number of power demand changes were also applied to the system during the 19min of the experiment. These step changes are randomly generated and cover the full operating range of the fuel cell (Fig. 6.51).

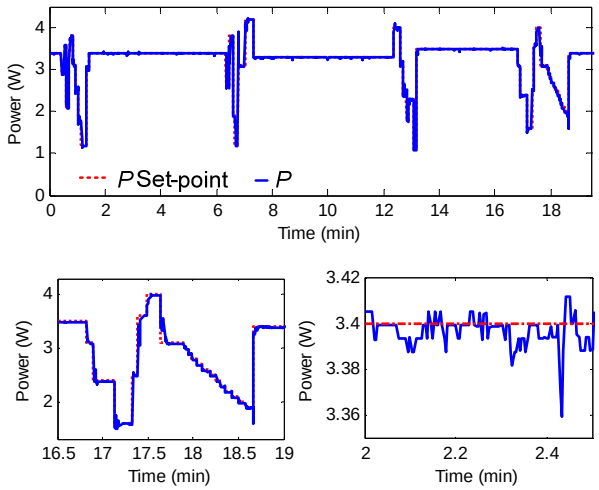

Figure 6.51 Power response a) whole scenario, b) few step changes, c) steady state

From the power delivery point of view the exNMPC framework exhibits a very good performance as it can respond to frequent and abrupt changes of the power demand. Finally the mean squared error (MSE) for each objective and some performance metrics are presented in Table 6.13.

Table 6.13 Performance of the Online exNMPC framework

MSE from set-point		Performance metrics	
Power	12mW	Max. opt. time	307ms
Temperature	0.1°C	Average opt. time	197ms
λ_{O2}	1.4×10^{-3}	Max. Iterations	162
λ_{H2}	7.2×10^{-4}	Max. func. calls	425

The MSE shows that the exNMPC can accurately fulfill the objective for power delivery (P_{SP}) in a safe operating region while minimizing the gas consumption ($\lambda_{O2,SP}, \lambda_{H2,SP}$) and concurrently provide a stable environment with respect to the temperature ($T_{fc,SP}$) condition. From the performance metrics of Table 6.13 it is evident that the computational constraints are satisfied and the results from the simulation study are verified by the online application of the controller to the fuel cell unit. Hence, the optimum operation of the fuel cell is achieved at varying operating conditions and rapid power changes.

Scenario E5 - System start up from the environmental temperature

In the fifth experimental scenario (E5) the use of the proposed exNMPC scheme for the start-up of the system is presented. The objective is to heat-up the system in a controlled way while delivering a stable power demand. Concurrently we want to control the inlet flows in order to avoid starvation and minimize fuel consumption. At the beginning of its operation the temperature is the same with the environmental one (~27°C) while the goal is to reach 60°C. As soon as the control scheme is enabled the power and subsequently the excess ratio profiles are set to a predefined point. The demanded power is 3.2W and the resulting oxygen and hydrogen excess ratio profiles are set to 3.2 and 1.55 respectively. Fig. 6.52 illustrates the power generation profile.

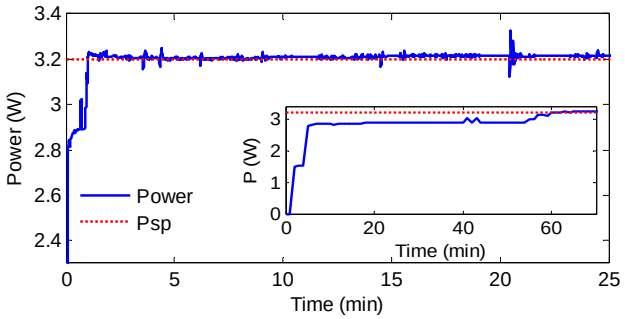

Figure 6.52 Produced power during temperature increase from 27°C to 60°C

As in the previous case study, the controller is able to deliver the demanded power even at low temperature conditions and during the temperature rise. The MSE for the power is 15.3mW while the values for λ_{O2} and λ_{H2} is 4.69×10^{-4} and 2.52×10^{-4}, respectively. Fig. 6.53 illustrates the temperature trajectory towards the set-point.

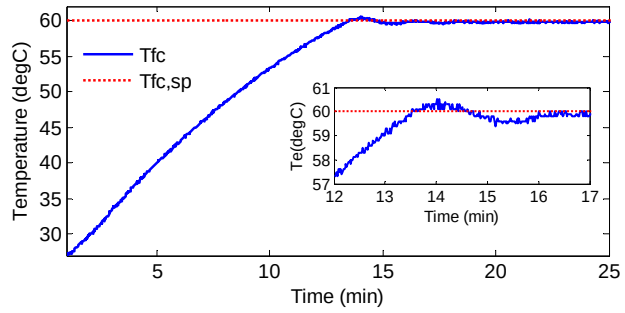

Figure 6.53 Temperature increase from 27°C to 60°C

From Fig. 6.53 it is clear that the desired temperature is accurately reached, with the use of the exNMPC controller, despite the existence of a large difference in the beginning of the operation between the set-point and the temperature of the system. The rise time of the temperature is 13.4min with an average steady-state error of 0.2°C. The percentage of operation for the heat-up resistance is shown is Fig. 6.54.

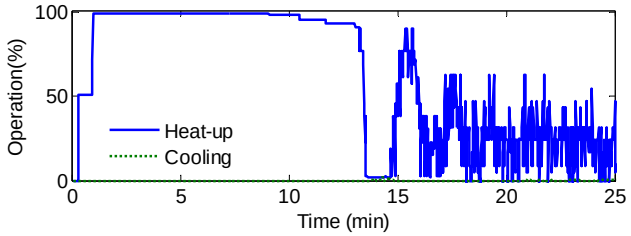

Figure 6.54 Heat-up % during temperature increase from 27°C to 60°C

At steady state the resistance operates at ~19.2% in order to maintain the temperature at the desired level (60°C). Finally from the computational point of view the maximum and the average optimization time is 181ms and 48ms respectively as shown in Fig. 6.55.

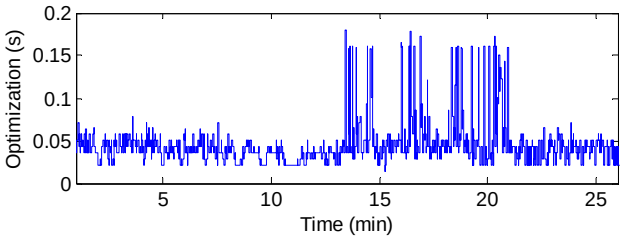

Figure 6.55 Optimization time during temperature increase from 27°C to 60°C

It is observed that the optimization time increases when the temperature approaches the set-point and decreases after the temperature settles to the desired value. Based on the results of the above analysis it clear that the exNMPC scheme can be used for the start-up of the system as it is able to compensate the difference between the measured and the desired temperature without increasing the computational requirements.

6.4.5 Overall assessment of the exNMPC controller

In this Section (6.4) the behavior of the newly proposed synergetic exNMPC controller is presented. A warm-start method is complemented by an SSR technique, relying on a PWA function that sets the basis for the improved behavior of the optimizer. By this cooperation the computational requirements for the solution of an NLP problem are reduced. The importance of this synergy is illustrated by a challenging multivariable nonlinear control problem with measured and unmeasured variables that involves concurrently four operation objectives for the PEM fuel cell system. The response of the proposed framework is initially demonstrated through a simulation case study that focuses on the influence of the SSR to the solution of the NLP problem under different initialization methods for the optimizer. Afterwards the exNMPC is deployed to the experimental fuel cell and a comparative analysis is resented between the exNMPC and the NMPC, mpMPC methods. Finally the exNMPC approach is validated online at various operating conditions and during system start-up.

6.5 Comparative experimental analysis between MPC controllers

The aim of this section is to explore the behavior of the exNMPC scheme compared to other control configurations. To this end an experimental scenario is formulated and applied to the PEM fuel cell unit under different control configurations (Fig. 6.56).

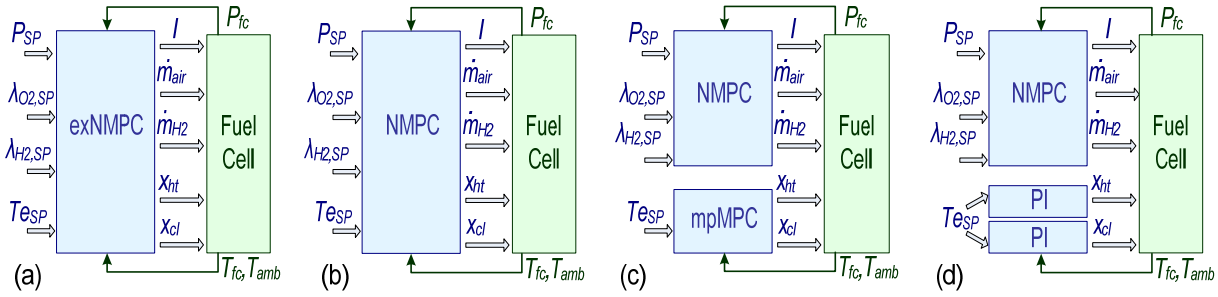

Figure 6.56 Control configurations deployed at the fuel cell system

As illustrated in Fig. 6.56 the power, oxygen and hydrogen excess ratio objectives are controlled by a nonlinear MPC approach based on the dynamic model presented at Chapter 3. Also, the same optimization problem (NLP problem with direct transcription of the model) is used at the exNMPC and NMPC approaches introduced in the previous sections of Chapter 6. The difference between the various control configurations (a-d) is the way that the temperature objective is handled. In configurations (a) and (b) the temperature is included in the objective function of the optimization problem while this is not the case in (c) and (d). More specifically in configuration (a) the temperature objective is achieved using the SSR algorithm whereas in (b) a typical NMPC approach is implemented with fixed bounds for the manipulated variables of the heat-up and cooling. In configuration (c) an mpMPC approach is applied for the temperature control and finally in (d) two independent PI controllers are utilized.

6.5.1 Desired power and temperature profile and derived excess ratios

During this case study a few steps changes at the power demand (2.8W, 3.4W, 2.4W, 3W) and at the operating temperature (60°C, 52°C, 63°C) are performed while the oxygen and hydrogen excess ratio set-points are determined by the feedforward scheme. Fig. 6.57 illustrates the power and temperature set-point profiles.

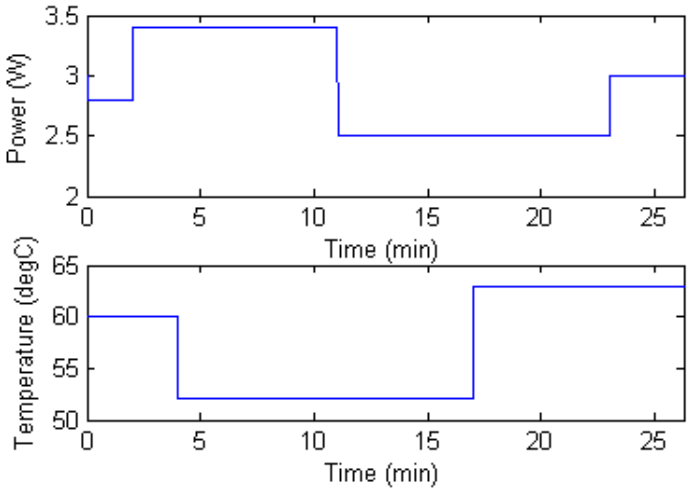

Figure 6.57 Power and temperature profiles

The adjustment of the excess ratio profiles (Fig. 6.58) are based on the desired power, therefore a respective step change concurrently with the change in the power demand is observed, while the excess ratio profiles remain constant when the temperature set-point changes. The derived excess ratio profiles are based on the polynomial functions that described at Chapter 4. In order to have an overview of the demanded profiles the profiles for the excess ratios are presented at Fig. 6.58.

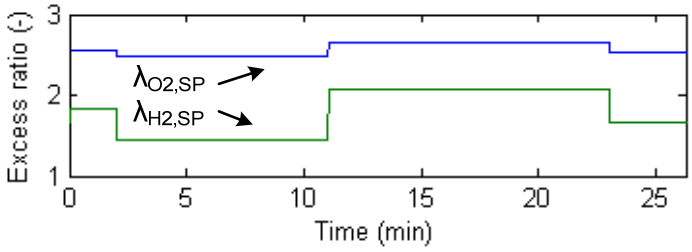

Figure 6.58 Oxygen and hydrogen excess ratio profiles

During the experiments these profiles are dynamically generated by the respective feedforward scheme at every time interval and the respective set-point is provided at the NMPC or exNMPC controller.

The results from the four experiments are presented in the following sections, beginning from the last configuration (d) to the first one (a). The performance of the underlying controllers is assessed based on:

- fast response and minimum error comparing to the set-point
- qualitative response characteristics: settling time, rise time, overshoot and undershoot
- required energy for the heat-up and the cooling during each experiment
- computational requirements of each configuration

Although there are four control objectives the emphasis is towards the temperature objective.

6.5.2 Power demand objective and excess ratios profiles

Based on the predefined power profile (Fig. 6.57) an experiment for each controller is performed. Fig. 6.59 illustrates the tracking of the power profile for all control configurations. It is observed that the fuel cell exhibits similar behavior regardless of the control configuration. For example for the exNMPC the maximum power error at steady state is 9.5mW with an average error of 4mW and for the NMPC the maximum power error at steady state is 12.0mW with an average error of 3mW. A snapshot of the steady state behavior is shown in Fig. 6.60a while Fig. 6.60b focuses on a step change at the power.

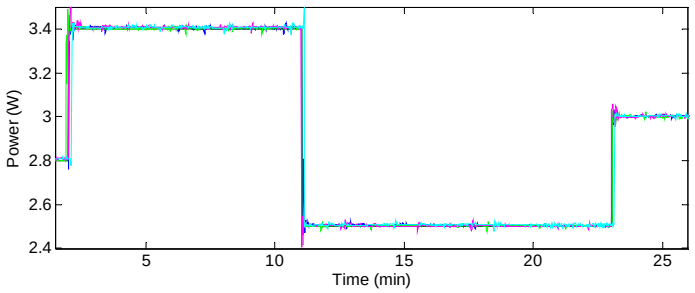

Figure 6.59 Demanded and produced power (all control configurations)

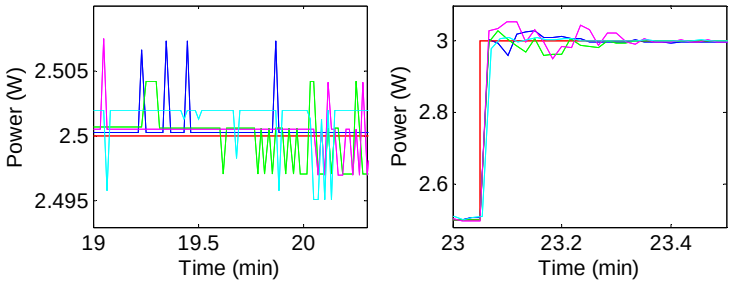

Figure 6.60 Steady state and transient power behavior (all control configurations)

The system is able to deliver the demanded power with very good response characteristics. In the case of the oxygen and hydrogen excess ratio profiles, a similar accurate behavior regarding the profile tracking is observed. A similar behavior is observed for the tracking of the oxygen and hydrogen excess ratios profiles. Table 6.14 presents the mean square error (MSE) for both of them.

Table 6.14 Mean Square Error of O_2 and H_2 excess ratio profiles

	O_2 Excess Ratio (-)	H_2 Excess Ratio (-)
exNMPC	4.21×10^{-4}	2.42×10^{-4}
NMPC	4.38×10^{-4}	3.81×10^{-4}
NMPC+mpMPC	3.52×10^{-4}	2.91×10^{-4}
NMPC+PI	3.82×10^{-4}	3.12×10^{-4}

A negligible difference exists between the various configurations. It is evident that the fuel cell operates at a safe region regardless of the power demand while avoiding oxygen starvation in all cases and minimizing the fuel supply to the required one.

Overall the four controllers can efficiently provide the necessary control actions in order to follow the power set-point changes and adjust the air and hydrogen flow rate according to the requirements for oxygen and hydrogen excess ratios and thus avoid oxygen starvation and minimize the supplied hydrogen to the required one.

6.5.3 Temperature objective

As stated earlier the difference between the various configurations is the way that the temperature objective is achieved. A brief analysis is provided for each controller's response in order to evaluate the behavior of the system in terms of accuracy, time response and overall energy consumption with respect to the temperature.

Temperature control using two independent PIs

Initially the control configuration with the two PI controllers (d), one for the heat-up and the other for the cooling of the fuel cell is presented. These controllers operate independently and they are properly tuned in order to achieve an adequate behavior as illustrated at Fig. 6.61.

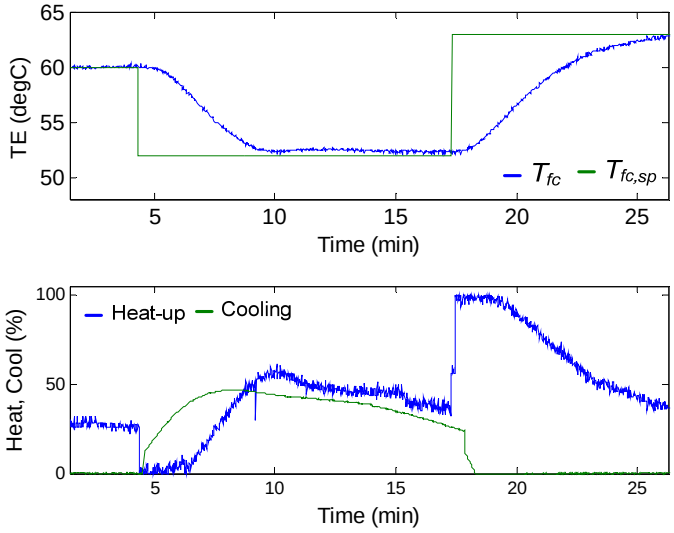

Figure 6.61 Temperature profile and heat-up/cooling actions (PI controllers)

Fig. 6.61 illustrates that the system is able to reach the desired temperature without any oscillations with an accuracy of -0.2°C/+0.7°C. When there is an increase in the set-point the rise time is 9min while at a set-point decrease it is 5.8min. Also, we observe that the heat-up resistance and the cooling fans operate concurrently for a long period. This behavior could be improved if another structure was used, but this is beyond the scope of the current study, where we want to show the response of simple PI loops compared to advanced model based controllers.

Temperature control using mpMPC

The next control scheme uses the mpMPC controller developed at Section 6.3 based on a linear state space model with two states. The temperature objective and the resulting behavior of the fuel cell are shown in Fig. 6.62.

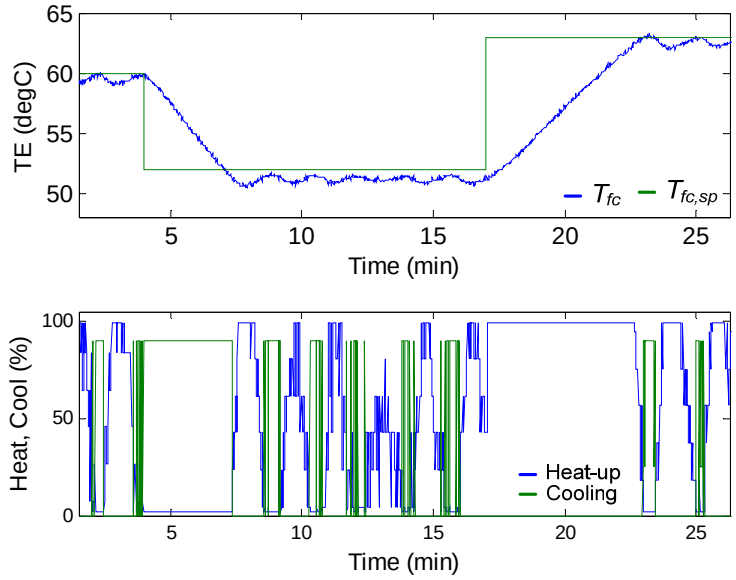

Figure 6.62 Temperature profile and heat-up/cooling actions (mpMPC)

By the use of the mpMPC undamped oscillations appear at the temperature which are caused by the fact that the heat-up and the cooling are enabled alternatively. Also, as the development of the mpMPC is based on a state space system derived at 65°C, the steady state error is decreased when the operating temperature gets closer to 65°C. At 52°C the average error from the set-point is 0.7°C, at 60°C is 0.5°C and at 63°C is 0.3°C. This behavior could be improved if a more sophisticated reduced order technique is used to derive the controller or a filter is used to avoid the oscillations, but this is out of the scope of the current study.

Temperature control using NMPC

The third configuration which is examined is the NMPC approach where the temperature objectives is fulfilled by the centralized controller along with the rest of the operation objectives. The fuel cell temperature and the control actions applied by the NMPC scheme is illustrated at Fig. 6.63.

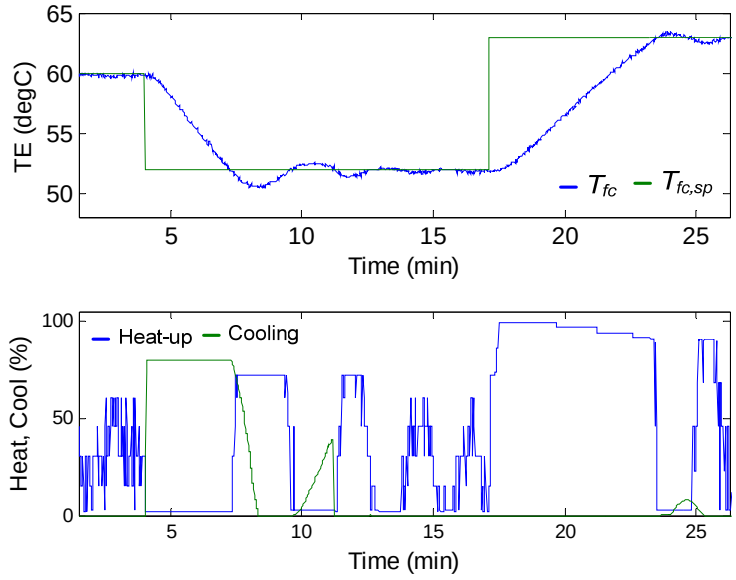

Figure 6.63 Temperature profile and heat-up/cooling actions (NMPC)

It is clearly illustrated that the temperature settles to its desired value after a few oscillations. The use of the NMPC controller results to an accurate profile tracking as at steady state the deviation from the set-point is ±0.3°C. Furthermore, the cooling fans are not used for the maintenance of the temperature after the set-point is reached (step change from 60°C to 52°C).

Temperature control using exNMPC

Finally Fig. 6.64 shows the fuel cell temperature controlled by the exNMPC scheme.

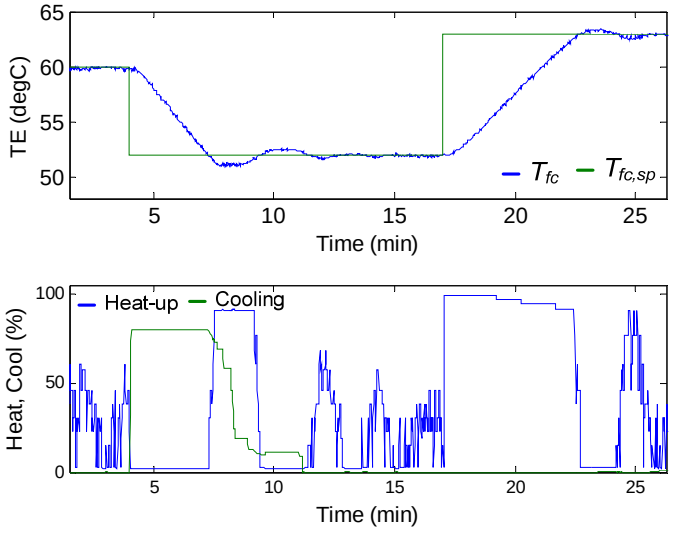

Figure 6.64 Temperature profile and heat-up/cooling actions (exNMPC)

The exNMPC scheme is able to control the fuel cell temperature and has the desired performance as described in Chapter 4. The heat-up resistance and the cooling fans do not operate concurrently and the temperature settles to its desired set-point with a negligible error (±0.2°C) after a few oscillations. Also, the maximum overshoot and undershoot is 0.6°C and 0.9°C respectively which are within the operating objectives. At steady state the temperature is maintained by proper manipulation of the operating percentage of the heat-up resistance while the cooling fans are used only to reach the decreased set-point (step change from 60°C to 52°C).

Although the response of the exNMPC seems like the NMPC's response there are some qualitative differences. More specifically they differ at the maximum undershoot, the rise time and the settling time which are described in Table 6.15.

Table 6.15 Overshoot, undershoot, rise and settling time (exNMPC, NMPC)

	exNMPC	NMPC
Max Overshoot	0.6°C	0.6°C
Max Undershoot	0.9°C	1.6°C
Rise time (SP increase)	3.26min	3.25min
Rise time (SP decrease)	5.6min	6.5min
Settling time (SP increase)	4min	5.5min
Settling time (SP decrease)	2.8min	4min

Compared to the configuration where the PI's are used, the use of exNMPC results in a 40% decrease of the time required to reach the set-point.

Energy consumption

A critical analysis of the energy which is consumed to heat-up or cool down the system is provided for each controller (Fig. 6.65). The maximum power that the heat-up resistance can provide to the fuel cell is 25W while the maximum operation of the two cooling fans requires 55.8W. Based on the operating percentage, the consumed energy can be derived for the duration of the experiment into consideration.

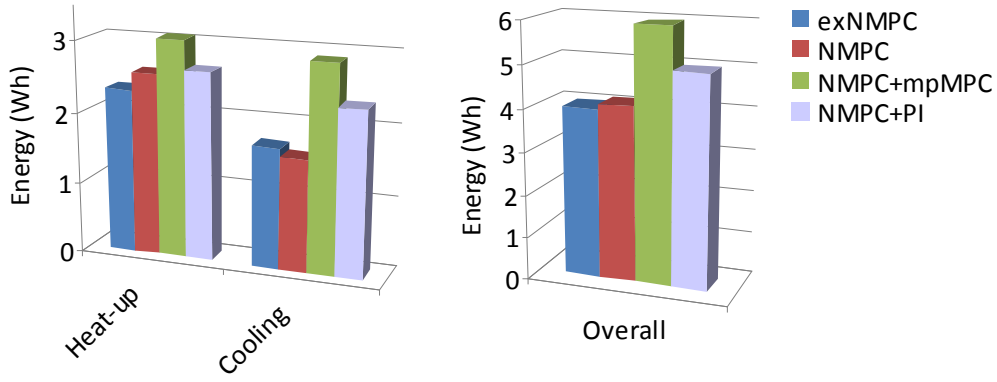

Figure 6.65 Energy consumed for the heat-up and the cooling of the system

The exNMPC scheme consumes the lowest energy for the heat-up (2.31Wh) compared to the other configurations while the NMPC is the one that requires the lowest energy for the cooling of the system (1.37Wh). Overall the exNMPC and the NMPC have similar energy requirements (exNMPC:4Wh, NMPC:4.1Wh). The two PI controllers require 23% more energy to achieve the same objective, while the energy demand of the mpMPC controller is increased by 47% compared to the exNMPC.

The primary objective regarding the heat management subsystem is to exhibit a smooth behavior throughout the whole operating range (45°C to 70°C). From the above analysis we can conclude that each approach has some benefits and some limitations. The PI scheme is easily developed and does not require any model of the system but it cannot handle efficiently conflicting objectives in terms of energy consumption. The mpMPC controller can be developed from input/output data of the fuel cell system or simplified linear models and it works adequately regarding the temperature objective but there is always the issue that its response is depended on the accuracy of the linear approximation of the system. Finally the NMPC and the exNMPC approach have similar behavior regarding the temperature control and are able to operate seamlessly independently of the operating range since a nonlinear model is in the core of their structure.

6.5.4 Computational requirements

One important challenge that arises from the online deployment of an advanced model-based controller, is the computational time required for the solution of the optimization problem which is repeated at every interval. Although a controller might achieve its objectives, the necessary time for the computation of the optimal values of the manipulated variables should also be considered in the development and implementation process. From the previous analysis we concluded that the exNMPC and NMPC approaches exhibit similar requirements in terms of profile tracking and energy consumption. However a significant difference exists between those two schemes related to the computational requirements. In fact this is the main contribution of the exNMPC

scheme, the reduction of the optimization time compare to the NMPC scheme, as illustrated in Fig. 6.66.

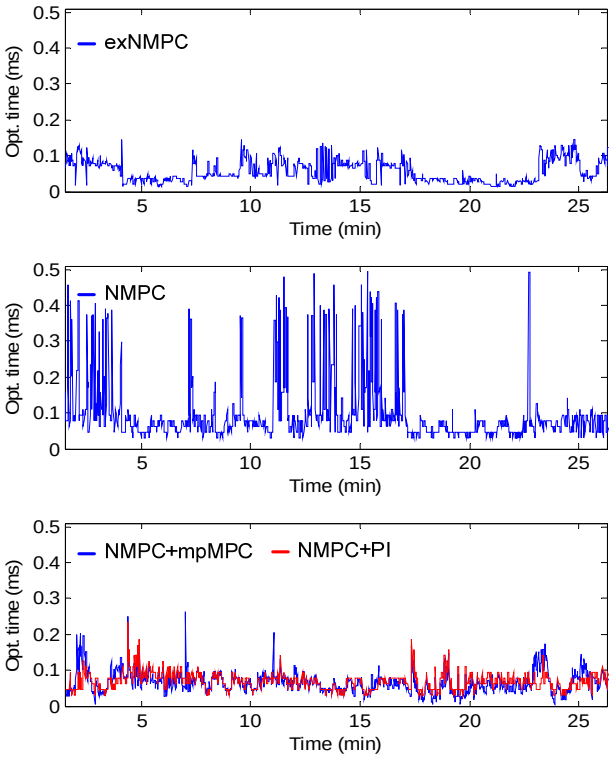

Figure 6.66 Optimization time for all control configurations

It is clear from Fig. 6.66a that the exNMPC can efficiently and faster compute the optimal values for the fuel cell system compared to the NMPC scheme (Fig. 6.66b). Even in the case where the NMPC has a reduced objective function (Fig. 6.66c), as the temperature is controlled by the mpMPC or the PI scheme, the exNMPC scheme outperforms those controllers too. From Figs 6.66b and 6.66c we can also observe the effect of the temperature objective on the computational requirements. Finally Fig. 6.67 shows the maximum and the average time of each controller.

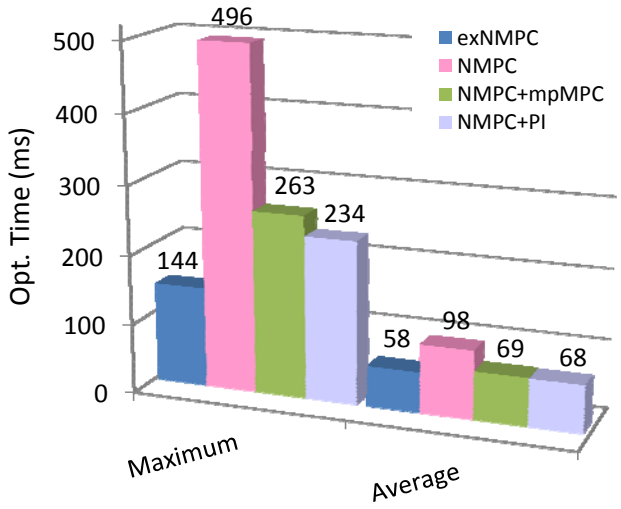

Figure 6.67 Maximum and average optimization time for all controllers

In the case of exNMPC the maximum optimization time is decreased by 70% compared to the NMPC scheme and by 47% compared to the reduced NMPC scheme. The above experiments clearly illustrate the computational performance of the proposed synergetic control scheme.

Overall in this section a thorough experimental case study was performed to reveal the benefits that arise from the deployment of the newly proposed exNMPC method. The results illustrate the salient characteristics of the proposed strategy. Apparently the combination of the NMPC with the PWA approximation, for the modification of the search space of the variable into consideration, shows interesting results for the underlying control problem. Furthermore, the fact that it is based on a nonlinear model of the fuel cell ensures that the exNMPC controller has the same performance, as with an NMPC controller, regardless of the varying operating conditions.

6.6 Concluding Remarks

This chapter presents the implementation of three advanced control schemes in the online operation of a PEMFC. Two well established MPC methods (NMPC, mpMPC) are initially developed for the control of the system and the key features of each method are outlined. Subsequently, an alternative way of combining the two advanced MPC methodologies into one cooperative approach is experimentally explored (exNMPC). More specifically, to improve the convergence speed without sacrificing the quality of the solution, a novel algorithm is proposed to dynamically adjust the search space of selected variables, based on a pre-computed augmented low-complexity PWA approximation of the feasible space. The applicability and efficiency of the proposed synergetic framework is illustrated in the real-time operation of the PEM fuel cell. The results illustrate that the response of the NMPC controller can be enhanced when it is combined with an SSR technique. A comparative simulation study and experimental analysis reveals the capabilities and the potential of the newly developed exNMPC algorithm.

The salient characteristics of the exNMPC scheme are demonstrated through a set of experimental case studies at nominal conditions, in the presence of disturbances and during system start-up. It is shown that the computational requirements of the exNMPC are within the desired sampling time constraints without compromising the fulfillment of the control objectives. The behavior of the resulting closed-loop system is optimal in terms of the performance measure considered, while the satisfaction of the various constraints imposed on the PEMFC unit operation is guaranteed by the underlying control formulation. Overall, the proposed exNMPC framework guarantees that the fuel cell system can deliver the demanded power upon request while operating at a safe region using the optimal quantities of air and hydrogen and simultaneously maintaining a stable temperature environment. The performance of the exNMPC controller also illustrates a promising behavior in terms of online computational requirements.

Chapter 7

Conclusions

In this chapter a brief summary of the main results of this thesis are presented along with an outline of the main contributions. Also, some suggestions for future developments are identified that could extend the research findings of this work.

7.1 Conclusions

This work has been motivated by the need to develop a model-based framework for advanced control of an integrated PEM fuel cell system. As the fuel cell system is an essential element of a promising, benign and environmental friendly technology that could be part of a decarbonized and sustainable future economy, a continuous and persistent effort in technological innovation is needed. Driven by this incentive, the multidisciplinary research effort of this work was built around a fuel cell system, which was supervised by an automation system, complimented by predictive control algorithms that act as a catalyst towards the improvement of the response and protection of the fuel cell's operation and safety.

Chapter 1 reviews the role of fuel cell system at the future energy landscape along with a brief analysis of the PEM fuel cell technology. Also, the context for the advanced process control methodology is presented and the importance of controlling the fuel cell behavior is presented.

A small-scale fully automated PEM fuel cell unit based on a SCADA architecture is described in Chapter 2. A custom-made interface was designed enabling the supervision and monitoring of the unit's distinct, yet interacting, subsystems namely the power, the temperature, the water and the gas flow supply management. The unit is equipped with a single PEM fuel cell that was successfully activated through a systematic experimental procedure and its response was stabilized according to the manufacturer's specifications. A number of tests were performed at various operating conditions (pressure, temperature, humidity, gas supply) that explored the behavior of the PEM fuel cell and the response of the unit.

A detailed semi-empirical model that relies on mass and energy conservation equations combined with equations having experimentally defined parametric coefficients is developed and experimentally validated in Chapter 3. The model accounts for mass dynamics in the gas flow channels, the gas diffusion layers (GDL) and the membrane. For the voltage calculation the activation, ohmic and concentration losses are taken into consideration and finally in this scheme the energy balance of the fuel cell was also considered. The results from the experimental validation of the model signified that it can capture accurately enough the behavior of the small-scale unit, a fact that guarantees its suitability for the subsequent model-based control studies.

Chapter 4 presents the control challenges and objectives in the context of PEMFC systems. The performance and longevity of the PEMFC are strongly influenced by the operating conditions and it is therefore important to control each subsystem in order to ensure a stable and optimum environment. The control objectives were the delivery of the demanded power while operating at a safe region and concurrently minimize the fuel consumption at stable temperature conditions ensuring proper gas humidification. In addition to the safety of the system, the overall performance was further improved by properly selecting the set-point for the gases excess ratios using two experimentally

determined feedforward functions that will derive the appropriate set-points for λ_{O2} and λ_{H2} based on the minimum gas criteria.

Chapter 5 presents two advanced model-based control methodologies. The first methodology is the online NMPC strategy, which is very appealing due to its ability to handle dynamic nonlinearities of the process under consideration. The second methodology is an mpMPC strategy, which provides the optimal solution in real-time, as the solution is computed offline. From their cooperation a novel approach is proposed relying on an NMPC formulation using a search space reduction (SSR) algorithm which is based on a PWA of the variable's feasible space, derived offline by the solution of an mpQP optimization problem.

Overall, three different MPC-based approaches were formulated and subsequently implemented and assessed in Chapter 6. More specifically, a modular control framework was developed, deployed online and systematically evaluated. A number of experiments were performed revealing the potential and the performance of each control method while the behavior of the overall framework was assessed. The salient capabilities of the proposed synergetic formulation were revealed through the multivariable nonlinear control problem involving the optimal operation of the PEM fuel cell system. The results illustrated that the computational demands of the NMPC controller were reduced when it was combined with an SSR technique as the solution of the NLP problem was significantly enhanced. Finally a comparative analysis between the various controllers revealed the potential of the combined approach.

7.2 Main Contribution of this Work

The main contributions of this work have been:

- A control-oriented dynamic nonlinear dynamic semi-empirical PEM fuel cell model is developed and its empirical parameters were determined using a systematic formal parameter estimation procedure based on a set of experimental data.
- A novel synergetic framework (exNMPC) between two well established control methods (mpMPC and NMPC) is developed, aiming at the reduction of the computational time without compromising the accuracy of the obtained solution.
- An algorithm is derived that bounds the active area of the variables so that the exploration of the search space by the NLP solver is reduced at every iteration during online control. This SSR algorithm augments the typical NMPC formulation.
- The online multivariable nonlinear controllers (NMPC, exNMPC) utilize the full dynamic nonlinear model of the fuel cell. This is greatly enhanced by the use of the direct transcription method that was part of the direct simultaneous optimization approach based on the reduced gradient projection NLP solver that was utilized.
- All the model-based algorithmic developments have been experimentally tested in a real-life fuel cell system at nominal conditions, in the presence of disturbances and during start-up. The multi-variable control problem is treated in a centralized way. A comparative analysis between the mpMPC, NMPC and exNMPC controllers reveals the merits and limitations of each approach.
- The newly proposed unified framework is developed and deployed online to an industrial automation system. The response of the multivariable nonlinear controller is assessed through a set of experimental studies, illustrating that the control objectives are achieved and the fuel cell system operates economically and at a stable environment regardless of the varying operating conditions.

7.2.1 Automation and Software Engineering Accomplishments

From the automation and software engineering point of view, the following accomplishments have been achieved:

- The interconnection of the controllers to the industrial SCADA system is achieved through state-of-the-art communication industrial protocols (OPC). A custom made OPC-based interface has been designed to establish the online communication between the NLP solver and the automation system. The selected software architecture ensures portability, easy deployment and most importantly universal access to any OPC-based system.
- A set of software routines were developed in Matlab code in order to extend the use of mpMPC to Fortran based environment, including an automatic transformation function of the critical regions from Matlab code to Fortran language along with an algorithm that implements a look-up function of the critical regions.
- The typical functionality of a SCADA system is extended to include various MPC based controllers. For this purpose a modular, supervisory and hierarchical structure was embedded at the SCADA system enabling the testing of several control configurations.
- A user-friendly interface is developed to speed-up the deployment of each control and enable monitoring of the status of the system leading to significant time savings, since everything is presented graphically. Also, via this interface it is possible to select not only the type of controller to test but also to isolate the objectives.

7.3 Recommendations for Future Directions

During the course of this thesis several interesting and challenging issues are revealed requiring further investigation. In particular:

❖ **Fuel Cell operation**

- Include efficiency considerations at the control objectives that could online drive the operation of the PEMFC towards an economic region of operation.
- Incorporate a diagnosis and fault-tolerant control mechanism to the automation system.
- Expand the dynamic model to PEMFC stacks and include the components of the BOP.
- Modify the dynamic model to high temperature PEMFC that have some advantages compared to low temperature PEMFCs, such as increased CO tolerance which mean that hydrogen from reforming can be used. HT-PEMs are currently at a research stage.

❖ **Additions to model-based control structure for the PEM fuel cell system**

- Include online estimation for the time varying parameters and the unmeasured variables and states (Moving Horizon Estimation (MHE) problem).
- Develop a real-time variant of the proposed NMPC and exNMPC controllers with convergence guarantees.
- Deploy the NMPC and the exNMPC methods to embedded systems.

❖ **Extensions of the SSR algorithm based the PWA approximation (exNMPC)**

- Extend the exNMPC approach to include stability and robustness properties.
- Incorporate online estimation of the linearization error that defines the active bounds of the selected manipulated variables.
- Derive a systematic methodology for the selection of variables that effect the computational requirements of the NLP problem.
- Explore how a multivariable SSR and a multiple single variable SSR affect the quality of the NLP solution.
- Determine which features of the mpMPC or the NMPC would be beneficial to the resulting exNMPC approach (e.g., robust mpQP combined with nominal NMPC vs. the nominal mpQP with robust NMPC).

7.4 Thesis Publications

7.4.1 Journal Articles

- C. Ziogou, E. N. Pistikopoulos, M. C. Georgiadis, S. Voutetakis, S. Papadopoulou, "Empowering the performance of advanced NMPC by multi-parametric programming – An application to a PEM fuel cell system*"*, *Industrial Engineering and Chemistry Research*, **52 (13)**, 2013, 4863–4873.
- C. Ziogou, S. Papadopoulou, M. C. Georgiadis, S. Voutetakis, "On-line nonlinear model predictive control of a PEM fuel cell system", *Journal of Process Control*, **23(4)**, 2013, 483-492.
- C. Ziogou, S. Voutetakis, S. Papadopoulou, M. C. Georgiadis, "Modeling, Simulation and Validation of a PEM Fuel Cell System", *Computers and Chemical Engineering*, **35**, 2011, 1886-1900.

7.4.2 Refereed conference proceedings

- C. Ziogou, M. C. Georgiadis, E. N. Pistikopoulos, S. Papadopoulou, S. Voutetakis, "Combining multi-parametric programming and NMPC for the efficient operation of a PEM fuel cell", *16th Conference Process Integration, Modelling and Optimisation for Energy Saving and Pollution Reduction (PRES13)*, 29 September - 2 October 2013, Rhodes, Greece (Accepted).
- C. Ziogou, M. C. Georgiadis, E. N. Pistikopoulos, S. Voutetakis, S. Papadopoulou, "Performance improvement of an NMPC problem by search space reduction and experimental validation to a PEM fuel cell system", *European Control Conference (ECC)*, 16-19 July 2013, Zurich, Switzerland (Accepted).
- C. Ziogou, S. Papadopoulou, S. Voutetakis, M. C. Georgiadis, *"Online* Implementation of an Integrated Explicit and Nonlinear Model Predictive Control (exNMPC) Framework for a PEM Fuel Cell System", *IFAC 5th Symposium on System, Structure and Control*, 4-6 February 2013, Grenoble, France.
- C. Ziogou, S. Voutetakis, S. Papadopoulou, M. C. Georgiadis, "Development of a Nonlinear Model Predictive Control Framework for a PEM Fuel Cell System", *Computer Aided Chemical Engineering*, **30**, 2012, 1342-1346.

- C. Ziogou, E. N. Pistikopoulos, S. Voutetakis, M. C. Georgiadis, S. Papadopoulou, "A Multivariable Nonlinear Model Predictive Control Framework for a PEM Fuel Cell System", *Computer Aided Chemical Engineering*, **31**, 2012, 1617-1621.
- C. Ziogou, C. Panos, K. Kouramas, S. Papadopoulou, M. C. Georgiadis, S. Voutetakis, E. N. Pistikopoulos, "Multi-Parametric Model Predictive Control of an Automated Integrated Fuel Cell Testing Unit", *Computer Aided Chemical Engineering*, **29**, 2011, 744-747.
- C. Ziogou, S. Voutetakis, S. Papadopoulou, M. C. Georgiadis, "Dynamic Modeling and Experimental Validation of a PEM Fuel Cell System", *Chemical Engineering Transactions*, **21**, 2010, 565-570.
- C. Ziogou, S. Voutetakis, S. Papadopoulou, M. C. Georgiadis, "Modeling and Experimental Validation of a PEM Fuel Cell System", *Computer Aided Chemical Engineering*, **29**, 2010, 721-726.

7.4.3 International peer-reviewed conferences

- C. Ziogou, S. Voutetakis, S. Papadopoulou, M. C. Georgiadis, "Power Control Of A PEM Fuel Cell System Using Nonlinear Model Predictive Control", *European Fuel Cell Conference (EFC11)*, 12-14 December 2011, Rome, Italy.
- C. Ziogou, S. Voutetakis, S. Papadopoulou, M. C. Georgiadis, "Experimental Validation of a PEM Fuel Cell Dynamic Model", *7th Symposium on Fuel Cell Modeling and Experimental Validation (MODVAL7),* March 2010, Lausanne, Switzerland.

7.4.4 National conferences

- C. Ziogou, E.N. Pistikopoulos, M. C. Georgiadis, S. Voutetakis, S. Papadopoulou, "Improving the performance of NMPC using mpQP and application to a PEMFC", *9th Panhellenic Chemical Engineering Conference*, 23-25 May, 2013, Athens, Greece.
- C. Ziogou, S. Voutetakis, S. Papadopoulou, M. C. Georgiadis, "Design of an integrated MPC system for a PEM fuel cell unit", *8th Panhellenic Chemical Engineering Conference*, 26-28 May, 2011, Thessaloniki, Greece.

References

Adamson, K., and Jerram, L. (2012). Fuel Cells Annual Report 2012, Market Development for Fuel Cells in the Stationary, Portable and Transport Sectors, Pike Research.

Adzakpa, K. P., Ramousse, J., Dube, Y., Akremi, H., Agbossou, K., Dostie, M., and Fournier, M. (2008). Transient air cooling thermal modeling of a PEM fuel cell. *Journal of Power Sources*, 179(1), 164-176.

Ahn, J. and Choe, S. (2008).Coolant controls of a PEM fuel cell system. *Journal of Power Sources*, 179, 252–264.

Al-Baghdadi, M., and Al-Janabi, H. (2007). Parametric and optimization study of a PEM fuel cell performance using three-dimensional computational fluid dynamics model. *Renewable Energy*, 32, 1077-1101.

Al-Baghdadi, M. A. (2005). Modelling of proton exchange membrane fuel cell performance based on semi-empirical equations. *Renewable Energy*, 30(10), 1587-1599.

Al-Dabbagh, A. W., Lu, L., and Mazza, A. (2010). Modelling, simulation and control of a proton exchange membrane fuel cell (PEMFC) power system. *International Journal of Hydrogen Energy*, 35(10), 5061-5069.

Alessio, A., and Bemporad, A. (2009). A survey on explicit model predictive control. *Nonlinear model predictive control*, 345-369. Springer Berlin Heidelberg.

Allgöwer, F., Badgwell, T. A., Qin, J. S., Rawlings, J. B. and Wright, S.J. (1999). Nonlinear Predictive Control and Moving Horizon Estimation - An Introductory Overview. *Advances in Control*, 391-449, Springer Verlag, Berlin.

Allgöwer, F., Findeisen, R., Nagy, Z. K. (2004). Nonlinear Model Predictive Control: From Theory to Application. *Jounral Chin. Inst. Chem. Engrs*, 35 (3), 299-315.

Altmüller, N., Grüne, L., Worthmann, K. (2010). Performance of NMPC schemes without stabilizing terminal constraints. *Recent Advances in Optimization and Its Applications in Engineering*, 289-298. Springer, Berlin.

Amphlett, J. C., Mann, R. F., Peppley, B. A., Roberge, P. R., Rodrigues, A. (1996). A model predicting transient responses of proton exchange membrane fuel cells. *Journal of Power Sources*, 61(1), 183-188.

Amphlett, J. C., Baumert, R. M., Mann, R. F., Peppley, B. A., Roberge, P. R., Harris, T. J. (1995a). Performance modeling of the Ballard Mark IV solid polymer electrolyte fuel cell II. Empirical model development. *Journal of the Electrochemical Society*, 142(1), 9-15.

Amphlett, J. C., Baumert, R. M., Mann, R. F., Peppley, B. A., Roberge, P. R., Harris, T. J. (1995b). Performance modeling of the Ballard Mark IV solid polymer electrolyte fuel cell I. Mechanistic model development. *Journal of the Electrochemical Society*, 142(1), 1-8.

Andujar, J. M., Segura, F. and Vasallo, M. J. (2008). A suitable model plant for control of the set fuel cell− DC/DC converter. *Renewable Energy*, 33(4), 813-826.

Arce, A., del Real, A.J., Bordons, C., Ramirez, D.R. (2010). Real-time implementation of a constrained MPC for efficient airflow control in a PEM fuel cell. *IEEE Transactions on Industrial Electronics*, 57(6), 1892–1905.

Arce, A., Panos, C., Bordons, C., and Pistikopoulos, E.N. (2011). Design and experimental validation of an explicit MPC controller for regulating temperature in PEM fuel cell systems. *In Proceedings of the 18th IFAC World Congress*, Milan, Italy.

Baluja, S., and Davies, S. (1997). Using optimal dependency-trees for combinatorial optimization: learning the structure of the search space. *Proceedings of the 14th International Conference on Machine Learning*, 1997, 30–38.

Bao, C., Ouyang, M., and Yi, B. (2006). Modeling and optimization of the air system in polymer exchange membrane fuel cell systems. *Journal of power sources*, 156(2), 232-243.

Bao, C., Ouyang, M., Yi, B. (2006) Modeling and control of air stream and hydrogen flow with recirculaion in a PEM fuel cell system–II. Linear and adaptive nonlinear control. *Int. Journal of Hydrogen Energy*, 31, 1897–1913.

Baschuk, J. and Li X. (2000). Modelling of polymer electrolyte membrane fuel cells with variable degrees of water flooding. *Journal of Power Sources*, 86, 181-196.

Baschuk, J. and Li X. (2005) A general formulation for a mathematical PEM fuel cell model. *Journal of Power Sources*, 142, 134-153.

Baschuk, J. and Li, X. (2009). A comprehensive, consistent and systematic mathematical model of PEM fuel cells. *Applied Energy*, 86, 181-193.

Bauer, M., and Craig, I.K. (2008). Economic assessment of advanced process control – A survey and framework. *Journal of Process Control*, 18 (1), 2-18.

Bavarian, M., Soroush, M., Kevrekidis I., Benziger J. (2010). Mathematical Modeling, Steady-State and Dynamic Behavior, and Control of Fuel Cells: A Review. *Industrial Engineering Chemistry Research*, 49, 7922–7950.

Beckhoff Automation, http://www.beckhoff.co.uk/

Bemporad, A., Morari, M., Dua, V., Pistikopoulos, E. N. (2002). The explicit linear quadratic regulator for constrained systems. *Automatica*, 38, 3-20.

Benson, H. Y., and Shanno, D. F. (2008). Interior-point methods for nonconvex nonlinear programming: regularization and warmstarts. *Computational Optimization and Applications*, 40, 143–189.

Benziger, J., Chia, E., Moxley, J.F., Kevrekidis, I.G. (2006). The dynamic response of PEM fuel cell to changes in load. *Chemical Engineering Science*, 60, 1743-59.

Berg, P., Promislow, K., Pierre, J. S., Stumper, J., Wetton, B. (2004). Water management in PEM fuel cells. *Journal of the Electrochemical Society*, 151(3), A341-A353.

Bernardi, D. M and Verbrugge, M. W. (1991). Mathematical model of gas diffusion electrode bonded to a polymer electrolyte. *AIChE Journal*, 37, 1151-1163.

Berning, T., and Djilali, N. (2003). Three-dimensional computational analysis of transport phenomena in a PEM fuel cell—a parametric study. *Journal of Power Sources*, 124(2), 440-452.

Berning, T., Lu, D. M., and Djilali, N. (2002). Three-dimensional computational analysis of transport phenomena in a PEM fuel cell. *Journal of power sources*, 106(1), 284-294.

Betts, J. T. (2001). Practical Methods for Optimal Control and Estimation Using Nonlinear Programming, *Advances in Design and Control*, 19, SIAM, Philadelphia.

Biegler, L. T., and Grossmann, I. E. (2004). Part I: Retrospective on Optimization. *Computers and Chemical Engineering*, 28, 8, 1169–1192.

Biegler, L.T., (1984). Solution of dynamic optimization problem by successive quadratic programming and orthogonal collocation, *Computers and Chemical Engineering*, 8, 243–248.

Biegler, L.T., Cervantes, A.M., Wachter, A. (2002). Advances in simultaneous strategies for dynamic process optimization. *Chem. Engineering Science*, 57, 575–593.

Booker A., Dennis, J., Frank, P., Serafini, D., Toroczon, V., and Tosset, M. (1999). A Rigorous Framework for Optimization of Expensive Functions by Surrogates, *Structural and Multidisciplinary Optimization*, 17(1), 1-13.

Buchi, F. N. and Scherer, G. G. (1996). In-situ resistance measurements of Nafion(R) 117 membranes in polymer electrolyte fuel cells. *Journal of Electroanalytical Chemistry,* 404(1), 37-43.

Cannon, M., Buerger, J., Kouvaritakis, B., Rakovic, S., (2011). Robust Tubes in Nonlinear Model Predictive Control, *IEEE Transactions On Automatic Control*, 56, 8, 34-42.

Cannon, M. (2004). Efficient nonlinear model predictive control algorithms. *Annual Reviews in Control*, 28, 229-237.

Caux, S., Lachaize, J., Fadel, M., Shott, P., Nicod, L. (2005). Modelling and control of a fuel cell system and storage elements in transport applications. *Journal of Process Control*, 15(4), 481-491.

Caux, S., Hankache, W., Fadel, M. and Hissel, D. (2010). PEM fuel cell model suitable for energy optimization purposes. *Energy Conversion and Management*, 51(2), 320-328.

Ceraolo, M., Miulli, C., Pozio, A. (2003). Modelling static and dynamic behaviour of proton exchange membrane fuel cells on the basis of electro-chemical description. *Journal of Power Sources*, 113(1), 131-144.

Cheddie, D. and Munroe, N. (2007). A two-phase model of an intermediate temperature PEM fuel cell. *International Journal of Hydrogen Energy*, 32, 832-841.

Cheddie, D. and Munroe, N. (2005). Review and comparison of approaches to proton exchange membrane fuel cell modeling. *Journal of Power Sources*, 147(1-2), 72-84.

Chen, H., and Allgöwer, F. (1998.). A quasi-infinite horizon nonlinear model predictive control scheme with guaranteed stability. *Automatica*, 34(10), 1205-1217.

Chen, J. and Zhou, B. (2008). Diagnosis of PEM fuel cell stack dynamic behavior. *Journal of Power Sources*, 177(1), 83-95.

Chen, W., Balance, D. J., and O'Reilly, J. (2000). Model predictive control of nonlinear systems: Computational burden and stability. *IEEE Proceedings of Control Theory and Applications*, 147(4), 387 394.

Cho, J., Kim, H.S., Min, K. (2008). Transient response of a unit proton-exchange membrane fuel cell under various operating conditions. *Journal of Power Sources*, 185, 118-28.

CSS (2011). The Impact of Control Technology. T. Samad and A.M. Annaswamy (eds.), IEEE Control Systems Society, www.ieeecss.org (Accessed Dec 2012).

Danzer, M. A., Wilhelm, J., Aschemann, H., Hofer, E. P. (2008). Model based control of cathode pressure and oxygen excess ratio of a PEM fuel cell system. *Journal of Power Sources*, 176 (2), 515–522.

DeHaan, D., and Guay, M. (2007). A real-time framework for model-predictive control of continuous-time nonlinear systems. *IEEE Transactions on Automatic Control*, 52(11), 2047-2057.

De Nicolao G., Magni, L., and Scattolini, R. (2000). Stability and robustness of nonlinear receding horizon control. In F. Allgower and A. Zheng, editors, *Nonlinear Predictive Control*, 3-23. Birkhauser.

del Real, A. J., Arce, A., Bordons, C. (2007). Development and experimental validation of a PEM fuel cell dynamic model. *Journal of power sources*, 173(1), 310-324.

Diehl, M., Ferreau, H. J., and Haverbeke, N. (2009). Efficient numerical methods for nonlinear MPC and moving horizon estimation. *Nonlinear Model Predictive Control*, 391-417, Springer Berlin Heidelberg.

Diehl, M., Findeisen, R., Bock, H. G., Schlöder, J. P., Allgöwer, F. (2005). Nominal stability of the real-time iteration scheme for nonlinear model predictive control. *IEEE Control Theory and Applications*, 152(3), 296-308.

Diehl, M., Bock, H., Schloder, J., Findeisen, R., Nagy, Z., Allgöwer, F. (2002). Real-time optimization and nonlinear model predictive control of processes governed by differential-algebraic equations. *Journal of Process Control*, 12(4), 577-585.

Djilali, N. and D. M. Lu (2002). Influence of heat transfer on gas and water transport in fuel cells. *International Journal of Thermal Sciences*, 41, 29-40.

Domahidi, A., Zgraggen, A.U., Zeilinger, M.N., Morari, M., Jones, C.N., (2012). Efficient interior point methods for multistage problems arising in receding horizon control, IEEE 51st Annual Conference on Decision and Control (CDC), 668,674, 10-13 Dec. 2012.

Dua, V., Bozinis, N.A. and Pistikopoulos, E.N. (2002). A multiparametric programming approach for mixed-integer quadratic engineering problems. *Computers and Chemical Engineering*, 26, 715-733.

Dutta, S., Shimpalee, S., and Van Zee, J. W. (2000). Three-dimensional numerical simulation of straight channel PEM fuel cells. *Journal of Applied Electrochemistry*, 30(2), 135-146.

Dutta, S., Shimpalee, S. and Van Zee, J. W. (2001). Numerical prediction of mass-exchange between cathode and anode channels in a PEM fuel cell. *International Journal of Heat and Mass Transfer*, 44(11), 2029-2042.

European Hydrogen Association (2008). Hydrogen and Fuel Cells as Strong Partners of Renewable Energy Systems, Brussels.

Eikerling, M. and Kornyshev, A. A. (1998). Modelling the performance of the cathode catalyst layer of polymer electrolyte fuel cells. *Journal of Electroanalytical Chemistry*, 453, 89-106.

ElectroChem Inc., http://www.electrocheminc.com (accessed Dec2012).

El-Sharkh, M. Y., Rahman, A., Alam, M. S., Byrne, P. C., Sakla, A. A., Thomas, T. (2004). A dynamic model for a stand-alone PEM fuel cell power plant for residential applications. *Journal of Power Sources*, 138(1), 199-204.

Engell, S. (2007) Feedback control for optimal process operation. *Journal of Process Control*, 17, 203–219.

Eqtami, A., Dimarogonas, D.V., and Kyriakopoulos, K.J., (2011). Novel event-triggered strategies for Model Predictive Controllers, *50th IEEE Conference on Decision and Control and European Control Conference (CDC-ECC)*, 3392-3397, 12-15 Dec. 2011.

European Commission (2011). A roadmap for moving to a competitive low carbon economy in 2050, COM(2011) 112, Brussels.

European Commission (2000). Towards a European Strategy for the Security of Energy Supply, Green Paper, COM(2000) 769, Brussels.

European Commission (2003). Hydrogen Energy and Fuel Cells, A vision of our future, EUR 20719 EN, Brussels.

Ferreau, H. J., Bock, H. G., and Diehl, M. (2008). An online active set strategy to overcome the limitations of explicit MPC. *International Journal of Robust and Nonlinear Control*, 18(8), 816-830.

Findeisen, R., Allgöwer, F., and Biegler, L. T. (2007). Assessment and Future Directions of Nonlinear Model Predictive Control, *Volume 358 of Lecture Notes in Control and Information Sciences*. Springer Verlag, Berlin.

Findeisen, R., Imsland, L., Allgower, F., and Foss, B. A. (2003). State and output feedback nonlinear model predictive control: An overview. *European Journal of Control*, 9, 2-3, 190-206.

Findeisen, R., and Allgöwer, F. (2004). Computational delay in nonlinear model predictive control. In Proceedings of IFAC Symp. *Adv. Control Chem. Processes*, 427-437.

Findeisen, R., Imsland, L., Allgöwer, F. and Foss, B. (2003). Towards a sampled-data theory for nonlinear model predictive control, New Trends in Nonlinear Dynamics and Control, *Lecture Notes in Control and Information Sciences*, 295–313, Springer-Verlag, New York.

Finlayson, B. (1992). Numerical Methods for Problems with Moving Fronts. Ravenna Park Publishing.

Fowler, M. (2002). Incorporation of voltage degradation into a generalised steady state electrochemical model for a PEM fuel cell. *Journal of Power Sources,* 106(1-2), 274-283.

Fuel Cells 2000 (2012). The Business Case for Fuel Cells 2012, http://www.fuecells.org (accessed Dec 2012).

Fuel Cell Today (2011). Industry Review 2011, http://www.fuelcelltoday.com (accessed Dec 2012).

Fuel Cell Today (2012). Industry Review 2012, http://www.fuelcelltoday.com (accessed Dec 2012).

Fuller, T. F. and Newman, J. (1993). Water and Thermal Management in Solid-Polymer-Electrolyte Fuel-Cells, *Journal of the Electrochemical Society*, 140, 1218-1225.

Garcia-Gabin, W., Dorado, F., and Bordons, C. (2010). Real-time implementation of a sliding mode controller for air supply on a PEM fuel cell. *Journal of Process Control*, 20, 325–336.

GE Intelligent Platforms Proficy iFIX, http://www.ge-ip.com/ (Accessed 2012).

Gill, P.E., Murray, W., Saunders, M.A., Wright, MH. (1984). Procedures for optimization problems with a mixture of bounds and general linear constraints. *ACM Transactions on Mathematical Software*, 10 (3), 282–298.

Golbert, J. and Lewin, D. R. (2004). Model-based control of fuel cells: (1) Regulatory control. *Journal of Power Sources*, 135(1-2), 135-151.

Gruber, J., Bordons, C., and Oliva, A. (2012). Nonlinear MPC for the air flow in a pem fuel cell using a Volterra series model. *Control Engineering Practice*, 20, 205–217.

Gurau, V., Liu, H., Kakac, S. (1998). Two-dimensional model for proton exchange membrane fuel cells. *AIChE Journal*, 44(11), 2410-2422.

Haraldsson, K. and Wipke, K. (2004). Evaluating PEM fuel cell system models. *Journal of Power Sources*, 126, 88-97.

Henson, M. A. (1998). Nonlinear model predictive control: current status and future directions. *Computers and Chemical Engineering*, 23(2), 187-202.

Hou, Y., Zhuang, M., and Wan, G. (2007). A transient semi-empirical voltage model of a fuel cell stack. *International journal of hydrogen energy*, 32(7), 857-862.

Huisseune, H., Willockx, A. and De Paepe, M. (2008). Semi-empirical along-the-channel model for a proton exchange membrane fuel cell. *International Journal of Hydrogen Energy*, 33(21), 6270-6280.

Hum, B. and X. G. Li (2004). Two-dimensional analysis of PEM fuel cells, *Journal of Applied Electrochemistry*, 34, 205-215.

IEA (2007). Energy Technology Essentials, April 2007, http://www.iea.org/techno/essentials5.pdf (Accessed Nov 2012)

Imsland L., Findeisen, R., Bullinger, E., Allgower, F., Foss, B. (2003). A note on stability, robustness and performance of output feedback nonlinear model predictive control, *Journal of Process Control*, 13, 7, 633-644.

Jang, J. H. and Chiu H. C. (2008). Effects of operating conditions on the performances of individual cell and stack of PEM fuel cell. *Journal of Power Sources,* 180(1), 476-483.

Jiang, Z., Gao, L., and Dougal, R. A. (2007). Adaptive control strategy for active power sharing in hybrid fuel cell/battery power sources. *Energy conversion, IEEE transactions on*, 22(2), 507-515.

Johansen, T.A., and Grancharova, A. (2003). Approximate explicit constrained linear model predictive control via orthogonal search tree. *IEEE Trans. Automatic Control*, 58(5), 810–815.

Jones, D., Schonlau M., and Welch, W. (2008). Efficient Global Optimization of Expensive Black-Box Functions, *Journal of Global Optimization*, 13(4), 455-492.

Kameswaran, S., and Biegler, L. T. (2008). Convergence rates for direct transcription of optimal control problems using collocation at Radau points. *Computational Optimization and Applications*, 41(1), 81-126.

Kelouwani, S., Adegnon, K., Agbossou, K., Dube Y. (2012). Online System Identification and Adaptive Control for PEM Fuel Cell Maximum Efficiency Tracking. *IEEE Transactions on Energy Conversion*, 27 (3), 580-592.

Kim, H. S., and Min, K. (2008). Experimental investigation of dynamic responses of a transparent PEM fuel cell to step changes in cell current density with operating temperature. *Journal of Mechanical Science and Technology*, 22(11), 2274-2285.

Kim, S., Shimpalee, S., and Van Zee, J. W. (2004). The effect of reservoirs and fuel dilution on the dynamic behavior of a PEMFC. *Journal of Power Sources*, 137(1), 43-52.

Kiparissides, C., Seferlis, P., Mourikas, G., Morris, A. J. (2002). Online optimisation control of molecular weight properties in batch free-radical polymerisation reactors. *Industrial Engineering Chemistry Research*, 41, 6120-6131.

Kolavennu, P. K., Palanki, S., Cartes, D. A., Telotte, J. C. (2008).Adaptive controller for tracking power profile in a fuel cell powered automobile. *Journal of Process Control*, 18 (6), 558-567.

Kulikovsky, A. (2001). Quasi three-dimensional modeling of the PEM fuel cell: comparison of the catalyst layers performance. *Fuel Cells*, 1, 162-169.

Kulikovsky, A. (2004). Semi-analytical ID plus ID model of a polymer electrolyte fuel cell. *Electrochemistry Communications*, 6, 969-977.

Kunusch, C., Puleston P.F., Mayosky, M., Fridman, L. (2013). Experimental results applying second order sliding mode control to a PEM fuel cell based system. *Control Engineering Practice*, 21, 5, 719-726.

Kunusch, C., Puleston P.F., Mayosky M., More J. (2010). Characterization and experimental results in PEM fuel cell electrical behaviour. *International Journal of Hydrogen Energy*, 35(11), 5876-5881.

Kurtz, J., Sprik, S., and Saur, G. (2012). State-of-the-art Fuel Cell Voltage Durability Status 2012 Composite Data Products, NREL, http://www.nrel.gov/hydrogen/pdfs/55288.pdf (accessed Dec. 2012).

Kvasnica, M., Grieder, P., Baotic, M., and Morari, M. (2004). Multi-Parametric Toolbox (MPT), 448–462.

Lauzze, K. C., and Chmielewski, D. J. (2006). Power control of a polymer electrolyte membrane fuel cell. *Ind. Eng. Chem. Res.*, 45 (13), 4661–4670.

Lazar, M., de la Peña, D. M., Heemels, W., and Alamo, T. (2008). On input-to-state stability of min-max nonlinear Model Predictive Control. *Systems and Control Letters*, 57, 39–48.

Lazarou, S., Pyrgioti, E. and Alexandridis, A. T. (2009). A simple electric circuit model for proton exchange membrane fuel cells. *Journal of Power Sources*, 190(2), 380-386.

Lee, Y. I., Kouvaritakis, B., and Cannon, M. (2002). Constrained receding horizon predictive control for nonlinear systems, *Automatica*, 38, 2093–2102.

Lee, J. H. and Lalk T. R. (1998). Modeling fuel cell stack systems. *Journal of Power Sources*, 73(2), 229-241.

Li, X. G., Cao, L. L., Liu, Z. X., and Wang, C. (2010). Development of a fast empirical design model for PEM stacks. *International Journal of Hydrogen Energy*, 35(7), 2698-2702.

Limon, D., Alamo, T., Raimondo, D., de la Peña, D. M., Bravo, J., Ferramosca, A., and Camacho, E. (2009). Input-to-State Stability: A Unifying Framework for Robust Model Predictive Control, *Volume 384 of Lecture Notes in Control and Information Sciences*, 1–26. Springer Verlag, Berlin.

Limon, D., Alamo, T., Salas, F., and Camacho, E. F. (2006). Input to State stability of min-max MPC controllers for nonlinear systems with bounded uncertainties. *Automatica*, 42, 797-803.

Litster, S. and Djilali, N. (2007). Mathematical modelling of ambient air-breathing fuel cells for portable devices. *Electrochimica Acta*, 52(11), 3849-3862.

Lum K. and McGuirk J. (2005). Three-dimensional model of a complete polymer electrolyte membrane fuel cell: model formulation, validation and parametric studies. *Journal of Power Sources*, 143, 103-124.

Magni, L. and Scattolini, R. (2004). Model Predictive Control of Continuous-Time Nonlinear Systems with Piecewise Constant Control. *IEEE Transactions on Automatic Control*, 49, 900-906.

Magni, L., Raimondo, D., and Allgöwer, F. (2009). Nonlinear Model Predictive Control: Towards New Challenging Applications, *Lecture Notes in Control and Information Sciences*, Volume 384, Springer Verlag, Berlin.

Magni, L., De Nicolao, G., Magnani, L., and Scattolini, R. (2001). A stabilizing model-based predictive control for nonlinear systems. *Automatica*, 37, 1351-1362.

Manenti, F. (2011). Considerations on nonlinear model predictive control techniques. *Computers and Chemical Engineering*, 35(11), 2491-2509.

Mann, R. F., Amphlett, J. C., Hooper, M. A., Jensen, H. M., Peppley, B. A., and Roberge, P. R. (2000). Development and application of a generalised steady-state electrochemical model for a PEM fuel cell. *Journal of Power Sources,* 86(1), 173-180.

Marr, C., and Li, X. G. (1999). Composition and performance modelling of catalyst layer in a proton exchange membrane fuel cell. *Journal of Power Sources*, 77, 17-27.

Martin, K. E., Kopasz, J. P., and McMurphy, K. W. (2010). Status of fuel cells and the challenges facing fuel cell technology today. *Fuel Cell Chemistry and Operation*, 1040, 1-13.

Martinsen, F., Biegler, L. T., and Foss, B. A. (2004). A new optimization algorithm with application to nonlinear MPC. *Journal of Process Control*, 14, 853-865.

Mathworks, Matlab, http://www.mathworks.com/matlabcentral/ (Accessed Dec 2012).

Mayne, D. Q., and Michalska, H. (1990). Receding horizon control of nonlinear systems. *IEEE Transactions on Automatic Control*, 35, 814-824.

Mayne, D.Q., Rawlings, J.B., Rao, C.V., Scokaert, P. O. M. (2000). Constrained model predictive control: Stability and optimality. *Automatica* 36, 789-814.

McKay, D. A., Ott, W. T., Stefanopoulou, A. G. (2005). Modeling, parameter identification, and validation of reactant and water dynamics for a fuel cell stack. *In ASME international mechanical engineering congres exposition*, 1177-1186.

McKinsey and Company (2010). A portofolio of powertrains for Europe: A fact-based analysis, Fuel Cells and Hydrogen Joint Undertaking, November 2010, Brussels.

Melo, V., Delbem, A., Junior, D., Federson, F. (2007). Improving Global Numerical Optimization Using a Search-Space Reduction Algorithm. *Genetic and Evolutionary Computation Conference (GECCO'07) 2007*, 1195-1202.

Methekar, R. N., Patwardhan, S. C., Gudi, R. D., Prasad, V. (2010). Adaptive peak seeking control of a proton exchange membrane fuel cell. *Journal of Process Control*, 20 (2), 73-82.

Methekar, R. N., Patwardhan, S. C., Rengaswamy, R., Gudi, R. D., Prasad, V. (2010b). Control of proton exchange membrane fuel cells using data driven state space models. *Chemical Engineering Research and Design*, 88(7), 861-874.

Miansari, M., Sedighi, K., Amidpour, M., Alizadeh, E., Miansari, M. (2009). Experimental and thermodynamic approach on proton exchange membrane fuel cell performance. *Journal of Power Sources*, 190(2), 356-361.

Mishra, V., Yang, F., and Pitchumani, R. (2005). Analysis and design of PEM fuel cells. *Journal of power sources*, 141(1), 47-64.

More, J., Puleston, P., Kunusch, C., and Visintin, A. (2010). Temperature control of a PEM fuel cell test bench for experimental MEA assessment. *Journal of Hydrogen Energy*, 35, 5985-5990.

Moreira, M. V. and da Silva, G. E. (2009). A practical model for evaluating the performance of proton exchange membrane fuel cells. *Renewable Energy* 34(7), 1734-1741.

Muller, E. A. and Stefanopoulou, A.G. (2006). Analysis, modeling, and validation for the thermal dynamics of a polymer electrolyte membrane fuel cell system. *Journal of Fuel Cell Science and Technology*, 3(2), 99-110.

Murtagh, B. A., Saunders, M.A. (1998). MINOS 5.5 User's Guide, Technical Report SOL 83-20R, Stanford University.

Murtagh, B. A., Saunders, M.A., (1978). Large-scale linearly constrained optimization. *Mathematical Programming*, 14, 41-72.

Nam, J. H. and Kaviany, M. (2003). Effective diffusivity and water-saturation distribution in single- and two-layer PEMFC diffusion medium. *International Journal of Heat and Mass Transfer*, 46(24), 4595-4611.

Natarajan, D., and Van Nguyen, T. (2001). A two-dimensional, two-phase, multicomponent, transient model for the cathode of a proton exchange membrane fuel cell using conventional gas distributors. *Journal of The Electrochemical Society*, 148(12), A1324-A1335.

National Instruments, Labview, http://www.ni.com/labview (Accessed 2012).

Nguyen, T. V., and Knobbe, M. W. (2003). A liquid water management strategy for PEM fuel cell stacks. *Journal of Power Sources*, 114(1), 70-79.

Nguyen, T. V., and White, R. E. (1993). A Water and Heat Management Model for Proton-Exchange-Membrane Fuel-Cells, *Journal of the Electrochemical Society*, 140, 2178-2186.

OPC Foundation, http://www.opcfoundation.org (Accessed 2012).

OSIsoft, PI System, http://www.osisoft.com (Accessed 2012).

Outeiro, M. T., Chibante, R., Carvalho, A. S., De Almeida, A. T. (2008). A parameter optimized model of a proton exchange membrane fuel cell including temperature effects. *Journal of Power Sources*, 185(2), 952-960.

Pannocchia, G., Rawlings, J.B., and Wright, S.J. (2007). Fast, large-scale model predictive control by partial enumeration. *Automatica*, 43, 852-860.

Pathapati, P. R., Xue, X., Tang, J. (2005). A new dynamic model for predicting transient phenomena in a PEM fuel cell system. *Renewable energy*, 30(1), 1-22.

Patrinos, P., and Bemporad, A., (2012). An accelerated dual gradient-projection algorithm for linear model predictive control, *IEEE 51st Annual Conference on Decision and Control (CDC)*, 662,667, 10-13 Dec. 2012.

Pistikopoulos, E. N. (2012). From multi-parametric programming theory to MPC-on-a-chip multi-scale systems applications, *Computers and Chemical Engineering*, 47, 57-66.

Pistikopoulos, E. N., Dominguez, L., Panos, C., Kouramas, K., Chinchuluun, A. (2012). Theoretical and algorithmic advances in multi-parametric programming and control, *Computational and Management Science*, 9(2), 183–203.

Pistikopoulos, E. N., Dua, V., Bozinis, N. A., Bemporad, A., Morari, M. (2002). On-line optimization via off-line parametric optimization tools. *Computers and Chemical Engineering*, 26 (2), 175-185.

Pistikopoulos, E.N., Georgiadis, M., Dua, V. (2007). Multi-parametric Model-based Control: Theory and Applications, Weinheim: Wiley-VCH.

POP (2007). Parametric Optimization Solutions (ParOS) Ltd.

Pregelj, B., Vrecko, D., and Jovana, V. (2011). Improving the operation of a fuel-cell power unit with supervision control – A simulation study. *Journal of Power Sources*, 196, 9419– 9428.

Promislow, K., and Wetton, B. (2005). A simple, mathematical model of thermal coupling in fuel cell stacks. *Journal of Power Sources*, 150, 129-135.

PSE Ltd, (2010). gPROMS Model Developer Guide, Process Systems Enterprise Ltd.

Puig, V., Rosich, A., Ocampo-Martínez, C., Sarrate, R. (2007). Fault-tolerant explicit mpc of pem fuel cells. *46th IEEE Conference on Decision and Control*, 2657-2662.

Pukrushpan, J. T., Peng H., and Stefanopoulou, A.G. (2004). Control-oriented modeling and analysis for automotive fuel cell systems. *Journal of Dynamic Systems Measurement and Control-Transactions of the ASME*, 126(1), 14-25.

Pukrushpan, J. T., Stefanopoulou, A. G., and Peng, H. (2004b). Control of fuel cell breathing. *Control Systems, IEEE*, 24(2), 30-46.

Qin, S. and Badgwell, T. (2003). A survey of industrial model predictive control technology. *Control Engineering Practice*, 11(7), 733-764.

Raimondo, D. M., Riverso, S., Summers, S., Jones, C., Lygeros, J., and Morari, M. (2012). A Set-Theoretic Method for Verifying Feasibility of a Fast Explicit Nonlinear Model Predictive Controller, *Distributed Decision Making and Control, LNCIS* , 417, 289– 311.

Rawlings, J.B. and Mayne, D.Q. (2009). Model Predictive Control: Theory and Design. Nob Hill Publishing, Madison.f

Reble, M., and Allgöwer, F. (2012). Unconstrained model predictive control and suboptimality estimates for nonlinear continuous-time systems, *Automatica*, 48 (8), 1812-1817.

Rodatz, P., Paganelli, G., Sciarretta, A., and Guzzella, L. (2005). Optimal power management of an experimental fuel cell/supercapacitor-powered hybrid vehicle. *Control Engineering Practice*, 13(1), 41-53.

Rowe, A., and Li, X. (2001). Mathematical modeling of proton exchange membrane fuel cells. *Journal of Power Sources*, 102, 82-96.

Rowhanimanesh, A., and Efati, S. (2012). A Novel Approach to Improve the Performance of Evolutionary Methods for Nonlinear Constrained Optimization. *Advances in Artificial Intelligence*, 2012, doi:10.1155/2012/540861.

Sahraoui, M., Kharrat, C., Halouani, K. (2009). Two-dimensional modeling of electrochemical and transport phenomena in the porous structures of a PEMFC. *International Journal of Hydrogen Energy*, 34(7), 3091-3103.

Schafer, A., Kuehl, P. Baschuk, Diehl, M., Schloder, J., Bock, H. (2007). Fast reduced multiple shooting methods for nonlinear model predictive control. *Chemical Engineering and Processing*, 46(11), 1200-1214.

Schmittinger, W. and Vahidi, A. (2008). A review of the main parameters influencing long-term performance and durability of PEM fuel cells. *Journal of Power Sources*, 180, 1– 14.

Shan, Y., and Choe, S. (2006). Modeling and simulation of a PEM fuel cell stack considering temperature effects. *Journal of Power Sources*, 158, 274-286.

Shimpalee, S., Lee, W. K., Van Zee, J. W., Naseri-Neshat, H. (2006). Predicting the transient response of a serpentine flow-field PEMFC: II: Normal to minimal fuel and Air. *Journal of Power Sources*, 156(2), 369-374.

Siegel, N. P., Ellis, M. W., Nelson, D. J., Von Spakovsky, M. R. (2004). A two-dimensional computational model of a PEMFC with liquid water transport. *Journal of Power Sources*, 128(2), 173-184.

Sousa, R., and Gonzalez, E. R. (2005). Mathematical modeling of polymer electrolyte fuel cells. *Journal of Power Sources*, 147(1), 32-45.

Springer, T. E., and Zawodzinski, T. A., Gottesfeld S. (1991). Polymer Electrolyte Fuel-Cell Model. *Journal of the Electrochemical Society*, 138(8), 2334-2342.

Stefanopoulou, A.G., and Suh, K.W. (2007). Mechatronics in fuel cell systems. *Control Engineering Practice*, 15, 277–289.

Sun, H., G. S. Zhang, Guo L.J., Liu H. (2009). A Study of dynamic characteristics of PEM fuel cells by measuring local currents. *International Journal of Hydrogen Energy*, 34(13), 5529-5536.

Sun, J., and Kolmanovsky, I. (2005). Load governor for fuel cell oxygen starvation protection: A robust nonlinear reference governor approach. *IEEE Transactions on Control Systems Technology*, 13 (6), 911–920.

Sundaresan, M., and Moore, R. M. (2005). Polymer electrolyte fuel cell stack thermal model to evaluate sub-freezing startup. *Journal of Power Sources*, 145, 534-545.

Talj, R., Hissel, D., Ortega, R., Becherif, M., Hilairet, M. (2010). Experimental validation of a PEM fuel-cell reduced-order model and a moto-compressor higher order sliding-mode control. *IEEE Transactions on Industrial Electronics*, 57, 1906–1913.

Tamimi, J., and Li, P. (2010). A combined approach to nonlinear model predictive control of fast systems. *Journal of Process Control*, 20(9), 1092-1102.

Tøndel, P., Johansen, T. A., and Bemporad, A. (2003). An algorithm for multi-parametric quadratic programming and explicit MPC solutions, *Automatica*, 39, 3, 489–497.

Tong, S., Liu, G., Wang, X.G., Tan M. (2009). Real-Time Implementation of Adaptive State Feedback Predictive Control of PEM Fuel Cell Flow Systems Using the Singular Pencil Model Method. *IEEE Transactions on Control Systems Technology*, 17 (3), 697-706.

U.S. Department of Energy (2012). Hydrogen and Fuel Cells Program, Record 12020: Fuel Cell System Cost - 2012, September 2012.

U.S. Department of Energy (2012b). Hydrogen and Fuel Cells Program, FY 2012 Annual Progress Report, DOE/GO-102012-3767, December 2012.

Ullah, B., Sarker, R., and Cornforth, D. (2008). Search space reduction technique for constrained optimization with tiny feasible space. *10th annual conference on Genetic and evolutionary computation (GECCO'08) 2008*, Atlanta, GA, USA, 881–888.

Um, S., and Wang, C. Y. (2004). Three-dimensional analysis of transport and electrochemical reactions in polymer electrolyte fuel cells. *Journal of Power Sources*, 125, 40-51.

Um, S., Wang, C. Y., and Chen, K. S. (2000). Computational fluid dynamics modeling of proton exchange membrane fuel cells. *Journal of the Electrochemical society*, 147(12), 4485-4493.

Vahidi, A., A. Stefanopoulou, H. Peng, (2006). Current Management in a Hybrid Fuel Cell Power System: A Model-Predictive Control Approach, *IEEE Trans. on Control Systems Technology*, 14, 6.

Varigonda, S., and Kamat, M. (2006). Control of stationary and transportation fuel cell systems: Progress and opportunities. *Computers and chemical engineering*, 30(10), 1735-1748.

Wang, Y. and Boyd, S. (2010). Fast model predictive control using online optimization. *IEEE Trans. on control systems technology*, 18 (2), 267-278.

Wang, Y. and Wang, C. Y. (2005). Simulation of flow and transport phenomena in a polymer electrolyte fuel cell under low-humidity operation,. *Journal of Power Sources*, 147, 148-161.

Wang, Y., Chen, K.S., Mishler, J., Cho, S.C., Adroher, X. C. (2011). A review of polymer electrolyte membrane fuel cells: Technology, applications, and needs on fundamental research, *Applied Energy*, 88, 981–1007.

Wang, Z. H., Wang, C. Y., and Chen, K. S. (2001). Two-phase flow and transport in the air cathode of proton exchange membrane fuel cells. *Journal of Power Sources*, 94(1), 40-50.

Weisbrod, K. R., Grot, SA, Vanderborgh, N. (1995). Through-the-electrode model of a proton exchange membrane fuel cell, *Electrochem. Soc. Proc.*, 153-167.

Wingelaar, P. J. H., Duarte, J. L., and Hendrix, M. A. M. (2007). PEM fuel cell model representing steady-state, small-signal and large-signal characteristics. *Journal of Power Sources*, 171(2), 754-762.

Wishart, J., Dong, Z., Secanell, M. (2006). Optimization of a PEM fuel cell system based on empirical data and a generalized electrochemical semi-empirical model. *Journal of Power Sources*, 161(2), 1041-1055.

Wohr, M., Bolwin, K., Schnurnberger, W., Fischer, M., Neubrand, W., Eigenberger, G. (1998). Dynamic modelling and simulation of a polymer membrane fuel cell including mass transport limitation. *International Journal of Hydrogen Energy*, 23, 213-218.

Woo, C. H., an Benziger, J. B. (2007). PEM fuel cell current regulation by fuel feed control. *Chemical engineering science*, 62(4), 957-968.

Wu, H., P. Berg, X. Li (2007). Non-isothermal transient modeling of water transport in PEM fuel cells. *Journal of Power Sources*, 165, 232-243.

Wu, H., Berg, P., Li, X. (2010). Steady and unsteady 3D non-isothermal modeling of PEM fuel cells with the effect of non-equilibrium phase transfer. *Applied Energy*, 87(9), 2778-2784.

Wu, W., Xu, J., and Hwang, J. (2009). Multi-loop nonlinear predictive control scheme for a simplistic hybrid energy system. *International Journal of Hydrogen Energy*, 34(9), 3953–3964.

Würth, L., Hannemann, R., and Marquardt, W. (2011). A two-layer architecture for economically optimal process control and operation. *Journal of Process Control*, 21(3), 311-321.

Xue, X., Tang, J., Smirnova, A., England, R., Sammes, N. (2004). System level lumped-parameter dynamic modeling of PEM fuel cell. *Journal of Power Sources*, 133(2), 188-204.

Yang, X. and Biegler, L.T. (2012). Advanced-multi-step Nonlinear Model Predictive Control, *8th IFAC Symposium on Advanced Control of Chemical Processes*, 426-431, Singapore, July 10-13, 2012.

Yang, Y., (2010). Portable Power Fuel Cell Manufacturing Cost Analyses, Austin Power Engineering. Fuel Cell Seminar, San Antonio, USA.

Yang, Y.P., Wang, C.F., Chang, H.P., Maa, Y.W., Weng, B.J. (2007). Low power proton exchange membrane fuel cell system identification and adaptive control. *Journal of Power Sources*, 164, 761–771.

Yerramalla, S., Davari, A., Feliachi, A., Biswas, T. (2003). Modeling and simulation of the dynamic behavior of a polymer electrolyte membrane fuel cell. *Journal of Power Sources*, 124(1), 104-113.

Yi, J. S., and Nguyen, T.V. (1998). An along-the-channel model for proton exchange membrane fuel cells, *Journal of the Electrochemical Society*, 145, 1149-1159.

Younis, A., and Dong, Z. (2010). Metamodeling Search Using Space Exploration and Unimodal Region Elimination for Design Optimization, *Engineering Optimization*, 42(6), 517-533.

Yuan, W., Tang, Y., Pan, M., Li, Z., and Tang, B. (2010). Model prediction of effects of operating parameters on proton exchange membrane fuel cell performance. *Renewable Energy*, 35(3), 656-666.

Zavala, V. M., Laird, C. D., and Biegler, L. T. (2008). A fast computational framework for large-scale moving horizon estimation. *Journal of Process Control*, 18(9), 876-884.

Zavala, V. M., and Biegler, L.T. (2009). The Advanced Step NMPC Controller: Optimality, Stability and Robustness. *Automatica*, 45(1), 86-93.

Zeilinger, M. N., Jones, C. N., and Morari, M. (2011). Real-Time Suboptimal Model Predictive Control Using a Combination of Explicit MPC and Online Optimization. *IEEE Trans. on control systems technology*, 56 (7), 1524-1534.

Zenith, F., and Skogestad, S. (2007). Control of fuel cell power output. *Journal of Process Control*, 17, 333–347.

Zenith, F., and Skogestad, S. (2009). Control of the mass and energy dynamics of polybenzimidazole-membrane fuel cells. *Journal of Process Control*, 19(3), 415-432.

Zhang, J., Liu, G., Yu, W., Ouyanga, M. (2008). Adaptive control of the airflow of a PEM fuel cell system. *Journal of Power Sources*, 179, 649–659.

Zong, Y., Zhou, B. and Sobiesiak, A. (2006). Water and thermal management in a single PEM fuel cell with non-uniform stack temperature. *Journal of power sources*, 161(1), 143-159.

Zumoffen, D., and Basualdo, M. (2010). Advanced control for fuel cells connected to a DC/DC converter and an electric motor. *Computers and Chemical Engineering*, 34(5), 643-655.

Appendix A. Interface of the developed software

The developed software consists of a number of custom designed user interfaces that facilitate the operation of the various controllers including:

- Communication interface for OPC data transmission
- Device driver for electronic load (using serial RS232C protocol)
- HMI interface at SCADA of the Unit
    - Analog, Digital, Alarms, Menu, Control, System, Trending

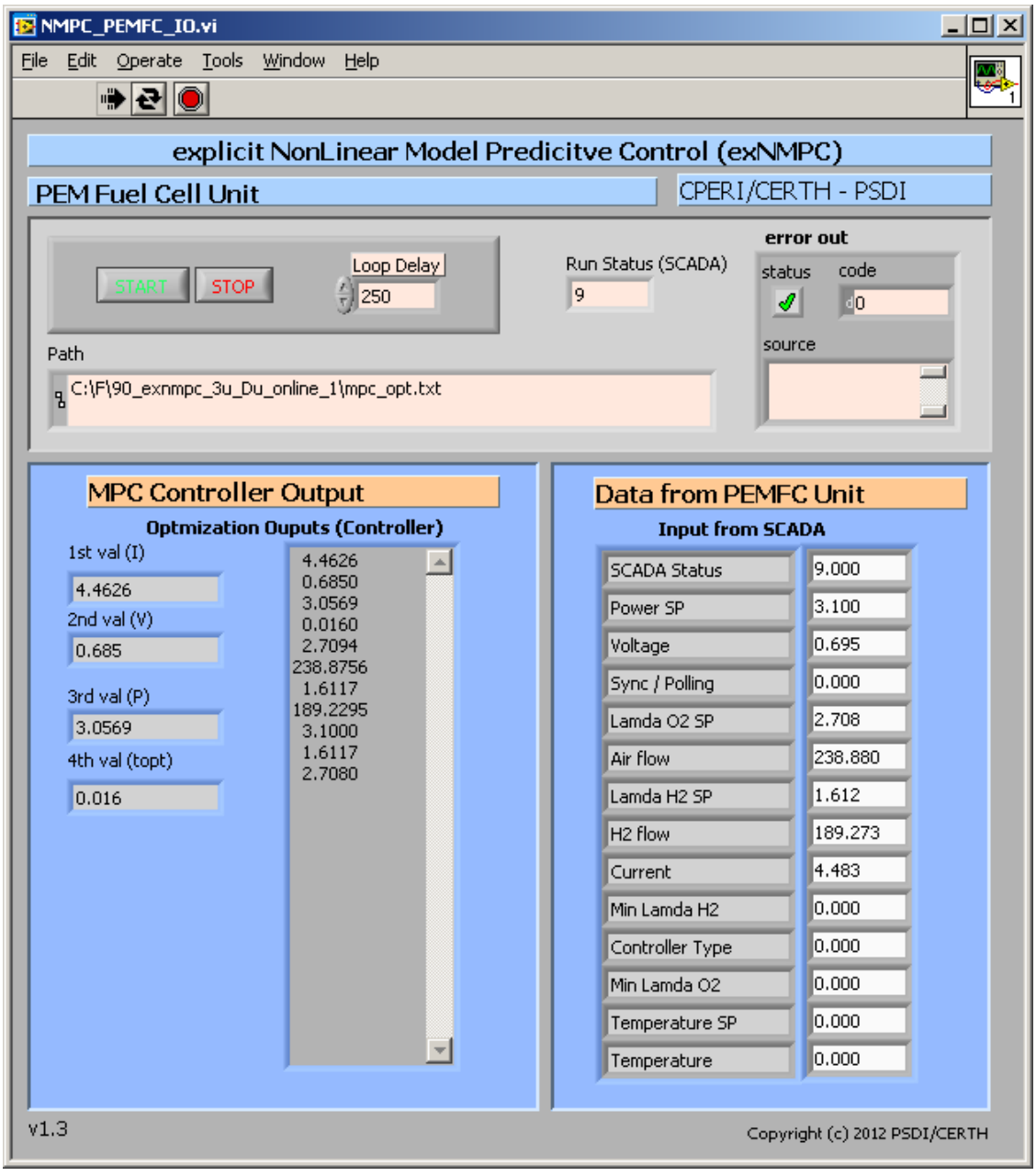

Interface of the I/O driver between the FORTRAN models and optimization solver and the SCADA system using OPC protocol

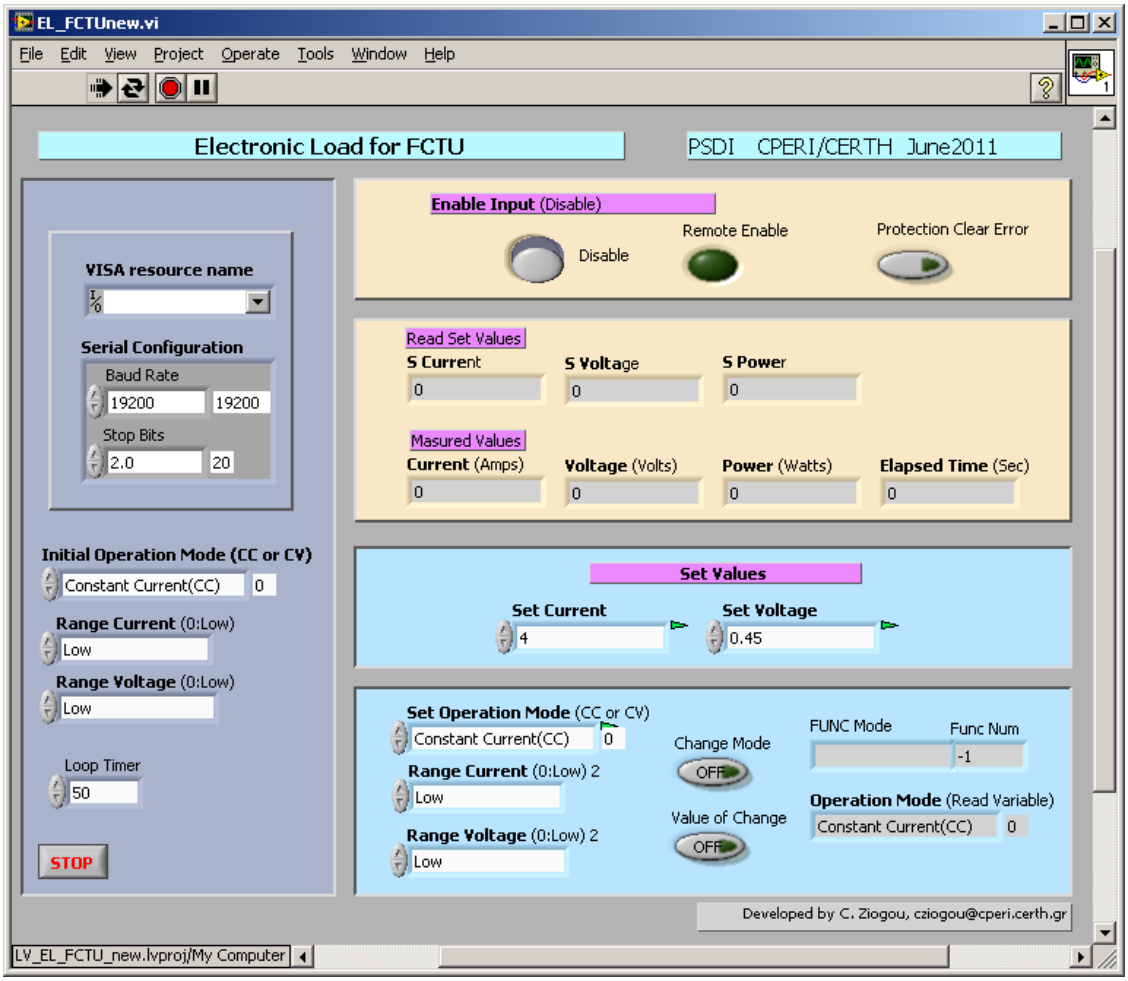

Serial I/O driver that enables the communication between the programmable DC Electronic Load and the SCADA system. The data communication is based on the OPC protocol.

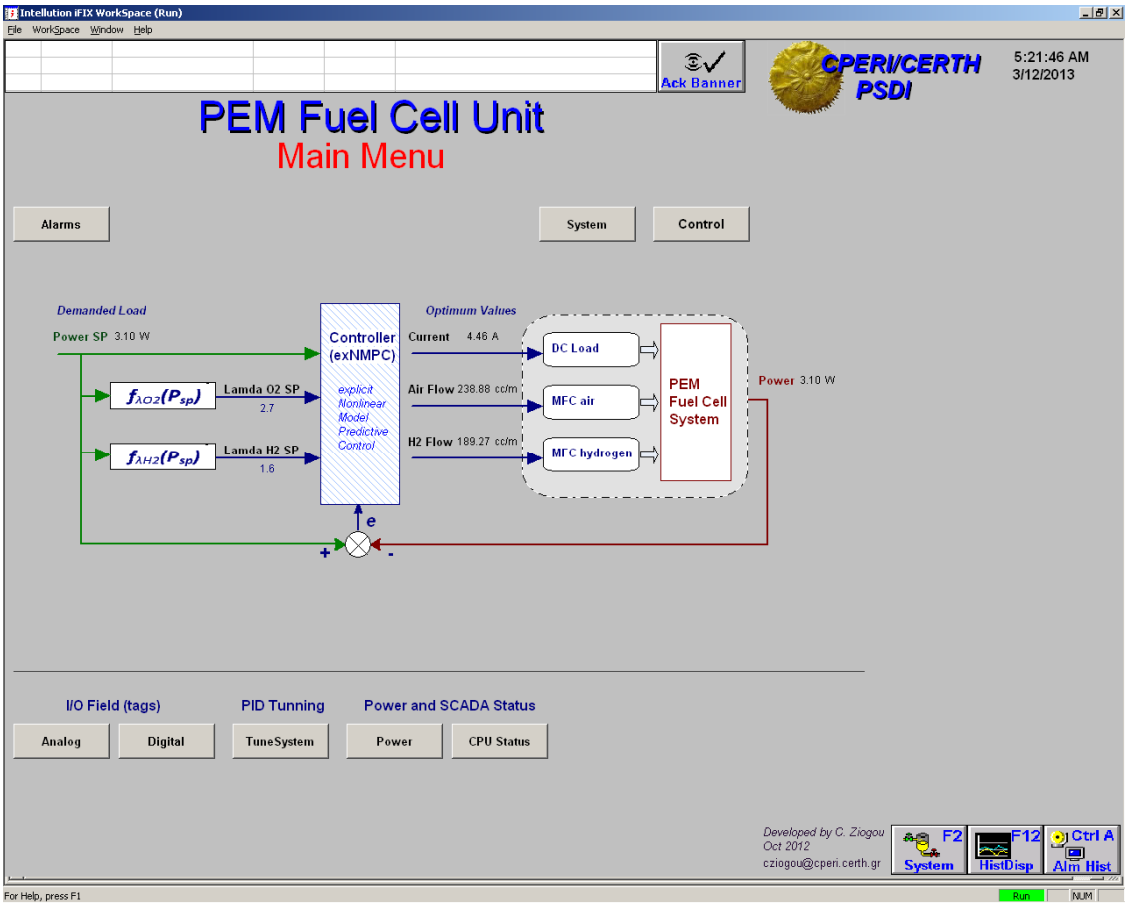

Main screen of the HMI/SCADA system.

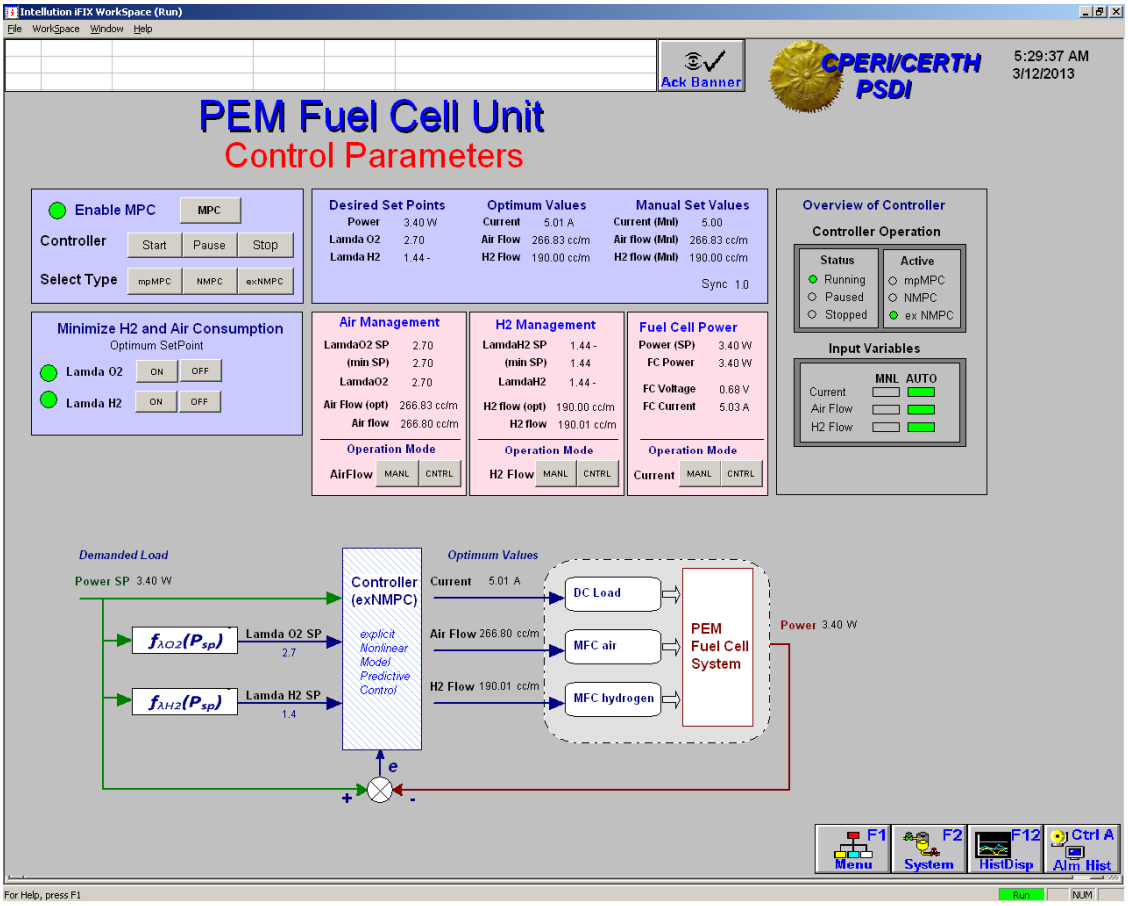

Supervisory screen with the available parameters for each controller.

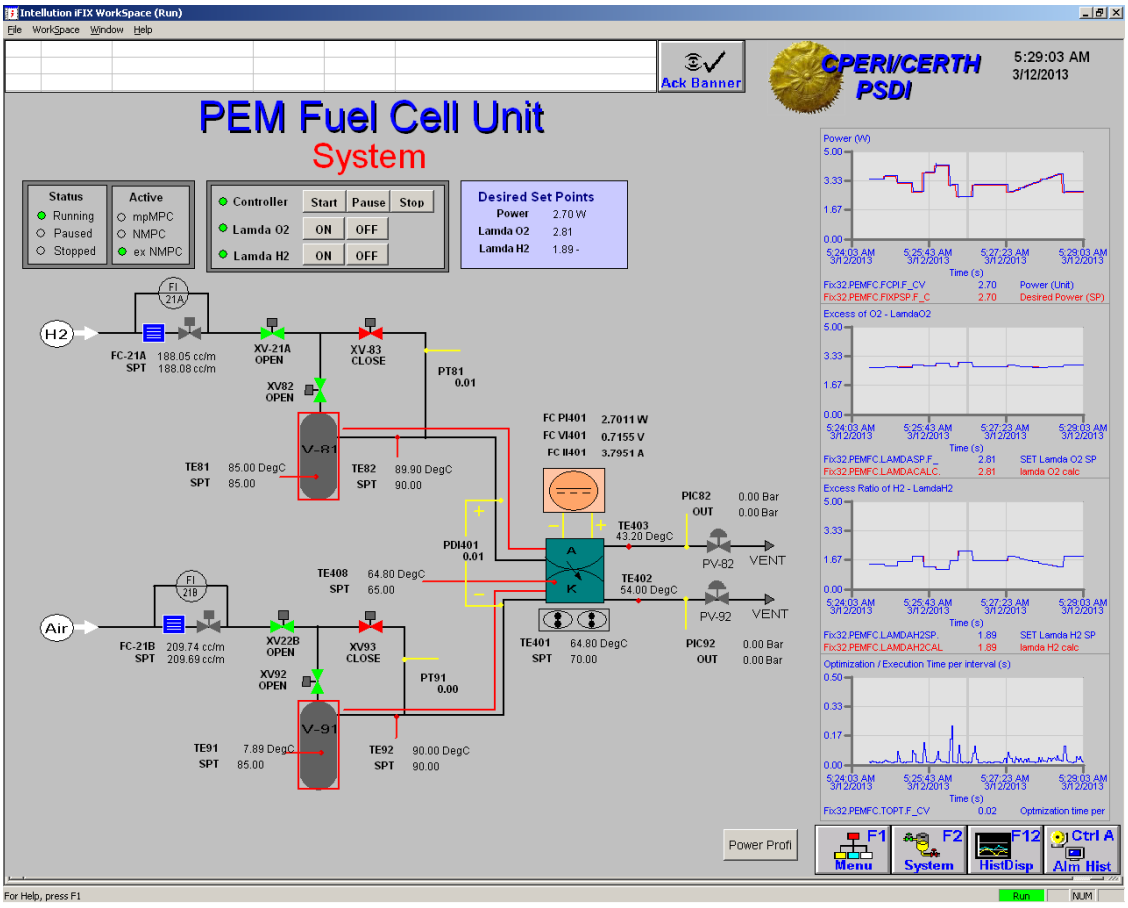

Overview of the status of the PEMFC system

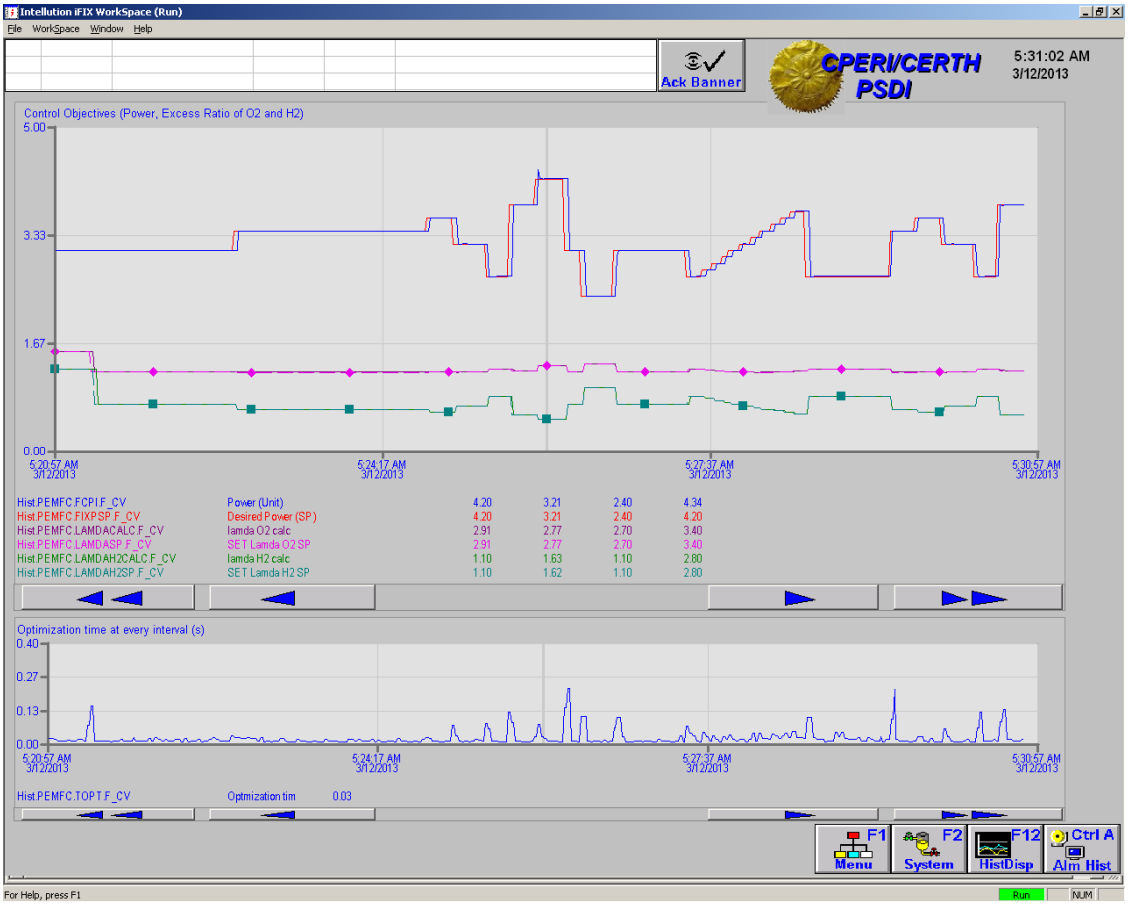

Indicative diagrams that present the online behavior of the fuel cell using data from the archiving system.

List of the analog signals of the PEMFC system.

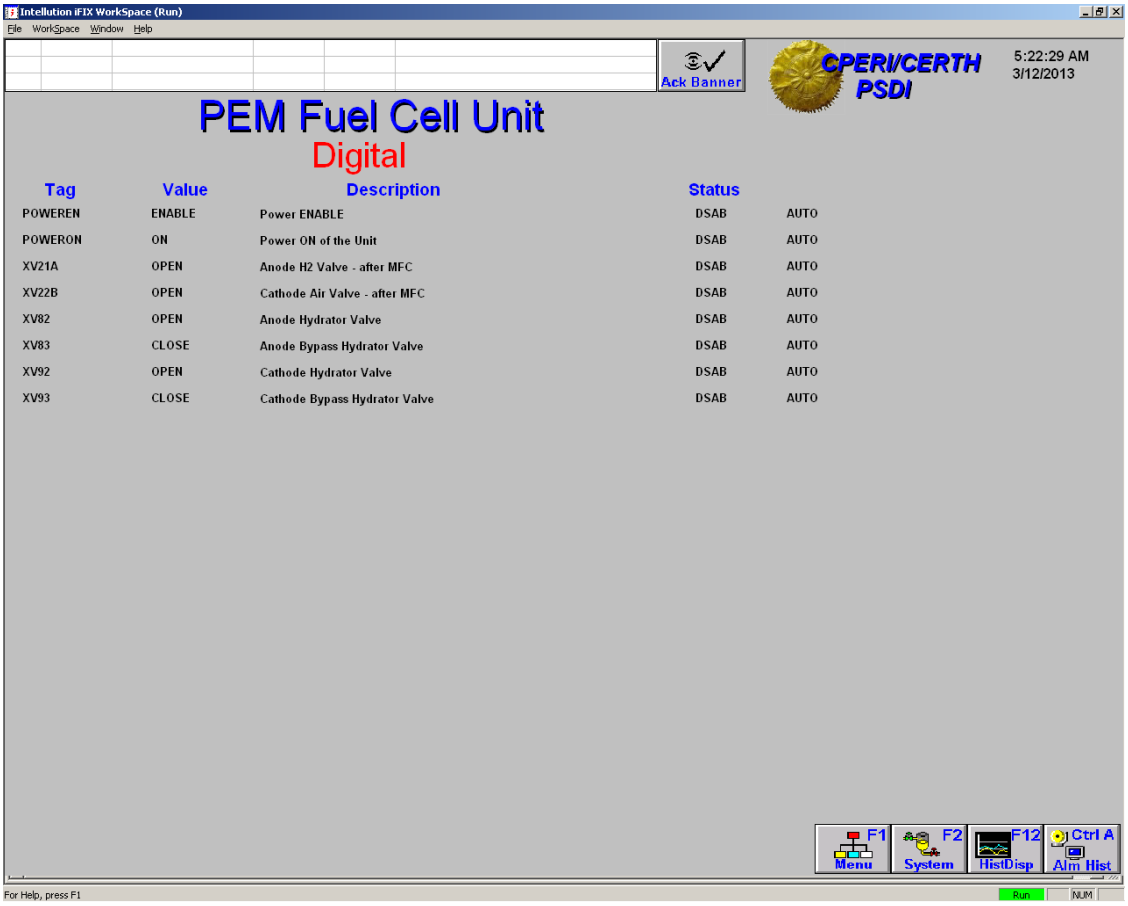

List of the digital signals of the PEMFC system.

Appendix B. Software routines for the mpMPC

---

1. Matalab function that was used to automatically translate the Critical Regions from Matlab code to Fortran subprograms

```
% ----- Subroutine for Automatic transformation ton CRs se fortran -----
% Jan2012, Dev by C. Ziogou (CPERI/CERTH - PSDI)
% cziogou@cperi.certh.gr
%
function retflag = crinf24transep(zcr, fonoma)
    retflag = logical(0);
    global ZERO;
    [unit, msg] = fopen(fonoma, 'wt');
    nCR = length(zcr); % NREGIONS pli8os ton crit regions
    nrX = size(zcr(1).X, 1); % NCONTROLS gia p , grmmes tou X
    ncX = size(zcr(1).X, 2) - 1; % NTHETA siles tou X -1
fprintf(unit, '!3/Jan/2012: when Matlab egine Fortran \n (C.Ziogou CPERI/CERTH)
cziogou@cperi.certh.gr \n\n');

fprintf(unit, 'SUBROUTINE CR24TRAN(stat) \n\n \t EXTERNAL stat \n');
fprintf(unit, '! critical region information \n');
fprintf(unit, '! original X-rows (discretized controls for all time periods) are %d
\n',nrX);
fprintf(unit, '! only the following rows have been included for the MPC: */');
fprintf(unit, '\n ! /* [ %d]*/ \n ', ZERO);
fprintf(unit, ' PARAMETER (NCONTROLS=2, NTHETA=6, NREGIONS=67) \n',nrX, ncX, nCR);

fprintf(unit, 'COMMON /CRPARAMS/ oNCONTROLS, oNTHETA, oNREGIONS \n');
fprintf(unit, 'INTEGER oNCONTROLS, oNTHETA, oNREGIONS \n');
fprintf(unit, '! NCONTROLS %d /* control variables # */\n', nrX);
fprintf(unit, '! NTHETA    %d /* "parameters" (states etc) # */\n', ncX);
fprintf(unit, '! NREGIONS  %d /* critical regions # */\n\n', nCR);

% ---- gia ka8e critical region : pinakes Ab declaration
for i = 1:nCR,
   fprintf(unit, 'DOUBLE PRECISION crA_raw%04d(26*(NTHETA)) \n\t', i);
end
for i = 1:nCR,
   fprintf(unit, 'DOUBLE PRECISION crb_raw%04d(26) \n\t', i);
end
% ---- gia ka8e critical region : X declaration
fprintf(unit,'\n \n !gia ka8e critical region : X declaration \n \t');
for i = 1:nCR,
   fprintf(unit, 'DOUBLE PRECISION XA_raw%04d(NCONTROLS*(NTHETA)) \n\t', i);
end
for i = 1:nCR,
   fprintf(unit, 'DOUBLE PRECISION Xb_raw%04d(NCONTROLS) \n\t', i);
```

```
end
fprintf(unit,'\n \n ');
% --- struct
fprintf(unit,'TYPE :: RegionInfo \n\t');
fprintf(unit,'    INTEGER     :: nEdges    ! inequalities defining this CR \n\t');
fprintf(unit,'DOUBLE PRECISION :: crA(26*(NTHETA)) ! combined constraints + RHS
[nEdges, NTHETA] \n\t');
fprintf(unit,'DOUBLE PRECISION :: crb(26) ! combined constraints + RHS [nEdges]
\n\t');
fprintf(unit,'DOUBLE PRECISION :: XA(NCONTROLS*(NTHETA))    ! control law including
constant term [NCONTROLS, NTHETA]\t');
fprintf(unit,'DOUBLE PRECISION :: Xb(NCONTROLS)    ! control law including constant
term [NCONTROLS]\n\t');

fprintf(unit,'END TYPE RegionInfo \n\t');
fprintf(unit,' TYPE(RegionInfo) :: CRInf(NREGIONS) \n\n');
% ------------------------------------------------------------------------
% ---- gia ka8e critical region : pinakes A
fprintf(unit,'! Raw critical region data: CRi = {t: Ai*t <= bi} ------ */\n');
max=26
for i = 1:nCR,
   lenb = length(zcr(i).cr.b); % pli8os ton b
   diplaAb = [zcr(i).cr.A ]; % dipla A b [cols: 6 1]
   fprintf(unit, 'crA_raw%04d = [ & \n\t', i );
    for j = 1:max
        if j<=lenb
            row = diplaAb(j, :);
            for k=1:length(row)
              if abs(row(k)) <= ZERO, row(k) = 0; end
            end
            format long
            fprintf(unit, '%12.7f, ', row);
        else
            fprintf(unit, '0.0 ,0.0, 0.0, 0.0 ,0.0, 0.000, ');
        end
    %last row or EOL
      if j==max
         fseek(unit, -2, 'cof');
         fprintf(unit,' &\n ] \n');
      else
         fprintf(unit,' & \n\t ');
      end
   end %end of CRs A
end
% ---- gia ka8e critical region : pinakas b
% mono b
fprintf(unit,'! Raw critical region data: CRi = {t: Ai*t <= bi} ---- */\n');
max=26
for i = 1:nCR
   lenb = length(zcr(i).cr.b); % pli8os ton b
   diplaAb = [zcr(i).cr.b]; % dipla A b [cols: 6 1]
   fprintf(unit, 'crb_raw%04d = [ & \n\t', i );
    for j = 1:max
        if j<=lenb
            row = diplaAb(j);
            for k=1:length(row)
              if abs(row(k)) <= ZERO, row(k) = 0; end
            end
            format long
            fprintf(unit, '%12.7f, ', row);
```

```
        else
            fprintf(unit, '0.000, ');
        end
    %last row or EOL
      if j==max
         fseek(unit, -2, 'cof');
         fprintf(unit,' &\n ] \n');
      else
         fprintf(unit,' & \n\t ');
      end
   end %end of CRs gia b
end
% ---- gia ka8e critical region : XA
fprintf(unit, '\n ! Control laws for each region: U = F*t + c --- \n');
colsX=1:nrX
for i = 1:nCR,
   fprintf(unit, 'XA_raw%04d= [ & \n\t', i);
   for j = 1:length(colsX)
      row = zcr(i).X(colsX(j),1:end-1);
              for k=1:length(row)
                     if abs(row(k)) <= ZERO, row(k) = 0; end
        end
      fprintf(unit, '%12.7f, ', row);
      if j==length(colsX)
         fseek(unit, -2, 'cof');
         fprintf(unit,' \t & \n] \n');
      else
         fprintf(unit,' & \n\t');
      end
   end
end
% ---- gia ka8e critical region : Xb
fprintf(unit, '\n ! Control laws for each region: U = F*t + c --- \n');
colsX=1:nrX
for i = 1:nCR,
   fprintf(unit, 'Xb_raw%04d= [ & \n\t', i);
   for j = 1:length(colsX)
      row = zcr(i).X(colsX(j), end);
              for k=1:length(row)
                     if abs(row(k)) <= ZERO, row(k) = 0; end
              end
      fprintf(unit, '%12.7f, ', row);
      if j==length(colsX)
         fseek(unit, -2, 'cof');
         fprintf(unit,' \t & \n] \n');
      else
         fprintf(unit,' & \n\t');
      end
   end
end
% ---- structure me nEdges, crAb, Xb
fprintf(unit,'\n ! Summary information for all regions ------------ \n');

for i = 1:(nCR),
   fprintf(unit,'\t      CRInf(%d)=      RegionInfo(%d,      crA_raw%04d,crb_raw%04d,
XA_raw%04d,Xb_raw%04d) \n', i,length(zcr(i).cr.b), i, i,i,i);
end
   fprintf(unit,'\n \n \n END SUBROUTINE CR24TRAN \n');
retflag = logical(1);
fclose(unit);
```

2. Fortran program that implements a look-up function for the selection of the corresponding Critical Region to the respective input.

```
! ----- Subroutine gia na brei to CR gia to dedomeno thita -----
! Jan2012, Dev by C. Ziogou (CPERI/CERTH - PSDI)
! cziogou@cperi.certh.gr
! epistrefei to status kai to id tou CR,(status ==1 brike, ==0 problima)

SUBROUTINE locateCR(thita)
       PARAMETER (NCONTROLS=NCO, NTHETA=NTH, NREGIONS=NCR, MAXINEQ=INEQ)
       DOUBLE PRECISION thita(NTHETA)
       INTEGER i,j,k,l,indx
       DOUBLE PRECISION crAtemp(MAXINEQ*(NTHETA)),crbtemp(MAXINEQ),aux
       DOUBLE PRECISION crA_epi_thita(MAXINEQ), crb_meion_crAt(MAXINEQ)
       TYPE :: RegionInfo
         INTEGER          :: nEdges
              DOUBLE PRECISION :: crA(MAXINEQ*(NTHETA))
              DOUBLE PRECISION :: crb(MAXINEQ)
              DOUBLE PRECISION :: XC(NCONTROLS*(NTHETA))
              DOUBLE PRECISION :: Xd(NCONTROLS)
       END TYPE RegionInfo
       COMMON /CRset/ CRInf
         TYPE(RegionInfo) :: CRInf(NREGIONS)
       COMMON /CRstatus/ status, CRid
       INTEGER status, CRid
       i=1
       aux=0
       DO while (i<=NREGIONS)  ! NREGIONS
          crAtemp=CRInf(i)%crA
          crbtemp=CRInf(i)%crb
!         form Ax gia ka8e region , i & soter it in crA_epi_thita[max_ineq]
          DO j=1, CRInf(i)%nEdges
                     aux=0
                     DO k=1,NTHETA
                        indx=((j-1)*NTHETA)+k
                        aux=aux+(crAtemp(indx)*thita(k))
                     ENDDO
                     crA_epi_thita(j)=aux
                     crb_meion_crAt(j)=crbtemp(j)-crA_epi_thita(j)
                     if (crb_meion_crAt(j) < 0 )then
                            status=0
                            exit
                     else
                            status=1
                     endif
          ENDDO
          if (status==1) then
!               write(6,*) 'all ineq < 0 !!!!!'
                CRid=i
                exit
          endif
          i=i+1
       end do
       END SUBROUTINE locateCR
```